UNIVERSITY OF MINING AND GEOLOGY "ST. IVAN RILSKI"

JOURNAL

OF

MINING AND GEOLOGICAL SCIENCES

Volume 61
Part II: MINING, TECHNOLOGY AND MINERAL PROCESSING

Sofia, 2018

ISSN 2535-1184

Printig: **Publishing House "St. Ivan Rilski"**

C O N T E N T S

Evgenia Alexandrova	Development of a 3D Model for the Assessment of the Stability of the Slopes in the Mizia Quarry	**5**
Daniel Georgiev	Optimisation of Sampling of Coal From the Obedinen Open Cast Mine and the Republika Mine	**10**
Stojance Mijalkovski **Zoran Despodov** **Dejan Mirakovski** **Vancho Adjiski** **Nikolinka Doneva**	Analysis of the Ore Recovery and Ore Dilution in the Underground Mine for Lead and Zinc „SASA“ - M. Kamenica	**13**
Tondera, D. **Beier, D.** **Tamaskovics, N.** **Pavlov, P.** **Totev, L.**	Groundwater Impact Investigation Due to Installation of a “LWS” Silicate Gel Sealing Sole in the Water Saturated Soil Zone	**19**
Babich A.V. **Vinnikov V.A.**	On the Determination of the Optimum Time of Microwave Exposure to Pyrite-Containing Ore	**24**
Valeriy Slobodyanyuk **Ivan Maksimov** **Roman Slobodyanyuk**	Influence of the Arrangement and Performance of Shovels on the Optimum Position for Run-of-Mine Stock Location	**28**
Roman Slobodyanyuk	Analysis and Development of Slope Hoisting Systems for Open Pit Mines	**33**
Zahari Dinchev **Yasen Gorbunov** **Nadezhda Kostadinova**	Velocity Field Visualization, Measured with 3D Ultrasonic Anemometer	**39**
Blagovesta Vladkova **Luka Arbaliev** **Veronika Karadjova**	Safe Treatment of Expired Medicines	**45**
Irena Grigorova **Marin Ranchev** **Ivan Nishkov**	Mass Measurement for Metal Accounting in Mineral Processing Plants	**53**
Marin Ranchev **Irena Grigorova** **Ivan Nishkov**	Sampling in Mineral Processing – Review of Practices	**59**
Tsvetelina Ivanova	Pre-Contact Column Flotation Machines – Design Features and Principles of Operation	**65**
Alexander A. Klemiatov **Alexander I. Kalugin** **Ilya A. Gribov** **Nikita A. Rozhdestvenskii** **Alexey Yu. Barabash** **Yulia S. Gordeeva**	Some Aspects of the Revamp of Existent Beneficiation Plants	**69**

Norov Andrey M. **Pagaleshkin Denis A.** **Fedotov Pavel S.**	The Effect of Impurity Composition of Phosphate Rock on the Technology of its Processing and Properties of Final Products	**75**
Petya Gencheva **Lubomir Djerahov**	High-Strength Synthetic Fibers and Nano-Sized Particles of SiO_2 Combined into one Composite System for Ballistic Protection	**82**
Marinela Panayotova **Neli Mintcheva** **Lubomir Djerahov** **Gospodinka Gicheva**	Kinetics and Thermodynamics of Silver Ion Immobilisation by Natural Clinoptilolite	**87**
Marinela Panayotova **Gospodinka Gicheva** **Nely Mintcheva** **Lubomir Djerahov**	Study on the Air Quality During the Operation of the *Mizia* Quarry	**92**
Gospodinka Gicheva **Neli Mincheva**	Effect of Amines on the Silver Nanoparticles Formation at Room Temperature	**97**
Maria Manastirli **Irena Spasova**	Leading Principles and Practices in the Management of Construction Wastes	**102**
M. Nikolova **I. Spasova** **S. Groudev** **P. Georgiev** **V. Groudeva**	Electricity Generation in Microbial Fuel Cells by Means of Different Microorganisms	**106**
Irena Spasova **Marina Nikolova** **Plamen Georgiev** **Stoyan Groudev**	Microbial Pre-Treatment Of A Gold-Bearing Flotation Pyrite Concentrate By Means Of Mesophilic And Moderate Thermophilic Bacteria And By Extreme Thermophilic Archaea	**109**
P. Georgiev **M. Nikolova** **I. Spasova** **S. Groudev** **V. Groudeva**	The Effect of the Pulp Density of a Copper Slag on the Efficiency of its Bioleaching by Means of Different Microorganisms	**112**
Violeta Trifonova-Genova	Analytical Expressions for Stresses in Steeply Stratified Rock Mass Around an Opening in the Shape of an Ellipse	**115**
Stefan Pulev	Self-Clearing of Vibrating Screening Systems	**119**
Ivan Nikolov **Alexandre Loukanov** **Elena Ustinovich** **Anatoliy Angelov** **Seiichiro Nakabayashi**	Iron Doped Carbon Nanodots as Efficient Electrocatalysts	**123**

DEVELOPMENT OF A 3D MODEL FOR THE ASSESSMENT OF THE STABILITY OF THE SLOPES IN THE *MIZIA* QUARRY

Evgenia Alexandrova

University of Mining and Geology "St. Ivan Rilski", 1700 Sofia, jogeni@abv.bg

ABSTRACT. The main aspects of three-dimensional modelling for the assessment of the resistance of the slopes in open pit mines and quarries are reviewed in the article. Methods based on the boundary equilibrium and the mechanics of the continuous environment are analysed. An example is presented for the assessment of the stability of the slopes in the Mizia quarry based on a 3D model.

Keywords: open pit mining, slope stability

РАЗРАБОТВАНЕ НА 3D МОДЕЛ ЗА ОЦЕНКА НА УСТОЙЧИВОСТТА НА ОТКОСИТЕ В КАРИЕРА „МИЗИЯ"

Евгения Александрова

Минно-геоложки университет „Св.Иван Рилски", 1700 София

РЕЗЮМЕ. В статията са разгледани основните аспекти при триизмерното моделиране за оценка на устойчивостта на откосите в открити рудници и кариери. Анализирани са методите, основани на граничното равновесие и на механиката на непрекъсната среда. Представен е пример за оценка на устойчивостта на откосите в кариера „Мизия" на базата на 3Dмодел.

Ключови думи: открит добив, оценка на устойчивостта

One of the important and increasingly developing areas in the field of slope stability assessment is the three-dimensional analysis, i.e. solving the so-called volume task.

Creating a 3D model is a widely used method for solving a number of practical engineering problems (for example, a numerical modelling of the strained distorted state of the object) as well as in solving a wide number of ecological and hydrogeological problems. Applying a 2D analysis for solving the planar task to estimate the stability of slopes remains one of the recent fundamental methods. Along with that, 2D modelling in this area has significantly changed in the past years. A large number of methods are developed for 3D analysis of slope stability based on the concepts of boundary equilibrium and the mechanics of continuous mediums. The first attempt to develop a three-dimensional method for estimating the slope stability dates back to the early 60's of the last century but 3D methods have been used more intensely during the past few years. A number of specialised software products are used that already have program modules for 3D modeling of slope stability, e.g. SoilVisionSystems, Inc. (Canada), TAGAsoft, Inc (USA), Itasca International, Inc. (USA), O.Hungr Geotechnical Research, Inc. (Canada), etc. It can be assumed that the popular companies like GEO-SLOPE Internatioanal, Inc. (Canada) and Rocsiense, Inc. (Canada) will soon develop similar products. Based on this information, a 3D innovation in slope stability assessment in the near future is coming.

Improving the analysis for slope stability assessment from 2D to 3D is a challenging task because of the additional dimension. Modelling the stability in three dimensions is undoubtedly the better and more perspective choice than the 2D models, and the advantages come from the volume analysis:

- In a 3D problem, the possible sliding surface is modelled (in conditions of continuous medium) as a segment of an elliptical surface, while the circular cylindrical surface in a 2D problem remains unchanged. In terms of mechanics, the problem in focus cannot be considered planar, so the 2D task could be solved appropriately in case of significant assumptions only.

- In solving the 2D problem for slope stability assessment, a large number of conditions that must be considered exist (for example, the homogeneity of the massif in the vertical profile and the topographical homogeneity of the slope in the direction of its incidence). But in practice, these factors significantly affect the stability (for example, tectonic leaps intersecting the slope at an angle or cutting the slope in parts when opening roads). These additional components can be taken into account only in 3D models.

- A significant advantage in 3D analysis for slope stability assessment is that these calculations make it possible to predict the development of a landslide or a deformation process not only in depth but also in plane. Besides, these can solve the problem with respect to the location of the most dangerous area of sink or loss of stability. The results are towards a more precise risk assessment with regards to the

spatial activation of a landslide process and for taking well-grounded constructive solutions for landslide prevention.

2D modelling of slope stability has basically used-up its long term potential. When solving the 2D problem, the main ideas and methods for slope stability assessment have been formed in their current state in the mid 60's of the last century and no significant scientific contributions are added nowadays. Only detailed analyses are added of the specifics of the earlier developed methods.

In most of the cases, the graphical presentation of the calculating work scheme for solving the 2D problem for slope stability assessment is significantly simplified and rarely corresponds to the real situation. Anyway, the practical solution of the 2D task is surprisingly successful. The main reasons for that are:

- In 1987, S. Cavounidis showed that the stability coefficient of a slope in 3D analysis was greater than the one in the planar problem. Thus, the 2D method is more conservative and contains significant reserves of stability.
- The mathematical realisation of 2D methods is much more developed in comparison with 3D modelling where there aren't important tools like probability analysis, analysis of the sensitivity, optimisation of the probable slope of sliding, etc.
- 3D methods of numerical analysis are less resistant than 2D calculations, especially when they are based on the consideration of force equilibrium conditions.
- 3D methods for slope stability assessment, as well as 2D models, require additional assumptions for achieving a static determination of the problem. There are several ways to do this: reduce the number of variables, increase the number of equations, or use them both. The introduction of additional assumptions in 3D methods depends on the specific area of application.

The best-known methods for spatial modelling of the slope stability are as follows:

Methods based on the boundary equilibrium theory

The Anagnosti method. In 1969, Anagnosti developed a 3D method for calculating the stability coefficient using potential surfaces with different shapes (Anagnosti, 1969). This method is actually an amplification of the 2D methods of Morgenstern-Price with the inclusion of additional equations for the equilibrium of a thin vertical plate. The main assumption concerns the distribution of the moving forces which satisfies all equilibrium conditions. The results show that the actual coefficient of stability increases more than 50%. Detailed investigations come to the conclusion that the calculated stability coefficients strongly depend on the assumptions concerning the moving forces between the plates. Anagnosti proves that all six equilibrium equations require four times more static assumptions than 2D calculations.

The Hovland method

The method which was developed by Hovland is based on the Fellenius method with additional assumptions in the third dimension (Hovland, 1977). Instead of plates, columns are used in this method. Here, all moving forces between the columns are ignored. The normal and tangential forces acting at the base of each column are obtained as a component of the weight of the column. Another assumption is that there is movement in only one direction and the equilibrium of the system is calculated for this direction.

The 3D stability coefficient is defined as the ratio of the total sum of the holding forces on the sliding surface and the total sum of the driving forces. The computational scheme of the Hovland method is presented in Figure 1.

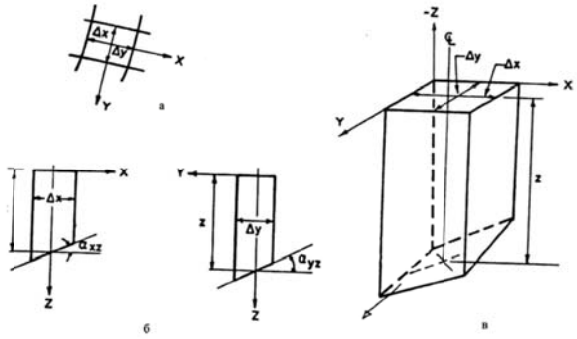

Fig. 1 The Hovland method
a) plan, b) profiles, c) 3D view of the column

It is assumed that the X and Y coordinates are perpendicular to each other in a horizontal plane, the Z coordinate is vertical, and the Y axis is along the side of the movement of the landslide (downstream). The column dimensions on a horizontal plane are determined by the Δx and Δy. Assuming that Δx и Δy are constant for all columns (the net is uniformly scaled), the stability coefficient can be calculated by the expression:

$$F = \frac{\sum x \sum y \left[cA_3 + W_3 \cos(DIP) tg\varphi \right]}{\sum x \sum y W_3 \sin \alpha_{yz}} \quad (1)$$

$$A_3 = \Delta x \Delta y \left[\frac{\sqrt{\left(1 - \sin^2 \alpha_{xz} \sin^2 \alpha_{yz}\right)}}{\cos \alpha_{xy} \cos \alpha_{yz}} \right] \quad (2)$$

$$\cos(DIP) = \frac{1}{\sqrt{\left(1 + tg^2 \alpha_{xz} + tg^2 \alpha_{yz}\right)}} \quad (3)$$

$$W_3 = yz \Delta x \Delta y \quad (4)$$

Hovland finds that any ratio between cohesion and the angle of internal friction of the mass may have its own critical surface of sinking and geometry. Studies also show that the ratio of the stability coefficient in the 2D and the 3D case is very sensitive

to the strength of the scales, as well as to the shape of the sliding surface, but are relatively insensitive to the width. The results obtained show that the 3D stability coefficient is much higher than the 2D coefficient, excluding some situations where the 3D coefficient could be lower (for example, for unbound soils).

The Chen method and the modified Chen and Chameau method

Chen and Chameau (1983) perform complex studies on the influence of the 3D model on the slope stability using a wide range of different mass properties. They offer two methods for calculating the stability coefficient based on the Spencer method for the 3D model and depending on the nature of the landslide movement. The landslide surfaces are presented in Figure 2 and Figure 3.

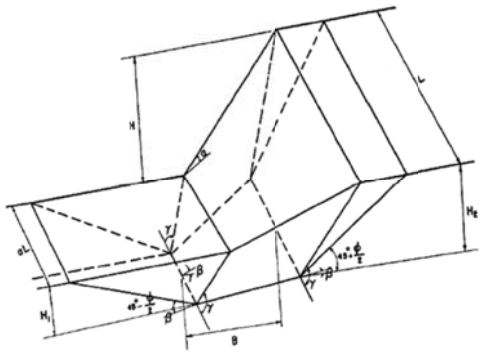

Fig 2 Calculation scheme for block shifting of a landslide body

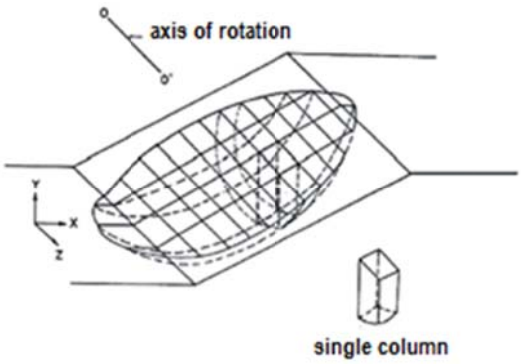

Fig 3 Calculation scheme with a landslide rotating body

Studying the block motion of the landslide in the 3D model, P. Chen makes the following conclusions:

- The 3D stability coefficient is always greater than the 2D coefficient;

- The 3D effect is greater for the slopes with connected masses;

- Staggering weak layers always give a smaller ratio of the stability coefficients obtained by the 3D and 2D models than those for sloping layers;

- In weak rocks, the 3D effect is more pronounced;

- When developing a wedge-shaped landslide, the ratio between the 3D and the 2D coefficient is usually less than one;

- Decreasing the surface slope of the landslide is the cause of a higher stability coefficient.

Based on the calculations for a rotating body, Chen concludes:

- The 3D effect is more significant when the landslide has a shorter length;

- For slanted slopes, the 3D effect is most significant for scales with a high coefficient of cohesion and a low internal friction angle;

- Pore pressure can cause significant three-dimensional effects.

In addition to the 3D modelling and slope analysis methods, there are also a number of methods based on 2D, such as the Hungr (1987) method (the Bishop method, the Yanbu simplified method), the Duncan method (1996), and others. In these methods, there is a tendency for higher values of the 3D stability coefficient.

Methods based on the mechanics of a continuous environment

Software products developed in recent years and based on the final difference method (FLAC3D, Itasca Consulting Group, Inc.) and the finite element method (PLAXIS3D) make it possible to solve the problem of slope stability with methods using the mechanics of non-continuous environments in three dimensional spaces.

An attempt of calculating a 3D slope stability coefficient has been made for the *Mizia* quarry by using the software product SVSlope 3D – SoilVisionSystems (Canada). Figure 4 presents the slope pattern used for the calculations. The properties of the mass are given in Table 1.

Table 1

Number	Density, kN/m^3	UCS,kPa	GSI	IRC	Distribance Factor
1	24.3	55000	25	9	0.7

UCS - Unconfined Compressive Strength
GSI - Geological Strength Index
IRC – Intact Rock Constant

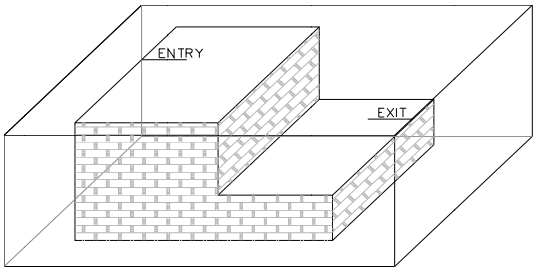

Fig.4 General overview of the model

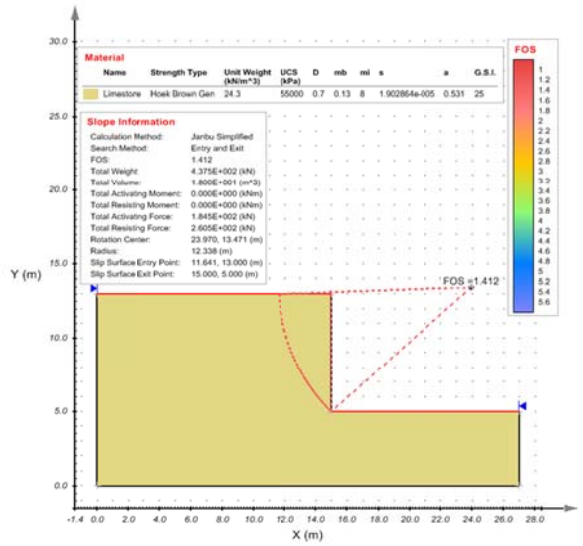

Fig.5 Results of estimating the 2D slope stability by the Bishop method

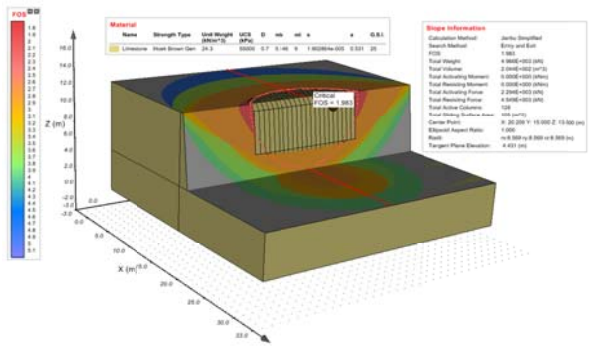

Fig.6 Results of the 3D model by the Janbu method

The following calculation methods were used for the modelling:

- The Yanbu method referring to the group of methods that satisfy the force equilibrium;

- The Bishop method referring to the group of methods that satisfy the moment equilibrium;

- The Spencer method referring to the group of methods satisfying the general equilibrium of moments and forces.

For searching the most dangerous sliding surfaces in the 3D model, the "entry and exit" algorithm is used. The results of the modelling are presented in Fig.5 and Fig 6.

A comparison between the results of 3D and 2D models is given in Table 2.

Table 2
Comparison of 3D and 2D computing results

Type	Estimation method		
	Spencer	Bishop	Yanbu
3D	2.866	1.969	1.893
2D	2.828	1.334	1.412
Ratio 3D/2D	1.01	1.48	1.34

Considering the obtained results, several important observations can be made:

1.The critical sliding surface obtained from the 3D model differs substantially from the sliding surface when solving the plane task.

2.The 3D stability coefficient is higher than the coefficient obtained by the 2D model.

Three-dimensional modelling based on boundary equilibrium methods has a number of significant constraints:

First, three-dimensional methods of analysis are less persistent than two-dimensional calculations. The analysis of the obtained results shows that the area of possible solution is not closed, and the result is significantly different from that obtained by the Entry and Exit method.

Secondly, it is necessary to mention that, in general, solving the slope stability task with the methods of the boundary equilibrium is statically undefined. In particular, using lamella methods, the task becomes statically determined for each element, but the need for accepting different assumptions arises.

Conclusions

Two-dimensional models based on the mechanics of the continuous medium imply conditions for flat stressed condition, which is not applicable for slopes with a complex structure and with a varying lithology and surface relief. The main methods of three-dimensional analysis of the slope stability are the methods of boundary equilibrium and the methods based on the mechanics of a continuous environment.

Several important conclusions can be drawn based on the results of the three-dimensional calculations of the slope stability:

- The values obtained for the slope coefficient by the 3D model are higher than those obtained in solving the planar task.

- When there is a transition from 2D modelling to 3D, it is necessary to take into account the following aspects:

1) The concept of describing the shape of the probable sliding surface is changed. In the 3D model, it is in the form of a segment of an elliptical surface. The circular-cylindrical sliding surface in the volume model can not be its analogue.

2) The forces at the boundary of the lamellae are distributed not in one but in two directions in the 3D modelling of slope stability and boundary equilibrium methods.

3) Three-dimensional methods of analysis are numerically less resistant than two-dimensional calculations.

Regardless of the limitations, it should be noted that in the near future, the implementation of the three-dimensional

models in the quantitative assessment of slope stability will be applied in the Bulgarian specialised software products, too, and the methods for three-dimensional calculations will be introduced and updated in the normative documents.

References

Anagnosti, P. Proceedings of the 7th International Conference on Soil Mechanics and Foundation Engineering // Three dimensional stability of fill dams. Mexico. 1969. - 275-280.

Chen, R. H., Chameau, J. L., Three-dimensional limit equilibrium analysis of slopes, In: Geotechnique, Vol. 32, No. 1, 1983. - 31-40.

Duncan J. M., "State of the Art: Limit Equilibrium and Finite Element Analysis of Slopes". Journal of Geotechnical Engineering, Vol. 122, No. 7, 1996. pp. 577-596.

Fomenko, I. K., Zerkal, O. V., Proceedings of the Technical Meeting TC207 - Workshop on Soil Structure Interaction and Retainig Walls // Three-dimensional slope stability analysis. Dubrovnic, 2011. - 125-129.

Hovland, H. J. Three-dimensional slope stability analysis method, In: Journal of the Geotechnical Engineering Division. ASCE, Vol. 103, No. 9, 1977. - 971-986.

Hungr, O. An extension of Bishop's Simplified Method of slope stability analysis to three dimensions, In: Geotechnique. London, Vol. 37, No. 1, 1987. - 113-117.

https://www.itascacg.com/software/flac3d

OPTIMISATION OF SAMPLING OF COAL FROM THE OBEDINEN OPEN CAST MINE AND THE REPUBLIKA MINE

Daniel Georgiev

University of Mining and Geology "St. Ivan Rilski", 1700 Sofia, daniel__georgiev@abv.bg

ABSTRACT. The article discusses in detail the processes that the coal undergoes after it enters the *Pernik* Preparation Plant. Special attention is paid to one of the main problems in the quality management of the coal from the *Obedinen* open cast mine and the *Republika* mine, namely the sampling of coal. Two modern sampling methods are presented, with instruments that provide the necessary information about the quality of the coal in real time, taking into account the problems of the *Pernik* Preparation Plant.

Keywords: open cast mining, quality management, coal

ОПТИМИЗИРАНЕ НА ПРОБОВЗЕМАНЕТО НА ВЪГЛИЩА ОТ ОТКРИТ РУДНИК ОБЕДИНЕН И РУДНИК РЕПУБЛИКА

Даниел Георгиев

Минно-геоложки университет „Св.Иван Рилски", 1700 София, daniel__georgiev@abv.bg

РЕЗЮМЕ. В статията подробно са разгледани процесите през които преминават въглищата след тяхното постъпване в Обогатителна фабрика "Перник" и по-специално внимание е обърнато на един от основните проблеми в управлението на качеството на въглищата от Открит Рудник Обединен и Рудник Република, а именно пробовземането на въглищата. Представени са два съвременни метода на пробовземане, с уреди, които дават необходимата информация за качеството на въглищата в реално време, съобразени с проблематиката на Обогатителна фабрика "Перник".

Ключови думи: открит добив, управление на качеството, въглища

Introduction

General information and technological processes in the *Obedinen* open cast mine and the *Republika* mine

The Pernik Coal Basin is located about 30 km southwest of Sofia, with the following approximate boundaries of the productive horizon: the Viskyar Mountain to the north; the Vitosha Mountain and the Lyulin Mountain to the southwest, to the east, and to the northeast; the village of Golo Bardo to the south; and the Chernogorski heights to the west.

Fig. 1. Location of the *Obedinen* and the *Republika* open pit mines

It includes two open pit mines: the *Republika* and the *Obedinen*. Their object of production is brown coal. They occupy an area of 5608 dka and cover terrains on the territory of the town of Pernik, the village of Divotino, the village of Lyulin, and the village of Golyamo Buchino.

The development system in the two open pit mines is a transport system with the removal of the waste rock by trucks. Segments use the cyclic-flow technology. Coal is loaded with excavators and transported to a reloading point. The maximum height of the benches in the mines is determined depending on the maximum height of rowing of the excavator and the conditions for drilling and blasting operations. The array is pre-crushed according to well-established drilling and blasting projects. The exploded waste rock is loaded onto trucks with excavators and transported to the internal embankments. The height of the benches is less than 15 m in order to improve the compaction of the array.

The annual program of the *Republika* and the *Obedinen* open pit mines is as follows:

- Coal = 1 078 000 t (with a Coal Volume = 1,82 t / m^3)
- Waste rock = 11 040 000 m^3

The mode of operation is continuous: two shifts of 12 hours. Work is suspended only on public (bank) holidays and due to annual repairs and planned repairs. Or:

365 days - the total number of days within a year;
less 7 days - the number of public (bank) holidays within a year;
less 18 days - planned repairs;
less 40 days - yearly repair is done for 40 days on average.

The development system is a transport system with the removal of the waste rock in the bulldozer embankments by trucks.

The coal-mining scheme is implemented as coal is transported with the help of trucks. For this purpose, reloading points have been constructed in the sections. Through bunkers in which coal is poured, they are transported along a conveyor belt that is connected to the main conveyor belt. Coal loading is done with hydraulic excavators.

Methods

Coal sampling and technological processes in the *Pernik* Preparation Plant

After elimination of the main processes at the *Pernik* Preparation Plant, the coal undergoes a process of sampling, charging, crushing, and sieving. The supply of coal for processing from the mines to the filling plant is carried out by railway transport.

After reaching the landfill by means of a folding ramp at the top of the wagons, the sampler enters the wagons and takes a sample, digging a hole at a depth of about 30 centimeters and then taking a sample of a few shovels large. Two samples are taken from each bunch from the wagons coming from the *Obedinen* open pit mine, a total of 6 samples from each wagon. One sample of each bundle is taken from the wagons coming from the *Republika* open pit mine, a total of 3 samples from each wagon, because the material there is relatively homogeneous. The sample results are obtained within 4 hours. Although the results have not been obtained yet, the coal is discharged into the receiving hoppers. Trains arriving from both pits can be unloaded simultaneously on two tracks: the wagons from the *Republika* open pit mine are unloaded on the sixth track, and the wagons from the *Obedinen* open pit mine are unloaded on the seventh track. The unbaked pieces are manually crushed on 400-250 mm grills. Once the material passes through the grate, it goes into a pick-up hopper. Under each track, there are eight receiving hoppers distributed in a column, but over them there can be precisely three wagons. Under each wagon, there are 2.67 bunkers making it impossible to accurately distribute the coal from the wagons to the bunkers. Each bunker has a volume of 90 tons. By means of four finers with a capacity of 300 tonnes/hour, coal is fed to two conveyors belts with a total output of 600 tonnes/hour. The two conveyor belts are then assembled into one that weighs the coal from the *Republika* open pit mine and from the *Obedinen* open pit mine and transports the material for screening. The sieve has a gradient of 15 degrees and 100 mm holes. The 200 mm offshore fraction is transported to another conveyor belt for further crushing in cone crushers where a 100 mm fraction is obtained. The cone crushers are two and below each there are five storage hoppers with a volume of 200 tons each, meaning that 1000 tons of coal can be stored under each tapering crusher. The submerged material of the size of 0-100 mm and the crushed material are combined onto one conveyor belt. This transports the material to a rotor crusher that crushes the material to a size of up to 30 mm, as is the requirement of the *Republika* thermal power plant.

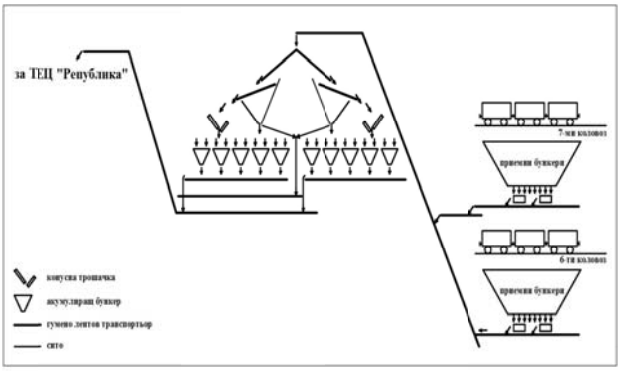

Fig. 2. Diagram of the processes in the *Pernik* Preparation Plant

After studying the ways of coal sampling and the mode of operation of the *Pernik* Preparation Plant, it was found that no more than 60÷62% of the coal supplied is suitable for energy fuel, which shows that the percentage of reduction of the useful component is about 35%.

Discusions

In view of what has been discussed in this article, the following could be proposed to improve the coal quality management and to increase the volume of coal used for energy use. This could be achieved after a change in the method of coal sampling.

1. After reaching the coal layers in both the *Obedinen* and the *Republika* open pit mines, samples must be taken with the ENELEX GE3030 device. Then, the results are set in a mathematical model for quality management, and only then can we proceed to loading the coal. After solving the algorithm, the two open pit mines receive accurate information about how many tons of coal they should take and transport to the preparation plant.

The GE 3030 coal fast-analyser enables fast analysis of the non-combustible content and the calorific value of coal samples immediately on site or in the laboratory. Operational evaluation of coal quality can significantly raise processing efficiency and, consequently, keep running costs lower, too. Coal is one of the most important energy sources. The need of saving all kinds of energy is strongly emphasised nowadays and though coal mining and efficient processing, it becomes the first-degree interest. The need of immediate coal quality evaluation or evaluation in reasonably short time results from the requirements of combustion and mining process optimisation. The unit is intended for fast measurement of ash content and calorific value of coal samples. The unit is produced as a desktop unit. The whole measurement is performed with no user manipulation of samples in the radiation beam. After putting the sample into the measurement

container and closing the cover, the sample is moved to the measurement radiation beam. The measurement is performed automatically. After finishing the measurement, the sample is automatically moved out of the radiation beam for user manipulation. The complete information on the measurement process is displayed on the touchscreen user interface panel with possibility of data transfer to the supervisory system. System setup and calibration can also be performed using the user interface panel in a simple and user-friendly way. The measurement method evaluates the coal non-combustible content according to differences of attenuation of two gamma beams of different energy passing through the coal. While the changes in chemical composition in the ash content are low, there's a significant correlation between the ash content and the average proton number. The measurement beam passes through coal sample while the resulting radiation is evaluated by a detector with a control unit. Based on the retrieved attenuation values of radiation beams, the control unit can compute the ash content and the calorific values within no longer than 10 minutes.

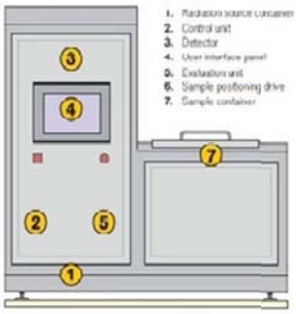

2. After the wagons arrive at the landfill, apart from the sampling that has already been performed to make a laboratory analysis of the coal, "The Ash Probe", produced by Bretby Gammatech, could also be employed. Again, the data from it is set in a mathematical model. On the basis of the decision taken, we can dispose of those wagons with which the decision of the algorithm for the average of the quality of the coal will be as accurate as possible.

The Ash Probe is a hand portable instrument for measuring the ash content of piles, wagons or trucks of coal. It provides the user with quick and accurate ash readings within seconds. It contains no radioactive sources. The Ash Probe consists of two parts: the Probe and the Display Unit. The ash measurement is obtained by inserting the probe into the coal and operating the Display Unit. The ash reading is displayed and its precision improves with measurement time. The desired precision is user selectable from four values ranging between 0.25% and 1% ash. The measurement times out once the required precision has been reached. In Pile Mode, the Ash Probe is used at several locations around the pile. Up to 99 readings per pile can be made. Both the individual readings and the pile average ash can be displayed, along with the standard error for the pile. Results from up to 99 piles can be displayed and stored. Calibration is readily achieved by the customer using the supplied sample gathering equipment. The Display Unit can store up to nine separate calibrations for different coal types. Stored data can be transferred to a PC for off-line data archiving and analysis.

Conclusion

The article discusses how coal was sampled at the *Pernik* Filling Plant which is served by the the *Obedinen* and the *Republika* open pit mines. The results of the study suggest that the use of the abovementioned coal sampling technique will improve the quality of coal management and the volume of coal that is suitable to be used for energy.

References

1. Passport for the operation of the *Pernik* plant.
2. http://www.enelex.cz/en/gamapopelomery-3030.htm
3. http://www.bretbygammatech.com/ash-probe.html

ANALYSIS OF THE ORE RECOVERY AND ORE DILUTION IN THE UNDERGROUND MINE FOR LEAD AND ZINC „SASA“ - M. KAMENICA

Stojance Mijalkovski[1], Zoran Despodov[2], Dejan Mirakovski[3], Vancho Adjiski[4], Nikolinka Doneva[5]

[1]University “Goce Delcev”, Faculty of Natural and Technical Sciences, 2000 Stip, stojance.mijalkovski@ugd.edu.mk
[2]University “Goce Delcev”, Faculty of Natural and Technical Sciences, 2000 Stip, zoran.despodov@ugd.edu.mk
[3]University “Goce Delcev”, Faculty of Natural and Technical Sciences, 2000 Stip, dejan.mirakovski@ugd.edu.mk
[4]University “Goce Delcev”, Faculty of Natural and Technical Sciences, 2000 Stip, vanco.adziski@ugd.edu.mk
[5]University “Goce Delcev”, Faculty of Natural and Technical Sciences, 2000 Stip, nikolinka.doneva@ugd.edu.mk

ABSTRACT. Ore recovery and ore dilution are very important parameters in all mining exploitation methods, butespecially in the sublevel caving mining method. In this exploitation method there is a functional dependence between the ore recovery and ore dilution, and for this reason it is very important to determine the optimal values for these parameters.
The paper presentsthe methodology for monitoring and analysis of the ore recovery and ore dilution in the underground mine for lead and zinc „SASA“ - M.Kamenica, by applying geodetic surveying measurements of the volume of excavated and unexcavated ore for each workplace.

Keywords: ore, recovery, dilution, sublevel caving, underground exploitation

АНАЛИЗ НА ИЗЗЕМВАНЕТО И ОБЕДНЯВАНЕТО НА РУДА В ПОДЗЕМЕН РУДНИК ЗА ОЛОВО И ЦИНК „САСА“ – М. КАМЕНИЦА

Стоянце Миялковски[1], Зоран Десподов[2], Деян Мираковски[3], Ванчо Аджийски[4], Николинка Донева[5]

[1]Университет “Гоце Делчев“, Факултет по естествени и технически науки, 2000 Щип, stojance.mijalkovski@ugd.edu.mk
[2]Университет “Гоце Делчев“, Факултет по естествени и технически науки, 2000 Щип, zoran.despodov@ugd.edu.mk
[3]Университет “Гоце Делчев“, Факултет по естествени и технически науки, 2000 Щип, dejan.mirakovski@ugd.edu.mk
[4]Университет “Гоце Делчев“, Факултет по естествени и технически науки, 2000 Щип, vanco.adziski@ugd.edu.mk
[5]Университет “Гоце Делчев“, Факултет по естествени и технически науки, 2000 Щип, nikolinka.doneva@ugd.edu.mk

РЕЗЮМЕ. Изземването и обедняването на руда са много важни параметри за всички минно-добивни методи, особено за системата на разработване с подетажно обрушаване. При този метод на разработване има функционална зависимост между изземването на рудата и нейното обедняване и поради тази причина е особено важно да се определят оптималните стойности на тези параметри.
В настоящия доклад е представена методология за мониторинг и анализ на изземването и обедняването на руда в подземен рудник за олово и цинк „САСА“ – М. Каменица чрез прилагането на геодезични маркшайдерски измервания на обемите иззета и неиззета руда за всяко работно място.

Ключови думи: руда, изземване, обедняване, подетажно обрушаване, подземен добив

Introduction

The sublevel caving mining method is applied in the underground mine for lead and zinc „SASA“ (Гоцевски и Мијалковски, 2008). In this exploitation method, the coefficients of ore recovery and ore dilution are in mutual functional dependence, that is, by increasing the ore recovery the ore dilution is also increased and vice versa. For this reason, it is necessary to calculate the optimal values for ore recovery and ore dilution (Mijalkovski et al., 2017; Mijalkovski, 2015).

When calculating the coefficient for recovery of geological reserves from the ore deposit, the ratio of the unexcavated ore and ore masses contained in the geological ore reserves is of high importance (Мијалковски, 2013). Classical methods (measuring surfaces with plan-meters, calculating volumes by approximating curved surfaces with a set of regular geometric bodies, etc.) to determine these masses were used in the past, which were not sufficiently accurate and therefore certain errors occurred, which indirectly affected the accuracy of calculating the coefficient for ore recovery. As a drawback, we can add the engagement of a large number of consultants and the increased number of working hours for performing this kind of analysis.

Due to the above-mentioned negative factors, today, computer graphics are used for faster and more accurate calculation of the excavated surfaces and volumes. This method is very favorable for 3D visual representation of ore bodies and mining objects, where the spatial distribution of all objects in the mine can be perceived (Mijalkovski et al., 2013). For this purpose, the software packages "Promine" and "Vulcan" were introduced in the underground mine „SASA“ (Mijalkovski et al., 2016).

Ore recovery and ore dilution in sublevel caving mining method

The sublevel caving mining method is characterized by a mutual connection between ore recovery and ore dilution, which in this case is such that by increasing the values of one parameter there is an increase in the values of the other parameter. In underground mining deposits with low thickness, ore recovery can be caused by the inability to monitor the contour of the deposit, which may be result in ore losses. When analysing the exploitation of ore deposits with big thickness, ore recovery and ore dilution arise primarily in the process of leached or caved ore (Mijalkovski et al., 2015).

In the leaching process of the mined ore, first the clean ore is leached, and then there is interference with the fragmented waste rock, which is in contact with the belt of the crushed ore. If an ore leak is stopped early, the ore dilution will be less, but the ore losses will be bigger. In order to have bigger ore recovery and at the same time reducing the ore losses, the leak continues, and as consequence of this the ore dilution is increasing according to the exponential dependence. This is the essence of the previously stated functional dependence of the ore recovery and ore dilution (Mijalkovski, 2015), where our goal is to obtain a high ore recovery for the purpose of small ore dilution.

These changes are particularly pronounced in the sublevel caving mining method with face loading. In the magnitude of the ore dilution the thickness of the blasting belt and its height have the biggest influence, also certain influence has the method of ore loading, i.e. the depth of engagement with the loading basket along the slope of the ore in the production drifts (Milicevic, 2008).

Ore dilution also occurs during exploitation. From this point of view, there are two types of ore dilution, planned and unplanned, shown schematically in Fig. 1 (Soyer, 2006; Stewart, 2012).

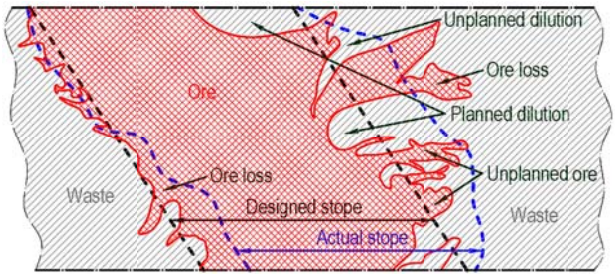

Fig. 1. Planned and unplanned dilution

Ore recovery is largely dependent on the human factor, that is, on the person managing the mining operations, but with disciplined work this influence can be reduced to a minimum.

Ore recovery (losses) of the reserves has an impact on the mine's exploitation period, and therefore on the size of the total revenue. While ore dilution, which is in direct functional dependence with ore recovery, has the greatest influence on the value of one ton of produced ore, that is, the value of a ton of produced concentrate, and thus on the size of the total revenues. Also, ore dilution has big impact both on the size of production costs and on the value of flotation utilization of metals in the technological processing (Mijalkovski, 2015).

Optimization of ore recovery and ore dilution in sublevel caving mining method

Taking into account the above-mentioned arguments, there is a necessity to determine the optimal values for the coefficients of ore recovery and ore dilution.

In order to optimize ore recovery and ore dilution when applying a sublevel caving mining method, the following steps have to be defined (Mijalkovski et al., 2017; Mijalkovski, 2015):

- Defining the geological parameters of the ore deposit (ore reserves, metal content, boundary content of metals);
- Defining the technological parameters for exploitation of the ore deposit (optimal annual production capacity, age of exploitation, content of metals in the ore, ore recovery during excavation, ore dilution during excavation, flotation utilization, metallurgical utilization of metals);
- Calculation of economic parameters (costs, revenues, net present value-NPV, internal rate of return of capital-IRR).

The last step is the decision making, whereby, by maximizing the net present value, the optimum values of the coefficient for ore recovery are reached (Mijalkovski et al., 2017; Mijalkovski, 2015). Net present value is obtained as the difference between total revenues and total cost of ore production.

Scientific research (Mijalkovski, 2015) has been carried out in order to calculate the optimal values for the coefficient of ore recovery and ore dilution for the sublevel caving mining method (Mijalkovski et al., 2017), applied for the conditions in mine „SASA“. On the basis of experimental tests of similarity models, the functional dependence between the coefficient of ore recovery and ore dilution was determined and also the optimization area for these two technical-economic parameters of the excavation (Fig. 2). The values for the coefficient of ore recovery are ranged from 70% to 90%, while the values of the coefficient of ore dilution are ranged from 10% to 30%. The optimization results showed that the optimal value for the coefficient of ore recovery for the conditions in mine „SASA“ is ir=80%, and for the coefficient of ore dilution is Or=20% (Mijalkovski, 2015).

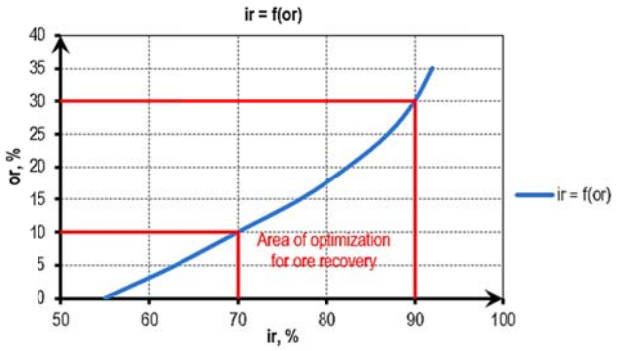

Fig. 2. Functional dependence between the coefficient of ore recovery and ore dilution with a display area of optimization

Monitoring of ore recovery and ore dilution in workplace areas in the mine „SASA"

Monitoring and calculation of the ore recovery and ore dilution are carried out by applying geodetic surveying

measurements for the volume of excavated and unexcavated ore for each workplace (Mijalkovski et al., 2013; Mijalkovski et al., 2016; Mijalkovski et al., 2015). After calculating the coefficient of ore recovery and ore dilution for each workplace individually, the next step is to calculate the average coefficient for ore recovery and ore dilution for each ore block and then for each horizon. At the end, the average coefficient for ore recovery and ore dilution for each month and for a whole year is calculated (Mijalkovski et al., 2015; Mijalkovski, 2015).

Measurement of the volume of excavated and unexcavated ore for each workplace is done with modern geodetic instruments which in themselves are mini computers and with their speed, accuracy and output data allow acceleration of many steps leading to the final product of the whole procedure, i.e. maps and plans (Mijalkovski et al., 2013; Mijalkovski et al., 2016).

The „SASA“ mine has the Total Station Leica Flex Line TS02/TS06/TS09/, which fully meets all the needs of the geometer when performing geodetic measurements in the pit. The advantage of this geodetic tool is that it does not need any trigonometric form template for recording the measured values (angles, lengths), because they store, process and output coordinates and elevation for all measured points. Furthermore, the measured data is very quickly and simply transferred to a computer and processed through the drawing program AutoCAD (Mijalkovski et al., 2016).

With the electronic mapping of mine maps, i.e. plans, high accuracy and precision is achieved, which in the past was complicated due to the size, type of paper, the way of storing the maps, the geodetic drawing tool, etc.

The maps and plans in the mining industry are of varying content, because the situation of the performed works is changed daily, and especially in the excavation zone, so that they have to be constantly updated, which is actually done in the „SASA" mine.

If safety conditions permit, after excavation of a certain production drift, a final measurement needs to be made for the safe production of some future mining facilities near the excavated part. In this way, the amount of excavated ore from the production drift is calculated and is compared with the value of the geologically projected quantity of ore, which calculates the ore recovery and ore dilution at that certain production drift (Mijalkovski et al., 2015; Mijalkovski, 2015).

The three geological profiles shown on Fig. 3 and in Fig. 4 display a plan for the given location between these three geological profiles. On the situation plan, as well as on the geological profiles, the forecast geological contours for the ore zone and the results of the geodetic survey of the mining workplace area are given, i.e., graphically we have the geological data before and after the excavation of that part in the ore zone.

Geodetic surveying of mining operations is carried out during excavation and in this way the monitoring of ore recovery and ore dilution is constantly done. According to the mining project, when ore dilution has increased above the planned, then the excavation of that part is stopped.

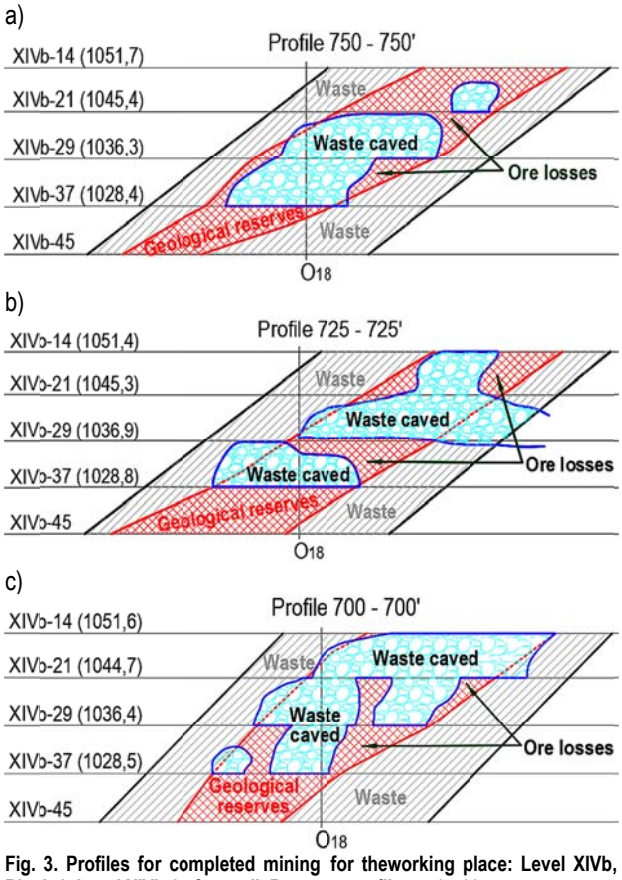

Fig. 3. Profiles for completed mining for theworking place: Level XIVb, Block 1, Level XIVb-37 footwall, Between profiles 750-700

When the excavation is completed at one workplace, then a final surveying is performed for that area, i.e., the final recording for the completed mining operations. From Fig. 3 and Fig. 4 (geological profiles and plan), the surface can be calculated, i.e. the volume of the excavated parts, as well as the parts where the ore is not excavated due to certain technical reasons (leaving the protective pillars, etc.) By comparing the quantities of geological reserves and quantities of excavated ore, the ore losses are calculated and compared with the planned losses according to the mining project. It is possible to calculate how much ore has been excavated without ore dilution and with ore dilution, i.e. with waste rock. In this way, the total ore dilution at the considered workplace can be calculated and then it can be compared with the planned ore dilution according to the mining project. In this way, it can be verified if there is a growth in geological ore reserves and its value, i.e. whether some unconfirmed geological reserves are involved (Mijalkovski et al., 2015; Mijalkovski, 2015). Then a report for each workplace is prepared and the values for the excavated parameters for each workplace are entered in a common table (Table 1), to make a record for the entire ore block or horizon.

Analysis of ore recovery and ore dilution for a specific workplace

An example for calculating the coefficient of ore recovery and ore dilution (Миланов, 2018) for the following workplace locations in the„SASA” mine is presented further on:

- Level XIVb;
- Mining Block 1;

Table 1.
Data for excavation parameters of some workplaces on level XV, mining block 3 in the "Sasa" mine

Workplace	Profile	Read geological reserves, (Q_{geol}) t	Total excavated ore without dilution, (Q_1) t	Total excavated ore with dilution, (Q_2) t	Total excavated rock waste, (Q_j) t	Dilution, (o_r) %	Ore in safety pillars, (Q_{zs}) t	Total excavate run of mine ore, (Q_v) t	Increment of geological reserves, (Q_{pr}) t
XV B3-0 f	1550-1500	10.2	9	9.4	0.4	4.3	1.8	10.8	0.6
XV B3-0 f	1500-1450	9.2	9.8	10.2	0.4	3.9	2.3	12.1	2.9
XV B3-0 f	1450-1400	13.3	8.6	10.4	1.8	17.3	5.2	13.8	0.5
XV B3-0 f	1400-1350	19.4	9.4	13.7	2.3	16.8	2.6	12	0
XV B3-0 f	1350-1300	12	10.7	13	2.3	17.7	2.6	13.3	1.3
XV B3+7 f	1550-1500	6.4	9.8	10.7	0.9	8.4	0.4	10.2	3.8
XV B3+7 f	1500-1450	12.1	16	16.9	0.9	5.3	3.6	19.6	7.5
XV B3+7 f	1450-1400	14.5	15.5	17.1	1.6	9.4	1.7	17.2	2.7
XV B3+7 f	1400-1350	18.1	15.8	17	1.2	7.1	2.7	18.5	0.6
XV B3+7 f	1350-1275	30.9	23	25	2	8	4	27	0
XV B3+7 f	1275-1225	10.5	8.3	9.3	1	10.8	2	10.3	0
XV B3-7 f	1550-1500	14.9	12.6	14.8	2.2	14.9	2.2	14.8	0
XV B3-7 f	1500-1450	26.8	21.2	23.2	2	8.6	5.6	26.8	0
XV B3-7 f	1450-1400	25.3	21.2	23.1	1.9	8.2	3.9	25.1	0
XV B3-7 f	1400-1350	19.5	17.6	19.7	2.1	10.7	2.3	19.9	0.4
XV B3-7 f	1350-1300		16.6	16.6		0		16.6	16.6
XV B3-7 f	1300-1250	7.8	5.1	5.6	0.5	8.9	2.7	7.8	0
XV B3-14 f	1525-1450	20.2	14	15.2	1.2	7.9	6.2	20.2	0
XV B3-14 f	1450-1400	21.8	18.2	19.9	1.7	8.5	3.8	22	0.2

- Sublevel XIVb – 37 (footwall ore body – north);
- Horizontal distance: L=50 m (from geological profile 700 to geological profile 750);
- Vertical distance: h = 8 m (from sublevel -37 to sublevel -29);
- Thickness of ore zone: variable (from 10 m to 20 m).

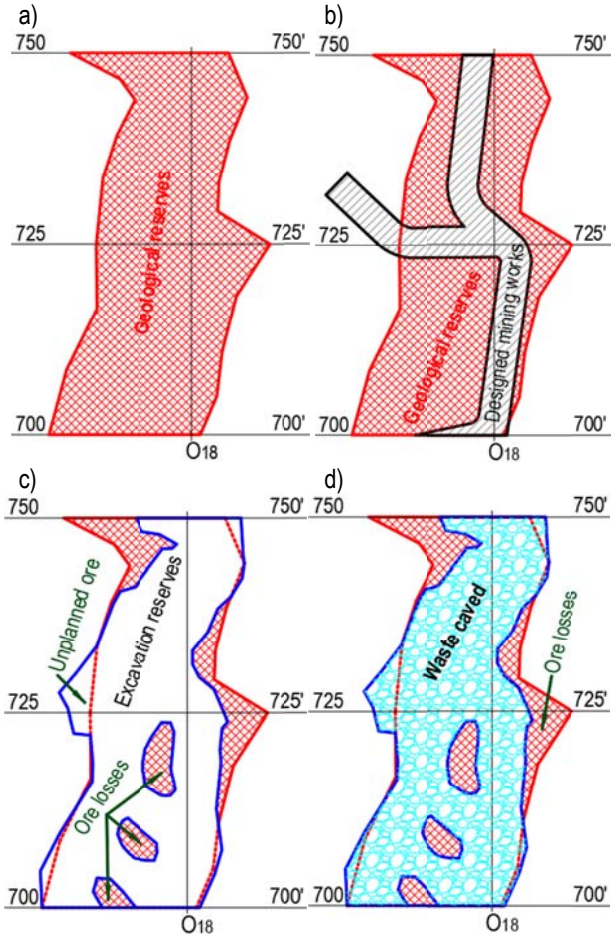

Fig. 4. Situation of the working place: Level XIVb, Block 1, Level XIVb-37 footwall, Between profiles 750-700, with excavation layout

On the basis of the geological data and the results of the geodetic surveying measurements of the mining works (Fig. 4 - *a*), it was stated that in the beginning, before , the preparatory mining works and the excavation of the ore, real geological reserves for excavation have been read for $Q_{geol.}$=18,9 t.

After the mining works, i.e. the excavation of the ore (Fig. 4 - *b* and *c*), the situation was as follows:

- quantity of excavated ore reserves without ore dilution Q_1=13,3t (from which 1,0 t is unconfined ore);
- quantity of excavated ore reserves with ore dilution Q_2=16,6t (from which 3,3 t is waste rock).

On the basis of the predetermined quantities of excavated ore reserves, the coefficient of ore dilution can be calculated (Mijalkovski et al., 2015), as follows:

$$o_r = \frac{Q_2 - Q_1}{Q_2} \cdot 100 = \frac{16{,}6 - 13{,}3}{16{,}6} \cdot 100 = 19{,}87\ \%$$

The planned average coefficient of ore dilution according to the mining project, which is actually the optimal coefficient, is: $o_{r,rp.} = 20\ \%$.

On the basis of volumetric measurements, the quantities of the remaining ore in the temporary protective pillars are determined (Fig. 4 - *c* and *d*) and their amount is Q_{zs} = 2,9 t. Knowing the geological reserves and the ore losses in the pillars, we can calculate the coefficient of ore losses:

$$z_{zs} = \frac{Q_{zs}}{Q_{geol.}} \cdot 100 = \frac{2{,}9}{18{,}9} \cdot 100 = 15{,}3\ \%$$

The planned average coefficient of ore losses according to the mining project, which is in fact the optimal coefficient, is: $z_{zs,rp.} = 20\ \%$.

The coefficient of ore recovery at excavation is:

$$i_r = 1 - z_{zs} = 1 - 0{,}153 = 0{,}847\ or\ 84{,}7\%$$

The total quantity of unexcavated ore and ore remaining in the protection pillars for this workplace is:

$$Q_{vk} = Q_1 + Q_{zs} = 16{,}6 + 2{,}9 = 19{,}5\ t$$

Now the ratio of total excavated ore with the ore in the geological reserves for this workplace can be calculated, expressed in percentages:

$$\frac{Q_{vk}}{Q_{geol.}} \cdot 100 = \frac{19{,}5}{18{,}9} \cdot 100 = 103{,}1\ \%$$

The explanation for the high ratio of the excavated ore for this workplace is proved by the following arguments:

- increment of geological reserves:

$$Q_{pr} = Q_{vk} - Q_{geol.} = 19{,}5 - 18{,}9 = 0{,}6\ t \text{ or } 3{,}1\ \%,$$

- unconfirmed geological reserves: 0 t or 0%,
- unexcavated ore for technical reasons: 0 t or 0%,

which can be seen from Fig. 3 and Fig. 4.

Conclusion

In the sublevel and block caving mining method the increasing of ore losses causes a reduction in ore recovery and ore dilution. Calculation of the parameters that have an impact on the ore recovery and ore dilution, can be carried out practically or through laboratory analyses.

In mining practice, the coefficients of ore recovery and ore dilution can be calculated with satisfactory accuracy using the already existing mathematical formulations with previously made detailed geodetic surveying measurements of the volume for excavated and unexcavated ore for each workplace.

The occurrence of losses or the utilization of the ore lead to significant economic consequences, which can be expressed in terms of value indicators. It must be kept in mind that the ore losses cannot be entirely avoided in practice, and therefore, as the main task, the question arises as how to minimize, i.e., how to achieve greater ore recovery, having in mind the fact that ore wealth is a non-renewable natural resource.

The „SASA“ mine constantly monitors the coefficients of ore recovery and ore dilution to provide optimum values for them, obtained on the basis of scientific research backed up by practical experiences.

References

Гоцевски В., Мијалковски С. Избор на оптимални вредности за искористување и осиромашување на рудата при подетажна метода со зарушување на кровината во ревир "Свиња река"-рудник "Саса", М. Каменица, Технологија на подземна експлоатација на минерални суровини, СРГИМ, Македонска Каменица, 2008. -158-171. (Gocevski V., Mijalkovski S. Izbor na optimalni vrednosti za iskoristuvanje i osiromasuvanje na rudata pri podetazna metoda so zarusuvanje na krovinata vo revir "Svinja reka" – rudnik "Sasa", M. Kamenica, Tehnologija na podzemna eksploatacija na mineralni surovini, SRGIM, Makedonska Kamenica, 2008. -158-171.)

Мијалковски С. Најважни показатели кои имаат влијание врз искористувањето (загубите) и осиромашувањето на рудата кај методата со подетажно зарушување, Македонско рударство и геологија, број 23, ЗРГИМ, Скопје, 2013. -30-33. (Mijalkovski S. Najvazni pokazateli koi imaat vlijanie vrz iskoristuvanjeto (zagubite) i osiromasuvanjeto na rudata kaj metodata so podetazno zarusuvanje, Makedonsko rudarstvo i geologija, broj 23, str.30-33, ZRGIM, Skopje, 2013. -30-33.)

Миланов С. Анализа на искористувањето / загубите на рудата во рудниците за олово и цинк "Саса"-М. Каменица, Дипломска работа (непубликувана), Факултет за природни и технички науки, Штип, 2018. - 32 с. (Milanov S. Analiza na iskoristuvanjeto / zagubite na rudata vo rudnicite za olovo i cink "Sasa" – M. Kamenica, Diplomska rabota (nepublikuvana), Fakultet za prirodni i tehnicki nauki, Stip, 2018. - 32 s.)

Mijalkovski S., Despodov Z., Gorgievski C., Bogdanovski G., Mirakovski G., Hadzi-Nikolova M., Doneva N., Modern geodesy approach in underground mining, Natural resources and technology Volume VII, No 7, University "Goce Delcev", Faculty of natural and technical sciences, Stip, 2013. -15-20.

Mijalkovski S., Despodov Z., Doneva N., Adjiski V., Modern trends of geodetic measurements in the underground mine "SASA" of lead and zinc ore, Mining and metallurgy engineering Bor, Nomber 1, Mining and Metallurgy Institute Bor, 2016. -89-94.

Mijalkovski S., Despodov Z., Mirakovski D., Adjiski V., Doneva N., Methodology for optimization of coefficient for ore recovery in sublevel caving mining method, Undergorund mining engineering, Year 23, Nomber 30, University of Belgrade – Faculty of Mining and Geology, Belgrade, 2017. -19-27.

Mijalkovski S., Despodov Z., Mirakovski D., Hadži-Nikolova M., Mitić S., Determination and monitoring of ore recovery and dilution coefficients in SASA lead and zinc mine - M. Kamenica, R. Macedonia, Underground mining engineering, Year 23, Nomber 26, University of Belgrade – Faculty of Mining and Geology, Belgrade, 2015. -1-9.

Mijalkovski S. Optimizing of the recovery of ore reserves for underground mining of metal ore deposits, Doctoral dissertation (unpublished), Faculty of natural and technical sciences, Stip, 2015. - 152 p.

Milicevic Z. Metode podetažnog i blokovskog zarušavanja, Tehnički fakultet u Boru, 2008. - 459 s.

Soyer N. An approach on dilution and ore recovery / loss calculations in mineral reserve estimations at the "Cayeli" mine, Turkey, School of natural and applied sciences of middle east technical University, 2006. - 102 p.

Stewart R. An introduction to underground mining, On the rocks, Dundee capital markets, Canada, 2012. - 30 p.

GROUNDWATER IMPACT INVESTIGATION DUE TO INSTALLATION OF A "LWS" SILICATE GEL SEALING SOLE IN THE WATER SATURATED SOIL ZONE

Tondera, D.[1], Beier, D.[2], Tamaskovics, N.[1], Pavlov, P.[3], Totev, L.[3]

[1] TU Bergakademie Freiberg (Freiberg University of Mining and Technology), D-09599 Freiberg, tondera@tu-freiberg.de
[2] BAUER Spezialtiefbau GmbH, Bauer-Straße 1, D-86529 Schrobenhausen, dirk.beier@bauer.de
[3] University of Mining and Geology "St. Ivan Rilski", 1700 Sofia, pavel.pavlov@abv.bg

ABSTRACT. The present study investigates the effects of the newly developed "BAUER LWS" silicate gel on the water-saturated soil zone on a test site in Berlin, Germany. For this purpose, a project comprising the grouting of a sealing sole of a construction trench has been accompanied by a groundwater sampling and analysis program. Four groundwater observation wells were sampled and analyzed at fixed time intervals over a period of 18 months to monitor changes in groundwater conditions due to the soft gel injection. For comparison with original conditions, a zero measurement has been performed at the beginning of the investigation programme in accordance with the groundwater regulatory framework in order to determine the groundwater chemistry affected by the grouting activities. It has been found, that some of the analyzed parameters showed no response to the gel injection. These parameters were not considered further during the monitoring programme. Other parameters changed significantly during the grouting operations. However, already after the completion of the grouting, all parameters dropped back to their original values. The pH-value of the tested silicate gel was adjusted to an acceptable level of less than 10 in permanent contact with groundwater in order to prevent mobilization processes into the subsoil. The investigation results show, that the injection of silicate gel "BAUER LWS" involves lower substance mobilization than other well established grout material. Therefore, the "BAUER LWS" silicate gel can be applied as environmentally friendly and beneficial grout material in construction projects without expecting large-scale impact on the groundwater replacing alternative substances, such as chemical grouts.

Keywords: Grouting, Silicate gel, Sealing sole layer, Water saturated soil, Groundwater, Chemical impact

ИЗСЛЕДВАНЕ НА ВЪЗДЕЙСТВИЕТО ВЪРХУ ПОДЗЕМНИТЕ ВОДИ СЛЕД ИНСТАЛИРАНЕТО НА УПЛЪТНЯВАЩА ОСНОВА "LWS" СЪС СИЛИКАТЕН ГЕЛ ВЪВ ВОДОНАСИТЕНА ПОЧВА

Тондера, Д.[1], Байер, Д.[2], Тамашкович, Н.[1], Павлов, П.[3], Тотев, Л.[3]

[1] Технически университет Минна академия Фрайберг, Д-09599 Фрайберг, tondera@tu-freiberg.de
[2] BAUER Spezialtiefbau GmbH, ул. Бауер 1, Д-86529 Шробенхаузен, dirk.beier@bauer.de
[3] Минно-геоложки университет „Св.Иван Рилски", 1700 София, pavel.pavlov@abv.bg

РЕЗЮМЕ: Настоящото изследване разглежда влиянието на новия силикатен гел "BAUER LWS" върху водонаситени почви в тестово поле в Берлин, Германия. За тази цел проектът включва тампониране на уплътняваща основа на строителна траншея, което е придружено от пробовземане на подземни води и програма за анализ. Взети са проби от четири сондажа за подземни води и са анализирани на фиксирани времеви интервали за период от 18 месеца, за да се наблюдават промени в състоянието на подземните води поради инжектирането на мекия гел. За сравнение с оригиналните условия е направено нулево измерване в началото на изследователската програма в съответствие с регулаторната рамка за подземните води, за да се определи химията на подземните води, повлияна от тампониращите дейности. Установено е, че някои от анализираните параметри не реагират на инжектирането на гела. Тези параметри не са разглеждани допълнително по време на мониторинга. Други параметри се променят значително по време на тампонирането. След приключване на тампонирането, обаче, всички параметри се връщат към първоначалните си стойности. Стойността на pH на тествания силикатен гел се коригира до приемливо ниво, по-малко от 10, в постоянен контакт с подземните води, за да се избегнат процесите на мобилизация в подпочвения слой. Резултатите от изследването показват, че инжектирането на силикатен гел "BAUER LWS" предполага по-ниска мобилизация на веществата, отколкото други добре установени тампониращи материали. Ето защо силикатният гел "BAUER LWS" може да се използва като екологичен и полезен тампониращ материал в строителните проекти, без да се очаква голямо въздействие върху подпочвените води, като се заменят алтернативните вещества, като например химическите тампониращи разтвори.

Ключови думи: Тампониране, силикатен гел, уплътняваща основа, водонаситени почви, подземни води, химическо въздействие

Introduction

In the mid-1990s, the Berlin Senate for Environment banned the construction of grouted sealing soles with aluminate-based soft gel base due to their alleged negative chemical influence on the groundwater. This ban has also been followed by other municipalities and their responsible authorities (especially Water Authorities).

In recent years, the composition of grouting materials has been significantly optimized towards a significantly better environmental compatibility.

Within the construction project "Ringcenter II" designed by Brauns et.al. (2001), the chemical influence of the grouting material on the groundwater has been investigated for the first time in detail (BRAUNS et al., 2001). At a construction site of Bauer Spezialtiefbau GmbH in Berlin, Germany, with grouting of a sealing sole in a construction trench, the influence of the grouting process and grouting material on the groundwater quality has been investigated in detail according to the current state of the art.

Investigation schedule

The present study examined the chemical impact on the groundwater resulting from the installation of a sealing sole in the water saturated soil zone using an "BAUER LWS" silicate gel grouting operation. (The letters “LWS” in the product name stand for the abbreviated initials in the names of its inventors and do not represent chemical components.)

In order to track the spreading of dissolved grout material components, four groundwater extraction wells with different horizontal distance to the silicate gel sealing sole layer have been installed at the project location, one extraction well located in the groundwater inflow and three other extraction wells located in the groundwater outflow area. The depth range of water extraction extended over a 2 meters long filter section installed both above and below the sealing sole layer.

Project description

The construction trench with an overall surface extension over an area of approximately 3000 m² has been created after installing a sheet pile wall along the outer contour line up to a depth of about 15 m to 16 m (see Fig.1 below).

After the removal of a 2m to 3m thick sediment layer mostly consisting of anthropogenic material fill, a working plane has been created and the grouting wells have been drilled. The grouting sealing sole has been created with an average thickness of one meter in a depth of 15 meters below the ground surface. After the groundwater lowering, a residual dewatering has been operated in the construction trench above the grouted sealing sole.

Subsequently, the excavated soil and the concrete floor slab of the building have been installed. After completion of the shell work in the construction trench (below the original groundwater level), the sheet pile wall has been pulled back, exposing the grouted sealing to the regenerating groundwater flow regime.

The groundwater and soil analyses took place over the entire construction period from May 2015 to July 2016. The groundwater extraction wells were positioned outside the construction trench in a depth of approximately 19m. The lower edge of the installed sheet pile walls reached a depth 0.5m below the grouted silicate gel sealing sole layer.

Fig.1. Construction trench during sheet pile wall installation

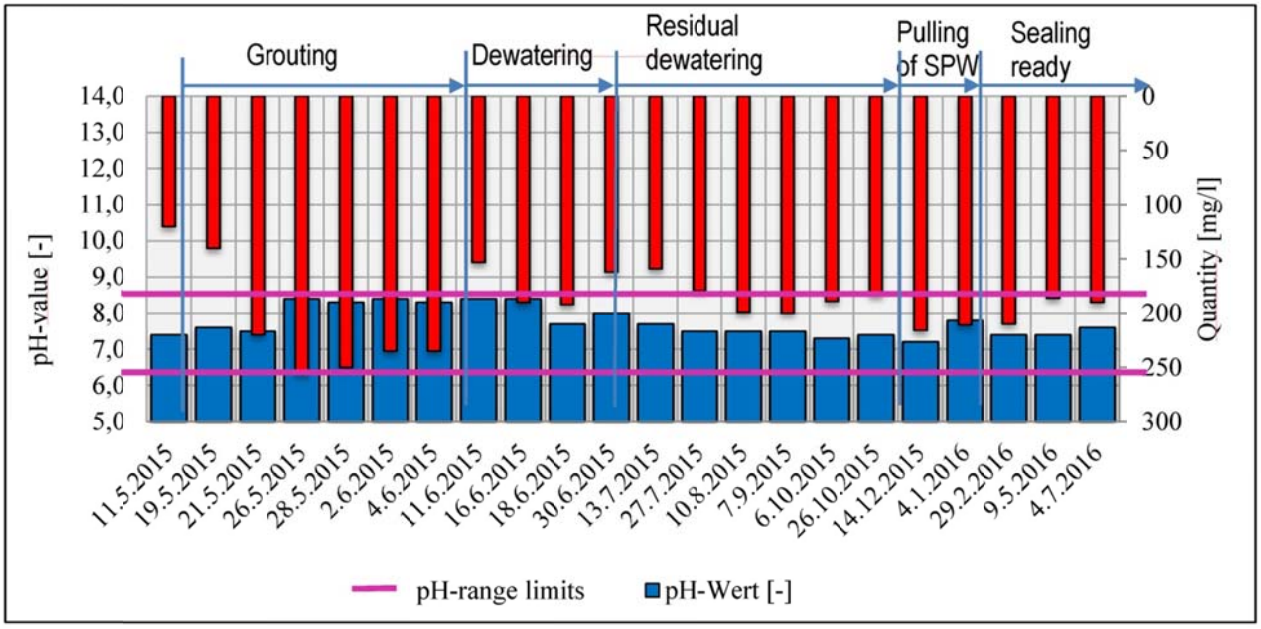

Fig.2. Analysis results at the first groundwater sampling well (GSW1) – ph-Wert=ph-value, Sulfat = Sulphate

Table 1.
Analysis result overview for the groundwater sampling wells GSW1 and GSW4

Parameter	Zero measurement	GSW1 (Grouting)	GSW1 (RDW²)	GSW4 (Grouting)	GSW4 (RDW²)	Eluate analysis E1 (14-16m)	Eluate analysis E2 (16-18m)
pH-value [-] (ALV¹: 6.5 – 8.5)	7.4	8.4	7.5	7.3	7.1	8.1	8.5
Filterable substances [mg/l] (ALV¹: 30 mg/l)	< 5 **- 110**	**5130**	22,8	11,0	8,0	--	--
Iron [mg/l] (ALV¹: 2,0 mg/l)	0,33 -4,2	25	1.7	**3.0**	**4.7**	0,18	0,065
Sulfate [mg/l] (ALV¹: 400 mg/l)	120 -240	256	200	367	**487**	6.9	2.1
Nitrate [mg/l] (ALV¹: 50 mg/l)	< 1- 2.7	< 1.0	< 1.0	< 1.0	< 1.0	< 1.0	< 1.0

ALV¹ – Admissible limit value; RDW² – Residual dewatering; GSW – Groundwater sampling well

Investigation programme

The effects of soft gel injection on groundwater quality have been observed over a time period of 18 months. In order to document the ground water conditions before the construction measures, a first zero measurement with an extensive analytical programme has been carried out on samples from four groundwater extraction points. A second zero measurement has been carried out after the installation of the sheet pile walls and immediately before the grouting operation has started.

The groundwater samples have been taken from four groundwater sampling wells accompanying the construction and grouting operations. During dewatering of the construction trench, the sampling period was extended to two weeks and during the residual dewatering to two months until the end of the observation in June 2016. In order to measure the chemical impact from the grouting material on the groundwater, the following analytical examination programme has been imposed:

- separable substances, filterable substances
- pH, electrical conductivity
- ammonium

- slightly soluble anions (sulphate, nitrate, chloride)
- metals (cations, iron, lead, chromium, nickel, etc.)
- cyanide, vinyl chloride
- volatile halogenated hydrocarbons (LHKW)
- polycyclic aromatic hydrocarbons (PAHs)
- aromatic hydrocarbons benzene, toluene, ethylbenzene, xylenes (BTEX)
- total organic carbon (TOC),
- dissolved organic carbon (DOC)

Depending on the results during the observation time, the analytical programme has been reduced to the relevant effects. The investigation programme has been adjusted to the construction operation in the trench and has been focussed on mobilization and transport processes in connection with the chemical influence on the groundwater from the grouting.

From the groundwater sampling wells GWS1 and GWS4, two liner soil samples (cores BK1 and BK4) have been extracted. After a sedimentological documentation, the grain size distribution and density have been measured in the laboratory. On two mixed samples from the liner BK1, an eluate test has been carried out in order to determine the potential hazard from leaching out the sand due to the grouting operation.

Investigation results

Soil analytics results

Below an approximately 2m to 3m thick local fill, a changing deposit of fine and coarse sands with obvious coal inclusions have been observed in the subsoil up to the investigation depth of 19m.

The heat loss examination of the soil samples has shown values of 0,2 to 2,6% in the sample BK1 and values of 0,2 to 2,3% in the sample BK4 and indicates the organic content that could be potentially mobilized due to the grouting measures.

For the determination of potential pollutants, samples have been taken from different depths in the liner sample cores. With the exception of the increased values for iron and sulphate, the results of the eluate analyses have generally shown a low pollutant content, so that the pollution of the groundwater triggered by the grouting operation measure could be expected to remain within tolerable limits.

Groundwater analytics results

The investigation results of the groundwater analyses can be readily demonstrated on the results in the inflow area at the groundwater sampling well GSW1 and in the outflow area at the groundwater sampling well GSW4 (see Tab.1).

The mobilization processes of substances influencing the groundwater are primarily triggered by a pH-value in the non-neutral range. The experimental results show, that the pH-value in the examined groundwater remained constant in a range of 6,5 to 8,5 and exceeded the higher limit of 8,5 in only one single measurement (see Fig.2). Although an elevated pH-value is inevitable in immediate contact with the grouted sealing sole, the investigations point out a strong dilution process due to the groundwater leaving very low potential for possible mobilizing processes around the sealing sole. During the grouting operation, the chemical impact on the groundwater could be kept very low with success.

After the start of grouting, a significant increase in iron and DOC (dissolved organic carbon) concentrations have been observed in the groundwater at the groundwater sampling well GSW1, reaching a maximum iron concentration value of 25.0 mg / l.

With completion of grouting and start of dewatering, the iron concentration in the groundwater has decreased, reaching values in the admissible range. An increase of the iron concentration above the tolerable limit has occurred during the removal of the sheet pile walls from the subsoil. At the end of the observation period, the measured iron concentration values have been in the legally admissible range. Significantly lower changes in iron concentration have been observed on other examined groundwater samples during the investigation period.

As a general result of the investigations on samples from all groundwater sampling wells can be derived that the observed parameters have shown an increased value immediately after the grouting operation, exceeding slightly the legally admissible limit values, returning to values of the zero measurements with increasing time after completion of grouting operations.

The analysis results from the groundwater sampling well GWS4 with larger distance to the grouted sealing sole have shown the slightest changes and due to limited mobilizing processes from the grouting operation. During the observation period, only the iron and sulphate concentrations have shown values exceeding the legally admissible limits. The content on filterable substances has also slightly exceeded tolerable limits, but only at the zero measurements before and thus, independently of the grouting operations.

The parameters of electrical conductivity, ammonium, nickel, cyanide, chloride, chromium, mercury, cadmium, copper, zinc, nitrate, ΣLHKW, vinyl chloride, ΣMKW, ΣBTEX and ΣPAH have always remained below the legally admissible limits of specific water authority regulations during the observation period. Some of the parameters have shown values below the limit of quantification and have been excluded from the investigation campaign.

Furthermore, from the analysis results at the groundwater sampling well GWS4 it could be obviously concluded, that spatial influence by the grouting operation on the groundwater was significantly low and the groundwater impact form grouting has apparently been restricted to the immediate vicinity of the silicate gel sealing sole. Due to dilution effects, obviously a water cleansing process must have taken place.

The analysis results from the last measurement series have shown a decreasing tendency reaching values corresponding to the natural initial groundwater chemistry over time.

Summary and Outlook

The present study has investigated the impact of a grouting operation with the newly developed "BAUER LWS" silicate gel on the water saturated soil zone at a construction trench in Berlin, Germany. During the investigation period, from the installation of the sheet pile walls until the exposition of the grouted sealing sole to the environment for a long period of time, the groundwater quality has been observed with systematic groundwater sampling and analytical measurements in order to detect changes and influences due to the grouting operation.

It has been observed, that the monitored analysis values have increased significantly during the grouting operations and returned to their initial zero measurement values after the grouting operations have been completed. It has also been found, that some of the observed analysis parameters have not been influenced by the installation of the grouted sealing sole.

The investigations have pointed out that the "BAUER LWS" silicate gel grouting material induces slighter mobilization processes than other comparable, known and practically utilized alternative grouting materials. The adjusted pH-value of the grouting material influences the groundwater and the grouted soil only over a limited time period and only in a limited extent. During contact between groundwater and "BAUER LWS" silicate gel, the pH-value of the groundwater has continuously remained in the upper neutral range.

The groundwater pH-value has been observed within a desired limit value range during the measurement campaign, restricting possible material transport and mobilizing processes to a minimum. The "BAUER LWS" silicate gel can be utilized in construction projects avoiding significant impact on the groundwater, where alternative chemical grouting materials are being planned to be used.

Conclusions

Despite fundamental improvements with the use of the new "BAUER LWS" silicate gel, there are still plenty of opportunities for further development. Since it has been observed that substances contained in the soil, especially during grouting, are dissolved and transferred into the groundwater, appropriate approaches are being examined in order to isolate and manage individual solution mechanisms by adjusting the gel properties in order to especially avoid the release of iron and sulphate. Due to the local variation of soil and groundwater conditions on different sites, the subsoil carries different reactive partners or even pollutant substances that could be dissolved and transported by the groundwater and a universal solution for the grout substance recipe appears to be difficult. Furthermore, other undesired side effects and drawbacks have to be excluded, also.

Finally it can be concluded, that with the "BAUER LWS" silicate gel, a well-designed, examined, tested and environmentally friendly grouting material is currently available for practical use.

References

Brauns, Josef; Eiswirth, Matthias; Hötzel, Heinz; Kast, Karl; Ohlenbusch, Renke; Schnell, Klaus (2001): Nachweis der Umweltverträglichkeit von Weichgelinjektionssohlen. Ernst & Sohn Verlag Bautechnik 78 (2001) Heft 7

Kempfert, Hans-Georg & Raithel, Marc (2015): Bodenmechanik und Grundbau, Geotechnik nach EUROCODE, Band 2: Grundbau. Bauwerk Verlag 4. Auflage

Kutzner, Christian (1991): Injektionen im Baugrund. Enke Verlag

Donel, Manfred (1990): Bodeninjektionstechnik. Verlag Glückauf GmbH

Schmidt, Hans-Henning (2006): Grundlagen der Geotechnik. Teubner Verlag 3. Auflage

Schnell, Wolfgang (1990): Verfahrenstechnik zur Sicherung von Baugruben. Teubner Verlag

DIN17892-04.2005. Baugrund, Untersuchung von Bodenproben – Bestimmung der Korngrößenverteilung

Geologische Skizze (2013):Analysebericht GuD vom 02.07.2015
http://www.stadtentwicklung.berlin.de/umwelt/umweltatlas/d117_02.htm#A3 abgerufen am 22.06.2016.

ON THE DETERMINATION OF THE OPTIMUM TIME OF MICROWAVE EXPOSURE TO PYRITE-CONTAINING ORE

Babich A.V.[1], Vinnikov V.A.[2]

[1] Ph.D. student at the FizGeo Department at the National University of Science and Technology MISiS, a.v.babich1992@yandex.ru
[2] Dr.Sc. (Phys.-Math.), Head of the FizGeo Department at the National University of Science and Technology MISiS, evgeny.vinnikov@gmail.com

ABSTRACT. The method of constructing an experimental dependence on temperature of the pyrite-containing ore samples during microwave exposure time is given. According to the results of the experiments, the stabilization temperature and the optimum microwave exposure time are determined. The character of the dependence of the stabilization temperature on the pyrite content in the samples is defined.

Keywords: pyrite-containing ore, microwave exposure, optimum microwave exposure time, stabilization temperature

ОПРЕДЕЛЯНЕ ОПТИМАЛНОТО ВРЕМЕ НА ЕЛЕКТРОМАГНИТНО ВЪЗДЕЙСТВИЕ ВЪРХУ ПИРИТСЪДЪРЖАЩИТЕ РУДИ

Бабич А.В.[1], Винников В.А.[2]

[1] докторант в катедра ФизГео на Минен институт НИТУ «МИСиС»; a.v.babich1992@yandex.ru
[2] д.ф.-м.н., завеждащ катедра ФизГео на Минен институт НИТУ «МИСиС»; evgeny.vinnikov@gmail.com

РЕЗЮМЕ. Описана е методика за построяване на експериментална зависимост на температурата на образец от пиритсъдържаща руда от времето на СВЧ въздействие. На основание на резултатите от експериментите е определена температурата на стабилизация и оптималното време на СВЧ въздействие. Установен е характерът на зависимостта на температурата на стабилизация от съдържанието на пирита в образците.

Ключови думи: пиритсъдържаща руда, СВЧ въздействие, оптимално време за облъчване, температура на стабилизация

Defining the task

It is well known that during the technological processes for mineral processing – crushing and grinding – a large quantity of hard to be ground ores and rocks is involved in order to extract the useful components. Since the ores of ferrous metals are, as a rule, of high strength, the use of traditional processing and grinding methods leads to a significant increase in energy costs, intensive wear on the metal parts of the mills, and considerable losses of extracted useful components due to the incomplete uncovering of the twins. Therefore, it is necessary to determine the methods for purposeful modification of the technological properties of the hard to be ground minerals, which increase the efficiency of their processing. Finding new approaches that take into account the heterogeneity of the rock types that make up the ore body and the reasons for the structural transformations of the ore minerals will make it possible to significantly reduce the energy intensity of the grinding process. Such studies have been carried out by well-known scholars – I.A.Birger, N.P.Vloh, Julij I. Zetser, M.G. Zilbershmidt, V.A.Kondrashov, J.M.Misnik, A.N. Moskalev, G.Y. Novik, A. D. Sashurin, R. M. Sultanalieva, K. Tazhibaev, M. Friedman and others.

One of the possible impacts on rock types with high hardness (strength), which increases the efficiency of their destruction, are the electrophysical fields. Their action is based on the absorption of the energy supplied to the rock and after its transformation, the rock is broken or there is a significant reduction of its hardness (strength). The electrophysical fields used can be classified into several groups: based on the use of direct current or industrial frequency current, high voltage electrical pulses, high and ultra-high frequency (UHF) electromagnetic field energy, infrared or optical effects.

From the point of view of impact on the physico-mechanical properties of the rocks and ores, the effect of the microwave exposure is quite perspective. The decrease in rock mass strength under such an impact is predetermined by the volumetric nature of the conversion of the radiated UHF energy into heat energy within the depth of waves' penetration as well as by the high heating temperature and the influence of the resulting thermal stresses which ensure the rate of the strength reduction, commensurate with the mechanical loading velocities [1,2].

Duration of the microwave exposure is one of the key points for determining the parameters of microwave exposure on minerals in hard rocks. Most of the scientists studying the effects of microwave exposure on rocks determined the temperature of the samples by using a calculation method based on their thermoformance and the experimental results for the relative (specific) volumetric intensity of the grinding depending on the optimum exposure time. Data show that this time ranges from 3 to 5 minutes [3]

This paper presents the results of the experimental studies of the heating temperature dependence of pyrite-containing

ores' samples on the microwave exposure time and the content of the metal-containing minerals.

Description of experimental studies

The following tools were used to perform the experimental tests:

• microwave oven «Electronics» (1300 Watt power, 2450 MHz frequency);

• DT-8868H high temperature pyrometer (temperature range from -50ºC to +1850ºC, 50: 1 optical resolution, ± 1.5% error, 0.1ºC resolution, double laser scope).

The tested specimen was placed in a microwave oven and subjected to repeated heating with a time step of 30 seconds. The temperature was fixed by the pyrometer at the time of completion of heating at an open door of the oven, whereby the pyrometer was mounted on a stand so that the spot of the beam was dropped into a fixed area of a stationary specimen containing pyrite grains. The tests were carried out by fixing the maximum of the measured temperature with an emission factor of 0.95. As a damper for protection from drilling the specimens with high content of pyrite, a 500 ml water cuvette was placed in all oven tests and the measurements were discontinued at the point when the water started to boil [4]. After the oven and the sample were completely cooled to room temperature (25° C), the measurements were repeated over a longer period of heating.

Figure 1 shows the installation with which the measurements were made. The results of the measurements are summarised in Table 1. 1 and shown in the graphs - Fig. 2.

The analysis of the temperature dependence of the sample on the microwave exposure time shows that with the general tendency to increase the temperature of the specimen with the increase of the microwave exposure time, at some of the intervals of impact there is a temporary temperature stabilization followed by a rise in temperature. The values of the stabilization temperature are shown in Table 2, and the microwave exposure time at which this stabilization occurs is in the range of 3 to 5 minutes, which coincides with the experimental data of other scientists who determined the optimal time for microwave exposure [3].

Fig. 1. Equipment for the experiments

Table 1.
Results from the experimental tests

Time for microwave exposure,s	Temperature of the sample, ºC			
	Sample № 3	Sample № 2	Sample № 6	Sample № 5
0	25	25	25	25
30	46.2	72.5	70.4	98.5
60	53.2	111	106.2	133.4
90	69.9	141.4	122.1	162.6
120	78	159.4	144.1	195.7
150	84.1	177.9	182.9	203.1
180	107.2	239	182.3	243.8
210	116.2	234	195.7	236.1
240	112.1	239	227.7	276.7
270	113.2	290.7	218.1	246.8
300	119.9	303.6	219.7	285.4
330	124.6	324.6	207.8	301

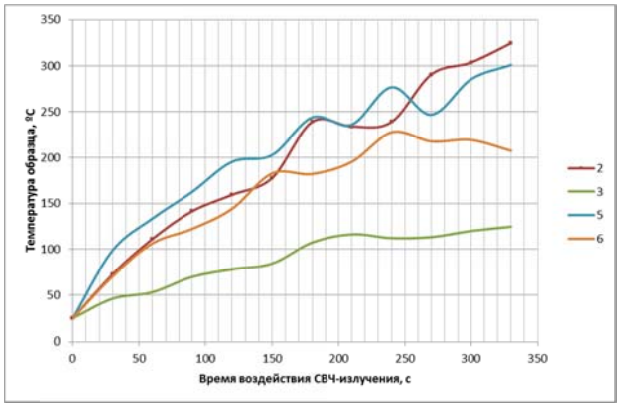

Fig. 2. Results from the experimental tests of samples of pyrite-containing ores №№ 2, 3, 5, 6

Since the specimens of the pyrite-containing ore contain different amounts of FeS2, it is necessary to determine the pyrite content in each specimen. Optical measurements were used for this purpose: in the microphotographs of the samples,

the percentage of pyrite in the samples was determined using a set of Microanalysis programmes to create special masks. The results of the measurements are shown in Fig. 3 and Table. 2 and the dependence of the stabilization temperature on the pyrite content in the sample is shown in Fig. 4.

Table 2

Dependence of stabilization temperature on pyrite content

№ of the sample	3	2	6	5
Pyrite content, %	0.8	2.8	16.7	52.9
Stabilization temperature, ºC	115	140	180	235

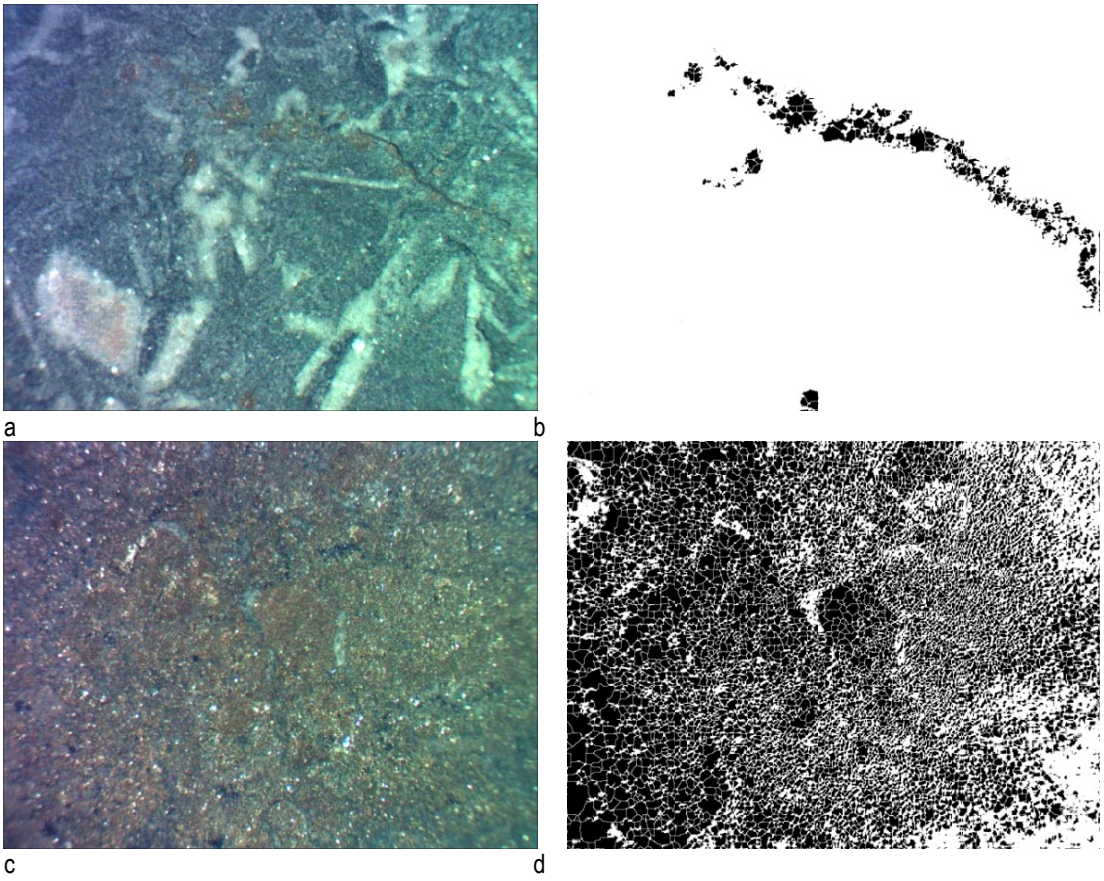

Fig. 3. Microsamples of specimens of pyrite-containing ore (a, c) and masks on pyrite (b, d) of samples of pyrite-containing ore No 2 (a, b) and No 5 (c, d)

Discussing the results

As a result of the tests, it has been found that in case of microwave exposure of pyrite-containing ores their heating temperature increases with the increase of the duration of exposure. Exposure time intervals (from 3 to 5 minutes) have been found in which the temperature stabilizes in the specimen (the time for microwave exposure increases, the temperature of the sample practically does not change). From the point of view of the energy intensity of the disintegration, these time intervals coincide with the optimal ones and with the time intervals for microwave exposure of samples of different rock types. The dependence of the stabilization temperature of the specimens on the pyrite content is similar to that of 0.5. The coincidence of the range of stabilization temperature with the optimum exposure time may allow the difficult tests for determining the energy intensity of rock disintegration in case of microwave exposure to be replaced with easier, but not less informative, results.

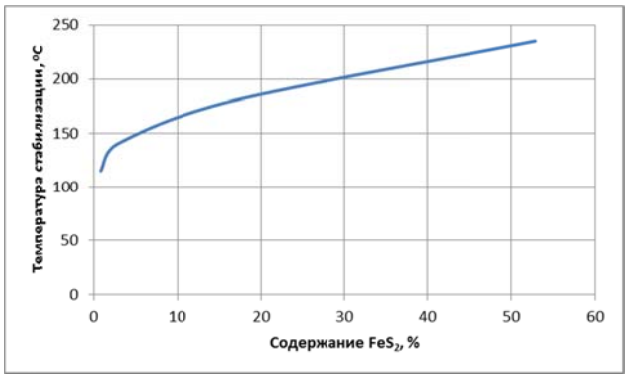

Fig. 4. Dependence of the stabilization temperature on the pyrite content of the sample

Bibliography

Максименко А.Г., Уваров А.П. Изследване на комбинираното СВЧ механично въздействие върху скалните породи // Общосъюзна VI научно-приложна конференция «Използване на СВЧ енергии в технологични процеси и научни изследвания». Саратов, 1991. – Стр. 71-73. Maksimenko A.G., Uvarov A.P. Izsledvane na kombiniranoto SVCh mehanichno vazdeystvie varhu skalnite porodi // Obshtosayuzna VI nauchno-prilozhna konferentsia «Izpolzvane na SVCh energii v tehnologichni protsesi i nauchni izsledvania». Saratov, 1991. – Str. 71-73

Петров В.М. Нови насоки в използване на радиоелектрониката: намаляване на якостта на скалните породи с помощта на мощно електромагнитно поле СВЧ // Информост «Радиоелектроника и Телекомуникации» - 22, 2002. – Стр. 63-72. Petrov V.M. Novi nasoki v izpolzvane na radioelektronikata: namalyavane na yakostta na skalnite porodi s pomoshtta na moshtno elektromagnitno pole SVCh // Informost «Radioelektronika i Telekomunikatsii» - 22, 2002. – Str. 63-72.

Султаналиева Р.М. Целенасочена промяна на механичните свойства на руди и минерали под въздействието на физичните полета // Дисертация за присъждане на научната степен докт. на техн. науки. – Бишкек, 2016. – Стр. 132. Sultanalieva R.M. Tselenasochena promyana na mehanichnite svoystva na rudi i minerali pod vazdeystvieto na fizichnite poleta // Disertatsia za prisazhdane na nauchnata stepen dokt. na tehn. nauki. – Bishkek, 2016. – Str. 132.

Martin Chaplin. Water and Microwaves / Water Structure and Science. Електронен ресурс: http://www1.lsbu.ac.uk/water/microwave_water.html

INFLUENCE OF THE ARRANGEMENT AND PERFORMANCE OF SHOVELS ON THE OPTIMUM POSITION FOR RUN-OF-MINE STOCK LOCATION

Valeriy Slobodyanyuk[1], Ivan Maksimov[1], Roman Slobodyanyuk[2]

[1] Ukraine, Krivoy Rog, "KNU" SIHE, slobod_v@i.ua
[2] France, Nancy, University of Lorraine; slobod.roman@gmail.com

ABSTRACT. The purpose of this paper is to develop a methodology to determine the coordinates of an optimum point for run-of-mine stock and influence of spacious arrangement of excavation faces on an optimum point of run-of-mine stock location. This article represents an overview of studies, where algorithms of the Fermat-Torricelli point are used in order to minimize the logistic processes. The methods of mathematical optimization and analytical geometry were applied in this work. It is proved that when the performance of one of the shovels is 1.7 times greater than the performance of the others, the Fermat-Torricelli point shifts to this shovel. The undertaken studies are aimed first at optimization of road and rail transport in the open pit mines. Considering an optimization of haulage for a group of three shovels, it is obvious that moving the rock mass from two shovels to the working area of the third one, which has the highest capacity we thereby determine an optimum position of the reloading point for the shovel. Since the depth of the open pit grows, the railway transport loses its efficiency mainly not because of the lesser gradient in comparison to the road transport, but because of the need to freeze a section of the pit wall in order to locate the reloading points for shovels. By eliminating the afore-mentioned shortcoming, it is possible to improve significantly the efficiency of haulage in the open pit mine. The article considers a new method of arranging and operating a reloading point for shovels.

Keywords: reloading station, Fermat-Torricelli point, minimum haulage

ВЛИЯНИЕТО НА РАЗПОЛОЖЕНИЕТО И ПРОИЗВОДИТЕЛНОСТТА НА ЕДНОКОФОВИТЕ БАГЕРИ ВЪРХУ ОПТИМАЛНОТО МЕСТОПОЛОЖЕНИЕ НА НЕОБРАБОТЕНАТА МИННА ПРОДУКЦИЯ ОТ ДНЕВНИЯ ДОБИВ

Валерий Слободянюк[1], Иван Максимов[1], Роман Слободянюк[2]
[1]Украйна, гр. Кривой Рог, ДВУЗ „КНУ"; slobod_v@i.ua
[2]Франция, гр. Нанси, Университет на Лотарингия; slobod.roman@gmail.com

РЕЗЮМЕ. Целта на настоящата разработка е да се разработи методология за определяне на координатите на оптималното местоположение на необработената минна продукция от дневния добив и влиянието на пространственото разположение на добивните забои върху оптималното местоположение на необработената минна продукция. В статията представен е прегледа на изследванията, в които за минимизиране на логистичните процеси се прилагат алгоритми с използване на точката на Торичели-Ферма. В работата се използват методите за математическа оптимизация и аналитична геометрия. Доказано е, че когато производителността на единия от еднокофовите багери е 1,7 пъти по-голяма от производителността на другите, точката на Ферма-Торичели се пренасочва към този багер. Извършените изследвания са насочени преди всичко към оптимизиране на автомобилния и железопътен транспорт в открити рудници. Като се има предвид оптимизирането на транспорта за група от три еднокофови багера, е очевидно, че чрез преместване на скалната маса от два багера в работния обхват на третия, който е с по-висока производителност, определяме оптималното положение на точката на претоварване на багера. С увеличаването на дълбочината на рудника, железопътният транспорт губи своята ефективност не поради по-малкия наклон в сравнение с автомобилния транспорт, а поради нуждата от замразяване на участък от рудничния борт, за да бъдат локализирани точки на претоварване на багерите. Преодолявайки гореспоменатите недостатъци, е възможно значително да се подобри ефективността на рудничния транспорт. В доклада се разглежда нов начин за разполагане и експлоатация на претоварните точки на багерите.

Ключови думи: точка за претоварване, точка на Торичели-Ферма, минимизиране на транспорта

Introduction

Background of the problem and its relation to practical issues

To minimize the transport work during open pit mine design, determination of the rational point of mining mass dumping is important. This task arises during the justification of the rational position of the reloading point of combined mine transport. The analysis of the design decisions on the combined transport usage shows that the position of reloading points often unfavorably affects the dynamics of mining operations (Яковлев, 1989; Вилкул и др., 2008; Vilkul et al., 2016; Белозеров, 2012; *Арсентьев*, 1986; Слободянюк и др., 2006). Reloading points that suspend mining operations in the lower part of the open pit mine side occur mainly in open pit mines. Such solutions reduce the economic efficiency of mining operations. In the theory of mining, insufficient attention has been devoted to problems of optimization of parameters, such as volume and location, of the reloading point (for instance temporary dump) that provides a minimization of the transportation work for haul trucks.

Analysis of recent studies and publications

In the mining and many other industries, the problem of determining an optimum point for run-of-mine (RoM) stock (an optimum location of the reloading point) that minimizes the cumulative haulage volume (S is Fermat-Torricelli point) is topical. Throughout 350 years, several methods have been

proposed for determining the optimum point, but they have some drawbacks and are not universal (*Протасов*, 1989; *Успенский*, 1958). A detailed analysis of the geometric methods (proposed in the XVII-XIX centuries) and an analysis of influence of the shape and dimensions of the triangle on the change in the position of the point S are made in (Slobodyanyuk et al., 2017), and formulas for the coordinates of the point S for the quadrangle are given. Similar formulas for the triangle cannot be applied because of the uncertainty of some intermediate operations (the uncertainty of the sign when the square root is found; the formulas vary for points "on the left" or "on the right", "on the top" or "on the bottom").

In (Slobodyanyuk et al., 2017; Максимов и.Слободянюк, 2017), the authors proposed a universal gradient method to find the point S for any quantity of points *n* with the same or different performance. Applying the simple formulas, we first find the coordinates of the gravity center (a starting point) and the volume of road haulage for the selected point and eight adjacent points (in different directions, at a distance of ±Δx; ±Δy); from nine points we choose the point with the lowest haulage volume and so on until the optimum point S is finally found.

Main Exposition

Formulation of the problem

The purpose of this article is to investigate the specific features of the influence of excavating face capacity on the position of the optimum point for RoM stock at three excavating faces, and to justify the results obtained in the context of further improvement of combined road and rail transport.

Presentation of the main study material

The methods proposed and developed earlier do not allow us to analyze the behavior of change in the cumulative haulage volume with change in the position (coordinates) of the RoM stock point; the dependence of the coordinates of the optimum point S on the parameters of the triangle is not determined. Similar methods have led to a system of irrational equations that do not give an unambiguous answer (the reasons were given above). In this paper we analyze the position of the optimum point for some symmetrical figures for which one of the coordinates is known (e.g., y_S=0). Let us consider an isosceles triangle with a center of the coordinate system located in the middle of the triangle base (Fig. 1).

If the face capacities are the same (Q), the cumulative transport operations are:

$$F(x) = Q\left[2\sqrt{\frac{a^2}{4}+x^2}+(b-x)\right] \Rightarrow \min \qquad (1)$$

Let us find the derivative, equate to zero and obtain the equation:

$$\frac{2x}{\sqrt{\frac{a^2}{4}+x^2}}-1=0 \qquad (2)$$

We finally find:

$$x=\frac{a\sqrt{3}}{6} \qquad (3)$$

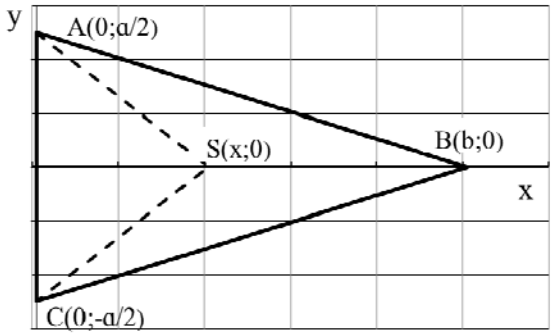

Fig.1. Diagram for finding the optimum point for RoM stock for an isosceles (symmetrical) triangle (AB = BC)

The resulted value corresponds to the geometric solution (Slobodyanyuk et al., 2017) and is equal to half the radius of the circle circumscribed about the Napoleon's equilateral triangle, constructed "on the left" on ***AC=a***. The conclusion that the position of the optimum point depends only on the parameter ***a*** and does not depend on the distance ***b***, where the point ***B*** is situated is confirmed. While the point ***B*** is moving off along the ***OX*** axis, the position of the optimum point does not change.

Let us consider a similar problem provided that the performance of point ***B*** is greater (or less) than the performance of points ***A*** and ***C*** and is equal to ***K·Q***, where ***K*** is some coefficient. Then, equation (2) takes the form as follows:

$$\frac{2x}{\sqrt{\frac{a^2}{4}+x^2}}-K=0 \qquad (4)$$

Finally, we find:

$$x=\frac{a}{2}\times\frac{K}{\sqrt{4-K^2}} \qquad (5)$$

At ***K = 1***, the performance of points ***A; B; C*** is the same, we get the value (3). At ***K=2*** (the performance of point ***B*** is twice the performance of points ***A*** and ***C***), we obtain ***x→∞***. In view of the physical and geometric meanings of the problem, the optimum point for RoM stock will be point ***B***. This conclusion coincides with the other researchers' conclusions obtained by modeling.

We set the positions of points ***A, B, C*** on the solid surface (model) and make holes in these points. Using the laces run through the holes, we hang the weights and tie the laces. The position of the knot corresponds to the position of the optimum point for RoM stock (*Протасов*, 1989; *Успенский*, 1958). If the weight corresponding to the point ***B*** is doubled, then the knot "falls through" to the point ***B*** (i.e., the point ***B*** is an optimum point for RoM stock). In (Максимов и.Слободянюк, 2017) this conclusion is proved by geometric methods. It is easy to verify this conclusion if two adjacent vertices of the

quadrangle infinitely approximate one another, then the point of intersection of the diagonals approaches this double point (the point of intersection of the diagonals for the quadrangle is the Fermat-Torricelli point). A similar conclusion follows from (5), being a more rigorous proof.

We substitute in formula (5) the value ***x=b*** and find the coefficient ***K*** at which the point ***B*** will be optimum:

$$b = \frac{a}{2} \times \frac{K}{\sqrt{4 - K^2}}; \quad \rightarrow \quad K = \frac{2b}{\sqrt{b^2 + \frac{a^2}{4}}} \tag{6}$$

For an equilateral triangle ABC $b = \frac{a\sqrt{3}}{2}$ and we have $K = \sqrt{3} \approx 1.73$.

The point ***B*** will be optimum at its performance (by 73% higher than the performance of points ***A*** and ***C***). When the point ***B*** is moving off, the value of the coefficient ***K*** increases, at ***b = 2a K = 1.95***. Fig. 2 shows a function graph (6), which reflects the nature of increasing the coefficient ***K*** when the point ***B*** moves off.

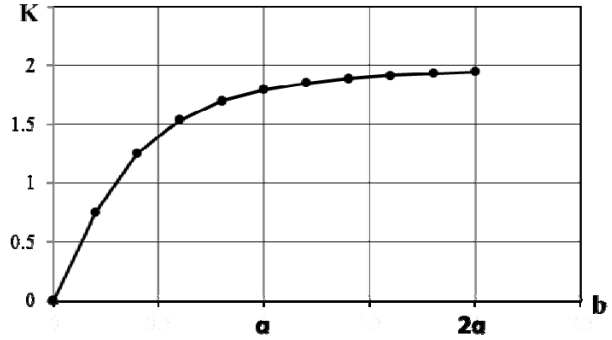

Fig.2 The graph of change in the parameter K when the point B moves off

Fig. 3 shows a graph of the function (1), i.e. the cumulative haulage volume. From the graph it is evident that the lowest tonnage will be available when the reloading point is located at the optimum point (Ferma-Torricelli) at $x = \frac{a\sqrt{3}}{6}$. With increasing ***x***, the cumulative tonnage increases, and with ***x>a***, the increase is proportional to the distance ***x***.

Function (1) has an oblique asymptote *y=Q(x+b)*, that indicates a proportional increase in tonnage (*x>a*). The efficiency of choosing the optimum point for RoM stock will be considered using an equilateral triangle. When hauling the rock mass to one of the triangle vertices, the cumulative haulage volume is ***2aQ***. When placing the point for RoM stock in the middle of either side (the point ***O***, Fig. 1) the cumulative tonnage is $a \times Q\left(1 + \frac{\sqrt{3}}{2}\right) \approx 1.87a \times Q$ (decreases by 6.7%), and when choosing the optimum Fermat-Torricelli point the cumulative tonnage is $a \times Q\sqrt{3} \approx 1.73a \times Q$ (decreases by another 7.2%).

A similar study of changing the cumulative haulage volume was made for the case when the performance of the point ***B*** was twice as large as the performance of points ***A*** and ***C***. Formula (1) looks like this:

$$F(x) = Q\left[2\sqrt{\frac{a^2}{4} + x^2} + 2(b - x)\right] \tag{7}$$

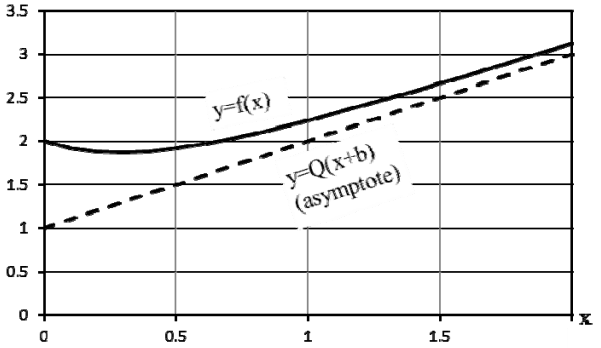

Fig.3. Change in the cumulative haulage volume when moving the point for RoM stock along the OX axis

However, the optimum point for RoM stock (Fermat-Torricelli) is point ***B***. Analysis of the graph (Fig. 4) shows that when shifting the point for RoM stock from the point O to the point ***B***, the cumulative haulage volume is reduced by 30%.

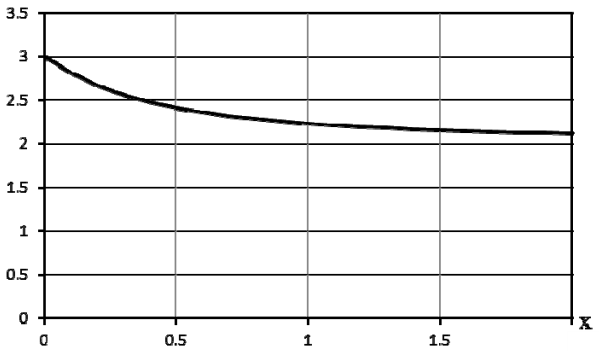

Fig.4. Change in the haulage volume for the case when the performance of the point B is twice as large as points A and C

Comparison of graphs (Fig. 3, 4) shows that with increasing the performance of the point ***B***, the behavior of the cumulative haulage changes drastically.

The undertaken studies are primarily aimed at optimization of road and rail transport in the open pit mines. Considering an optimization of haulage for a group of three shovels, it is obvious that moving the rock mass from two shovels to the working area of the third one, which has the highest capacity, we thereby determine an optimum position of the reloading point and open pit face for the shovel with a "zero" truck haulage (i.e. for the shovel operating for the second link of combined transport - rail transport).

Since the depth of the open pit grows, the rail transport loses its efficiency mainly not because of the lesser gradient (30-40‰ vs. 80‰) in comparison to the road transport, but because of the need to freeze a section of the pit wall in order to locate the reloading points for shovels. By eliminating the afore-mentioned shortcoming, it is possible to improve

significantly the efficiency of road and rail haulage in the open pit mine. The article (Slobodyanyuk, Turchin; 2017) proposes a new method of arranging and operating a reloading point for shovels.

The drawbacks of reloading points equipped with the rope shovels are that during operation of the reloading point, the trucks and dump cars intersect, which leads to a decrease in the tonnage capacity of trucks, and unloading the trucks at a level higher than the shovel is located makes it impossible to combine the handling operations in time and space. This causes a decrease in the shovel performance and an increase in the distance haulage of rock mass by trucks. In order to locate the reloading point, it is necessary to deactivate a section of the pit wall that resulted in a decrease in the rock mass output. The developed technology reduces the negative impact of reloading points on the dynamics of mining operations, increases the tonnage capacity of trucks due to eliminating the additional lift of rock mass by trucks and avoiding the intersection of roads and railways (Fig.5).

The mining operations using the developed technology are made as follows (Figure 5). A backhoe hydraulic shovel (1) excavates a receiving trench (2). This trench (2) is conditionally divided by width into two sections: the unloading wall (3) and the loading wall (4). The receiving trench (2) is filled with rock mass on the unloading wall (3) by trucks (5). In the general case, in order to prevent from intersecting the haul roads, the receiving trench wall (2) located closer to the lower pit benches is the unloading wall (3). The receiving trench wall located closer to the higher pit benches is the loading wall (4). The rail track is located (7) along the loading wall (4) of the receiving trench (2).

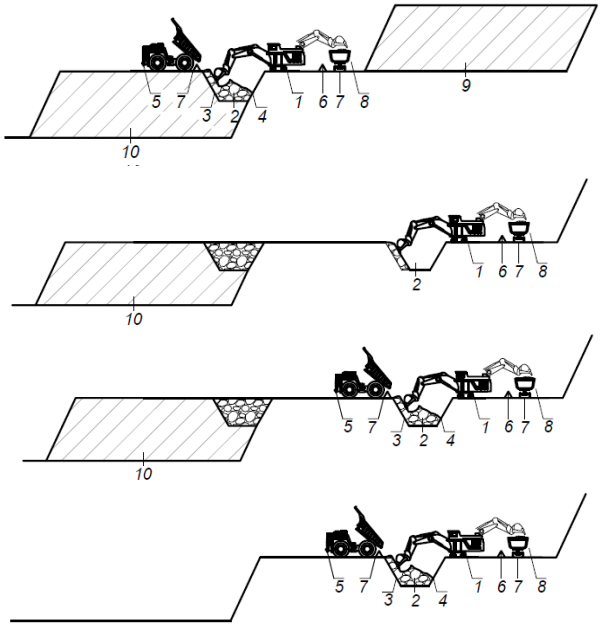

Fig.5. Diagram of mining operations when shifting a reloading point

The rock mass from the receiving trench (2) is reloaded by a hydraulic shovel (1), located on the loading wall (4) of the receiving trench (2) onto dump cars (8) located at the level of the hydraulic shovel.

The reloading point in the given place operates until the higher benches (8) are mined out. After this, a backhoe hydraulic shovel (1) excavates a new receiving trench (2) on the extended site. After commissioning the relocated reloading point, the lower benches (9) are mined out. In order to increase the capacity of the reloading point, two or more backhoe hydraulic shovels are placed on the loading trench wall at a safe distance from each other. The use of the proposed reloading point design provides an increase in the capacity of mining equipment and reduces the negative impact of open pit transport on the dynamics of mining operations. The reloading point of the proposed design is easily relocated as the mining operations progresses and does not freeze the pit wall.

Conclusions and trends for further studies

The use of a simplified model (an isosceles triangle) made it possible to conduct an analytical study, to find the coordinates of the optimum point for RoM stock at different performance of three points, to determine the behavior of change in the haulage volume when the point of stock was moved. In the future, similar studies are planned to be conducted for more points.

Minimum operation of three shovels, one of which has a higher performance (1.5-1.7 times higher) is ensured if the point for RoM stock tends to the location of the shovel with maximum performance. This rule determines the general approach to separation of open pit space into the operating zones for combined transport.

Minimum operation of the open pit transport, being the first link of road and rail transport, will be provided, if the truck haulage distance of maximum rock tonnage to the reloading point will be minimum. This imposes a number of requirements on the optimum mining technology, such as the use of more powerful shovels on the border of adjacent links of combined transport and the possibility of operating the second link of combined transport without freezing the working pit wall. The second requirement is fulfilled when using the developed design of the reloading point for shovels.

In further studies, the developed mathematical apparatus will be used to establish the regularities for the optimum location of reloading points and temporary truck dumps and to provide the conditions for circular truck routing.

References

Арсентьев А.И. Законы формирования рабочей зоны карьера: учеб. пособие. Ленинград: Изд-во ЛГИ, 1986. 54 с. (Arsent'ev A.I. Zakony formirovaniya rabochey zony kar'era: ucheb. posobie. Leningrad: Izd-vo LGI, 1986. 54 p.)

Белозеров В.И. Оптимизация вскрытия рабочих горизонтов карьера. ГИАБ. Москва: Изд-во МГГУ. 2012. № 6. С. 88–94. (Belozerov V.I. Optimizatsiya vskrytiya rabochikh gorizontov kar'era. GIAB. Moskva: Izd-vo MGGU. 2012. № 6. pp. 88–94.)

Вилкул Ю.Г., Слободянюк В.К., Максимов И.И. Обоснование рациональных зон использования карьерных автосамосвалов разной грузоподъемности. Разработка рудных месторождений. Кривой Рог. 2008. № 92. С. 3–7. (Vilkul Yu.G., Slobodyanyuk V.K., Maksimov I.I. Obosnovanie ratsional'nykh zon ispol'zovaniya kar'ernykh avtosamosvalov raznoy gruzopod"emnosti. Razrabotka rudnykh mestorozhdeniy. Krivoy Rog. 2008. № 92. pp. 3–7.)

Vilkul Y., Slobodyanyuk V., Maximov I. Optimization of capacity and the number of crushing and transfer stations at the deep open pits. Metallurgical and Mining Industry. 2016. № 4. pp. 116–120.

Максимов І.І.,Слободянюк Р.В. Особливості визначення раціонального положення перевантажувального пункту у кар'єрі. Вісник Криворізького національного університету. Кривий Ріг: КНУ, 2017. Вип. 44. С. 73-79. (Maksymov I.I.,Slobodjanjuk R.V. Osoblyvosti vyznachennja racional'nogo polozhennja perevantazhuval'nogo punktu u kar'jeri. Visnyk Kryvoriz'kogo nacional'nogo universytetu. Kryvyj Rig: KNU, 2017. Vyp. 44. pp. 73-79.)

Протасов В.Ю. Максимумы и минимумы в геометрии. Москва: МЦНМО, 2005. 56 с. (Protasov V.Ju. Maksimumy i minimumy v geometrii. Moskva: MCNMO, 2005. 56 p.)

Слободянюк В.К., Данілов М.М., Письменний О.В., Саприкін В.С. Дослідження умов та особливостей використання рудоспусків для розкриття глибоких горизонтів залізорудних кар'єрів. Вісник ЖДТУ. Серія: Технічні науки. Житомир: ЖДТУ, 2006. № 1 (36). С. 163–171. (Slobodyanyuk V.K., Danilov M.M., Pys'mennyj O.V., Saprykin V.S. Doslidzhennja umov ta osoblyvostej vykorystannja rudospuskiv dlja rozkryttja glybokyh goryzontiv zalizorudnyh kar'jeriv. Visnyk ZhDTU. Serija: Tehnichni nauky. Zhytomyr: ZhDTU, 2006. № 1 (36). pp. 163–171.)

Слободянюк В.К., Максимов І.І., Слободянюк Р.В. Вплив взаємного розташування вибоїв на положення оптимальної точки звозу гірничої маси і аналітичне визначення її координат. Вісник ЖДТУ. Серія: Технічні науки. Житомир: ЖДТУ, 2017. №1 (79). С. 202-208.(Slobodyanyuk V.K., Maksymov I.I., Slobodyanyuk R.V. Vplyv vzajemnogo roztashuvannja vyboi'v na polozhennja optymal'noi' tochky zvozu girnychoi' masy i analitychne vyznachennja i'i' koordynat. Visnyk ZhDTU. Serija: Tehnichni nauky. Zhytomyr: ZhDTU, 2017. №1 (79). pp. 202-208.)

Slobodyanyuk V., Turchin Yu. Rational use of hydraulic excavators in iron ore pits. Journal of Mining and Geological Sciences. University of Mining and Geology "St. Ivan Rilski". 2017. № 60. pp. 21–26

Слободянюк Р.В., Пижик М.М Вдосконалення технології гірничих робіт з кільцевою схемою руху кар'єрних автосамоскидів. Вісник ЖДТУ. Серія: Технічні науки. Житомир: ЖДТУ, 2016. № 1 (76). С. 151–157. (*Slobodyanyuk* R.V., Pyzhyk M.M Vdoskonalennja tehnologii' girnychyh robit z kil'cevoju shemoju ruhu kar'jernyh avtosamoskydiv. Visnyk ZhDTU. Serija: Tehnichni nauky. Zhytomyr: ZhDTU, 2016. № 1 (76). pp. 151–157.)

Успенский В.А. Некоторые приложения механики к математике. Москва: Физматгиз, 1958. 48 с. (Uspenskij V.A. Nekotorye prilozhenija mehaniki k matematike. Moskva: Fizmatgiz, 1958. 48 p.)

Яковлев В.Л. Теория и практика выбора транспорта глубоких карьеров. Новосибирск: Наука, 1989. 240 с. (Yakovlev V.L. Teoriya i praktika vybora transporta glubokikh kar'erov. Novosibirsk: Nauka, 1989. 240 p.).

ANALYSIS AND DEVELOPMENT OF SLOPE HOISTING SYSTEMS FOR OPEN PIT MINES

Roman Slobodyanyuk[1]

[1]France, Nancy, University of Lorraine; slobod.roman@gmail.com

ABSTRACT. The purpose of this article is to develop and substantiate rational designs of slope hoisting systems for dump trucks in open pit mines to reduce the time losses associated with an idle mileage in the transport cycle. The basic arrangements of slope hoisting systems have been analyzed and a rational field of their application has been determined. The lack of experience in operation of slope hoisting systems with multi-rope friction winders, the possibility of reducing a friction ratio due to freezing and wetting the rope leave no chance to recognize this technical solution as a reliable. The article presents the results of the design study and determination of parameters of a hoister with a reeving system for suspension of one platform to haul down the 130-ton trucks. The developed hoisting plant consists of the following main parts two 1-6 x 5.6/0.8 single-drum hoisters; a platform for transporting the truck; a headframe for placing the deflection sheaves; two deflection sheaves; two inclined rail tracks to move the platform. The article proposes new technical solutions for hoisting plants with two platforms. The developed technology promotes improvement of the operational performance of haul trucks in open pit mines.

Keywords: slope hoisting plant, haul trucks, drum hoister, reeving system of vehicles, resource-saving technology

АНАЛИЗ И РАЗРАБОТВАНЕ НА КОНСТРУКЦИИ ЗА НАКЛОНЕНИ КЪМ КАРИЕРА СИСТЕМИ ЗА ПОДЕМ

Роман Слободянюк[1]

[1]Франция, гр. Нанси, Университет на Лотарингия; slobod.roman@gmail.com

РЕЗЮМЕ. Целта на работата е разработване и обосноваване на рационални конструкции за кариерни наклонени кранове за самосвали, за да се намалят времевите загуби, свързани с напразния път в транспортния цикъл на самосвалните камиони. Извършен е анализ на основните схеми на кариерните подемни системи с наклон и е определен рационалния обхват на тяхното използване. Липсата на опит в експлоатацията в кариерите на подемни системи с теглителни снопове на триене, възможността за намаляване на коефициента на триене, дължащ се на замръзване и омокряне на въжето, не определят това техническо решение като надеждно. В статията са представени резултатите от изследването и определянето на параметрите на подемна машина с ремъчна спирачка на една платформа, която служи за спускане на самосвали с полезен товар от 130 тона. Разработената подемна система се състои от следните основни части: две еднобарабанни подемни машини тип 1-6x5,6/0,8; платформа за транспортиране на камиона; куп за поставяне на шайби за отклоняване; две отклоняващи шайби; две наклонени релсови линии за преместване на платформата. Предлагат се нови технически решения за подемни машини с две платформи. Разработената технология създава необходимите условия за подобряване на експлоатационните характеристики на кариерните самосвали.

Ключови думи: кариерна подемна система с наклон, транспортни камиони, барабанна подемна машина, полиспаст, технология за спестяване на ресурси

Introduction

Articulation of the problem

By the end of the 20th century, considerable progress had been made in the development and implementation of heavy hoisting plants in the underground mines. There are examples of mines with a depth exceeding 2 000 m, the lifting capacity of hoisting plants has reached over 50-60 tons. Advances in the development of mine hoisting plants have awaken fresh interest in the use of steep-slope hoisting plants in deep open pit mines (Новожилов и др., 1962; Носырев, 1972; Shilling and Adams, 1971; Васильев, 1975; Кульбида и др., 1981; Садыков, 2011). In the 60s, in the US, South America and China, more than 10 projects of slope skip hoisting plants were implemented (Новожилов и др., 1962; Shilling and Adams, 1971). In 1972, Siemag, the West German company, built the only slope skip hoisting plant in the USSR in the Sibaisky Open Pit Mine (Васильев, 1975). Along with the development and implementation of slope skip hoisting plants, a number of teams of authors elaborated an idea of using a slope hoisting plant to haul down the empty and lift the laden dump trucks in the open pit mines (Дремин и др., 1993; Листопад, 2001; Бондарєв и др.1, 2011). However, numerous projects in this regard have not been implemented. The reason for this is not only the technical complexity of slope hoisting plants, which should conform to the pit dump trucks in their parameters, but also the doubts about the economic efficiency of such plants at a state-of-the-art open pit. The systems designed for hauling down the empty and lifting the laden trucks are distinguished by high metal consumption and complexity of technical solutions on multi-rope hoisting.

Progress in mining machinery manufacturing has increased reliability of pit dump trucks and led to an increase in the reasonable distance of rock mass haulage. There are examples when the rock haulage by trucks reaches over 10 km. In these conditions, the main negative factor that needs to be solved is the idle run of trucks. One-way traffic and equal number of loaded and idle runs of trucks are the main features of truck haulage at the open pit; elimination of idle runs can be considered as the key method for improvement of truck haulage efficiency.

Analysis of recent research and publications

A great contribution to the development of the theory of slope hoisting systems was made by Белобров (2002). His work deals with multi-rope slope hoisting plants designed to haul down and lift the trucks, as well as to lift the skips of over 120 ton capacity. However, the main orientation of research was focused on lifting the cargo to the surface. In order to solve the problem, we used a multi-rope hoisting system with a large angle of the drive sheave contact (**α=3π**). With increasing **α**, the lifting capacity of the hoister is increased:

$$S_2 = S_1 e^{\alpha f}, \quad (1)$$

where S_2 is the tension of the rope lifting the laden vehicle; S_1 is the same from the side of the empty vehicle; *f* is an adhesion (friction) factor between the rope and the lining of drive sheaves (0.2 ÷ 0.3).

The hoisting plants with several drive sheaves of friction have a lifting capacity 3 to 6 times greater than single-drive machines. A weak point of this plant (Садыков, 2011) is that the hoisting ropes are subjected to multiple (up to 8-9 times) kinking on the sheaves during a lifting cycle, half of them bends in different directions, that will lead to a short lifespan of the ropes.

Siemag has developed a project for a slope hoisting plant for laden trucks, which is equipped with a single platform with a counterweight. In this project, a multi-rope hoisting system with a large angle of the drive sheave contact is also used. In the world, there are several examples of using the hoisting plants for dump trucks in the mining operations under extreme conditions - in the construction of hydraulic structures in the highlands (Nant de Drance, Tokuyama, Tateyama, Miyagase, Kaprun, etc.). The capacity of these plants does not exceed 40 tons.

Main Exposition

Statement of the problem

The purpose of this article is to develop and substantiate rational designs of slope hoisting systems for dump trucks in the open pit mines, the use of which will reduce the idle runs.

Presentation of the main study material

The main idea of this study is to increase the truck capacity by reducing the downtime associated with idle mileage in the transport cycle using the slope hoisting plants to haul down the empty trucks to the open pit. Obviously, the hoisting systems equipped with two lifting platforms alternately used for hauling down the trucks can achieve maximum economic effect.

It is known that when lifting vertically using drum winders or hoisters with friction sheaves, the vehicles move in two mutually perpendicular vertical planes: in plane, where the head sheave is located and in plane being tangential to the sheave circle (the rope leaving point from the sheave). The line of intersection of these planes coincides with the axis of the hoisting rope. When lifting vertically there are no critical difficulties with creating conditions for movement of two skips in the shaft. The skips used for vertical lifting are structurally adapted to move within a limited section of the shaft (the height of the skip is greater than its dimensions in plan).

This principle is maintained even at slope hoisting – the vehicle moves along the line of intersection of two mutually perpendicular planes, but one of them (tangent to the sheave) is located at an angle to the horizon. In this case, the design solution to arrange the movement of two vehicles (skips or platforms) associated with one or more hoisters is more difficult, especially when the trucks are lowered on the platform (the length of 130-ton truck is about 12 m, the width is 6 m, the weight is 105 t, the weight of lifting platform is 50 t). In most of proposed slope hoisting systems for dump trucks, this has led to placing the deflection sheaves on the headframes or in the hoist house, which makes these hoisting plants complex and unreliable.

A great contribution to the development of the theory of slope hoisting systems was made by *Б.А.Носырев*. In his work (1972), eight basic arrangements of slope hoisting plants are defined, the estimation is given and the rational application area is specified. Fig.1 shows the schematic diagrams of slope hoisting plants in the open pit mines, the analysis of these plants is given in Table 1. The absolute lack of experience in operation of slope hoisting systems with multi-rope friction winders in the open pit environment does not optimize the possible increase in the calculated friction factor and even more, the friction factor may be reduced due to rope freezing and wetting during the periods of rain and snow melt (Носырев, 1972).

In order to determine the main technical characteristics of the plant for hauling the empty trucks (Fig. 2), the design was elaborated for the following mining conditions: the hoisting plant is single-end type; lifting height, Hn = 400 m; a slope angle of the lifting way, α = 40 °; lifting length, L_H = 622.48 m; the type of vehicle is a platform; capacity of the platform is Q_{gr} = 105 000 kgf; mass of the platform, Q_{pl} = 50 000 kg; the purpose of the hoisting plant is men and cargo hoisting.

The maximum static load of the slope hoisting plant is 155t. At present, the mine hoisters manufactured by the industry have no capacity required to meet a target. The hoisting plant with two synchronized hoisters and a reeving system for suspension of the cargo platform is proposed, that will allow reducing the suspended load on the hoisting ropes. The suspended load is:

$$Q_0 = \frac{Q_{st}}{n \times i_n \times \eta_n} = \frac{155000}{2 \times 2 \times 0{,}99} = 39142\ kgf \quad (2)$$

where: n = 2 - number of hoisting ropes;
i_n = 2 - mechanical advantage of a tackle block (number of ropes);
η_n = 0.99 - efficiency of a tackle block on the roller bearings

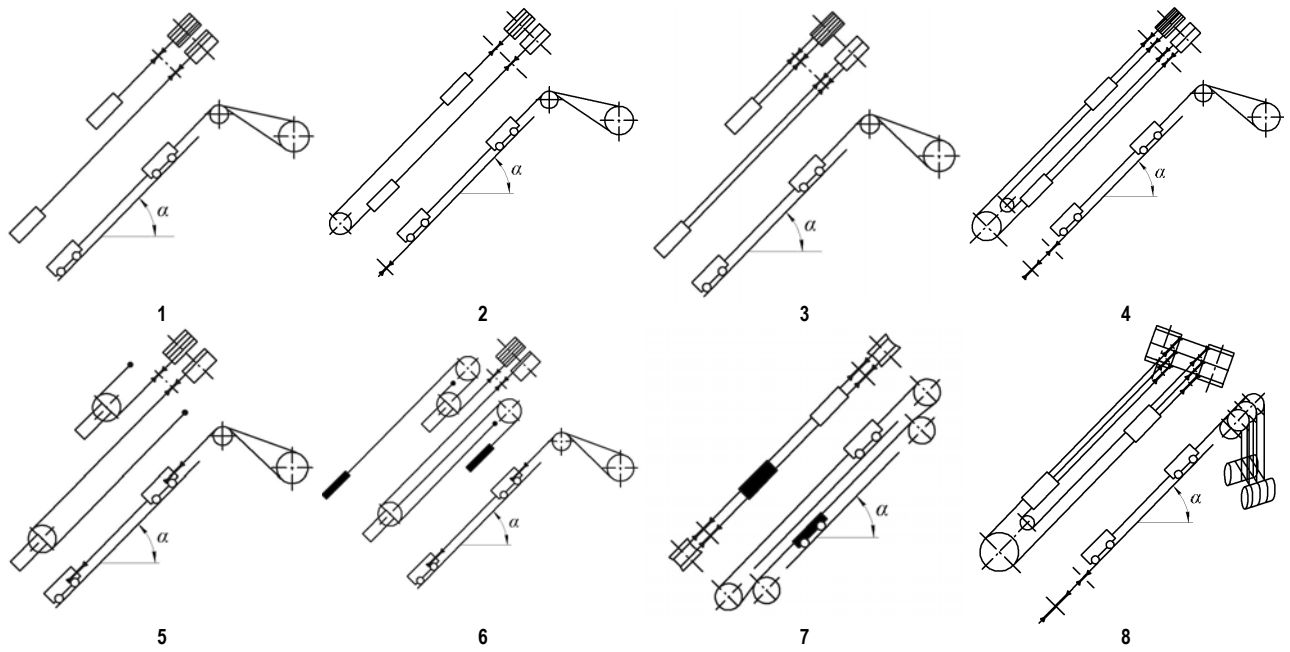

Fig.1. Diagrams of hoisting plants (Носырев, 1972)

Table 1
Analysis of arrangements of slope hoisting plants

Design features	Advantages	Disadvantages
A single-rope hoisting plant with multilayer rope winding on a cylindrical hoist drum (Fig. 1.1, 1.2), (drum hoist). Capacity is up to 40 tons.	Simplicity and reliability of the plant; the possibility of using the lubricated ropes.	The use of this plant is limited by the traction properties of the rope, the static tension of the rope line and the greatest static unbalanced circumferential force. With a greater unbalanced circumferential force, it is necessary to balance the hoisting system (Fig. 1.2).
A multi-rope hoisting plant with multilayer rope winding on the section of cylindrical drums (Fig. 1.3), (Blair hoist). Capacity is over 40 t, lifting height is over 400 m.	Simplicity and reliability of the plant; the possibility of using the lubricated ropes, the use of a winding reel of smaller diameter than in the case of friction sheaves; lower consumption of ropes.	When lifting cargo from deep levels, the improvement of energy effect may be achieved by using lower balancing ropes (Fig. 1.4).
The hoisting plants with a reeving system for suspended vehicles (Fig. 1.5, 1.6).	The harmful phenomenon of uneven force distribution along the rope lines has been eliminated; due to the high speed of the rope, it is possible to use gearless drives. The use of block hoisting arrangements is reasonable for cage hoisting plants with a low lifting speed of the cage (platform).	Complication of the vehicle construction due to placing the circumferential sheave on its frame, an increase in the vehicle weight by 10-15 tons; increased wear of the rope, because of the doubled speed of its movement and additional bending on the by-pass sheave; the use of double-length ropes.
A multi-rope hoisting plant with friction sheaves (Fig. 1.7, 1.8), (Koepe hoists). Capacity is over 40 t, lifting height is over 400 m. A hoister with one driving friction sheave provides no high traction and requires balancing ropes. In the hoisters with several driving friction sheaves, the angle of the drive sheave contact is 3π.	It can be used with long ropes; decrease in inertial masses of the winding reel; increase in efficiency of the hoisting plant; rope rupture hazard prevention when the vehicle is derailed (jammed) and re-lifted.	Limited use due to the rope stress ratios; increase in wear and corrosion of the rope due to the lack of protective lubrication; reduction of the friction factor due to rope freezing and wetting during the periods of rain and snow melt; constructive complexity of two-vehicle slope hoisting plants; the low balance ropes considerably complicate the design and reduce the reliability of the hoisting plant.

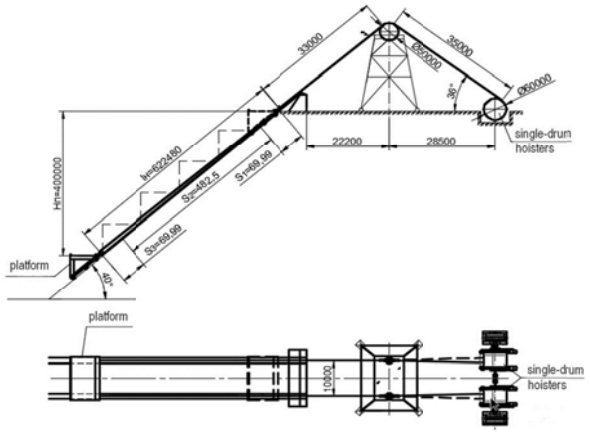

Fig.2. Diagram of a hoisting plant

As a hoister, it is rational to use the mine hoister with one cylindrical drum that has been developed by NKMZ. Based on the dimensions of the winding reel and suspended loads, the 1-6x5.6/0.8 mine hoister fits well having the following parameters: 6 000 mm drum diameter; 5 600 mm drum width; 560 kN static rope tension; 400 kN difference in static rope tension and 11 200 kNm^2 flywheel effect.

The developed hoisting plant consists of the following parts:
- two 1-6x5.6/0.8 single-drum hoisters;
- a platform for transporting the truck;
- a headframe for placing the deflection sheaves;
- two deflection sheaves (Ø 5 000 mm);
- two inclined rail tracks to move the platform.

In order to reduce the suspended load on the hoisting ropes, provision is made for two hoisters with fixing the ropes via a tackle block to the platform frame. This type of arrangement makes it possible to use commercially available hoisters. In order to distribute an even load, the operation of hoisters should be synchronized in terms of rope speed and tension. The parameters of the hoisting plant are determined by calculation as follows: the hoisting speed is 9.9 m/s, the time of one cycle is 214.2 s, the time for a truck to drive on and off the platform is 60 s, the cycles per hour are 12-15. Fig. 3 shows the diagrams of acceleration, speed and force. When the loaded platform is lowered, 1÷3 periods (Fig. 3), the values of driving forces on the circumference of the rope winders have negative values, i.e. the engines operate in a dynamic braking mode. When the platform is lifted, the drive motors operate in a traction mode, overcoming the static resistance of the hoisting system and at the same time ensuring the actual linear speed with the proper acceleration and deceleration adopted according to the requirements of design standards. The hoisting plant is equipped with two P2-800-217-8SUHL4 electric motors of 3 150 kW nominal.

The efficiency of mining operations with the use of a developed system for hauling the trucks to the working area depends on the number of downward trips per hour. The performance of the hoisting plant with one platform is sufficient to provide operation of one shovel with a 12-15 m^3 bucket capacity. In order to provide a working area of the open pit with twice as many trucks, it is necessary to build two similar single-rope hoisting plants or to develop a hoisting plant with two platforms. The main idea that needs to be implemented in the hoisting plant with two platforms is to balance the hoisting system and haul down the trucks when engines are operating in a regeneration mode.

The arrangements can be classified as per location of tracks with respect to the longitudinal hoister and the position of tracks relative to each other. We will compare the advantages and disadvantages of alternative arrangements of hoisting plants having two platforms with two independent hoisting plants having one platform. Analysis of possible kinematic diagrams allowed the following solutions to be called competitive. From the position relative to the hoister, both tracks can be located either on one side (Fig.4, 5) or on opposite sides of the hoister (Fig.6). When the tracks are located on opposite sides of the hoister, they are located in the same vertical plane, but not parallel to each other (Fig.6). In order to ensure mining technical conditions for this track location, it is necessary to provide the hoister's site on a rock pillar, protruding in plan from the general strike trend of the pit wall. This design of the hoisting plant allows to haul down the trucks at two different sections of the working area. The distance between in-pit sites of the hoisting plant can reach 600-800m. When the tracks are located on one side of the hoisting plant, they are also located in the same plane, in general, parallel to each other, but this plane can be either parallel to the pit wall plane (Fig.4)or vertical and pass through the hoisting sheaves of the hoisting plant (Fig.5).

Fig.5 shows a general view of the hoisting plant with one-sided arrangement in a vertical plane of two parallel tracks (the top and bottom tracks), where 1,2 - platforms; 3 - dump truck; 4,5 - inclined rail tracks; 6,12 - hoisting ropes; 7,13 - headframes; 8,14 – top headframe sheaves; 11,17 - bottom headframe sheaves; 9,15 – rope winding reel; 10,16 - electric motors; 18 - a hoist house (deflection sheaves on the platforms and a reeving system are not shown in the figure). Fig.6 shows a general view of the hoisting plant with an opposite-sided arrangement (in relation to a vertical plane passing through the longitudinal axis of the drum) in a vertical plane of two tracks (conditionally applied to Fig.7, left and right tracks), where 1 is platform of the right track; 2 - platform of the left track; 3 - dump truck; 4,5 - inclined rail tracks; 6,14,13,21 - hoisting ropes; 7,15,11,19 - headframes; 8,16,12,20 - headframe sheaves; 9,17 – rope winding reels; 10,18 - electric motors; 22 - a hoist house (deflection sheaves on the platforms and a reeving system are not shown in the figure).

The arrangement shown in Fig.4 differs from two independent, side-by-side located hoisting plants with one platform in that the adjacent single-drum hoisters are replaced by one double-drum hoister. The double-drum hoister serves both tracks and operates all the time in a regeneration mode, the single-drum hoisters operate alternately. In this case, the hoisting plant is equipped with three hoisters. One of the main drawbacks of this arrangement is that there is no possibility to provide a through movement of trucks, that is, when driving on or off the platform, the truck drives in reverse.

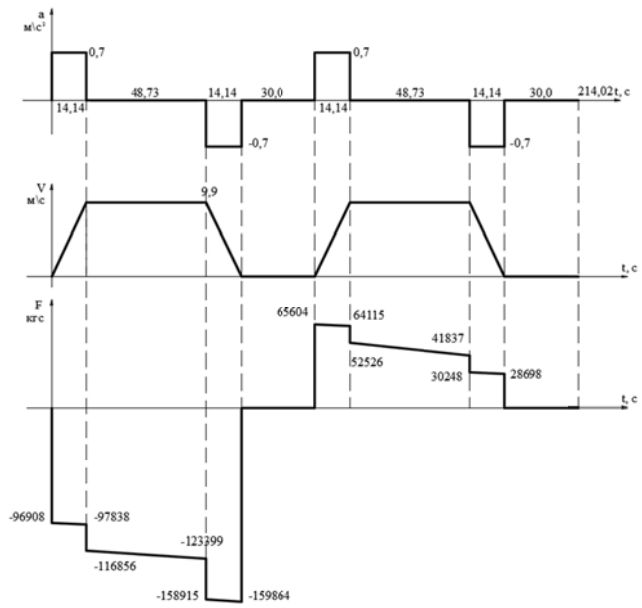

Fig.3. Diagrams of acceleration, speed and force

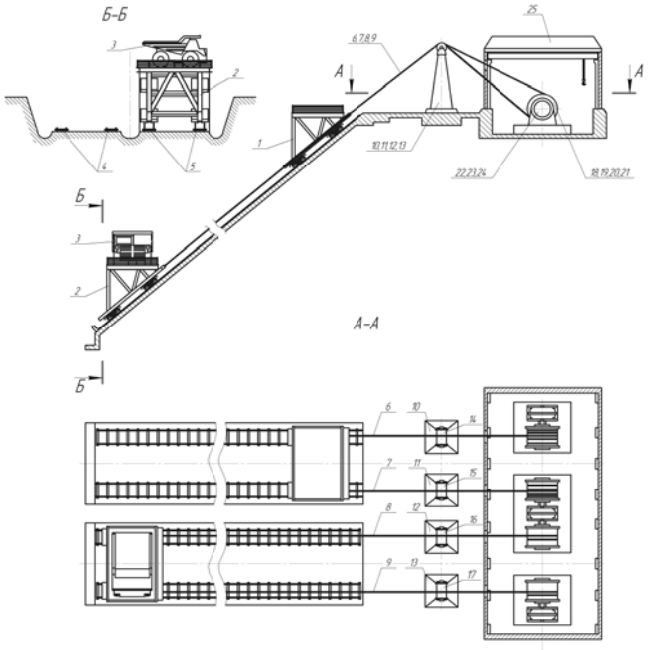

Fig.4. General view of a hoisting plant with a single-sided arrangement of two parallel tracks in a plane of a pit wall

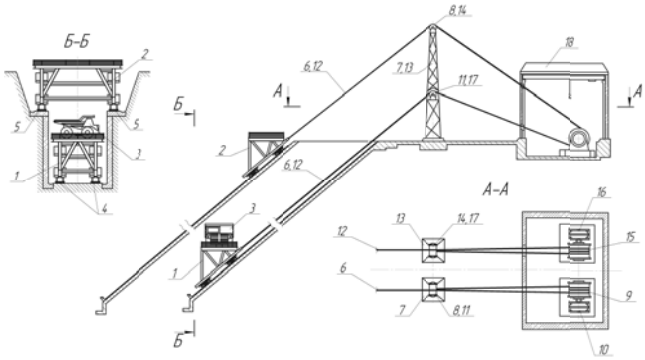

Fig.5. General view of a single-sided hoisting plant in a vertical plane of two parallel tracks

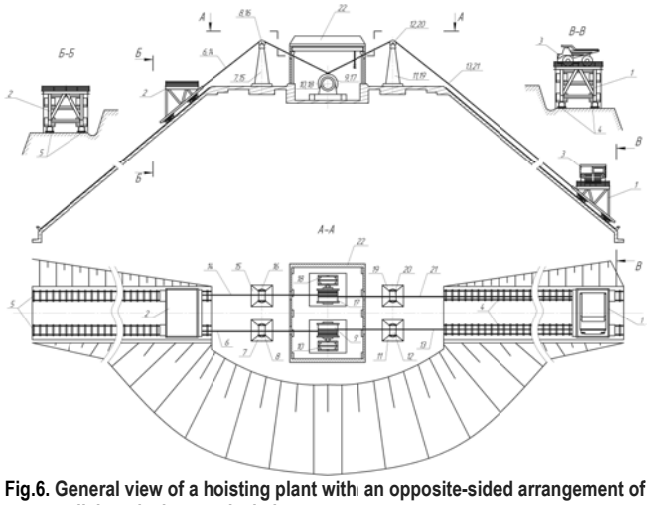

Fig.6. General view of a hoisting plant with an opposite-sided arrangement of two parallel tracks in a vertical plane

The diagram in Fig. 5 differs from the diagram in Fig. 4 in that the hoisters are statically more balanced, two ropes are wound on the cylindrical drums: when one rope reels in, another one reels out. Two hoisting plants provide hauling two platforms up and down, and operate all the time in a regeneration mode. The location of tracks in section of one step-shaped trench allows the trucks to arrive and depart without additional maneuvers. The drawback of this arrangement is the need to construct a special trench with the location of rail tracks at two levels. The upper platform is structurally more complex than the lower one.

The diagram shown in Fig. 6, in terms of arrangement of hoister operation is similar to the diagram in Fig.5. However, in this case, two tracks of the hoisting plant are located in diametrically opposite directions. This design is characterized by a safer arrangement of the truck movement on the upper loading station and provides driving the trucks off the platform in the lower position without additional maneuvers. This arrangement is characterized by a large amount of mining and capital work to prepare the sites for construction of a hoist house and a track and can be used at the open pit with a long-distance haulage.

Conclusions and trends for further research

The article presents the results of research on the development and substantiation of rational designs of slope hoisting systems for hauling the empty dump trucks in the open pit mines, the use of which will reduce the idle runs.

The basic arrangements of slope hoisting plants using drum hoisters and hoisters with friction sheaves have been analyzed. The design complexity of slope hoisting plants with friction sheaves, the rope exposure to atmospheric precipitation (wetting and frosting), the increased rope wear due to friction against the supporting rollers and sheaves cause the low reliability of the hoisting plant. The hoisters with cylindrical drums do not have the above-mentioned drawbacks.

The issue of providing the required hauling ability of the hoisting plant is proposed to be solved by using several drum-type hoisters in its construction.

The results of the design study of the hoisting plant for hauling the trucks of 130-ton capacity are presented. The arrangement of the hoisting plant with two synchronized drum hoisters and a reeving system for suspension of one cargo platform, that allow reducing the suspended load on the hoisting ropes is considered.

The developed hoisting plant consists of the following main parts: two 1-6x5.6/0.8 single-drum hoisters (manufactured by NKMZ); a platform for transporting the truck; a headframe for placing the deflection sheaves; two deflection sheaves; two inclined rail tracks for moving the platform. When lowering the dump trucks, the hoisters operate in generator mode that allows for electrical energy regeneration.

The efficiency of mining operations with the use of a developed system for hauling down the trucks to the working area depends on the number of downward trips per hour. In order to provide a working area of the open pit with more trucks, it is necessary to build two similar hoisting plants or to develop a hoister with two platforms. The article proposes new technical solutions for hoisters with two platforms, which are alternately used for hauling the trucks. The developed technology promotes improvement of the operational performance of trucks in the open pit mines.

References

Белобров В.И., Белоброва Е.А. Многоканатные наклонные подъемные установки для карьеров и шахт. Наук.-техн. зб. «Гірнича електромеханіка та автоматика». 2002. №69. С. 155-159. (Belobrov V.I., Belobrova E.A. Mnogokanatnye naklonnye pod"emnye ustanovki dlya kar'erov i shaht. Nauk.-tekhn. zb. «Girnicha elektromekhanika ta avtomatika». 2002. №69. pp. 155-159.)

Бондарєв С.В., Горбатенко Ю.П. Застосування підіймачів для переміщеннятrack автомобілів по крутих схилах. Будівництво України. 2011. № 1. С. 26-28. (Bondariev S.V., Horbatenko Yu.P. Zastosuvannia pidiimachiv dlia peremishchenniatrack avtomobiliv po krutykh skhylakh. Budivnytstvo Ukrainy. 2011. № 1. pp. 26-28.)

Васильев М.В. Устройство, опыт эксплуатации и перспективы карьерного скипового подъема. Тр. ИГД МЧМ СССР. 1975. Вып. 46. С. 37-52. (Vasil'ev M.V. Ustrojstvo, opyt ekspluatacii i perspektivy kar'ernogo skipovogo pod"ema. Tr. IGD MChM SSSR. 1975. Vyp. 46. pp. 37-52.)

Дремин А.И., Перепелицын А.И., Крутиков Н.Н. и др. Подъемник для доставки груженых автосамосвалов со дна карьера на поверхность. Горный журнал. 1993. № 7. С. 49-51. (Dremin A.I., Perepelicyn A.I., Krutikov N.N. i dr. Pod"emnik dlya dostavki gruzhenyh avtosamosvalov so dna kar'era na poverhnost'. Gornyj zhurnal. 1993. № 7. pp. 49-51.)

Кульбида П.Б., Ройзен В.В., Сербин В.И. и др. Большегрузные скиповые подъемники для отработки глубоких карьеров. Горный журнал. 1981. № 7. С. 48-50. (Kul'bida P.B., Rojzen V.V., Serbin V.I. i dr. Bol'shegruznye skipovye pod"emniki dlya otrabotki glubokih kar'erov. Gornyj zhurnal. 1981. № 7. pp. 48-50.)

Листопад Г.Г. Наклонные подъемники карьерного автотранспорта. Горная промышленность.-2001. -№ 2. -С. 57-58. (Listopad G.G. Naklonnye pod"emniki kar'ernogo avtotransporta. Gornaya promyshlennost'.2001. -№ 2. -pp. 57-58.)

Новожилов М.Г., Селянин В.Г., Троп А.Е. Глубокие карьеры. – М: Госгортехиздат, 1962. – 256с. (Novozhilov M.G., Selyanin V.G., Trop A.E. Glubokie kar'ery. – M: Gosgortekhizdat, 1962. – 256p.)

Носырев Б.А. Схемы карьерных наклонных подъемных установок, их оценка и области применения. Труды Свердловского горного института. 1972. Вып. 97. С.3-6 (Nosyrev B.A. Skhemy kar'ernyh naklonnyh pod"emnyh ustanovok, ih ocenka i oblasti primeneniya. Trudy Sverdlovskogo gornogo instituta. 1972. Vyp. 97. pp.3-6)

Садыков Е.Л. Повышение эффективности многоканатных наклонных подъемных установок: дис. …канд. техн. наук: 05.05.06. Екатеринбург, 2011. 159 с. (Sadykov E.L. Povyshenie effektivnosti mnogokanatnyh naklonnyh pod"emnyh ustanovok: dis. …kand. tekhn. nauk: 05.05.06. Ekaterinburg, 2011. 159 p.)

Шиллинг Р., Адамс Б. Наклонные скиповые подъемники // Научн. тр. американского института горных инженеров, инженеров–металлургов и нефтяников. – М.: Недра, 1971. – С. 151 – 155. (Shilling R., Adams B. Naklonnye skipovye pod"emniki // Nauchn. tr. amerikanskogo instituta gornyh inzhenerov, inzhenerov–metallurgov i neftyanikov. – M.: Nedra, 1971. – pp. 151 – 155.)

Build Unique Truck Skip Hoist in Belgian Congo. Mining World. 1959. №6. p. 28.

Trucklift System. Innovative transport technology for open pit mines. URL:http://www.siemag-tecberg.com/infocentre/technical-information/ti_27-trucklift.html (accessed 25 May 2018).

VELOCITY FIELD VISUALIZATION, MEASURED WITH 3D ULTRASONIC ANEMOMETER

Zahari Dinchev[1], Yasen Gorbunov[2], Nadezhda Kostadinova[3]

[1] University of Mining and Geology "St. Ivan Rilski", dinchev@mgu.bg
[2] University of Mining and Geology "St. Ivan Rilski", y.gorbounov@mgu.bg
[3] University of Mining and Geology "St. Ivan Rilski", nadezhda.kost@gmail.com

ABSTRACT. The advance in technology development makes it possible to use state of the art devices for 3D measurements such as ultrasonic anemometers. These devices are able to acquire great amounts of data which need to be further processed. By adding a GPS device and SD card storage the data can be analysed by engineers in offline mode or can be accessed wirelessly through Bluetooth connection. The above mentioned improvements are presented in this paper in their final version. A very important point in the overall practical application of the device is the visualization of the obtained velocity vector field. Several possible ways of visualization with the aid of different software packages such as Surfer and Grapher are discussed. A real 3D velocity vector field, measured with ultrasonic anemometer MODEL 81000 by R.M. YOUNG COMPANY, USA is presented in the paper along with cross sections in the xy, yz and xz planes.

Keywords: ultrasonic anemometer, velocity field measurement and visualization, data logging

ВИЗУАЛИЗАЦИЯ НА ВЕКТОРНО ПОЛЕ, ИЗМЕРЕНО С 3D УЛТРАЗВУКОВ АНЕМОМЕТЪР

Захари Динчев[1], Ясен Горбунов[2], Надежда Костадинова[3]

[1] Минно-геоложки университет "Св. Иван Рилски", 1700 София, e-mail: dinchev@mgu.bg
[2] Минно-геоложки университет "Св. Иван Рилски", 1700 София, e-mail: y.gorbounov@mgu.bg
[3] Минно-геоложки университет "Св. Иван Рилски", 1700 София, e-mail: nadezhda.kost@gmail.com

РЕЗЮМЕ. Развитието на технологиите прави възможно използването на съвременни устройства за тридименсионни измервания като например ултразвуковите анемометри. Чрез тези устройства се получават голям обем измерени данни, които чрез GPS позиционираща система и запис на SD карта посредством безжична връзка са на разположение на инженерните специалисти в електронен вид. Усъвършенстванията на уреда са реализирани от авторите и са представени в окончателния си вариант. Важно продължение на работата е визуализация на векторното поле. Статията представя няколко начина за визуализация с използване на приложните софтуерни продукти Surfer и Grapher. Представено е реално измерено 3D векторно поле и разрези по xy, yz и xz равнините.

Ключови думи: ултразвуков анемометър, скоростно поле, измерване, визуализация, регистриране на данни

Introduction

Real time velocity field measurement is a valuable and highly useful technique in many spheres of aerodynamics and ventilation (Francia V. at. all, (2016)). In the Report of Project MTF 159/2017 and in the paper (Dinchev Z., Gorbunov Y., 2017) the main features of the ultrasonic 3D anemometer are presented, together with the possibilities for instrumentation improvements in the following aspects: automation of measurements by implementing a data logging device with a possibility for storing on a SD card, automatic location registration via GPS, addition of a Bluetooth connection for easing mobile data transfer and for user convenience. Other authors also present modernization and special approaches in measurement technique with ultrasonic anemometers (Hietanen J. 2010).

This paper presents the ultimate realization of these device modernizations. The great amount of acquired data in the process of measurement needs specific treatment in order to get the output in applicable engineering presentation in a plane, surface and volume. Special attention is paid to the methodology for visualization of velocity fields by utilizing different software products.

Connecting the anemometer with the data logging device

A general overview of the setup is given in Fig. 1. As a main controller unit an 8-bit MCU-based Arduino platform is used. It represents an open software and open hardware project and provides short development times and easy programmability at a rational price. Programming is performed in the Arduino IDE via built-in libraries. The source code of the program is given in Appendix 2 of Report of Project MTF 159/2017, while the description of the included components is in Appendix 3 of the same project.

The anemometer has battery power supply of 12-24V which is further reduced by a DC-DC converter down to 3.3V. Such voltage is required by the Arduino system and the attached GPS, SD card (Elecrow Model MCS01107S) and Bluetooth. The anemometer communicates with the controller via the four provided analog voltages for the U, V, W and T vectors. The MCU reads the GPS data, adding coordinates to measured values of velocity vectors in the x, y and z directions. Next, it records the full information about the measured values and coordinates on the SD card.

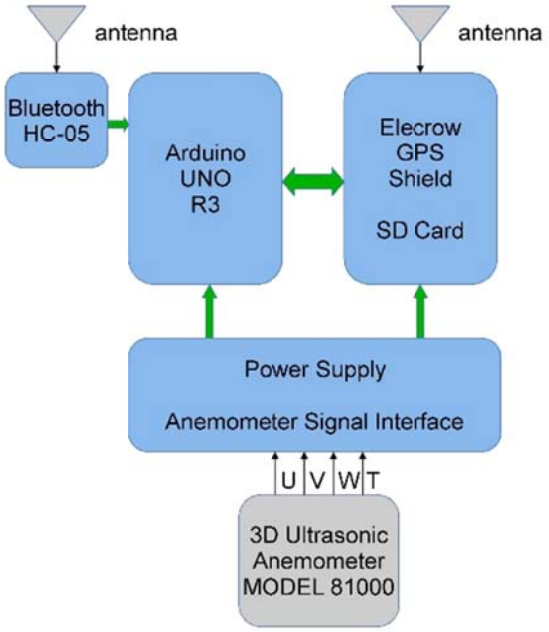

Fig.1. A general overview of the system

In Fig. 2 the final view of the controller is shown.

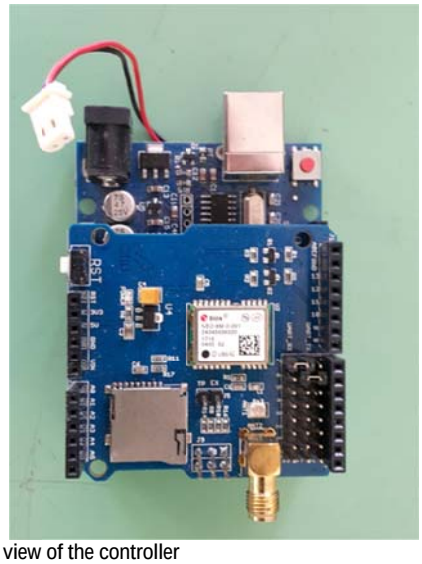

Fig.2. Final view of the controller

The Arduino board is located into a secure plastic box, which is mounted on the anemometer stand – see Fig.3. The external GPS antenna and the Bluetooth receiver placed inside the box are not shown.

Fig.3. Anemometer with the attached controller box

Performed measurements with MODEL 8100

First, it is important to place and orient the anemometer in the right position (fig. 4) – ideally facing the north geomagnetic pole or in the position that is along the tube. After this step the anemometer performs synchronization of devices for link to GPS and Bluetooth and initiates measurement. A new file in the comma-separated (CSV) format is created for every measurement cycle and the data is saved every second. The content of the file has the structure given in Table 1:

Table 1.

GPS_ LAT	GPS_ LON	GPS_ DATE	GPS _TIME	U [m/s]	V [m/s]	W [m/s]	T ['K]
				x	y	z	

where:
GPS_LAT – latitude, deg
GPS_LON - longitude, deg
GPS_DATE – data in format dd/mm/yyyy
GPS_UTC_TIME –time of record, UTC hh:mm:ss
U [m/s] – velocity vector, m/s (orientation east / west) – Fig. 4;
V [m/s] – velocity vector, m/s (orientation north/ south) –Fig.4.;
W [m/s] - velocity vector, m/s (orientation down/up), Fig. 5 m/s
T['K] – temperature of air flow, °K.

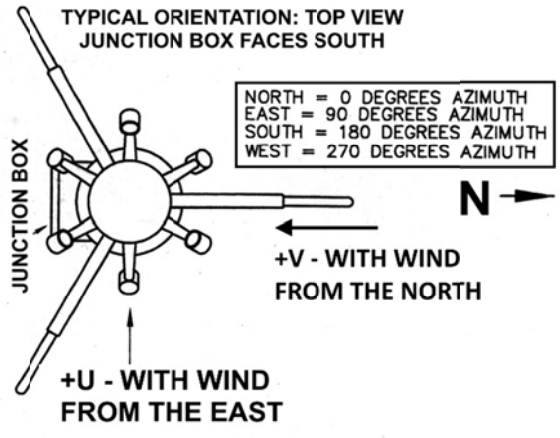

Fig.4. Orientation of the anemometer device

In case if no GPS connection is available (for instance underground) or the measurement is performed in a restricted area where the latitude and the longitude in different points are negligible, a close spare scenario is developed. The GPS data is switched off by a hardware button. Then the user inputs unique coordinates in the measuring points.

The orientation shown in Fig. 4 and 5 is used when performing measurements outdoor. When measurements are being taken indoor, the device orientation is the following: the direction north should coincide with the ordinate Y, thus receiving data in XY coordinated system – 2D surface velocity field. Changing the orientation allows 2D visualization in all planes (XY, XZ, YZ). Using three coordinates (X - GPS_LAT , Y - GPS_LON , Z – height) it makes it possible to achieve 3D visualization of the vectors – this is called the volumetric velocity field. Special attention is paid to data transformations, depending on specific application of results (Walker Ian J., 2004). Different approaches are possible to perform graphical

visualization in the chosen view. Further presented in the paper are 2D and 3D visualizations with specialized software products of Golden Software company – Grapher and Surfer, as well as with MatLab.

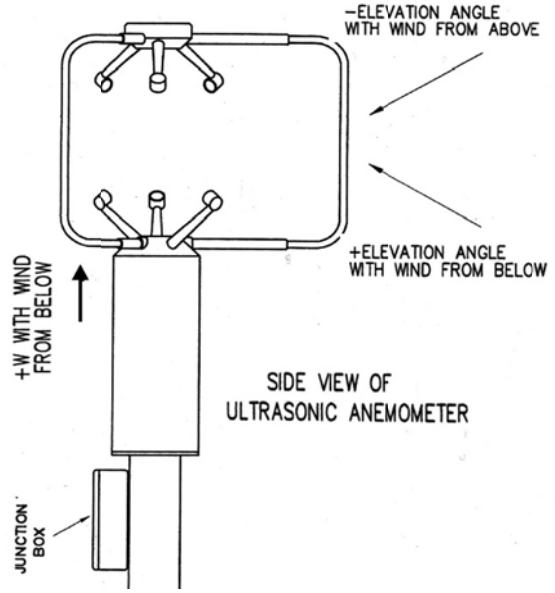

Fig.5. Side view of the anemometer device

The collected data from the file is transformed into EXCEL columns, representing vectors in three dimensions, thus giving a chance to calculate velocity scalar – Table 2.

Table 2.

tau	u	v	w	скорост
1	-0.3	-0.2	0.86	0.932523
2	-0.7	0.28	-0.3	0.811419
3	-1.18	0.96	0.68	1.666253
4	-0.8	0.48	0.58	1.098544
5	0.68	0.08	0.48	0.836182

Velocity field visualization

2D Visualization

The 2D visualization requires selection of surface in which velocity field needs to be drawn - XY, XZ or YZ. To do so additional transformations of measured data are fulfilled. The purpose of these transformations is to locate each vector direction, value and azimuth angle. As stated above, the planes for visualization and data required for each of them are:

- for plane XY – U and V
- for plane XZ –U and W
- for plane YZ – V and W).

The approach for each plane is similar to the one presented hereafter for plane XY. Vector's scalar mXY is:

$$mXY = \sqrt{U^2 + V^2} \ ,m/s \qquad (1)$$

The azimuth angle is defined depending on the vector position, bearing in mind that the anemometer measures the direction from where the wind flows, while the picture should visualize the direction of the vector. Following the structure given in Table 1, the value of U follows the East-West direction, while the value of V follows the direction Nord-South. Which means that if U<0 and V<0, the azimuth angle is in Ist quadrant, i.e. $0^\circ < \theta < 90^\circ$. The azimuth angles θ, representing the values of U and V are defined in the following way:

- if U<0 and V<0 $an = \theta = \arctan|U/V|$ - angle is in Ist quadrant;
- if U<0 and V>0 $an = \theta = 180 - \arctan|U/V|$ - angle is in IInd quadrant;
- if – U>0 and V>0 $an = \theta = 180 + \arctan|U/V|$ angle is in IIIrd quadrant;
- if U>0 и V<0 $an = \theta = 360 - \arctan|U/V|$ - angle is in IVth quadrant.

The velocity vectors on other planes are drawn in similar way, changing measured data for V and W (YZ) and for U and W (XZ) respectively.

Table 3 shows an EXCEL file, which is used by the software applied by authors to draw the velocity field.

Table 3.

x	y	z	u- dx	v-dy	w-dz	V-xy	angle
0	0	0	-0.3	-0.2	0.86	0.36	56.31
2	0	0	-0.7	0.28	-0.3	0.75	111.80
4	0	0	-1.18	0.96	0.68	1.52	129.13
0	2	0	-0.8	0.48	0.58	0.93	120.96
2	2	0	0.68	0.08	0.48	0.68	263.29
4	2	0	0.08	0.78	0.18	0.78	185.86
0	4	0	0.28	0.48	0.38	0.56	210.26
2	4	0	-0.1	-0.6	0.18	0.61	9.46
4	4	0	0.28	0.38	-0.1	0.47	216.38
0	6	0	0.38	0.58	0.58	0.69	213.23
2	6	0	-0.2	0.86	1.06	0.88	166.91
4	6	0	0.38	0.68	0.6	0.78	209.20

Visualization, after the above presented modification (Tabl.3) of measured data, is presented by Grapher and Surfer. Both ways are discussed below. Grapher software makes 2d and 3D visualization without interpolation between measuring points – i.e. it only registers the measurement. Surfer software makes interpolation between measured points and its velocity field is more fluent, but it can make only 2D plots. Very useful product of the same company (Golden Software) is Voxler, which creates 3D grid and surface diagram of isolines of equal velocities.

Visualization with GRAPHER

Fig. 6b shows 12 vectors in the XY plane, achieved by the data transformation shown in Table 3. Starting from the point of origin (X,Y), then taking into account angle (an) and scalar value mXY, vectors are drawn in the plane with size, representing measured area. Parts of GRAPHER's properties are shown in Fig. 6a, while the diagram itself – in Fig 6b.

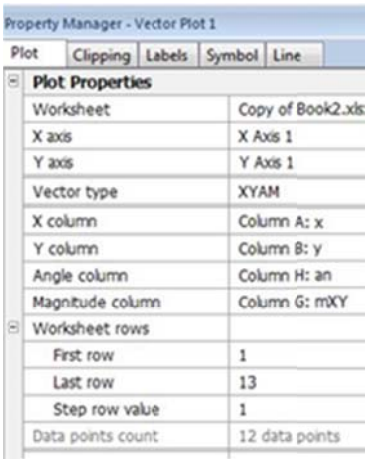

Fig. 6a. Golden Software Grapher properties

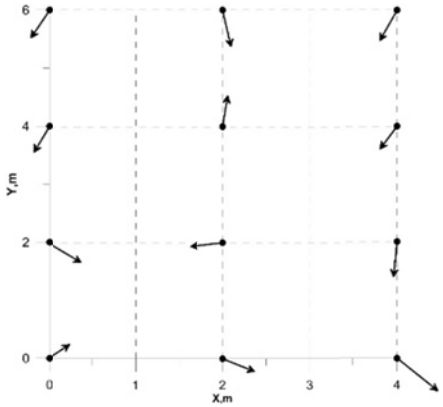

Fig. 6b. Golden Software Grapher plot of 12 vectors

Visualization with SURFER

This software generates 2D velocity field by interpolation between measured single vectors in a chosen plane (XY, YZ or XZ). If selecting „2 – Grid Vector Map" from the program menu two interpolation grid files with extension GDR are created. First of them holds information about the initial coordinates of the vector in the plane (XY) and the azimuth angle, while the second one contains the coordinates and scalars. The two files are created sequentially by „Surfer", taking as an input file the one, shown in Table 3. Fig. 7a shows part of the positions in Surfer, while Fig 7b shows the velocity field in the XY plane.

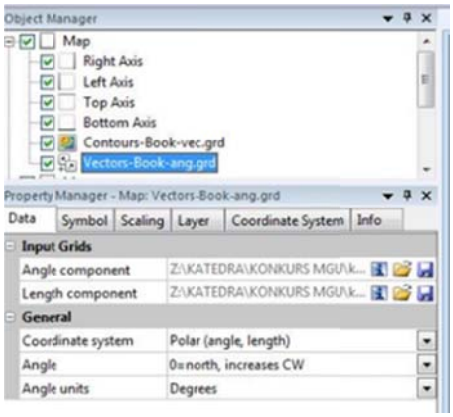

Fig. 7a. Golden Software Surfer Object Manager screen

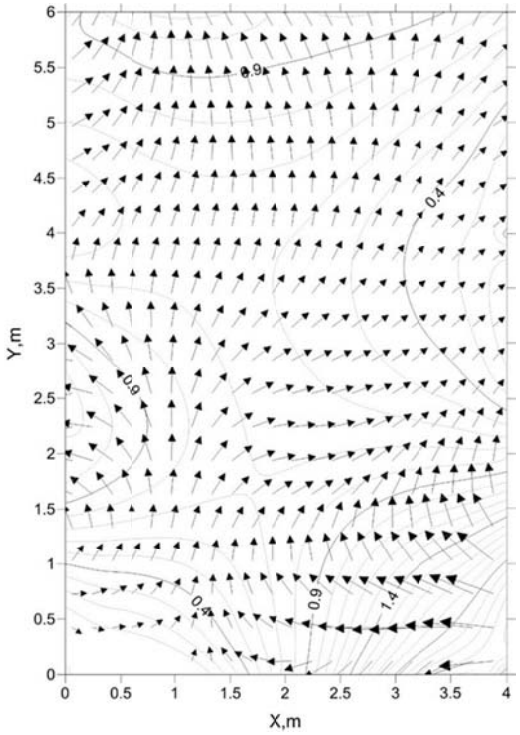

Fig. 7b. Golden Software Surfer velocity field plot in the XY plane

3D Visualization with GRAPHER

3D visualization with "Grapher" is performed by using the function "XYZ vector plot". The diagram may be in two different views according to the available data:

- absolute coordinates given by the GPS device of origin point of vectors (X, Y, Z) in the measured region and vector projections on three axes (dx, dy, dz) or relative coordinates given by the user when the GPS is switched off;
- evaluation of vector's end (X2, Y2, Z2) coordinates based on vector's origin (X1, Y1, Z1) and azimuth angle. This approach is complicated, because it requires numerous mathematical transformations, but when the location is important it may be used for special purposes.

Fig. 8a shows part of the Grapher parameters used in function "XYZ Vector Plot", while Fig 8b – the 3D velocity field.

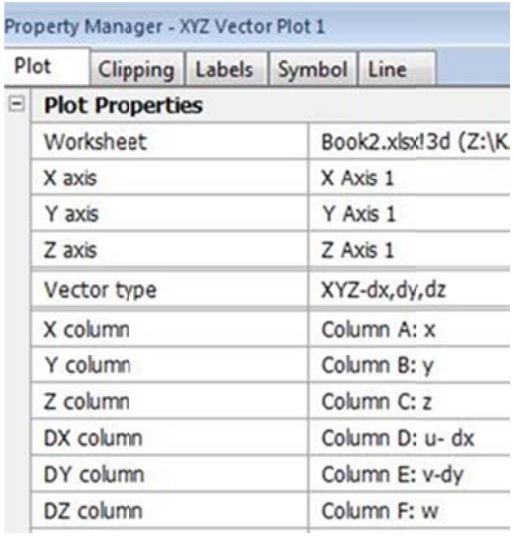

Fig. 8a. Golden Software Grapher XYZ vector plot settings

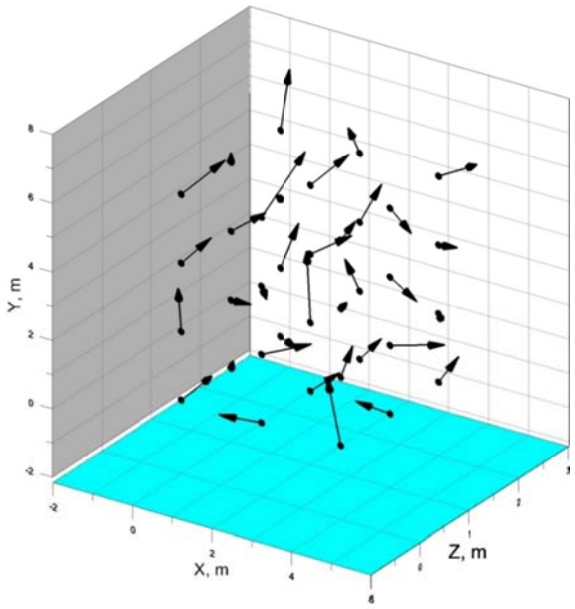

Fig. 8b. Golden Software Grapher 3D velocity field plot

3D Visualization with MATLAB

A 3D data visualization can be performed with the aid of the MathWorks Matlab matrix laboratory mathematical package. This visualization is performed by Matlab's function "quiver3" with the following syntax:

```
quiver3(x,y,z,u,v,w)
quiver3(z,u,v,w)
quiver3(...,scale)
quiver3(...,LineSpec)
quiver3(...,LineSpec,'filled')
quiver3(...,'PropertyName',PropertyValue,...)
quiver3(ax,...)
h = quiver3(...)
```

A velocity field plot obtained by using the "quiver3" function is shown on Fig. 9.

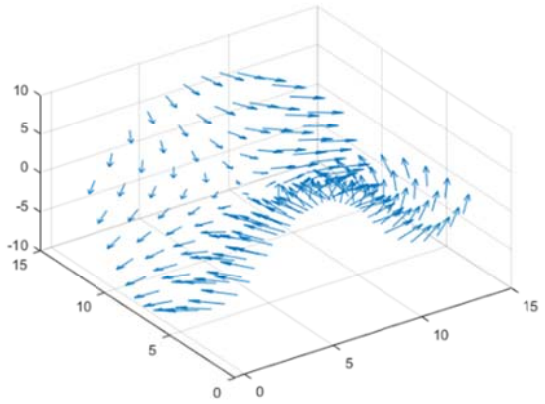

Fig. 9. Velocity field plot obtained by using the 'quiver3' function

In situ experiment

Fig. 10 shows the experimental measurement setup, which is performed in a restricted space with dimensions: L= 30 m, W= 2,7 m. An axial fan, located 10 meters away from measurement points, is connected to a flexible duct. The 3D anemometer is consecutively located into 20 points, at three levels:

- Z_0=1.1 m below center axis of the pipeline;
- Z_1=1.55 m along the center axis of the pipeline;
- Z_2=1.8 m above the center axis of the pipeline.

The points create a regular mesh in rows and columns. The space between the points in a row is 0.54 m, while the row to row distance is 2 m.

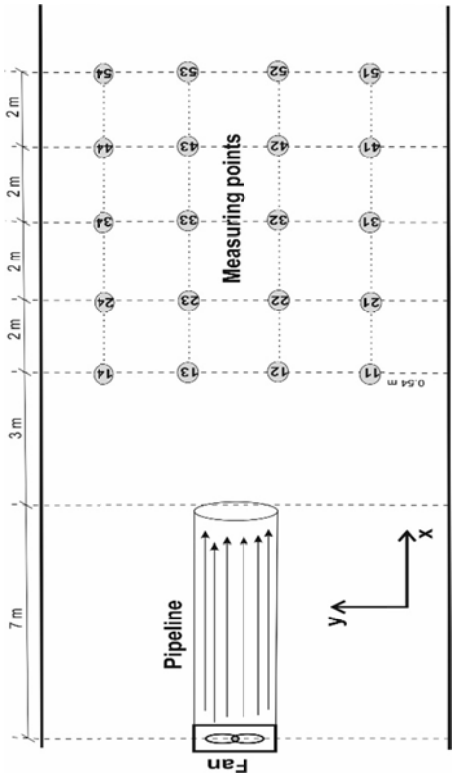

Fig. 10. The experimental measurement setup

As the anemometer measures 32 values per second, the measurement in each point has a duration of 1 min and data is saved into a file with a unique name. The results of the measurements are saved into 20x3=60 data files. Then, following the methodology explained above, velocity vectors in each point can be evaluated and different visualizations can be performed.

Fig. 11 shows the XY velocity vectors and lines of equal velocities for two elevations:

- for Z=1.1 m on fig. 11a;
- for Z=1.55 m on fig. 11b.

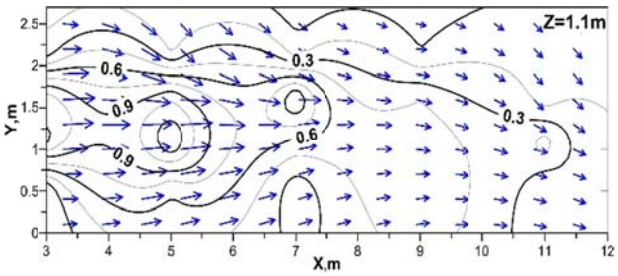

Fig. 11a. The XY velocity vectors and the isolines for Z=1.1[m]

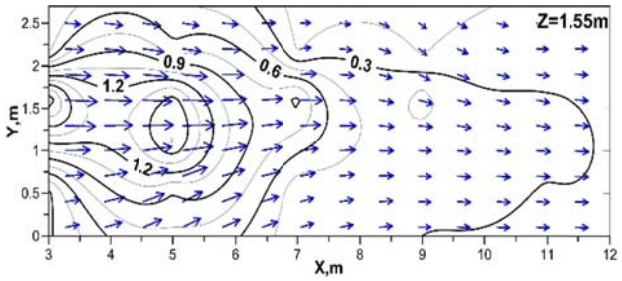

Fig. 11b. The XY velocity vectors and the isolines for Z=1.55[m]

The elevation Z=1.55 m is in plane, parallel to the main flow current from the pipeline. There velocities are higher, compared to Figure 11a. They are within a range of 1.2 m/s to 0.3 m/s, while on the lower level maximum velocity is 0.9 m/s. Another interesting point is that at the lower level wall the effect is bigger and can be observed in Fig. 11a.

Fig. 12 shows velocity field with vectors and scalars in plane XZ for two Y locations:

- For Y=1.1 m in fig 12a – i.e. in the middle of the space in Y direction;
- For Y=0.54 m on fig 12b – close to the wall.

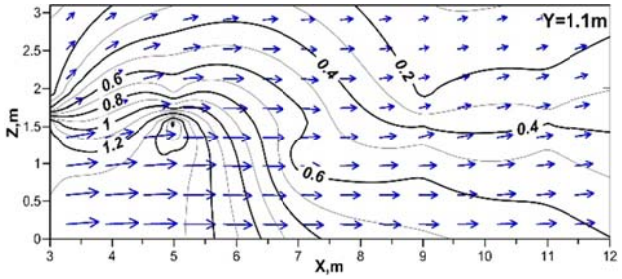

Fig. 12a. The XZ velocity vectors and the isolines for Y=1.1[m]

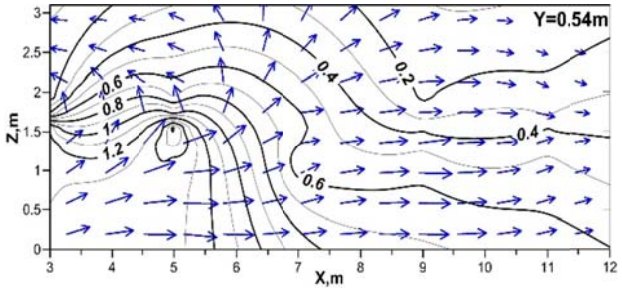

Fig. 12b. The XZ velocity vectors and the isolines for Y=0.54[m]

The wall effect is perfectly observed in Fig. 12b, leading to recirculation of the current. In Fig. 12a one can notice well developed flow in the middle of the area with minimum fluctuations toward walls and nearly missing recirculation.

Conclusion

The 3D anemometer, being a modern measuring device, is capable of collecting great amounts of data when performing flow velocity measurements. However, its ability to measure so many values – 32 measurement per second, raise the necessity of special data treatment in order to present the measured velocity field in practically applicable view. This paper shows several approaches which can be applied.

In general, measurements with 3D anemometer have several very practical applications:

- point measurement may serve as a tool to define coefficient of turbulence;
- as seen from Figures 11 and 12, wall effect can be seen and also the recirculation along it;
- it is also highly important to see how far from the end of a pipeline, the influence of the fan can take place.

All that directions will be explored in future work.

Acknowledgements

This work is supported by contract No MTF-159/2017, University of Mining and Geology "St. Ivan Rilski", Sofia.

References

Dinchev Z., Gorbunov Y., Improvement of Measurements of 3d Air Flows in Free and Semi-Restricted Space, Journal of Mining&Geological Sciences, 2017, vol. 60, Part II, Mining, Technology and Mineral Processing, p. 39-42

Gill Instruments Limited, How do Gill Ultrasonic Anemometers Work

Hietanen J. New Standard Ultrasonic Wind Sensor Platform, WMO Technical Conference on Meteorological and Environmental Instruments and Methods of Observation, 2010, P1-19

Taylor C., Timko R., Thimons E., Mal T. Using Ultrasonic Anemometers to Evaluate Factors Affecting Face Ventilation Effectiveness, Presented at the Society for Mining, Metallurgy, and Exploration (SME) Annual Meeting, Salt Lake City (2005)

Ultrasonic Anemometer Model 81000, R.M. Young Company, USA, 2801 Aero Park Drive, Traverse City, Michigan 49686, Rev. I102210, 2017

Wilson N., Paldanius J., Hietanen J., Practical Applications of Ultrasonic Wind Sensors for Resource Assessment, EWEA The European Wind Energy Association, Copenhagen, Denmark. April 16th - 19th 2012

Динчев, З. Изследвания върху нетрадиционни методи и конструкции за проветряване на минни и индустриални обекти, дипломна работа, МГУ „Св. Иван Рилски", 2014 (Izsledvania varhu netraditsionni metodi i konstruktsii za provetryavane na minni i industrialni obekti, diplomna rabota, MGU „Sv. Ivan Rilski")

Проект МТФ – 159/2017, Усъвършенстване на измерванията на 3D въздушни течения в свободно и полуограничено пространство, Архив НИС МГУ, София (Proekt MTF – 159/2017, Usavarshenstvane na izmerva-niyata na 3D vazdushni techenia v svobodno i poluogranicheno prostranstvo, Arhiv NIS MGU, Sofia) (bg text)

Walker Ian J., Physical and Logistical Considerations of Using Ultrasonic Anemometers in Aeolian Sediment Transport Research, Elsevier, Geomorphology 68 (2005) 57–76

Francia V., L. Martín, A.E.Bayly, M.J.H.Simmons, (Use of Sonic Anemometry for the Study of Confined Swirling Flows in Large Industrial Units, 2016, Elsiever, Flow Measurement and Instrumentation 50216–228

Arduino Elecrow Model MCS01107S GPS Logging Shield, https://www.elecrow.com/wiki/index.php?title=GPS_shield

SAFE TREATMENT OF EXPIRED MEDICINES

Blagovesta Vladkova[1], Luka Arbaliev[1], Veronika Karadjova[2]

[1]University of Mining and Geology "St. Ivan Rilski", 1700 Sofia, b_vladkova@yahoo.com
[2]University of Chemical Technology and Metallurgy, Sofia, vkar@mail.bg

SUMMARY: Every household has medicaments that have become time-expired. In this case, the following issues arise: what to do with these medicaments, how medical waste is treated, and what potential environmental impacts such medicines would have. In an attempt to answer these questions, a study was carried out in two directions. In the first direction, matters of administrative nature were clarified, such as correspondence with institutions, structures and organisations involved in this activity, as well as public awareness of the approaches applied. An experimental part was also carried out, namely experiments with soils contaminated with drugs and tracking the development of crops in such soils.

Keywords: time-expired medicaments, waste treatment, safety, environment, health, sustainable development

БЕЗОПАСНО ТРЕТИРАНЕ НА МЕДИКАМЕНТИ С ИЗТЕКЪЛ СРОК НА ГОДНОСТ

Благовеста Владкова[1], Лука Арбалиев[1], Вероника Караджова[2]
[1]Минно-геоложки университет "Св. Иван Рилски", 1700 София, b_vladkova@yahoo.com
[2]Химико - технологичен и металургичен университет, София, vkar@mail.bg

РЕЗЮМЕ: Почти във всяко едно домакинство се случва да се съберат лекарства, които с времето са остарели и срокът им на годност е изтекъл. В такъв случай възниква въпросът какво да се направи с тези медикаменти, как се третират отпадъците, какви биха потенциалните въздействие върху околната среда. В опит да се отговори на тези въпроси бе направено проучване в две направления – приложна част, състояща се в кореспонденция с ключови държавни структури и организации, изясняване на проблема и предложения за увеличаване на степента на информираност на населението; експериментална част – извършване на практически опити със замърсени с лекарства почви и проследяване развитието на посеви в такива почви.

Ключови думи: медикаменти, третиране на отпадъци, изтекъл срок на годност, здраве, околна среда, устойчиво развитие

Introduction

The problem with the collection and treatment of waste from household chemicals (empty packs of detergents, paints, varnishes, etc.) as well as expired medicaments is particularly relevant. The trend in recent years is for the flow of such waste to be managed. Thus, and the culture of separate collection of waste was imposed on the population.

This article is part of a conducted overview of the current status of the topic for the treatment of pharmaceutical waste from the households. The material discusses two directions-results of correspondence with key institutions (the Ministry of Health, BDA /the Bulgarian Drug Agency/, etc.) as well as the completed experimental part [31, 32].

The correspondence with different control authorities has shown gaps in the algorithms for providing information to the community. People are not responsible and committed to the common culture of treating household waste (household chemistry, old medicines, etc.). The lack of a single media bearer and the low information of society as a whole contribute to this situation, too.

The experiment aims to trace how the soil composition contaminated with expired medicines changes and, subsequently, to monitor the crops to be planted in this soil and their growth. It has been found that different medicaments affect the composition and the properties of the soil solution and, consequently, the growth of crops. Conducting of such tests is topical, both in environmental and in agricultural aspects, as it makes it possible to obtain information of the ongoing processes in the soil [1, 2].

Setting the Experiment

For the represent studies, an approach was chosen in which plots were used separately with soil from a random uncovered area which is not prepared or pre-treated. The soil was placed in monolithic containers (pots) whose volume and height were adapted to the needs of talking samples.

Seven pots of soil were prepared (Fig. 1), in five of them the selected medicaments were placed (pots № 8, 10, 11, 12, and 13) and in one of the pots a mixture of the powdered medicaments was placed. In the last pot (№14), only soil from a randomly selected uncovered area was placed, which served as a benchmark.

Fig. 1.

During the experiment, several types of expired medicaments which the authors have at their home "pharmacy" were selected arbitrarily. Their composition and properties are described in Table 1 [1].

Table 1.

medicine	*Composition*	*Undesirable medicine effects*	*Quantity*
Medicament *(film-coated tablets)*	*Atenolol 50 mg Additional ingredients: lactose monohydrate, wheat starch, microcrystalline cellulose, sodium starch glycollate, gelatin, talc, silicon dioxide, magnesium stearate, sparing white*	*Rash or itching, swelling of the face and / or difficulty in breathing, pain in joints, with or without fever, redness, severe diarrhea with bleeding*	*6 g*
Medicament *(tablets)*	*Magnesium citrate 600 mg Magnesium 98.6 mg Other Ingredients: sucrose, powdered cellulose, citric acid, xanthan gum, calcium kakonoat, sodium cyclamate, flavoring materials, coloring agent E 104*	*Diarrhea*	*21 g*
Medicine 3 *(eye drops - solution)*	*20 mg Dorzolamide like (Dorzolamidovhidrohlorid) and 5 mgTimolol (as Timololovmaleat). excipient substancecs mannitol, hydroxyethyl cellulose, sodium citrate, sodium hydroxide, benzalkonium chloride, water for injections*	*Facial swelling, itchy skin, difficulty breathing, hives, burning and stinging eyes, change in taste, burning sensation in the eye, itching of the eye, blurred vision, headache, dizziness,*	*5 ml*
Medicine 4 *(powder solution for injection)*	*Cefazolin sodium 1.048 g*	*Nausea, vomiting, loss of appetite, diarrhea, oral candidiasis, fever, skin rashes, in patients with renal insufficiency, nephritis, hepatic reaction and others.*	*1 g*
Medicine 5 *(hard capsules)*	*Cefaclor 500 mg as (cefaclormonohydrate). Other Ingredients: натриев нишестен глюколат, магнезиев стеарат, желатин, титанов диоксид, еритрозин, индигокармин*	*Rash or itching, swelling of the face and / or difficulty in breathing, pain in joints, with or without fever, redness, severe diarrhea with bleeding*	*4 g*
Medicine 6 *(Mixture of powdered pharmaceutical forms)*	*Atenolol, Magnesium Diasporal, Cefazolin, Medoclor*		*10.2 g*

Note: The names of the medicaments used for the studies are not indicated to avoid conflict with the manufacturer

Conducting the experiment

Sample preparation

The first stage of the preparation of the samples was powdering the tablet forms of pharmaceutical products and the preparation of a powder mixture. Such a preparation is not applicable to the capsules which are in manufactured in a powder form and the drops - they come in a liquid form [1].

The next step is the weighing of the medicaments to determine the exact quantities to be placed in the soil studied (Figure 2).

Fig. 2. Sample preparation

The samples (medicaments) were placed in soil under normal atmospheric conditions on 30th March 2018. The sites prepared for testing are shown in Figure 3.

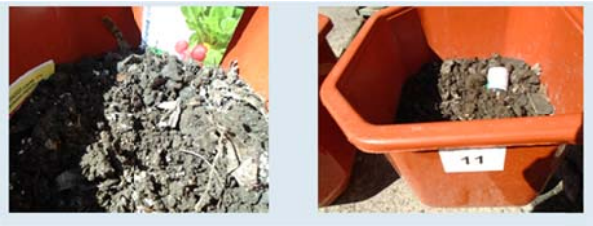

Fig. 3. Sowing the seeds of radishes

On 2nd April 2018, the pots with the time-expired medicament samples were planted with radish seeds (fig. 3). The experience with the planting of crops aimed to check the effect of medicines on the plants. The sowing was chosen due to the rapid growth of the radishes and its large contact surface with the soil.

The contents of the pot and the precise amounts of medicaments therein are presented in Table 2.

Table 2.
Distribution of the drugs in the individual pots with samples

Number of sample pot	***Medicinal product***	***Quantities placed in the soil***
Pot №8	*Medicinal product 1*	*4 g*
Pot No. 9 (mixture)	*A mixture of the medicinal product 6*	*10.2 g*
Pot №10	*Medicinal product 2*	*14 g*
Pot №11	*Medicinal product 4*	*0.2 g*
Pot №12	*Medicinal product 5*	*3 g*
Pot №13	*Medicinal product 3*	*5 ml*
Pot No. 14 benchmark sample	*BENCHMARK- Free of medicinal products*	*no*

Figures 4, 5, and 6 illustrate a crop image material and show the growth of the crops at different stages of the study, tracking the effect of the medicaments or lack of such (pot 14) on the radishes.

Fig. 4. Image of the crops from 12th April 2018

Fig. 5. Image of the crops from 26th April 2018.

Fig. 6. Image crop of radishes on 8th May 2018

Analysis of soil samples

The study of structure and properties of the soil solution gives valuable information on ongoing soil processes and is of important theoretical and practical importance [3-5, 10, 11].

In a study of soils in practice, a number of analyses can be carried out and their selection depends on the needs. Analyses may include:

1. Microbiological indicators
2. Physiochemical Indicators:
   - Determination of pH
   - Determination of total and organic carbon
   - Determination of total nitrogen (Kjeldahl)
   - Determination of nitrate nitrogen, ammoniac nitrogen and total soluble nitrogen
   - Determination of phosphorus
   - Determination of carbonates
   - Analysis of metals
   - Determination of water and acid-soluble sulphates
   - Determination of total sulphur
   - Determining the mechanical structure
   - General exchangeable acidity/Free hydrogen
   - Determination of mercury
   - Determination of the specific electrical conductivity
   - Bulk density
   - Dry matter/moisture content

Two methods of analysis were selected to study the effects of the selected medicaments on the soil solution - for the determination of pH and metals which are not notably expensive and at the same time provide information on the changes occurred as a result of the medicaments [4-9].

The tests carried out complied with the requirements for soil sampling, namely:

- Soil samples were taken in dry weather;
- The samples were taken from a depth of 0-30 cm;
- The transportation and storage of the test sample was carried out in a in a way which ensured steadiness in the composition of the sample taken for analysis from the time of collection at the time of testing (Fig. 7).

Fig. 7.

Study of pH

To study the pH of the soil samples, a soil solution was taken which passed through the following three stages (Fig. 8, Table 3):

- 1. Taking of soil samples and preparation of bulk monoliths.
- 2. Preparation of a soil solution.
- 3. Analysis of the resulting solution composition.

Fig. 8.

Table 3. Results from the pH analysis of the test samples

Sample-benchmark No. 14 * pH = 7.20, No 14 ** pH = 7.22						
Sample	**8***	**8****	**9***	**9****	**10***	**10****
pH	6.88	6.90	7.10	7.10	7.07	7.09
Sample	**11***	**11***	**12***	**12****	**13***	**13****
pH	6.98	6.91	7.02	7.02	7.10	7.11

Note: The numbering of the samples is as follows:

The first and the second sample of the different tested soils taken at an interval of 30 days are marked with * and **, respectively. In such a way, the change of pH is monitored over time and under the influence of the atmospheric conditions.

Analysis of metals

The test samples were prepared by the method of acid dissolution of the sediments, sludge and soils to comply with procedures and preparation for analysis by means of atomic-emission spectrometry with inductively coupled plasma (ICP-AES) [9, 11]. Samples prepared by this method were analysed by ICP-AES, with the *Prodigy* High Dispersion ICP-OES apparatus (Fig. 9 and 10).

Fig. 9. Preparation of the samples by the method of acid dissolution

Fig. 10. The *Prodigy* HighDispersion ICP-OES Apparatus

Table 4.
Results from the ICP-OES analysis of the test samples in mmol / l

	Sample							
element	**8***	**8****	**9***	**9****	**10***	**10****	**11***	**11****
Barium / Ba	4.982	4.443	5.831	7.011	5.342	6.339	5.311	5.568
Cadmium / Cd	0.446	0.387	0.203	0.205	0.205	0.249	0.215	0.219
Chromium / Cr	2.880	3.129	1.379	1.351	3.458	3.804	3.001	3.255
Copper / Cu	6.715	6.130	4.479	4.653	4.506	5.796	4.719	4.546
Lead / Pb	7.020	6.315	4.458	4.580	5.264	6.042	5.357	6.994
Manganese / Mn	8.253	7.209	8.175	8.089	6.024	7.057	7.533	7.555
Nickel / Ni	0.270	0.412	0.322	0.333	0.304	0.399	0.356	0.386
Sodium / Na	7.759	7.718	7.442	7.312	5.388	6.913	7.343	7.156
Strontium / Sr	0.822	0.736	0.674	0.692	0.566	0.682	0.576	0.572
Cobalt / Co	0.144	0.149	0.184	0.186	0.186	0.174	0.167	0.184
Aluminum / Al	93.71	95.02	115.6	120.4	98.01	122.5	114.1	115.1
Calcium / Ca	689.1	578.6	366.8	356.3	284.2	337.9	279.6	287.6
Iron / Fe	264.8	235.3	416.5	439.5	267.8	334.6	407.3	408.6
Magnesium / Mg	100.1	88.93	87.78	85.71	62.51	77.77	66.60	74.31
Potassium/K	11.16	11.32	14.59	15.08	12.08	15.04	12.54	14.07
Zinc / Zn	44.60	40.69	41.27	44.64	36.45	43.94	40.92	39.74
Arsenic / As	0.073	0.062	0.097	0.083	0.086	0.122	0.098	0.113
Sulfur / S	7.158	7.357	8.320	9.460	8.520	10.93	10.92	11.71
Phosphorus / P	6.739	6.229	8.100	8.427	7.918	8.584	8.782	9.154
Tin / Sn	0.149	0.133	0.062	0.053	0.067	0.118	0.076	0.083

	Sample					
Element	**12***	**12****	**13***	**13****	**14***	**14****
Barium / Ba	5.591	5.819	6.300	5.642	5.475	5.418
Cadmium / Cd	0.204	0.198	0.172	0.165	0.275	0.267
Chromium / Cr	1.895	1.890	2.551	2.517	2.192	2.464
Copper / Cu	4.330	5.101	3.610	3.642	4.032	3.987
Lead / Pb	5.818	5.782	4.583	4.212	4.676	4.716
Manganese / Mn	6.911	6.878	7.718	7.221	7.468	7.437
Nickel / Ni	0.366	0.358	0.275	0.278	0.319	0.312
Sodium / Na	7.177	8.616	6.172	6.907	4.758	5.664
Strontium / Sr	0.525	0.541	0.692	0.684	0.704	0.582
Cobalt / Co	0.159	0.152	0.119	0.112	0.168	0.160
Aluminum / Al	128.3	125.3	106.7	106.1	109.8	109.7
Calcium / Ca	266.2	275.7	342.5	326.9	346.4	327.8
Iron / Fe	424.7	435.9	305.7	297.0	365.1	357.4
Magnesium / Mg	70.52	70.05	74.91	70.31	71.65	74.48
Potassium/K	13.61	14.47	13.08	12.86	13.80	13.37
Zinc / Zn	45.25	44.74	38.24	36.02	39.38	39.68
Arsenic / As	0.084	0.091	0.090	0.085	0.081	0.071
Sulfur / S	11.68	11.91	10.61	10.31	10.48	10.30
Phosphorus / P	8.673	8.806	7.223	7.025	8.071	8.245
Tin / Sn	0.066	0.104	0.073	0.074	0.066	0.062

The change in the content of some of the heavy metals in the studied soils against the reference soil is presented graphically in Figure 11.

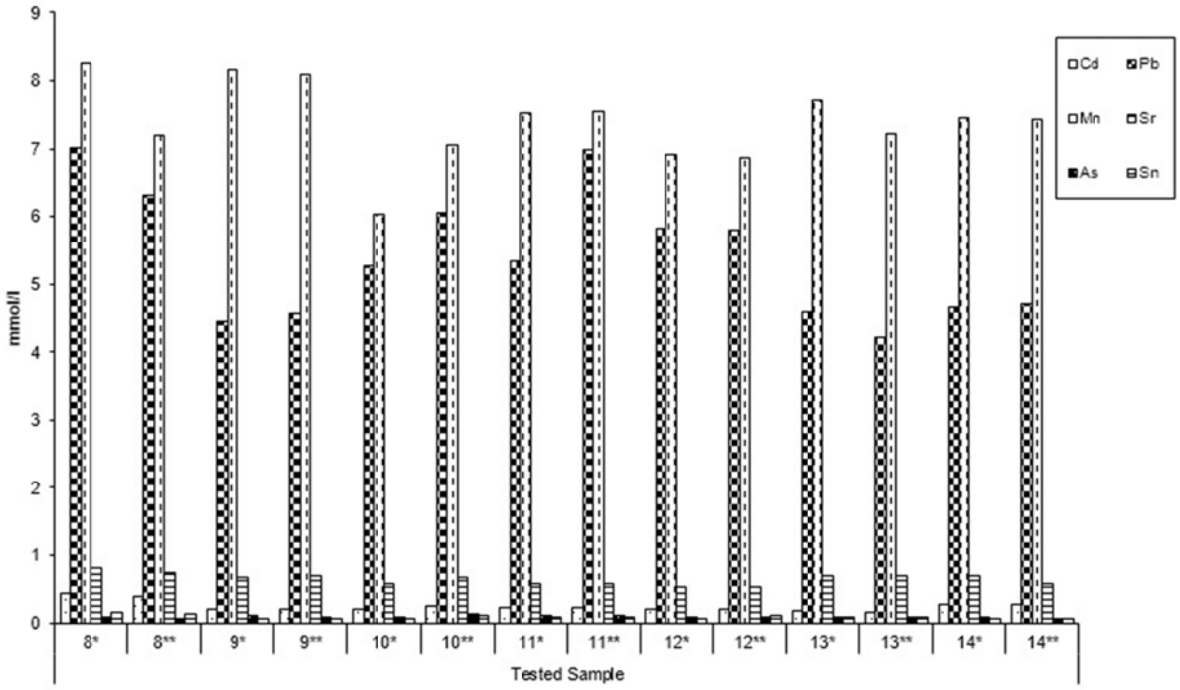

Fig. 11. Content of some heavy metals in the tested soils, compared to the soil-benchmark

Outcomes of the chemical analysis made:

- It has been found that the chemical composition of the soil solution in the tested soil is influenced by the composition of the medicament product.
- From all the studied soil samples in samples №9 and №13, the pH values are close to the basic of the used soil-benchmark pH = 7.22. In the other samples tested, the pH values ≤ 7, i.e. a lowering the pH was observed. The lowest value wasrecorded with the samples №8 (active component Atenolol) and №11 (active ingredient cefazolin sodium) (pH ≈6.90)
- From the medicaments included in the experiment, medicaments with highest content of heavy metals such as Cadmium (Cd), lead (Plumbum (Pb)), Manganese (Manganum (Mn)), Tin (Stannum (Sn)), and Strontium (Sr) were observed in soil sample №8 compared to sample №14 which is the benchmark soil.
- The obtained values shall not be compared to the acceptable benchmarks for the metal content and pH in the soil but they aimed to find a change in the composition of soils containing medicaments relative to the benchmarked soil.
- There is a difference in the growth of the crops, depending on the soil composition containing medicaments. Samples №9 and №13 were with better growth. Insufficient development of the plants was observed in the sample №10 (Fig. 6.).

Conclusion

The effect on the environment when disposing of time-expired medicaments should not be overlooked. In any case, this affects the quality and composition of the soil, and there is a danger from the passage of harmful substances in groundwater. The results from the chemical analyses (pH and metals) provide the basis from which the team can further expand their studies and conduct a more detailed research on the impact of medicinal products on the composition and properties of the soil and on crop growth.

Broader research and detailled analyses are needed to establish the precise degree of influence of medicaments on the soil composition and properties (and the ongoing soil processes). The studies presented in the present work may be the beginning of in-depth and comprehensive experiments with contaminated soils with medicaments. They should be conducted on an experimental site and with larger quantities of medicaments.

As a result of the conducted survey, notifications and suggestions to different institutions were submitted. Thus, the authors hope to have made the first steps towards improving the culture of the population in the field of waste treatment.

References

[1] Лука Арбалиев: "Безопасно управление на медицински и фармацевтични отпадъци от аптеки и болници" - дипломна работа за получаване на ОКС „Магистър", МГУ, Катедра „РВ и ТБ", София, юли, 2018 г. / (Luka Arbaliev, Master thesis, "Bezopasno uprawlenie na medicinski I pharmacevtichnii otpadaci ot apteki i bolnitzi" University of Mining and Geology, Sofia, July, 2018)

[2] Цецка Симеонова: "Състав и свойства на почвения разтвор при различни начини на земеползване", Автореферат на дисертация за даване на образователна и научна степен "Доктор", ИП "Н.Пушкаров" – София, 2010 г. / (Tzetzka Simeonova, PhD-Thesis, "Sastav i swoistwa na pochvenia raztwor pri razlichni nachini na zemepolzvaneto" N. Pushkarov, Sofia, 2010)

[3] Stela Georgieva, Petar Todorov, Emilia Naydenova, Electrochemical behavior of biologically active cycloalkanespiro-5-hydantoins, Analytical and bioanalytical electrochemistry, 2, vol.9, 2017, 214-231.

[4] Angelina Stoyanova-Ivanova, Denitsa Mitkova, Stela Georgieva, Victoria Vitkova, "Lipid bilayers as biocompatible model systems – does the acidity of the aqueous solution alter the membrane elasticity?", Advances in Natural Science: Theory & Applications, Volume 1 No. 1 2012, 29-35.

[5] Denitsa Mitkova, Angelina Stoyanova-Ivanova, Stela Georgieva, Petar Todorov, Nikolay Kozarev, Yury A. Ermakov, Victoria Vitkova, „Charged Lipid Bilayers in Aqueous Surroundings with Low pH", Advances in Planar Lipid Bilayers and Liposomes, Chapter one, Volume 18, 2013, p. 1-20.

[6] T. Nedeltcheva, M. Hristova, St. Georgieva, L. Vladimirova, Spectrophotometric determination of Cu (II) by the system I- - starch in the presence of Fe (III), Journal of the University of Chemical Technology and Metallurgy, 42, 4, 2007, 427-430.

[7] Kristina Gartsiyanova, Stela Georgieva, Assessment of the anthropogenic pollution of the Chepinska River, Proceedings of National conference with international participation "Natural Sciences 2017" (NCNS2017) (2017)-online;

[8] S Georgieva, K Gartsiyanova, V Ivanova and L Vladimirova, Assessment of Physical-Chemical Characteristics of Surface Water from Key Sites of the Mesta River: State and Environmental Implications, IOP Conf. Series: Materials Science and Engineering 374 (2018) 012093 doi:10.1088/1757-899X/374/1/012093

[9] D. Ilieva, A. Surleva, G Drochioiu, M. Murariu, M. Abdulah, Evaluation of ICP-OES Method for Heavy Metal and Metalloids Determination in Sterile Dump Material", Solid State Phenomena, Vol. 273, pp. 159-166, 2018

[10] G. Drochioiu, A. Surleva, D. Ilieva, L. Tudorachi, R. Necula, Heavy metal toxicity around a closed barite mine in Tarnita-Romania, 16th International Multidisciplinary Scientific GeoConference SGEM 2016, www.sgem.org, SGEM2016 Conference Proceedings, ISBN 978-619-7105-62-9 / ISSN 1314-2704, June 28 - July 6, 2016, Book3 Vol. 2, 525-532 ppDOI: 10.5593/SGEM2016/B32/S14.069

[11] M. Zaharia, G. Drochioiu, D. Ilieva, A. E. Butnariu, A. Surleva, Heavy metal toxicity and decontamination: tarnita closed mine pollution case, SGEM2017 Vienna GREEN Conference Proceedings, Vol. 17, Issue 43, 397-404 pp; DOI: 10.5593/sgem2017H/43/S19.050

[12] http://sembodja.bg/wp-content/uploads/2016/02/Указание-за-вземане-на-почвени-проби.pdf, 02/2016

[13] ttps://www.naas.government.bg/data/image/Lab/Ukazanie%20za%20vzemane%20na%20pochveni%20probi2017.pdf, 09. 2017

[14] http://www.globaltest-bg.com/testing/анализ-на-почви/, 20.05.2018

[15] http://eea.government.bg/bg/labs/vtr/instrumental, 25.04.2018

http://www.eurotest-control.bg/uslugi/izpitvane/pochvi, 14.01.2018

[16] https://sites.google.com/site/poushkarov/home/vzemane-na-pocveni-probi, 12. 2017

[17] http://pudoos.bg/2016/05; Пилотни модели за екологосъобразно събиране и временно съхранение на опасни битови отпадъци от домакинствата; ПУДООС; 28.11.2016 г. / "Pilotni modeli za ekologosaobrazno sabirane I wremenno sahranenie na opasni bitovi otpadaci ot doamkinstwata", PUDOOS, 28.11.2016

[18] http://www.balbok.com/bg/about/Sybirane-na-opasni-otpadytsi-ot-domakinstvata; Сайт на „Балбок Инженеринг" АД; Събиране на опасни отпадъци от домакинствата; 07.09.2017 г. Site of Balbok Engeneering, Sabirane na opasni otpadaci ot domakinstwata, 07.09.2017

[19] https://fakti.bg/bulgaria/94218-iznasame-opasni-otpadaci-za-prerabotka-v-chujbina; Изнасяне на опасни отпадъци за преработка в чужбина; Публикувана: 29 Април, 2014 / Iznasjane na opsni otpadaci za prerabotka w chujzbina, 29.04.2014

[20] https://noharm-global.org/issues/global/treating-pharmaceutical-waste; 12.2017

[21] https://www.actualno.com/sliven/otvarjat-punkt-za-sybirane-na-opasni-otpadyci-v-sliven-news_570529.html; Мобилен събирателен пункт за безвъзмездно приемане на опасни отпадъци от домакинствата и последващото им третиране; 23.10.2016 г.,"Mobilen sabiratelen punkt za bezwazmezno premane na opasni otpadaciot domakinstwata i posledwasto tretirane", 23.10.2016

[22] https://www.sofia.bg/documents/20182/283420/2017-12-22; Сайт на Столична община; График на мобилен събирателен пункт за 2018 година; 22.12.2017 г. Stolichna obstina, Grafik za mobilen sabiratelen punkt za 2818, 22.12.2017

[23] Практическо ръководство за безопасно управление на отпадъците от лечебните и здравни заведения, Авторски колектив от Национален център по обществено здраве и анализи, София 2017 г. Praktichesko rakowodstwo za bezopasno uprawlenie na otpadacite ot lechebnite zdrawni zawedenia, Awtorski kolektiv na Nacionalen centar po obstestweno zdrawe I analizi, Sofia, 2017

[24] Анализ на състоянието и прогноза за вида, количествата и източниците на отпадъците, образувани на територията на страната, както и за отпадъците, които е вероятно да бъдат обект на трансграничен превоз от или до националната територия; Оперативна програма Околна среда 2007-2013 г. Analiz na sastoqnieto i prognoza za wida, kolichestwoto i iztochnicite na otpadaci, obrazuwani na teriotoriata na stranata, kakto I za otpadacite, koito verojatno da badta obekt na transgranichen prevoz ot ili do nacionalnata teritoria, Opeativna programa okolna sreda 2007-2013

[25] Закон за управление на отпадъците Обн., ДВ, бр. 53 от 13.07.2012 г., в сила от 13.07.2012 г., изм., бр. 66 от 26.07.2013 г., в сила от 26.07.2013 г.; изм. с Решение № 11 от 10.07.2014 г. на КС на РБ - бр. 61 от 25.07.2014 г.; бр. 98 от 28.11.2014 г., в сила от 28.11.2014 г., бр. 14 от 20.02.2015 г., изм. и доп., бр. 105 от 30.12.2016 г. / Zakon za uprawlenie na otpadacite, obn. DW, br. 53 ot 13.07.2012

[26] Национален доклад за състоянието и опазването на околната среда в Република България през 2009 г,

Изпълнителна агенция по околна среда; 2009 / Nacionalen doklad za sastojanieto I opazawaneto na okolnata sreda w Republika Bulgraia prez 2009, Izpalnitelna agencia po okolna sreda, 2009

[27] Конференция на страните по Базелската конвекция за контрол на трансграничното движение на опасни отпадъци и тяхното депониране; Програма на Обединените нации за околна среда; Шеста среща Женева 9-13 Декември 2002 г. / Conferencia na stranite po Baselskata convencia za control na transgranichnoto dwizhenie na opasni otpadaci I tjahnoto deponirane, Programma na Obedinenite nacii za okolna sreda, 6 sresta Geneva 9-12 decemvri 2002

[28] Наредба № 28 от 9 Декември 2008 г. за устройството, реда и организацията на работата на аптеките и номенклатурата на лекарствените продукти; обн. ДВ бр. 109 от 23 Декември 2008 г., Министерство на здравеопазването / Naredba 8 ot 9 dekemwri 2008 za ustrojstwoto, reda I organizaciata na rabotata na aptekite I nomenklaturata na lekarstwenite produkti, obn. DW, br. 109 ot 23.12.2008

[29] Наредба №28 от 14 Декември 2000 г. за условията и реда за унищожаването, преработването или използването за други цели на лекарствата; Обн. ДВ. бр.106 от 22 Декември 2000 г., Министерство на здравеопазването, Naredba 28 ot 14.12.2000 za usloviata I reda za unistozhavaneto, prerabotwaneto ili izpolzwaneto za drugi celi na lekarstwata, obn. DW, br. 106 ot 22.12.2000

[30] Наредба №4 от 5 Април 2013 г. За условията и изискванията за изграждането и експлоатацията на инсталации за изгаряне и инсталации за съвместно изгаряне на отпадъци; Обн. Бр. 36 от 16.04.2013 г. В сила от 20.04.2013 г., Министерство на околната среда и водите/ Naredba 4 ot 5 april 2013 za usloviata I iziskwaniata za izgrazhdaneto I exploataciata na instalacii za izgarjane I instalacii za savmestno izgarjane na otpadaci, obn. DW, br. 36 ot 16.04.2013

[31] Национален план за управление на отпадъците 2014-2020 г; Оперативна програма Околна среда 2007- 2013 г.; Министерство на околната среда и водите, Август 2014 г. София Nacionalen plan za upravlenie na otpadacite 2014-2020, Operativna prgrama Okolna sreda 2007-2013, Ministerstwo na okolnata sreda I wodite, august 2014

[32] Наредба № 1 от 09.02.2015 г. за изискванията към дейностите по събиране и третиране на отпадъците на територията на лечебните и здравните заведения; обн., ДВ, бр. 13 от 17.02.2015 г., Министър на здравеопазването и министър на околната среда и водите, Naredba 1 ot 09.02.2015 za iziskwaniata kum deinostite po sabirane I tretirane na tpadacite na teritoriata na lechebnite I zdrawnite zawedenia, obn. DW, br. 13 ot 17.02.2015, Ministar na zdraweopazwaneto i minstar na oklnata sreda i wodite

[33] Ралица Ангелова „Балбок Инженеринг" АД, Петър Трайков Столична община: Практически опит в събирането на опасни битови отпадъци в България Въпроси, свързани с управление на риска при събиране на опасни отпадъци" ППП по Проект „Проучване и разработване на пилотни модели за екологосъобразно събиране и временно съхраняване на опасни битови отпадъци" „Опасни битови отпадъци-добри практики и опит" 24 Септември 2013 г. София., Ralitza Angelova, Balbok Engeneering, Petar Traikov, Stolichna obstina-Prakticheski opit w sabiraneto na opasni bitowi otpadaci w Bulgaria, Waprosi, swarzani s uprawlenieto na riska pri sabirane na opasni otpadaci, PPP po proekt Prouchvane I razrabotwane na pilotni modeli za ecologosaobrazno sabirane I wremenno sahranjawane na opasni bitowi otpadaci, "Opasni bitowi otpadaci- dobri praktiki I opit", 24.09.2013

[34] news7.bg;http://botevgrad.com/news/55213/Nezakonno-smetishte-za-lekarstveni-otpadaci-iznikna-v-gorata-kray-Botevgrad/#gallery; Незаконно сметище за лекарствени отпадъци;09.05.2014, 07:25

MASS MEASUREMENT FOR METAL ACCOUNTING IN MINERAL PROCESSING PLANTS

Irena Grigorova[1], Marin Ranchev[1], Ivan Nishkov[1]

[1]University of Mining and Geology "St. Ivan Rilski"; 1700 Sofia, Department of Mineral Processing and Recycling; irena_mt@abv.bg

ABSTRACT. In the course of mass and metal balancing in mineral processing plants, the mass measurement of particular products which are part of the evaluation process of the operation efficiency of the technological operations has a significant role. Unfortunately, accurate mass measurement is often overlooked, both in primary design and in subsequent operation, and this leads to compromised results and conclusions. This paper focuses on the most common methods for mass measurement in the mineral processing plants, as well as on the types of weighing equipment, their design features and operation characteristics. Some important aspects of mass measurement are also discussed, e.g. sources of error, calibration methods, and requirements for the correct mass and metal accounting.

Keywords: mass measurements, metal accounting, errors, calibration

ИЗМЕРВАНЕ НА МАСИТЕ ЗА ОТЧИТАНЕ БАЛАНСА НА МЕТАЛА В ОБОГАТИТЕЛНИТЕ ФАБРИКИ

Ирена Григорова[1], Марин Ранчев[1], Иван Нишков[1]

[1]Минно-геоложки университет "Св. Иван Рилски", 1700 София, катедра "Обогатяване и рециклиране на суровини", irena_mt@abv.bg

РЕЗЮМЕ. При отчитане на масовия и металния баланс в обогатителната фабрика, основна роля заема измерването на масите (теглата) на съответните продукти, участващи в изчисляване ефективността на работа на заложените технологични операции. Акуратното измерване на масите е много често пренебрегвано, както при първичното проектиране, така и при последващата експлоатация, което довежда до компрометирани резултати и заключения. Настоящата разработка се фокусира върху най-разпространените методи за измерване на масите в обогатителните фабрики, както и върху видовете измервателни уреди, техните конструктивни и експлоатационни особености. Разгледани са и някои важни аспекти при измерване на масите, като източници на грешки, методи за калибриране и изисквания за коректното отчитане на масовия и металния баланс.

Ключови думи: измерване на масите, баланс на метала, грешки, калибриране

Introduction

In literature, metal accounting is defined as a system whereby selected process data is collected from various sources, including mass measurement and analysis, and transformed into a coherent report format that is delivered in a timely fashion in order to meet specified reporting requirements (Morrison et al., 2008).

As reported by Gaylard et al. (2014), in the mineral processing industry, reliable metal accounting is essential to sound corporate governance and it is also becoming a focus of increased attention and concern, particularly as the figures generated by the metal accounting system feed directly into the financial accounts of mining companies. Mass measurement, sampling, and analysis provide the input data for the metal accounting system. Sound corporate governance requires that the procedures used be based on best practice and that the data generated be accurate and handled correctly, transparently, and consistently to produce the accounting reports.

It is also important to give an appropriate definition of mass balancing as a valuable aspect of metal accounting and reconciliation: this is the process whereby input and process streams, or the individual components of the streams, stocks and in-process inventory are measured, sampled, and analysed in order to calculate the mass of each and reconcile the output to the input, plus or minus the stock change.

It is worth mentioning some of the commonly used terms in the field of mass measurement. Authors such as Morrison et al. (2008) suggest the following terminology:

Belt Scale/Weigher – A mass measurement device that continuously integrates and records the load on a belt while it passes the suspended scale or the measuring section of the belt;

Bin Scale – A bin that is fitted with load sensors or other mass detecting devices and has been calibrated so that the weight of the contents can be established and weighed on a continuous or batch basis;

In-Motion Weighing – The weighing of objects that are in motion. Usually applied to rail or road trucks;

Platform Scale – A compound lever scale whose load-receiving element is a platform that is supported by four or (rarely) more main bearings;

Weighbridges – Weigh scales designed to weigh road trucks or rail wagons where the lever system is usually below ground in a pit so that the vehicle or rail wagon can pass over and stop on the scale. In a large capacity, the scale also refers to the structural frame carried by the main bearing which supports the load-receiving element.

Weigh Idlers – Idlers positioned in the weigh carriage assembly so that they sense the weight of the material on the conveyer and transmit the weight through the carriage to the load sensor.

According to Morrison et al. (2008), the primary goal of mass measurement for metal accounting is to establish the mass of the particular material or component present at a specific time, or the mass flow of that component over a defined time period, with a defined accuracy suitable for mass and metal balancing.

Mass measurement can be classified into: measurements that are necessary for custody transfer and primary accounting of the input and output streams to a plant or operation, and measurements that are required for secondary accounting, or management control (Wortley, 2009).

In his introduction, Wortley (2009) describes some of the essentials for any mass measurement system which should be followed if we want to achieve reliable results for primary metal accounting:

- Selection of the most suitable stream and location for measurement;
- Correct specifications and selection of the method and equipment to suit the application;
- Optimum design, location, and installation to permit measurement and calibration by recognised techniques;
- Regular calibration by approved techniques and procedures and certification in the case of custody transfer applications;
- Record keeping and logging of all calibration results, corrections, and readings in order to facilitate error detection and statistical analysis in order to enable the accuracy/precision of the measurement to be calculated;
- Cleanliness, good housekeeping, and maintenance.

The first three requirements should be incorporated into the design of the plant. This is often not the case and thus modifications to existing plants may be required with associated costs and, in some cases, they may be difficult to achieve. However, the latter three are totally under the control of the existing management and are basically part of good management practice.

In mineral processing plants, the mass measurements are usually accomplished using:

- Platform, truck, and rail weighbridges;
- Weigh tanks, hoppers or bins;
- Conveyer belt weighers;
- Flow meters (volume and mass measurement).

The mass measurements could be carried out in rail cars or road trucks, in bins, hoppers, drums, tanks or other vessels, on conveyer belts or in conduits, as well as in open channels. The mass of bulk commodities is usually measured in ships or bulk carriers.

Some of the most common problems related with the mass measurement techniques for metal accounting are as follows: design and equipment selection; record keeping; certification and calibration; plant management and housekeeping.

Methods of measuring mass

Static weighing

According to Gaylard et al. (2009), the road/rail weighbridges (Figure 1) and platform scales are the most accurate form of mass measurement as there are no dynamic effects and they can be easily and frequently checked in operation by the use of internal check weights.

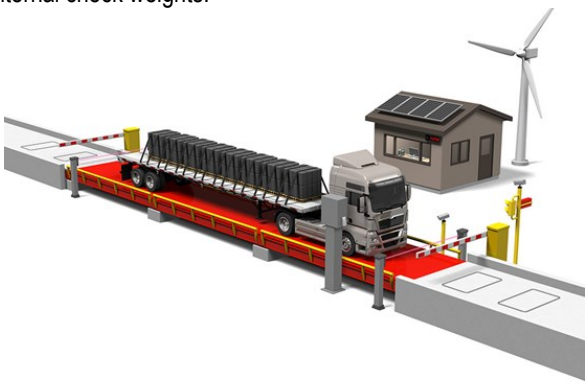

Fig. 1. View of Avery Weigh-Tronix weighbridge (Avery Weigh-Tronix Ltd.)

The mass measurement by truck/platform scale is usually performed by weighing the mass of the truck while it enters the plant area empty and when it leaves fully loaded. Truck scales are a practical solution for mineral processing plants with huge production volumes and constant material flow out of the plant through trucks. They are used particularly if the end products are stored in the plant area and transported out later. This way, the producer can monitor the amounts of end products when they leave the plant (www.weighingsystems.com, 2018).

In cases where the ore entering the processing plant is owned by one company and is treated by another company, the most practical solution to measuring the mass of the ore treated is in-motion rail weighing or through conveyor belt weighers. This equipment is capable of reasonable accuracy if the best practices for selection, installation, and calibration as detailed in the AMIRA Code and the textbook (Morrison et al., 2008) are followed and providing the equipment is kept well-maintained and clean, which is often not the case (Gaylard et al., 2014).

Road trucks, rail wagons or ships are commonly used for the transportation of concentrates where the material could be transferred in tankers in a slurry form, as filter cake, or as dry powder, usually weighed several times during the transfer.

Fig. 2. Railroad track scales (Rice Lake Weighing Systems Ltd.)

Usually, the in-motion weighing of materials in road or rail trucks (Fig. 2) is used for large quantities of ore or bulk commodities. The accuracy of in-motion weighing for rail trucks depends on:

- The truck layout at both ends of the weighing section;
- The fastening of the rails on these approaches (concrete or ballast);
- Constant speed over the weighing section, at a speed within the capability of the system;
- Good maintenance of the track, bogeys, and trucks in order to reduce impact and vibrations such as flat spots on the wheel.

The authors (Gaylard et al., 2009) also suggest that the weighbridges or platform scales should be designed in accordance with the following principles if they are going to be used for primary metal accounting purposes:

- The design range must take account of the various loads being measured to ensure that the mass to be measured is as high a proportion of the maximum range as possible without overloading;
- Ingress of water should be eliminated or a facility for ongoing regular removal incorporated;
- The installation must be level and the construction of the weigh frame must be such that distortion be eliminated;
- The weight indicator or print-out must have sufficient graduations in order to show the measured weight with the significant figures that are required to meet the specified accuracy requirement for the operation;
- Maintenance and operating personnel should undergo training in the correct operation, maintenance, and calibration of these scales;
- The indicator and other measuring elements should be in a weather- and tamper-proof casing;
- The zero reading should be checked every shift; ideally, scales should be checked by the operating personnel on a daily basis using internal check weighs;
- Results of these checks and of the regular inspections should be logged and analysed in order to establish the measuring error and any trends or bias;
- The weighing platforms should be checked regularly and kept clean;
- Access to the weighbridges/scales should be restricted to authorised operating and maintenance personnel only;
- The truck being weighed should be clean before loading or after offloading and the correct tare must be used (allowing for the driver, fuel, and packing equipment, such as tarpaulin covers);
- Free movement of the platform should not be restricted in any way, e.g. by touching the external frame or by spillage jamming in the gaps between the weighing platform and the frame;
- Overloading must not occur and loads must not be dropped onto the platform as this may damage the load cell and/or distort the platform;
- To eliminate the possibility of fraud, good supervision is required to ensure that checks are in operation.

In Chapter 3, entitled “Mass measurement” (Morrison et al., 2008), the authors discuss the design and usage of hopper/bin scales which are also capable of good accuracy although they require a more elaborate installation for loading and offloading the materials for weighing. Three or four load cells will be usually spaced equidistantly around the circumference. Authors propose that a rigid framework of support and stabilisation of the bin or tank should be introduced, so that the load cells are not affected by factors such as agitation, material flow or wind.

Dynamic weighing

Belt scales

Belt scales (weighers) (Fig. 3) enable the continuous weighing of large quantities of solid materials travelling on conveyer belts without the disruption to the process that batch weighing can produce. However, static scales are in general more accurate and capable of greater “sensitivity” since a larger quantity of material is being weighed at one time. In addition, in practice, the accuracy of belt scales in operation is often considerably poorer than should be expected because of the poor choice, system design, installation or bad operation or calibration (Morrison et al., 2008).

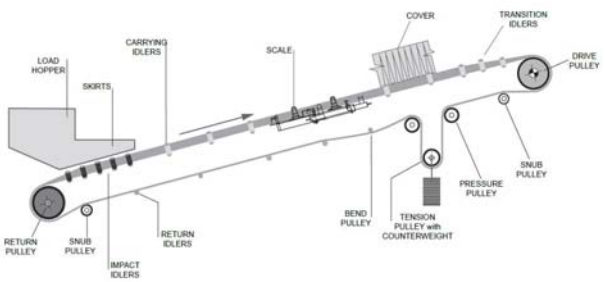

Fig. 3. Schematic diagram of belt conveyer system (Belt Scale Handbook 2016, Thayer Scale-Hyer Industries, Inc. Ltd.)

The weight on the conveyor belt is measured by sensing the force on one or more conveyor idlers. The motion of the material is measured by sensing the travel of the belt with a device which produces an "output" representing a fixed distance of belt travel. Because the measured force represents weight per unit of length (kg/m), it can be multiplied by the belt travel to acquire total weight. This function can be accomplished with an electro-mechanical or electronic integrator. With proper scaling, total weight may be accumulated in tons, long tons, or metric tons. In addition to displaying total weight passed over the belt conveyor scale, the most modern integrators also display instantaneous rate (i.e. kg/h or tons/h) and provide the transmitted output for remote monitoring and control requirements. The most viable belt conveyor scale systems operate in conformity with the above mentioned method of measuring weight per unit of length and multiplying that by the belt travel in order to determine the total material weight (Thermo Scientific Belt Conveyor Scale Handbook, 2012).

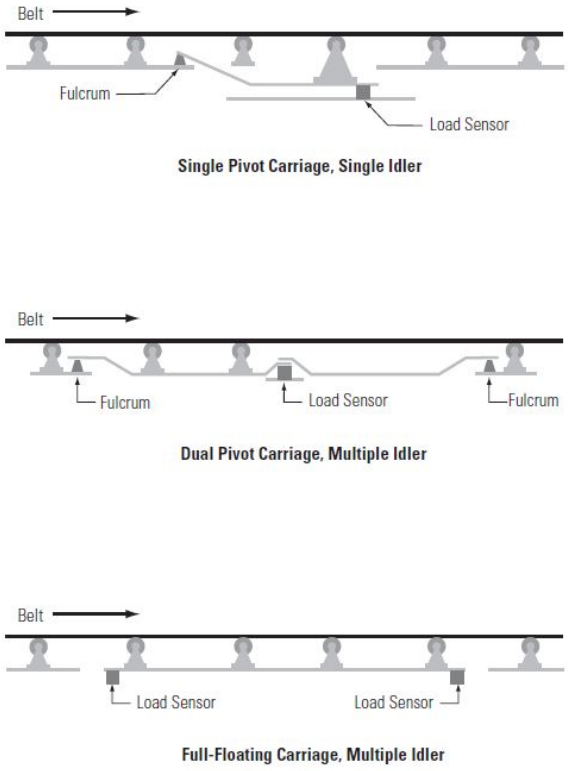

Fig. 4. Various common carriage designs of the conveyer belt measuring system (Thermo Scientific Belt Conveyor Scale Handbook, 2012)

Many manufacturers can be found in the field of mass measurement, and in particular in the conveyer belt weighing, but one of the world leaders and a most recognizable company in this area is Thermo Fisher Scientific Inc. Detailed and useful information has been presented in their Belt Conveyor Scale Handbook (2012). The following basic components and their function are quoted below:

- The scale carriage (Fig. 4) transmits the forces resulting from the belt load and directs those forces to the load sensor(s);
- The load sensor transduces the load force to a form acceptable to the mass totaliser;
- The belt travel (speed) pick-up contacts the belt and transmits belt travel (speed) to the speed sensor;
- The belt travel (speed) sensor transduces the belt travel (speed) to a form acceptable to the mass totaliser;
- The mass totaliser (integrator) computes the total mass that has passed over the belt conveyor scale and provides for the indication and recording of that value. Typically, the mass totaliser will also provide a mass flow rate indication.

The scale carriage must transmit the forces resulting from the material on the conveyor belt to the load sensor without adding any extraneous forces. It is important that no forces originating from belt travel or belt side travel be converted to a force on the load sensor. A draw of a single weigh idler showing forces in two dimensions is shown on Figure 5. Force F actually is sensed by the idler, but the scale carriage must transmit only force V to the load sensor. Force H must not be changed to a force acting on the load cell as a false representation of force V.

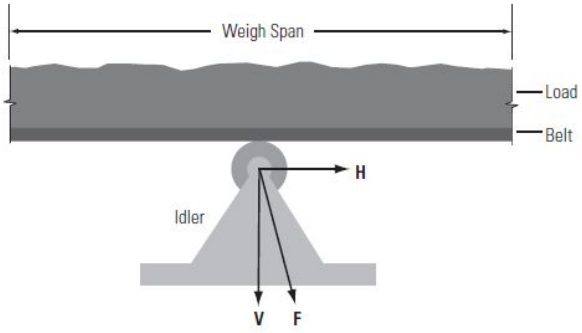

Fig. 5. Single weigh idler (Thermo Scientific Belt Conveyor Scale Handbook, 2012)

Morrison et al. (2008) suggest that the accuracy of conveyer belt (Fig. 6) weighing could be affected by the following:

- Flexibility of the weigh carriage;
- Spillage onto the weigh section;
- Belt effects such as tension, stiffness, and misalignment of the belt or idlers;
- Error in the belt speed measurement;
- Errors in the various processes of the measurement chain;
- Calibration errors and poor calibration techniques;
- Changes in the material being conveyed;
- Belt loading (proportion of design and variability);
- Poor operation, housekeeping, and maintenance;
- External environmental factors such as wind, dust, and excessive vibration or shocks;

Fig. 6. Four Idler Belt Weigher - Thermo Scientific Ramsey Series 14 (Ramsey Catalogue, Thermo Fisher Scientific Inc., 2018)

Morrison et al. (2008) explain that various methods could be applied for accurate measurement of the conveyor belt travel speed, which is as important as the mass on the conveyer because any error is directly proportional to the mass flow. The authors also suggest that, for authentic metal accounting, high quality equipment should be used and the belt speed measurement be derived from a cylinder or wheel (Fig. 7) in contact with the belt itself. This wheel should be: fitted so that it is in contact with the belt at all times (spring loaded); fitted at 90° to the direction of belt travel in the centre of the belt; of as large a diameter as is practical and as close to the weigher as possible. In general, the more idlers on a weigh frame, the less the effect of belt tension and alignment and the longer the instrument will remain in calibration (Amira, 2007).

Fig. 7. Tachometer for belt speed measurement (Spangenberg, 2012)

Various calibration methods exist such as: dead (static) test weights with the belt stopped or operating; use of an installed calibration test weight with the empty belt running; test chains or the material-run (bulk test) method. Calibration should cover a range of 20-100% of the belt loading for static tests. Testing over a range is not possible with an installed calibration weight, nor is it practical for material tests (Annon, 2003).

It has been suggested (Thermo Scientific Belt Conveyor Scale Handbook, 2012) that frequent zero calibrations may be impractical although it is recommended to do a daily zero calibration or zero balance. A change in zero balance can be expected over a long period of time due to material buildup on the carriage or to belt and idler wear. Zero calibration should only be performed by making a whole number of revolutions. The belt weight variance will be compensated for only if whole numbers of revolutions are used for zero calibration. Zero shifts in the order of 0.1 to 0.2% of full scale are normally the result of major weather changes, material buildup on the weighbridge, belt tracking, etc. Zero shifts of a larger magnitude normally are conveyor belt related and should be corrected prior to zero calibration. Most belt conveyor scale weighing errors result from improper zero calibration and lack of understanding of factors that cause zero calibration shifts or errors.

Morrison et al. (2008) propose that the static weights are the easiest and most convenient method but suffer from the following disadvantages: the dynamic effect of the normally loaded belt is excluded; the weight length must be accurately known and if the weigher is a pivoted type, the leverage ration must be accurately established.

The “material–run” method is preferred since it involves passing a known weight of the material (measured statistically in a weigh bin or a weigh bridge), which is normally measured by the weigher, over the specific weigher in the normal operating mode, thus incorporating the operating belt effects. This method is a requisite if the scale is to be certified but it necessitates facilities such as reference weigh bins or weighbridges to test weigh the material passing over the scale to a higher level of accuracy than that required for the belt scale being calibrated (Considine, 1993).

According to NIST 44 (Specifications, Tolerance, and Other Technical Requirements for Weighing and Measuring Devices, Handbook 44, 2015), some of the significant requirements for a material run test are presented below:

- The test shall be conducted at normal operating load;
- The test shall be conducted over a period of:
  - not less than 1000 scale divisions;
  - at least three complete revolutions of the belt;
  - at least 10 minutes of operation.
- A zero load test shall be conducted prior to the material test for at least three complete revolutions and ten minutes and immediately after the material test. The zero error for the former shall not exceed ± 0.06% or ±1 scale division after the zero adjustment, and for the latter test it shall not exceed ± 0.12% or ±2 divisions, whichever is less;
- The check weight scale must be capable of an accuracy of at least ±0.1%;
- After a zero load test, the totaliser must not change more than 3 scale divisions for one complete belt revolution;
- If the error shown by the material test is less than 0.25%, no adjustments should be made. If it is grater than 0.25% but less than 0.75%, adjustment may be made after notifying the statutory authority. If it is over 0.75%, adjustment may only be made by a

competent person after notifying the authority and if the error is over 0.75% an official test is required.

Nuclear Belt Weighers

Nuclear belt weighers use the principle of the adsorption of nuclear (gamma) radiation to measure belt loading. Suppliers provide guides to help select electro-mechanical or nuclear weighers for a specific application (Morrison et al, 2008). Such a belt weigher is shown on figure 8, where a fan-shaped collimated beam of radiation is transmitted from the source through the process material and the conveyor to the detector.

The nuclear belt weighers are simple to install and are less affected by belt tension or misalignment, so the conveyer design is not as important. Besides, they are not susceptible to external forces such as wind, they are less maintenance intensive, and easier to calibrate. However, they have the some operational limitations as to the measurement of belt speed, plant housekeeping moisture determination and regular calibration as any type of belt weigher. Most importantly, they are affected by variation in the size, composition, and shape of the material being measured and are therefore normally less accurate than electro-echanical weighers, with maximum errors of ±1 to ±2% of full scale being achievable but higher levels being normal (Jost, 1986).

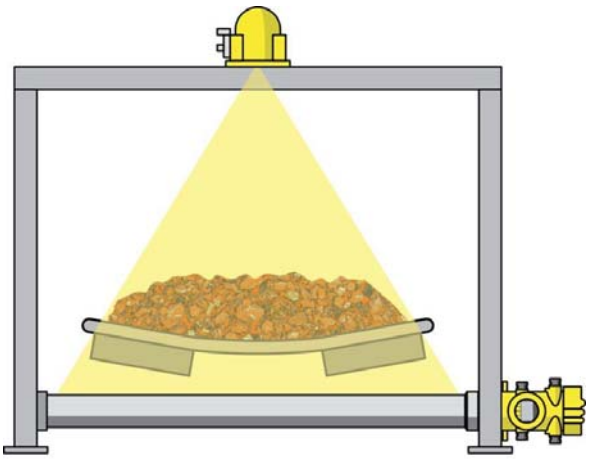

Fig. 8. Nuclear Belt Scale (Measuring Bulk Solids on a Conveyor, http://www.powderbulksolids.com, 2018)

The relevant national nuclear authorities control their use and maintenance. In certain applications, they can also be used, with neutron or microwave gauges to determine moisture content. They should not be used for metal accounting measurements.

Conclusion

As was mentioned in the Introduction and thanks to researchers such as Rob Morrison, Peter Gaylard, Ralph Holmes, Neville Randolph, Mike Wortley, Richard Beck etc., who were included in AMIRA P754 project, 'Metal Accounting and Reconciliation' and developed the Code of Practice for Metal Accounting for the Mining and Metallurgical Industry, the primary objective of mass measurement for metal accounting has been determined. It is to provide a result for the mass or mass flow of the component of interest that is free of bias, or at least such bias that can be established, and with a random error that is within the maximum limits required for the metal accounting system.

This review was made possible by the research carried out by the AMIRA International P754 Program and by the above mentioned scientists whose efforts and knowledge have contributed to the publication of various textbooks, research papers, and industrial reports. More details on this topic can be found in the literature sources listed below.

References

Annon B., Preparation of calibration curves. A guide to Best Practice. Published by the Laboratory of the Government Chemist (England) LGC/VAM/2003/032. 2003.

Considine, D. M., Process Instruments and Control Handbook, Forth Edition (McGraw-Hill: New York). 1993.

Gaylard P., Morrison, R., Randolph, N., Wortley, M., Beck, R., Extending the application of the AMIRA P754 code of practice for metal accounting. The Southern African Institute of Mining and Metallurgy Base Metals Conference 2009. -15 – 38.

Gaylard, P. G., Randolph, N. G. and Wortley, C. M. G. Metal accounting and corporate governance. Journal of the Southern African Institute of Mining and Metallurgy 114 (1), 2014. - 83–90.

Jost G., Comparison of Nuclear and Gravimetric Systems for the Continuous Weighing of Bulk Solid Flows, Bulk Solids Handling, 6 (6). 1986.

Measuring Bulk Solids on a Conveyor, [Online]. http://www.powderbulksolids.com, 2018.

Morrison, R., Wortley, M., Holmes, R., Randolph, N., Dunglison, M., An introduction to Metal Balancing and Reconciliation (ed. Morrison, R. D.) Julius Kruttschnitt Mineral Research Centre Monograph Series #4. 2008.

Spangenberg C. I., The status of sampling practice in the gold mining industry in Africa: Working towards an international standard for gold mining sample practices. A dissertation submitted to the Faculty of Engineering and the Built Environment, University of the Witwatersrand, Johannesburg. 2012.

Specifications, Tolerances, and Other Technical Requirements for Weighing and Measuring Devices as adopted by the 99th National Conference on Weights and Measures, NIST Handbook 44, 2015 Edition.

Thayer Scale Belt Scale Handbook, Application Guidelines for Installing a High Accuracy Conveyor Belt Scale Version 2016.

Thermo Scientific Belt Conveyor Scale Handbook, Thermo Fisher Scientific Inc., 2012.

Weighing-systems.com. Vehicle Weighing principles, [Online] http://www.weighingsystems.com/TechnologyCentre/vehicleweigh.html, 2018.

Wortley, C. M. G., Mass measurement for metal accounting — principles, practice, and pitfalls. Fourth World Conference on Sampling & Blending, The Southern African Institute of Mining and Metallurgy, 2009.

SAMPLING IN MINERAL PROCESSING – REVIEW OF PRACTICES

Marin Ranchev[1], Irena Grigorova[1], Ivan Nishkov[1]

[1]University of Mining and Geology "St. Ivan Rilski"; 1700 Sofia, Department of Mineral Processing and Recycling; inishkov@gmail.com

ABSTRACT The past few decades have witnessed a significant progress in the development of various sampling and control methods, sampling equipment, and standards. Sampling of various product streams in mineral processing plant is an extremely important process in providing information that allows the management and optimisation of the operation in a processing plant. In order to obtain a representative sample of the lot, we must ensure that all material in the process flow should have an equal probability of being sampled. The primary reasons for sampling in mineral processing plants, as well as some basic statistical concepts are discussed in this paper. However, the main aim of this review is to explore and summarise the various types of sampling equipment (mechanical, manual and on-line), sampling procedures (methods), and practices carried out in modern mineral processing plants.

Keywords: sampling, sample, mineral processing, practices, procedures

ОПРОБВАНЕ ПРИ ОБОГАТЯВАНЕТО НА ПОЛЕЗНИ ИЗКОПАЕМИ – ПРЕГЛЕД НА ПРАКТИКАТА

Марин Ранчев[1], Ирена Григорова[1], Иван Нишков[1]

[1]Минно-геоложки университет "Св. Иван Рилски", 1700 София, катедра "Обогатяване и рециклиране на суровини", inishkov@gmail.com

РЕЗЮМЕ. През последните няколко десетилетия се наблюдава значителен прогрес в разработването на различни методи за опробване и контрол, както и стандарти и оборудване за осъществяване на процеса опробване. Опробването на различни технологични потоци е много важен процес, осигуряващ информация, чрез която управляваме и оптимизираме работата на обогатителната фабрика. С цел осигуряване на представителна проба, трябва да гарантираме, че всички части на материала който се опробва, трябва да бъдат равнопоставени по отношение на вероятността да попаднат в крайната проба за анализ. В настоящата разработка са разгледани главните причини, поради които се осъществява процеса опробване в обогатителните фабрики, както и някои основни статистически понятия. Основната цел на този преглед е да се проучат и обобщят разнообразните опробващи устройства (механични, ръчни и онлайн устройства), практики и процедури (методики) на опробване, прилагани в съвременните обогатителни фабрики.

Ключови думи: опробване, проба, обогатяване на полезни изкопаеми, практики, процедури

Introduction

According to Gy (1982) and Pitard (1993), the fundamental rule for correct sampling and sample processing is that all parts of the ore, concentrate or slurry being sampled must have an equal probability of being collected and becoming part of the final sample for analysis; otherwise, bias is easily introduced and the sample will not be representative.

Before doing into detail concerning the processes of sampling practice, measurements and procedures, it is worth mentioning some of the terms commonly used in this field. Authors such as Morrison et al. (2008) suggest the following definitions:

- Best practices – The most precise method of performing a measurement with the information and equipment available at that time;
- Bias – The difference between the mean result of one or more measurements and the true value of the quantity being measured;
- Cross-Stream Sampler – A mechanical sampling device that is used to collect an increment from a falling stream of material either from a conveyor or particulate material or from a slurry stream;
- Increment – A quantity of material collected in a single operation of a sampling device;
- Lot – A defined quantity of the material being measured to which the mass and analysis is applicable. For accounting purposes, a weighed average sample of all the production or shipment batches making up that lot is prepared and submitted for analysis;
- Representative – A sample can be said to be representative of the lot from which it was taken if the mean square of the total sampling accuracy is less than some standard of representativeness;
- Sample – A subset of population chosen in such a way that it can be taken to represent the population with respect to some characteristics.

Overall, sampling procedures cover the practice of selecting representative quantities of test material in the field in order to evaluate bulk materials. Examples of the test materials are bulk granular solids, slurries, sludge, grains, and solid fuels. It

is necessary to be able to sample bulk materials during shipment and during processing operations.

Taggart (1945) defined sampling as: "The operation of removing a part convenient in size for testing, from a whole which is of much greater bulk, in such a way that the proportion and distribution of the quality to be tested (e.g. specific gravity, metal content, recoverability) are the same in both the whole and the part removed."

After the primary sampling stage, the increments taken by the mechanical sampling system are usually processed on-line to reduce the sample mass that is taken back to the laboratory for final sample preparation and analysis. Primary increments are either processed individually or combined into a sub-lot or gross sample in a number of stages of crushing, division and drying if necessary (Morrison et al., 2008).

Very important decisions, such as process flowsheet developments, methods of improving recoveries and grades, and reducing losses etc., are usually made in a metallurgical plant thanks to the results obtained from sampling processes. Logically, this confirms the need for reliability of the samples and the methods used in obtaining them, as well as careful control and quantitative determination (Chibwe et al., 2005).

Morrison et al. (2008) highlight the principal steps in establishing a sampling regime and they are listed below:

- Determine what needs to be sampled – a shift production, a stockpile or a shipment;
- Specify the purpose of sampling and the required precision – the purpose of sampling is particularly important as it determines the overall precision required;
- Identify the nominal top size of the material to be sampled and, hence, the dimensions of the sample cutter and mass of increment;
- Characterise the variability of the material being sampled for determining the number of primary increments needed to obtain the required sampling precision;
- Determine the sampling intervals in tonnes for mass-basis sampling and in minutes for time-basis sampling;
- Establish the procedure for combining increments into sub-lot samples or a gross sample in order to achieve the required overall precision of sampling, sample preparation and analysis.

The sampling intervals mentioned above are usually based on time or mass principle, i.e. mass-basis and time-basis systematic sampling. Morrison et al. (2008) suggest that when mass-basis sampling is adopted, the increment masses extracted need to be of almost uniform mass to ensure that each increment caries the correct weighting information. This could be achieved by using a variable speed cutter, discussed below, that adjusts its speed increment-by-increment so that it is proportional to the flow rate at the time of taking the increment, thereby ensuring that the increment masses are almost uniform. On the other hand, when time-basis sampling is adopted, the increment mass must be proportional to the flow rate, so a fixed speed cutter needs to be used. Both mass-basis and time-basis sampling are equally acceptable, although time-basis sampling is easier to implement and does not require measurement of flow rate and control of cutter speed.

Sampling in concentrators

Holmes (2010) suggests that the most appropriate location for sampling a process stream in a mineral processing plant is at the discharge point of a conveyor belt or chute where the complete stream can be intersected at regular intervals.

This article begins with a look at the manual, mechanical and on-line sampling techniques, requirements, and instruments that are most widely used in practice.

Manual Sampling

According to Morrison et al. (2008), the requirements for manual sampling of a process stream are very similar to those for mechanical sampling, even though manual sampling can only be conducted at relatively low flow rates.

Smith (2004) points out that the most important and influential aspect of sampling, in the Gy sense, is the correct sampling equipment which is also used properly. Conversely, the incorrect equipment commonly results in biased samples. Another essential conclusion, according to Smith (2004), is that the sampling equipment may not perform well in practice even though it is designed correctly. Operators (those taking the samples) may not be properly trained in correct sampling. Without correctness, sampling bias is introduced and sampling variation is increased, sometimes substantially, beyond the unavoidable statistical sampling variation. Since samples are only as good as the sampling systems that generate them, incorrect sampling will remain undetected without an examination and evaluation of the sampling systems.

Fig. 1. Sampling from the top of conveyor belt (Holmes, 2010)

Taking a manual sample from the top of conveyor belt (Fig. 1) is undesirable, because the material at the bottom of the conveyor is ignored, therefore the representativeness of the

sample is not provided. Furthermore, sampling from the top of railway wagons (Fig. 2A) or from the side of a stockpile (Fig. 2B) it is not recommended due to the segregation which occurs in stockpiles because the coarser particles tend to rill down the outside leaving the finer particles in the centre of the stockpile, thus introducing unsatisfactory results.

Fig. 2. Taking samples from the top of railway wagons (A) and the side of stockpiles (B) (Morrison et al., 2008)

According to Petersen et al. (2005) due to the material heterogeneity, the Grouping and Segregation Error (GSE) is usually inevitable in any sampling practice. The GSE mostly depends on the level of fragment segregation which strongly depends on the material differences in particle size, shape, and density. Segregation usually occurs when dealing with particulate materials, both stationary and in motion.

Figure 3 illustrates the effect of sampling a segregated (Fig. 3A) and mixed material (Fig.3B). The authors (Peterson et al., 2005) suggest that it may be appreciated how compositing a number of small samples gives a much more representative sample than extracting only one large sample of the same mass/volume. In order to minimise the grouping and segregation error, mixing or blending the material before primary or/and secondary sampling should be carried out; if this is not possible, a composite sampling is the most appropriate action that must be taken.

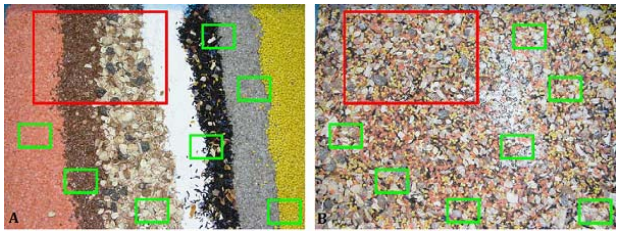

Fig. 3. Illustration of segregated (A) and mixed (B) material (Peterson et al., 2005)

Mechanical Sampling

Sample cutters are known as devices for taking samples from a broad range of locations in the mineral processing plant, and the portions of material extracted by a single operation of a sample cutter are referred to as ‘‘increments’’. Holmes and Robinson (2004) suggest that the two main classes of sample cutters are ‘‘cross-stream cutters’’ which pass a bucket or a chute through a stream of falling material, and ‘‘cross-belt cutters’’ which remove material from a conveyor belt by passing a device across the belt, generally by having it rotate around an axis that is parallel to the belt.

Cross-Belt Cutters

As reported by Morrison et al. (2008), cross-belt cutters are widely used in the resource industries, especially as cutters that take samples in-situ from conveyor belts, as well as for ore, concentrate, and particularly coal sampling rather than falling stream cutters. Generally, the cross-stream cutters are cheaper to install and the increment mass is smaller than for falling stream cutters.

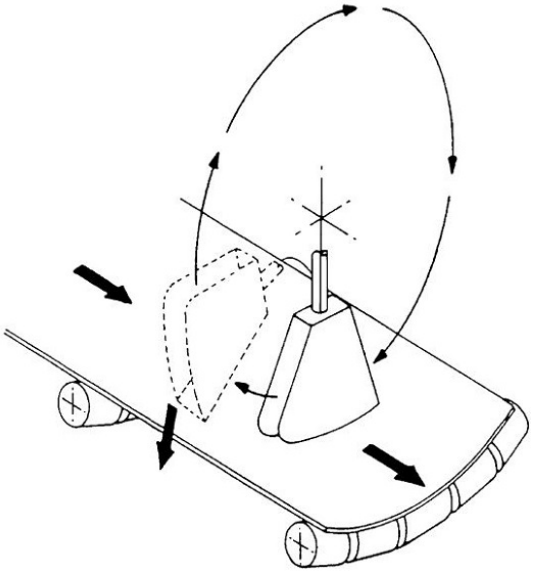

Fig. 4. Cross-belt sample cutter illustration (Holmes and Robinson, 2004)

The most appropriate cross-belt cutters (Fig.4) should comprise cutter blades which delimit the sample but use other parts of the cutter to extract the sample, as reported by Holmes and Robinson (2004). However, even the best designed cross-belt cutters are likely to undersample any material, therefore they are not recommended for metallurgical accounting for the following reasons (Morrison et al., 2008):

- Generation of considerable turbulence when passing through the stream, resulting in loss of material that should have been included in the increment, as well as in the introduction of other material into the increment that should not be included;

- Cross-belt cutters could leave a layer of material on the conveyor belt if the profile of the belt does not match the cutter path and/or if the skirts at the bottom of the cutter are not correctly adjusted. An example of an incorrectly designed cross-belt cutter installation where the conveyor profile does not match the cutter trajectory is shown in Figure 5 (Docherty, 2005);

- It is virtually impossible to check visually whether a cross-belt cutter is performing correctly in terms of correct increment delimitation and increment extraction because considerable turbulence is created as the cutter traverses the stream.

Fig. 5. Cross-belt sample cutter- the conveyor belt profile does not match the trajectory of the cutter (Docherty, 2005; Morrison et al., 2008)

Gy (1992) considers the "Pollock samplers", "hammer samplers", "strip samplers", and "swing samplers" as having "definitely incorrect extraction" because they undersample the material which is near the belt.

Linear Falling Stream Samplers

The appropriate design of sample cutters is of a great importance with respect to obtaining representative samples from process streams. The installation of the falling stream linear sampler (Fig. 6) at the discharge end of a belt conveyor is the internationally preferred method of sampling the conveyor. Correct design of the cutter shape and positioning is critical to obtaining a correct representative sample (http://www.flsmidth.com, 2018).

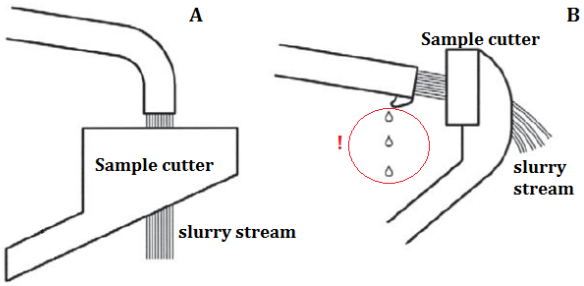

Fig. 6. Correct (A) and incorrect (B) slurry stream sampling (Holmes, 2010)

One of the world's pioneers in the design and manufacture of sampling and sample preparation equipment is the Australian company Essa which was acquired by FLSmidth in 2011. Now Essa Australia Limited are worldwide distributors of a range of electric motor driven ball screw samplers that find particular application in collecting representative samples from the material stream being discharged over the head pulley of a belt conveyor. These are setting new standards of performance and reliability that traditional chain, pneumatic, and hydraulic drive samplers can find difficult to match.

Fig. 7. Ball Screw Linear Cross Stream Sampler - Essa® Sampling Systems (http://www.flsmidth.com, 2018)

For cross-stream cutters (Figures 7, 8), the commonly accepted conditions for correct sampling are based on Gy's consulting experience and on trials discussed by Gy and Marin (1978). As mentioned by Holmes (2015), the cutter aperture must be at least 3 times the nominal top size (d) of the material being sampled, i.e. 3d, to prevent preferential loss of the larger particles, subject to a minimum of 10 mm for fine dry solids. The cutter speed is also an important design requirement for falling stream cutters and according to Gy (1982) must not exceed 0.6 m/s

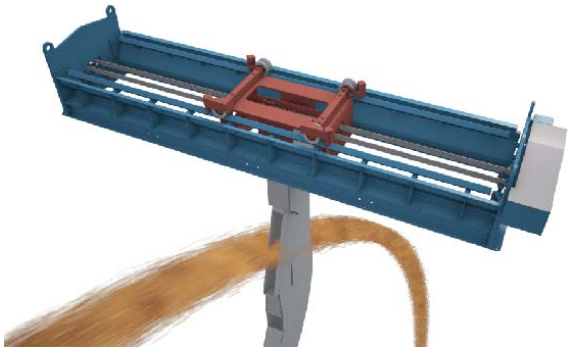

Fig. 8. Belt Drive Linear Cross Stream Sampler - Essa® Sampling Systems (http://www.flsmidth.com, 2018)

The synchronous belt drive samplers (Fig. 9, SBD), engineered and manufactured by FLSmidth (Essa®), are used where the sampler drive has to be mounted below the discharge point. A single electric motor drives two synchronised toothed belts located at either side of the ore stream. This allows the sampler drive and cutter to operate on the same plane across the falling ore stream.

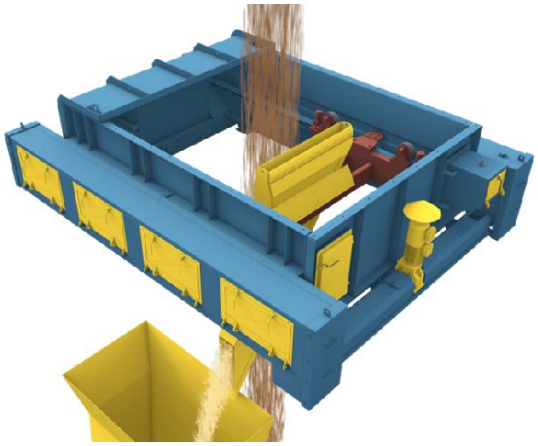

Fig. 9. Synchronous Belt Drive Linear Cross Stream Sampler - Essa® Sampling Systems (http://www.flsmidth.com, 2018)

On-line sampling and analysis

Wills and Napier-Munn (2006) suggest that the key to effective control is online chemical analysis which produces real-time analysis of the metal composition of process streams. On-line X-ray fluorescence (XRF) analysers provide elemental assays from process flow streams and are now considered standard hardware on large scale flotation plants (Garrido et al., 2008). Furthermore, various measurement techniques have been used for on-line particle size analysis of slurries. The main analytical procedure in comminution circuit performance measurement is the determination of the size distribution of the solids in the samples taken during surveys. Many techniques exist for particle size analysis (Napier-Munn et al., 2005). Grinding circuit reduces particle size to a desired distribution. It is important to measure the grinding product particle size for grinding circuit monitoring and control. On-line particle size measurement is the industry practice today.

Fig. 10. Courier® slurry analyser system (www.outotec.com, 2018)

Nowadays, many mine sites use analysers to replace the time-consuming and labour-intensive laboratory methods for routine process control assays. One of the main suppliers of advanced process automation systems, control solutions, and intelligent instruments to the mineral and metal processing industries is the well known Finland Company Outotec Oyj. One of the primary uses of on-stream slurry analysers is in flotation control. Outotec's Courier analyser (Fig. 10) family, for example, can measure elemental content in each stream of the flotation process.

The Courier range of analysers includes Courier 5X SL, Courier 6X SL, and Courier 8 SL (Table 1). It cannot be sufficiently specified how essential it is to choose the most suitable analyser since this entirely depends on your application and on the primary process control goal (Outotec SEAP Customer eNewsletter, 2018).

Several points of the process can be sampled with some modern XRF analysers handling up to 24 streams and with most machines capable of analysing for several elements and solids content. The time to analyse a single sample can range from 15 s to a minute, and the sampling cycle time is between 10 and 20 min — depending on the number of sample points attached to the analyser (Laurila et al., 2002; Bergh and Yianatos, 2011).

Table 1.
Various courier analyser details

	Courier 5X SL	Courier 6X SL	Courier 8 SL
Source	X-ray tube (35 W)	W-ray tube (200 W)	Laser
Detector	WDXRF / EDXRF	WDXRF / EDXRF	LIBS
Elements	Ca and heavier	Ca and heavier	Li and heavier
Measurement time	30 – 120 s	15 – 60 s	60 – 300 s
Sensitivity	0.01 %	0.003 %	0.05 %
Samples	Up to 12	Up to 24	Up to 12
Typical applications	Base metals, Fe ore, rare earths	Base metals, Fe ore, rare earths, precious metals, PGMs	Fe ore, phosphates, Ni concentrates with Mg/Si impurities, sulphide (Au), $CaCo_3$, coal

It is well-documented that different particle size measurement techniques will yield different results. This is due to the fact that each technique measures a different dimension of a three-dimensional particle. For on-stream particle measurement, the focus is on repeatability, precision, and reliability of the equipment (Kongas and Saloheimo, 2008).

An example of a commonly used analyser that provides real-time, accurate particle size distribution measurements is the PSI 500i Particle Size Analyser manufactured by Outotec. Usually, PSI 500i is used in: monitoring grinding circuit products with wide or bimodal distributions; monitoring regrind circuits; controlling thickeners for optimum water recovery; monitoring mine backfill and tailings disposal; monitoring feed to slurry pipeline product quality measurement for industrial minerals.

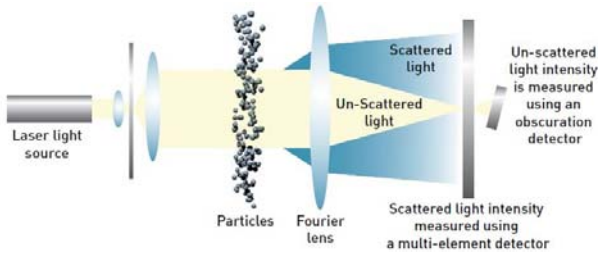

Fig. 11. Principle of laser diffraction measurement (www.outotec.com, 2018)

Laser diffraction (Fig. 11) gives a consistent volumetric particle size analysis result without any external calibration which is a significant advantage. There is a small difference to the particle size analysis measured by other methods, such as sieve analysis. However, the repeatability and precision over a wide particle size range are the most important features in process control applications. Plant results have shown that laser diffraction is a viable method for the on-line particle size analysis of wet slurries in mineral processes (www.outotec.com, 2018).

Conclusion

The objective of all sampling is to obtain a representative sample. This is an ideal concept which is rarely realised in practice. As mentioned above, the fundamental rule for taking representative samples is that all parts of the material sampled must have an equal probability of being collected and becoming part of the final sample for analysis. There is little point in using the latest metallurgical accounting package to improve metal balancing if the data used are unreliable in the first place. As pointed by Holmes and Robinson (2004) and Morrison et al. (2008), the financial consequences can be huge, ranging from sub-optimum utilisation of ore resources to poor recovery in the processing plant and loss of revenue from product sales. Therefore, it is vital for accurate metallurgical accounting that sampling be carried out correctly to ensure that samples are representative; otherwise the entire measurement chain is corrupted at the outset.

References

Bergh, L. G., Yianatos, J. B., The long way toward multivariate predictive control of flotation processes. Journal of Process Control 21, 2011. - 226–234.

Chibwe, P., Simukanga, S., Witika, L. K., Chisanga, P., Powell, M., African Journal of Science and Technology (AJST) Science and Engineering Series 6, 2, 2005. - 102 – 112.

Docherty, J. Mechanical sample plants. in: Proceedings Second World Conference on Sampling and Blending (WCSB2), Sunshine Coast, Australia (The Australasian Institute of Mining and Metallurgy: Melbourne), 2005. - 83-93.

Garrido, C., Toledo, H., San Martin, P., Villanueva, A., Calibration methodology and calibration maintenance in courier analyzers for copper - molybdenum flotation process. International Mineral Processing Seminar, 6, 2008. - 339–345.

Gy, P, Marin, L., Unbiased sampling from a falling stream of particulate material. International Journal of Mineral Processing, 5, 1978. - 297- 315.

Gy, P. Sampling of Heterogeneous and Dynamic Material Systems. Theories of Heterogeneity, Sampling and Homogenizing, Elsevier, Amsterdam, 1992.

Gy, P., Sampling of Particulate Materials - Theory and Practice, 2nd edition, Elsevier, Amsterdam, 1982.

Holmes, R. J. Sample station design and operation. WCSB7 Proceedings, TOS Forum, Issue 5, 2015. -119-128

Holmes, R. J. Sampling mineral commodities - the good, the bad, and the ugly. Journal of the South African Institute of Mining and Metallurgy, 110, 2010. - 269 – 276.

Holmes, R., Robinson, G., Codifying the principles of sampling into mineral standards. Chemometrics and Intelligent Laboratory Systems 74, 2004. - 231–236.

Kongas, M, Saloheimo, K., On-Stream Particle Analysis. Fine chemical processing, Filtration and Separation, May, 2008.

Laurila, H., Karesvuori, J., Tiili, O., 2002. Strategies for instrumentation and control of flotation circuits. Mineral Processing Plant Design, Practise and Control, 1, 2002. - 2174–2195 p.

Linear Falling Stream Samplers [Online] http://www.flsmidth.com, 06.2018.

Morrison, R., Wortley, M., Holmes, R., Randolph, N., Dunglison, M., An introduction to Metal Balancing and Reconciliation. (Ed. Morrison, R. D.). Julius Kruttschnitt Mineral Research Centre Monograph Series 4, 2008.

Napier-Munn, T. J., Morrell, S., Morrison, R. D., Kojovic, T., Mineral Comminution Circuits - Their Operation and Optimization, JKMRC, The University of Queensland, Brisbane, 2005. – 121 p.

Outotec SEAP Customer eNewsletter 2. A quick guide to the best analyzer for your application, 2018.

Petersen, L., Minkkinen, P., Esbensen, K., Representative sampling for reliable data analysis: Theory of Sampling. Chemometrics and Intelligent Laboratory Systems, 77, 2005. - 261– 277.

Pitard, F. Pierre Gy's Sampling Theory and Sampling Practice, 2nd edition, CRC Press, Florida, 1993.

Smith, L. P. Audit and assessment of sampling systems. Chemometrics and Intelligent Laboratory Systems, 74, 2004. - 225 – 230.

Taggart, M. Handbook of Mineral Dressing. Section 19, Wiley, 1945.

Wills, B. A., T. Napier-Munn, Mineral Processing Technology: an Introduction to the Practical Aspects of Ore Treatment and Mineral Recovery. Butterworth-Heinemann, Oxford, 2006.

PRE-CONTACT COLUMN FLOTATION MACHINES – DESIGN FEATURES AND PRINCIPLES OF OPERATION

Tsvetelina Ivanova

University of Mining and Geology "St. Ivan Rilski"; 1700 Sofia, Department of Mineral Processing and Recycling; inishkov@gmail.com

ABSTRACT. Over the past few decades, flotation has been one of the fastest developing and commonly applied processes in the mineral processing industry. Along with that, the flotation machines are constantly developed, modified and improved. The pneumatic pre-contact flotation machines are representatives of a new generation of flotation machines with a number of design features that improve the flotation process. This article discusses several types of pneumatic pre-contact flotation machines e.g., PNEUFLOT, SFR (Staged Flotation Reactor), IMHOFLOT, and SIMINE Hybrid Flot.

Keywords: column flotation machines, pre-contact flotation

КОНСТРУКТИВНИ ОСОБЕНОСТИ НА ФЛОТАЦИОННИТЕ КОЛОННИ МАШИНИ С ПРЕДВАРИТЕЛЕН КОНТАКТ

Цветелина Иванова

Минно-геоложки университет "Св. Иван Рилски", 1700 София, катедра "Обогатяване и рециклиране на суровини", inishkov@gmail.com

РЕЗЮМЕ. През последните няколко десетилетия флотацията е един от най-бързо развиващите се и прилагани процеси при преработката на полезни изкопаеми. Паралелно с това се развиват, модифицират и усъвършенстват флотационните машини. Представители на едно ново поколение флотационни машини са флотационните машини от колонен тип с предварителен контакт. Те притежават редица конструктивни особености, които подобряват флотационния процес. В настоящата статия разглеждаме няколко типа колонни флотационни машини с предварителен контакт, а именно PNEUFLOT, SFR (Staged Flotation Reactor – Стъпков флотационен реактор), IMHOFLOT и SIMINE Hybrid Flot.

Ключови думи: колонни флотационни машини, флотация с предварителен контакт

Introduction

Contemporary requirements in the field of pulp aeration theory and air bubble mineralisation require the creation of pneumatic pre-contact flotation machines. Those are representatives of a new generation of floating machines which are used in the flotation of ores of ferrous and non-ferrous metals, precious metals, coal, and other minerals.

The pneumatic pre-contact flotation machines are representatives of a new generation of flotation machines with a number of design features that improve the flotation process. The mixing of the solid and gas phases in an aqueous medium is carried out in advance, outside the volume of the flotation cell, in heterogeneous devices designated by the various manufacturers, such as aeration devices, mixing chambers, and others. The elementary flotation act (attachment of hydrophilic solid particles to air bubbles) occurs in these devices. Pre-contact flotation machines do not have an impeller system which means there is no wear and tear in the stator-rotor system. Another important feature is the ability to create finer air bubbles and lower air consumption than conventional pneumo-mechanical machines, resulting in flotation of fine products and production of high-quality concentrates.

This paper explores some of the most widely used column pneumatic flotation machines operating under the flotation method with pre-contact, in the process of studying the efficiency of the processing of a variety of raw materials (the feeding of the flotation cell, the pulp aeration, the residence time, and others). They are as follows: PNEUFLOT (MBE Coal & MINERALS TECHNOLOGY), SFR (Woodgrove Technologies), IMHOFLOT G-Cell (Maelgwyn Mineral Services Ltd.), and SIMINE Hybrid Flot (SIEMENS).

IMHOFLOT

Pneumatic flotation, as developed by Dr Rainer Imhof, has been applied in commercial beneficiation operations since 1987. Over 85 flotation cells have been installed in more than 30 operations successfully treating a wide range of minerals. Flotation machines with a pre-contact collar type column include: power supply, air bubble generation, bubble/particle contact, and phase separation of the froth from the tailings. The Imhoflot V-Cell design is presented in Figure 1. The suspension is pumped with sufficient fluid to obtain intense aeration of the air and rapid dispersion for efficient air bubble/particle contact (Imhof et al., 2005).

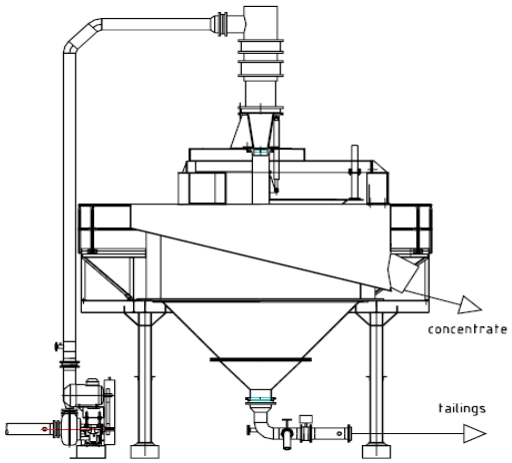

Fig. 1. Imhoflot V-Cell (Imhof, et al., 2005)

The aeration unit, or bubble generator, is a fundamental component of the process and is constructed of fused silicon carbide components to protect it from wear. Bubble sizes generated by the aerator have been measured in the range of 10 μm to 1500 μm, with the statistical average being around 300 μm (Brown, 2001). Figure 2 shows an Imhoflot aerator in assembly. The Imhoflot V-Cell incorporates froth level control and variable cross sectional area for froth removal; both can be used to control mineral enrichment and mass pull (Imhof, 2000).

Fig. 2. Imhoflot – aerator in assembly (Imhof, et al., 2005)

Pneumatic flotation technology of Imhoflot has been developing over a period of over 25 years. This has led to the development and patenting of G-Cell Imhoflot, where the application of centrifugal forces to accelerate the elemental flotation act results in a significant reduction in the amount of space required for the flotation equipment (Imhof, et al., 2005). Figure 3 shows the Imhoflot G-cell flotation machine.

The Imhoflot flotation machines are characterised by high selectivity and a number of advantages such as: efficiency in the extraction of fine (<20 μm) and large (> 350 μm) particles; absence of moving parts; low power consumption because no rotor/stator is needed to stir the flotation pulp.

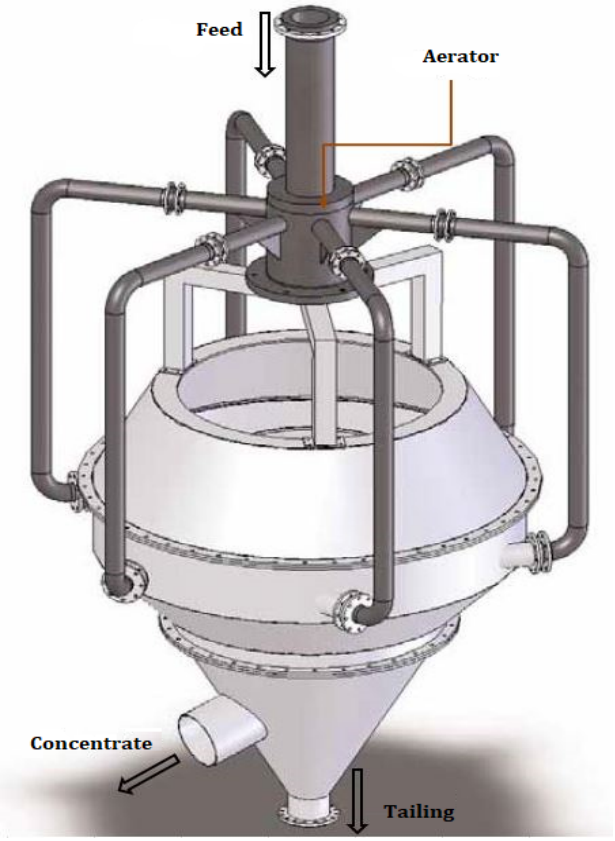

Fig. 3. Imhoflot G-Cell (https://www.maelgwyn.com, 2018)

The elemental flotation act in the Imhoflot flotation machine takes place outside the cell where pre-contact is taking place. The separation and recovery of the valuable component is performed in the cell without requiring mechanical dispersion of the air phase. The flotation process takes place at a high speed. The pulp is discharged through the aeration facility by means of a centrifugal pump which provides the necessary energy for complete aeration of the pulp. The aeration system has a self-priming aeration device. With the Imhoflot pre-contact flotation machines, a higher recovery is achieved, with a very short retention time of the flotation pulp in the cell. It is also possible to make large variations in the feed rate and the grain size of mineral particles. The design of the distribution pipes, the aeration unit, and the flotation cell allow easy assembly and replacement of the parts (repairs). The main parts are made of ceramics and wear-resistant materials. The flotation line is fully automated and operated using a PLC. The process is suitable for recovery hard-to-float minerals, resulting in reduced initial investment and subsequent operating costs (Imhof, 2000).

PNEUFLOT

The first PNEUFLOT pneumatic flotation plant was put into operation in Pennsylvania in 1987. The installation, owned by Pittstone Coal Co., is for coal flotation, and since then PNEUFLOT has been widely applied in the processing of coal and coal slimes, industrial minerals, iron minerals, and non-ferrous metals such as copper, lead, nickel, and zinc and precious metals - platinum, gold, silver and etc.

The PNEUFLOT pneumatic flotation machine with a pre-contact collar type column is based on the principle of mixing the air and solid phases in a continuous flow. The preliminary contact between hydrophobic mineral particles and fine air bubbles takes place in special aeration devices. The introduction of the aerated pulp into the flotation cell ensures the formation of air bubbles with a size appropriate for the respective flotation cycle. The flotation pulp is fed forward to the aerator located in a vertical tube above the flotation cell. After aeration, the pulp stream is introduced through the central tube into the distribution nozzles located at the bottom of the cell. Air bubbles covered with hydrophobic particles rise to the top of the cell and form a froth layer on the surface that separates around the cell. The particles that remain unattached to the air bubbles are detached at the bottom of the cell. The pulp level is kept constant by means of a gooseneck that actuates a control valve. The kinetic energy required for bubble/particle adhesion is generated by the turbulent flow of pulp in the aerator. The required flow and pressure are achieved by a feed pump for the suspension. The slurry is pressed through small wear-proof ceramic nozzles distributed in circles pointing to a large Venturi, thus creating a vacuum when the pulp is pumped through it. This effect pulls air into the pulp. The circular arrangement of the nozzles distributes the pulp flow creating the necessary turbulence for intensive air bubble/mineral particle contact. The air supplied serves both to aerate the slurry and to stabilise it. Furthermore, all parts exposed to friction are made of special rubber and ceramic materials that ensure their wear resistance. These aerators are offered in various sizes to suit different pulp flow rates and different mineral throughputs. Therefore, only one aerator unit per flotation cell is needed to achieve high performance. Another advantage of PNEUFLOT is the ability to obtain bubbles with a very wide range of sizes (0.00-1000 μm), with the same equipment being used in all stages of flotation - from rougher to scavenger and cleaner flotation (MBE Coal & Minerals Technology GMBH – Pneuflot, www.mbe-cmt.de, 2018).

Figure 4 shows industrial installations of the PNEUFLOT flotation machine (left) and the PNEUFLOT laboratory flotation machine (right) used for the laboratory flotation experiments.

Fig. 4. Industrial installation (left) and PNEUFLOT laboratory flotation machine (right)

SFR - Staged Flotation Reactor

The Staged Flotation Reactor has been developed thanks to the efforts of a team of specialists who have explored the shortcomings of both conventional flotation machines and those of a new generation, trying to improve the major stages of the flotation process. In this way, the team has created a flotation machine with a pre-contact column type which separates the three stages of the flotation process into three different reaction zones represented in Fig. 5: zone 1- particle collection unit (PCU); zone 2 - bubble disengagement unit (BDU); and zone 3 - froth recovery unit (FRU).

SFR is a technical and technological innovation in the flotation practice. It has several advantages: flotation conditions with pre-contact between the solid and air phases; reduced electricity consumption; less equipment area; significantly lower air consumption; a smaller number of cells; lower maintenance costs; better control scheme and easier automated control. The rate of the flotation process and the content of the valuable component in the concentrate is higher (www.woodgrovetech.com/SFR.html, 2018).

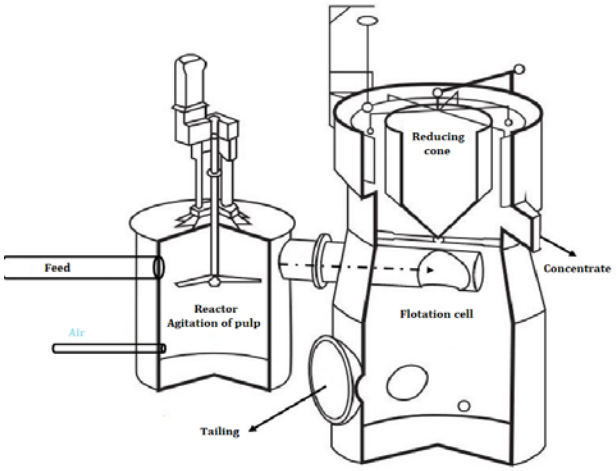

Fig. 5. Staged Flotation Reactor Flotation Machine (www.woodgrovetech.com/SFR.html, 2018)

Staged Flotation Reactor - Woodgrove Technologies Inc. is applied for a second time in the world and for the first time in Bulgaria, at Chelopech Mining EAD. Its implementation is planned by Dundee Precious Metals Inc. for the processing of the ore from the "Khan Krum" deposit, "Ada Tepe" section, until a gold-silver concentrate is obtained.

Figure 6 presents the industrial pneumatic flotation machines (SFR), put into operation at the Dundee Precious Metals processing plant in Chelopech, Bulgaria.

Fig. 6. SFR Flotation Machines at „Dundee Precious Metals Chelopech“, Chelopech, Bulgaria

Pneumatic flotation machine SIMINE Hybrid Flot

The SIMINE Hybrid Flot pre-contact flotation machine effectively combines the operation of pneumatic and column flotation machines. In the design of the cell, two basic construction stages are identified: upper and lower. The upper section works pneumatically with a three-phase injector - a solid/liquid phase (flotation pulp) and a gas phase through which the feed pulp passes where it is saturated with air. As a result of saturation, pre-contact occurs. In the froth product, the floating fractions of the recovery raw material are most easily extracted, the concentrate being drawn to launders circumferentially spaced around the flotation cell. The circular movement in the pneumatic section, along with the conical intersection between the upper and lower section, lead to a centrifugal effect while the turbulent flow is destroyed to enable a laminar flow in the second stage (column section). At the bottom of the column, the bigger gas bubbles catch coarse particles that have not attached in the first stage at lower enrichment factors. This significantly increases the total recovery while providing a high selectivity. Froth washing is possible to lower entrainment into the froth product. The concentrate from the second (lower) section is directed to a separate collection chute located at the top of the flotation cell. The regulation of the aeration device located at the bottom of the flotation cell provides a good opportunity to optimise the contact between the mineral particles and the air bubbles.

As with other pre-contact flotation machines, the SIMINE Hybrid Flot does not have a flotation pulp stirring device which contributes to the lower electricity costs and the insignificant wear on work surfaces. Figure 7 presents a general view of the SIMINE Hybrid Flot Flotation Machine (Primetals Technologies Hybrid Flotation FTC LAB, https://www.primetals.com, 2018).

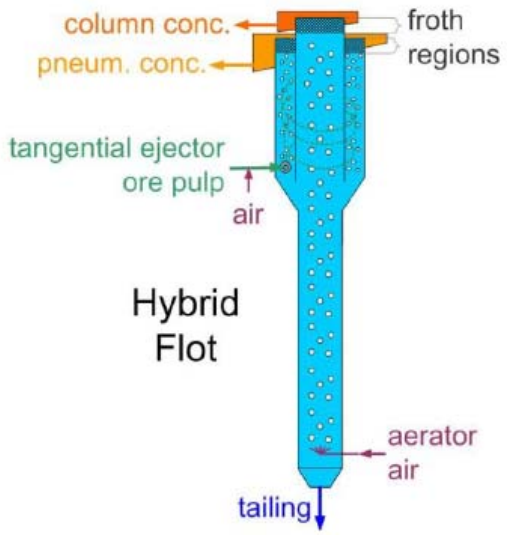

Fig. 7: Principle of the Hybrid Flotation Cell (https://www.primetals.com, 2018)

Conclusion

In the course of the past few years, constant attempts to improve the design and optimise the operation of the flotation machines have led to the development of a new generation of pneumatic flotation machines with a pre-contact column type. The established long-term trend towards decreasing the content of valuable components, especially for ore minerals, is one of the reasons for exploring the possibilities to optimise and improve the efficiency of both flotation machines and overall technological operations. One of the most important tasks that the mineral-raw material industry faces is the development of innovative engineering solutions aimed at improving the efficiency of the flotation process and leading to the full utilisation of increasingly used raw materials. The implementation of pre-contact flotation machines in the process of the concentrator plants and the hydrometallurgy plant is one of the most reliable solutions for the optimisation of the production process.

References

Brown, J., Imhof, R. and Lotzien, R., Self-aspirating aeration reactors for pneumatic flotation and other applications. In: Proceedings, Ninth Balkan Mineral Processing Congress, Istanbul, Turkey, 2001, 11-13 September.

Imhof, R., Battersby, M., Parra, F., Sanchez-Pino, S., The successful application of pneumatic flotation technology for the removal of silica by reverse flotation at the iron ore pellet plant of Compañía Minera Huasco, Chile. Proceedings of the AusIMM Centenary of Flotation Symposium, Brisbane, 2005, - 861–867 p.

Imhof, R. M., Brown, J. V., Imhoflot-Evolution of pneumatic flotation. In: Proceedings, Major Trends in Development of Sulfide Ores Up-Grading in the 21st Century Conference, Norilsk, Rissia, 2000, 24-28 April.

Imhoflot G-Cell, [Online] https://www.maelgwyn.com, 2018.

IMBE Coal & Minerals Technology GMBH – Pneuflot, [Online] http://www.mbe-cmt.de, 2018.

Primetals Technologies Hybrid Flotation FTC LAB, [Online] https://www.primetals.com/, 2018.

Staged Flotation Reactor - Woodgrove Technologies, [Online] http://www.woodgrovetech.com/SFR.html, 2018.

SOME ASPECTS OF THE REVAMP OF EXISTENT BENEFICIATION PLANTS

Alexander A. Klemiatov[1], Alexander I. Kalugin[2], Ilya A. Gribov[3], Nikita A. Rozhdestvenskii[4], Alexey Yu. Barabash[5], Yulia S. Gordeeva[6]

[1] JSC "NIUIF", Russia, Saint-Petersburg, AKlemyatov@phosagro.ru
[2] JSC "Apatit", Russia, Kirovsk, AKalugin@phosagro.ru
[3] JSC "NIUIF", Russia, Saint-Petersburg, IGribov@phosagro.ru
[4] JSC "NIUIF", Russia, Saint-Petersburg, NRozhdestvenskiy@phosagro.ru
[5] JSC "Apatit", Russia, Kirovsk, ABarabash@phosagro.ru
[6] JSC "NIUIF", Russia, Saint-Petersburg, YSGordeeva@phosagro.ru

ABSTRACT. The majority of beneficiation plants face the need for revamp in the conditions of currently operating technology, equipment, and limited space of production units. Illustrating the example of two beneficiation plants processing apatite-nepheline ore (ANOF-2 and ANOF-3), we considered some aspects, steps and results of solving a number of tasks for revamp. In the course of the work, a comprehensive approach was applied, including: setting and clarifying the task, analysing the plant operation, identifying limiting factors, identifying possible ways to solve the problem followed by selection of the most appropriate way, determining the impact on the other process stages, implementing the planned activities, and assessing the efficiency of the work performed. We reviewed the elements of forecasting applied for beneficiation process indicators and modeling with some dependences considered. High efficiency of fine screening is proved, same as of column flotation and some other processes in the conditions of available spaces of the plants considered.

Keywords: beneficiation, apatite, nepheline, revamp, column flotation, beneficiation plants processing apatite-nepheline ore (ANOF-2 and ANOF-3)

НЯКОИ АСПЕКТИ ПРИ ПРЕУСТРОЙСТВОТО НА СЪЩЕСТВУВАЩИ ОБОГАТИТЕЛНИ ФАБРИКИ

Александър А. Клемятов[1], Александър И. Калугин[2], Иля А. Грибов[3], Никита А. Рождественский[4], Алексей Ю. Барабаш[5], Юлия С. Гордеева[6]

[1] „НИУИФ" АД, Санкт Петербург, Русия, AKlemyatov@phosagro.ru
[2] „Апатит" АД, Кировск, Русия, AKalugin@phosagro.ru
[3] „НИУИФ" АД, Санкт Петербург, Русия, IGribov@phosagro.ru
[4] „НИУИФ" АД, Санкт Петербург, Русия, NRozhdestvenskiy@phosagro.ru
[5] „Апатит" АД, Кировск, Русия, ABarabash@phosagro.ru
[6] „НИУИФ" АД, Санкт Петербург, Русия, YSGordeeva@phosagro.ru

РЕЗЮМЕ. Болшинството от обогатителните фабрики са изправени пред необходимостта от преустройство в условията на непрекъснато действащи технология и оборудване и при ограничено пространство на производствените единици. Илюстрирайки с примери за две обогатителни фабрики за апатит-нефелинова руда (ANOF-2 и ANOF-3), разглеждаме някои аспекти, стъпки и резултати от решаването на редица задачи, свързани с преустройството. В хода на работата е приложен комплексен подход, включващ: поставяне и изясняване на задачата; анализ на работата на фабриката; идентифициране на възможните ограничаващи фактори; идентифициране на възможните начини за решаване на проблема, последвано от избор на най-подходящия начин; определяне на въздействието върху другите етапи на процеса; прилагане на планираните дейности; оценка на ефективността на извършената работа. Направен е преглед на приложените елементите на прогнозиране и моделиране на индикаторите в обогатителните процеси. Отчетени са и определени зависимости. Доказва се високата ефективност на финото пресяване, както и на флотационната колона и на някои други процеси в условията на наличните работни пространства на разглежданите фабрики.

Ключови думи: обогатяване, апатит, нефелин, преустройство, флотационна колона, обогатителни фабрики за апатит-нефелинова руда (ANOF-2 и ANOF-3)

Introduction

The implementation of a new production unit at a new location allows to apply the standard and already proven solutions, efficient (at the time of construction) technologies and equipment. However, in the process of operation, the production unit is supposed to be continuously improved. The following conditions may precede that: change in the properties of processed ores, the need to increase beneficiation and production indices, ageing of the existing equipment, and other factors. The revamp process consists of a number of stages. The goal of the initial stage is to determine the main criteria that need improvement or modification. In the course of work, these criteria can be specified, followed by data retrieval and identification of limiting factors of the existent production unit that prevent from achieving the assigned task. Then the possible ways to eliminate the revealed bottlenecks are identified. The general effect of the revamp on production is confirmed. Accordingly, the measures are developed and implemented to eliminate the bottlenecks, taking into consideration the integrated approach to solving the task. Thereupon, the efficiency of the completed works is assessed

and synergy of operation of all process stages is specified. Based on this, a decision is taken on the need for additional work. At all stages, the decisions are evaluated and compared not only from the process point of view, but also from economic point of view.

In many ways, the revamp of the existent production unit is a more difficult task compared to the construction of a new one due to the necessity to consider the previously implemented solutions.

Some aspects of revamp of two beneficiation plants, ANOF-2 and ANOF-3, processing apatite-nepheline ore are considered below. These beneficiation plants are part of *Apatite JSC* ("PhosAgro" company, the Russian Federation).

The reasons for revamp and succession of tasks

At the time of commencement of the revamp (technical re-equipment) of the production unit, the considered plants had similar capacity for ore. ANOF-2 produced apatite concentrate (in the main production building) and nepheline concentrate (in a separate building) whereas ANOF-3 produced only apatite concentrate.

The reasons preceding the revamp of the production units were as follows:

- the necessity to shutdown the main production building of ANOF-2 due to its ageing (in operation since 1963) and high operating costs to maintain it;
- the need to increase the yield of apatite concentrate.

An important condition was to carry out works without reducing the yield of concentrates with maximum use of existent production areas and equipment.

The complicating factor was a continuous decrease in P_2O_5 content in the ore by an average of 0.07% per annum, currently it is about 12.5% (2018).

As a consequence, at ANOF-2, it was required to allocate a new space for the apatite concentrate production unit. The initial product supplied for the production of nepheline concentrate is apatite flotation tailings with a certain content of minerals. If the main amount of apatite concentrate is produced at ANOF-3 from ore rich in P_2O_5, the quantity and quality of the tailings may not be sufficient for the stable production of nepheline concentrate at ANOF-2. Reduction of content of the useful component in the ore requires a more complicated technological process. In case a non-flexible beneficiation process is applied, any fluctuations in composition inevitably lead to a decrease in process indices.

As a result of the analysis of the set tasks, the following sequence of solutions was proposed:

1. arranging of the nepheline concentrate production unit at ANOF-3, followed by its further shutdown at ANOF-2;
2. a step-by-step increase of capacity of the apatite concentrate production unit at ANOF-3;
3. the construction of a new process chain for the production of apatite concentrate at ANOF-2 within the nepheline production areas;
4. the shutdown of the main production building at ANOF-2;
5. further expansion of the new process chain at ANOF-2 in order to make possible the beneficiation of ores of different composition and further increase of the capacity of the apatite concentrate production unit at ANOF-3.

Such succession of tasks shall allow to use the existing areas and equipment as much as possible, as well as to carry out the revamp without reducing the yield of concentrates. Thus, as a result of transferring the nepheline concentrate production unit to ANOF-3, the issue regarding the compact placement of the apatite concentrate production unit at ANOF 2 is solved. Since poorer ore is processed at ANOF-2, as well as ore with a less stable composition, the production process shall stabilise at ANOF-3. The step-by-step transferring of the most functional flotation machines, with their preliminary renewal and re-equipment, from the main production building of ANOF-2 to the new flotation production areas will make it possible to reduce the amount of equipment to be purchased.

Arrangement of the nepheline concentrate production unit at ANOF-3

According to the project (as of 1979), it was planned to construct three identical production lines of apatite flotation in the main production building at ANOF-3. Additional space for the production of nepheline concentrate was not reserved.

By the time when the revamp began, two production lines of apatite flotation had been implemented. There were areas available for the construction of the third production line. To increase the yield of apatite concentrate, the third flotation line shall be ultimately required.

The tasks for the construction of the third line for apatite flotation and for the production of nepheline concentrate were considered together. This solution is reasonable because production units of both considered concentrates were planned to be placed within one production building of the beneficiation plant. Also, it should be taken into account that the production of nepheline concentrate is a sequential process following the production of apatite concentrate in terms of comprehensive processing of apatite-nepheline ores.

In this regard, it was decided to consider the possibility to implement a more compact version of the third line of apatite flotation (compared with the existent lines) within the available areas. And the production capacities of the lines should be similar.

As a result of the optimisation of technologies and the integrated approach regarding the layout solutions, the apatite flotation line and the nepheline concentrate production unit were placed within the areas reserved for one flotation line.

The flexible process chain of the nepheline concentrate production unit includes: segregation of the required volume of apatite flotation tailings, screening by their size, magnetic separation in a weak field, reverse nepheline flotation, and, if necessary, refinement of nepheline concentrate by magnetic separation in a strong field. It is possible to use the equipment at dehydration and drying stage both for nepheline and apatite concentrates. Filtration is performed via belt vacuum filters. Storing and load handling of the nepheline concentrate is arranged within the new areas.

Increase of the apatite concentrate yield at ANOF-3

The technology of the production of apatite concentrate at ANOF-3 included: three-stage crushing and one-stage grinding of ore with screening in hydrocyclones, the basic, control and three re-cleaning flotations, dewatering, drying, storing, and

loading. Flotation is performed by pneumo-mechanical flotation machines OK-38.

Consideration of the process indices, test results, and further calculations proved that in a revamp process all major process stages are concerned, and it is reasonable to increase production capacity gradually by segregating the stages of work. This approach makes it possible to detail and correct the implemented solutions.

Analysis of the process schemes of new beneficiation plants (Baranov, 2004) shows that semi-autogenous ore grinding is the most common ore-preparation process. However, the introduction of this process at an existent plant shall require one-time drastic restructuring of the technological process with great financial investments.

This clearly does not fit into our general concept. For the revamp of ANOF-3, it was decided to gradually introduce modifications into the units which are limiting at this stage of general increase of production capacity of the plant. To identify the limiting factors, the following sequence of actions was performed: monitoring - measuring - calculating - analysing. Any of these actions may be skipped, and it is possible to come back to the previous action. This approach is used for all major process stages.

The performed calculations proved that the production capacity of the large crushing cycle would be sufficient.

At the stage of intermediate crushing, the screens GIST-72M were replaced with GTS 72MT (Korovnikov et al., 2013) and crushers KSD-3000T were replaced with GP7 (Metso Minerals). These measures, in addition to the increase of capacity, reduced the fraction size of fine crushing feed. The number of pieces of equipment did not change. It confirms the trend of the successful introduction of new crushers that operate as part of a standard ore preparation process which takes place mainly during the revamp of the operating beneficiation plants. At the same time, the obsolete equipment is replaced with new one.

Currently, the options for a revamp of the fine crushing unit are under consideration. The cone crusher MP-800 (Metso Minerals) was tested and commissioned.

It is important to arrange a rational load distribution between the stages of ore preparation, as well as between crushing and grinding. In our case, there is a task to increase the production capacity in conditions of limited spaces at grinding stage. In this regard, the issue of the increase of the efficiency factor of the crushing cycle, together with the reduction of a fraction size in the crushing-grinding cycle, has become very acute.

Taking this into account, one of the promising trends for a further revamp is the use of high-pressure grinding rolls (HPGR) at the final stage of crushing. The results of testing of ores processed at ANOF-2 and 3 by the use of HPGR confirm the possibility of efficient implementation of this technology within the existent production areas. In this regard, the development of a design for the installation of this equipment was started.

The sieving surface greatly influences the efficiency of screen operation. Currently, screening surfaces made of synthetic materials are widely used in the grinding cycle. The use of synthetic materials, in comparison with traditional metal surfaces, allows to increase their service life several times, to facilitate installation, and to reduce the extent of clogging. This leads to anincreased capacity due to the improving of the efficiency of screening and the equipment operating factor.

Increasing the capacity of the grinding process is possible by increasing the efficiency of screening. At the considered beneficiation plants, was applied a screening system several times by hydraulic size with the use of spiral classifiers (at ANOF-2) and hydrocyclones (at ANOF-2 and ANOF-3).

One of the trends in terms of increase of the capacity of the grinding cycle is the use of the fine screening process (Sukhoruchenkov et al., 2001; Baranov et al., 2005).

The results of the operation experience at the beneficiation plants (ANOF-2 and ANOF 3) showed that the curve of dependencies of apatite extraction on the grain size is typical with a reduced extraction of small (less than 20 μm) and large (more than 320 μm) grains of material into the apatite concentrate. The replacement in the grinding cycle of the screening process by hydraulic size for fine screening provides an increase in content of the most productive fractions in the flotation feed due to the reduction of the sludge content, the increase in the ore-grain release, and the reduction of the coarse fractions in the finished milled product. In the hydrocyclone, the separation of the material by its size is of a statistical nature, and in the hydrocyclone discharge, there are always particles of a much larger size that are considered to be the reference size for separation. Unlike the hydrocyclones, when screening into the sub-grid product, the material which is larger than the specified size does not pass through (in case of integrity of the screening surface). Also, the use of fine screening makes it possible to increase the capacity of a grinding cycle due to more efficient removal of the material of the required size from the circulating load of the mill. Compared to hydrocyclones, however, the screens have a number of drawbacks as well: lack of self-regulation of the process when the load changes, and there is often higher water content in the milled product.

Semi-industrial and further industrial tests of the fine-screening technology were conducted in 2006 (Brylyakov et al., 2006). Based on the test results, a step-by-step revamp of all existent mills at ANOF-3 was performed (Figure 1).

Fig. 1. The crushing unit at ANOF-3 after revamp

In addition, the total capacity of the grinding cycle was increased due to the installation of new mills that initially implied the use of screens. During the revamp of the mills, the circulating load decreased from ~ 400% to ~ 130% and the capacity increased by ~ 25-30% (Kalugin et al., 2014). An important point is that the revamp of the mills does not involve

additional areas, and the content of solids in flotation feed varies insignificantly.

The earlier revamp of the mill automatic control system made it possible to achieve a capacity increase by 7-8% and increased the process stability.

The results of the analysis of process indices at ANOF-3 and further industrial tests proved the possibility of a step-by-step load increase at two existent apatite flotation lines. Their optimum capacities were determined that allowed to conduct the process without reducing the process indices. Currently, based on the performed calculations, the pumps that limited the production capacity of the lines are being replaced step-by-step.

The remaining excess load is routed (recycled) to further flotation lines.

While arranging for the third flotation line, the experience of ANOF-2 was taken into account. Thus, the results of semi-industrial tests at ANOF-2 in 2000 showed the potential applicability of column flotation machines for basic and control flotation. Compared to pneumo-mechanical flotation machines, column ones turned to be much more effective when used in the re-cleaning cycle. Thus, the use of this type of equipment made it possible to replace three re-cleaning units by one modification. This led to a reduction of the production area occupied by those re-cleaning units by about 2/3. In this regard, since 2006, after additional testing, flotation machines of this type are involved in the re-cleaning cycle of apatite flotation in the main production building of ANOF-2

The third line of flotation which was set in operation at ANOF-3 includes: basic and control flotation, as well as one re-cleaning which is performed by column flotation machines operating in parallel (Figure 2). The flotation machines of the ore and re-cleaning flotation cycles were step-by-step moved out from the main production building of ANOF-2. The diameter of the chambers of the column flotation machines is 4.6 meters; once they were set in operation, the height of the chambers was increased from 8 to 10 meters.

Fig. 2. Re-cleaning of the 3rd line at ANOF-3

The result of the already completed revamp work of theore preparation unit, flotation, the tailings facility, and other process stages has been an increase in capacity of the plant for ore by 2.3 times over the last 7 years. Besides, the nepheline concentrate production unit was established with use of approximately 1/3 of the total volume of apatite flotation tailings. A further increase in the yield of apatite concentrate is planned, and the possibilities for increasing the yield of nepheline concentrate are considered, as well as for expanding the range of concentrates produced.

Arrangement of a new process chain for apatite concentrate production at ANOF-2

The next, and in many respects more difficult, task is arranging the production of apatite concentrate at ANOF-2 in the production building of nepheline concentrate. The complicating issue here is the fact that, in future, the technology should allow processing not only of ordinary ore but also of poor and off-balance ores. After revamp, the existent crushing complex shall stay the same, the transportation of the crushed ore shall be performed by a conveyor of about 1000 meters long, and grinding shall be done in mills operating together with screens. The dewatering unit, previously used for the nepheline concentrate, has undergone drastic modifications. The thickeners were modified, a flocculant supply system was implemented, the vacuum filters were replaced, the automation system for all process stages was redesigned and expanded, and the flotation agent preparation section was reconstructed, as well as the tailings facility. Currently, the first production line was started-up using the slurry supplied from the main production building. Flotation includes: basic, control, and one re-cleaning operation. The OK-38 flotation machines, previously used in the production of nepheline and apatite concentrates at ANOF-2, are used for the main and control flotation. Six column flotation machines with chambers of 4.6 meters in diameter and 8 meters in height are used in the re-cleaning flotation. Four column flotation machines are being transferred from the main production building, two are under purchasing. At the time of writing of this article, two transferred column flotation machines are operated (Figure 3).

Fig. 3. Re-cleaning of apatite concentrate in the former nepheline concentrate production building at ANOF-2

When developing and analysing the beneficiation options, the modelling of the process was done involving a number of dependencies.

The analysis of processes indices and lab tests for different ores and beneficiation processes has revealed a clear linear

relationship between the amount of the target component passing to the concentrate ($\gamma*\beta$) and the content of this component in the ore (Klemyatov et al., 2011). Thus, having a data array for the operation or for the entire technological process, we can consider the following dependence:

$$\gamma \cdot \beta = a \cdot \beta_{feed} + b \quad (1)$$

where:
γ is the concentrate yield (in %);
β is the component content in the concentrate;
β_{feed} is the component content in operation feed (in %);
a and b are equation coefficients.

At the same time, there is a close to linear dependence of the concentrate yield on the content of the target component in the ore.

In this regard, for each operation of beneficiation flotation cycle, there were found the coefficients of the regression equations linking the main beneficiation indices. The coefficients of the equations were calculated based on the array of the flotation process tests performed during the beneficiation of ores with different P_2O_5 contents. For the re-cleaning flotation, another regression equation term was added which is responsible for the effect of the apatite concentrate quantity (produced by one column of the flotation machine) on the beneficiation indices.

Then, by iterative calculations, the expected values for the intermediate beneficiation products were determined. The process configuration was designed taking into consideration the real possible layouts of the equipment, due to strict limitations in terms of spaces and elevations, and the need for self-transportation of products by gravity.

The approach using this or similar equations is quite universal. Here, it was used for forecasting of the final beneficiation indices, for estimating the effect of line ore load on the beneficiation indices, for identifying process failures, and in a number of other cases.

For example, when evaluating the effect of ore quantity (supplied into the processing from different mines) on the beneficiation indices and forecasting the beneficiation indices of this ore, the following option of the considered dependence can be applied (the simplest option is provided):

$$\varepsilon = \frac{\beta_{ore\Sigma} \cdot \sum(\gamma_{ore(n)} \cdot a_{\varepsilon(n)}) + b_{\varepsilon}}{\beta_{ore\Sigma}} \quad (2),$$

$$\gamma = \beta_{ore\Sigma} \cdot \sum(\gamma_{ore(n)} \cdot a_{\gamma(n)}) + b_{\gamma} \quad (3)$$

where:
ε is the extraction of the considered component into the concentrate (%);
γ is the concentrate yield (%);
n is the trend of ore supply;
$\beta_{ore\Sigma}$ is the contents of the considered component in the ore supplied to the plant (in %);
$\gamma_{ore(n)}$ is ore fraction in the trend of the total ore supply to the plant (in %);
$a_{\gamma(n)}$, $a_{\varepsilon(n)}$, b_{ε}, b_{γ} are equation coefficients.

Currently, an option is being elaborated for the second re-cleaning flotation for the implemented process. Considering the area limits for this operation, the possibility of using pneumatic flotation machines is considered: Pneuflot, Jameson Cell, or similar ones.

Conclusion

The example of the two beneficiation plants has shown that the process of revamp of existent production units requires a systematic approach. According to the authors, the process of revamp of the plant should proceed almost continuously from its start-up to its shutdown due to a constant change of ore composition, optimisation of operation parameters and new processes emerging, the existent equipment getting obsolete, and new equipment developed. An important factor is achieving maximum profit with minimum operating costs.

When choosing the options for revamp, we considered not only the process indices, but also compared the expected economic effects. A positive economic effect has been achieved for already completed upgrades. Calculations show that a positive economic effect is also expected from all works currently performed.

The methods for solving each task can vary and there are no unambiguous templates to follow. The main thing is always to keep to a systematic approach and consider more than just a local issue.

As a result of the already completed activities for the revamp of ANOF-2 and ANOF-3, the total yield of apatite concentrate at the two beneficiation plants has increased by 1.2-1.3 times over the past seven years and a further capacity increase is planned.

BIBLIOGRAPHICAL REFERENCES

Баранов, В. Ф. Современная мировая практика в области рудоподготовки (зарубежный опыт). - Обогащение руд, 3, 2004. - 41-47. (Baranov, V. F. Sovremennaya mirovaya praktika v oblasti rudopodgotovki (zarubezhnyj opyt). - Obogashchenie rud, 3, 2004. - 41-47.)

Баранов, В. Ф., В. А. Сентемова, А. А. Ядрышников. О модернизации технологии рудоподготовки отечественных железнорудных фабрик. - Обогащение руд, 1, 2005. - 5-8. (Baranov, V. F., V. A. Sentemova, A. A. YAdryshnikov. O modernizacii tekhnologii rudopodgotovki otechestvennyh zheleznorudnyh fabrik. - Obogashchenie rud, 1, 2005. – 5-8.)

Брыляков, Ю. Е., С. П. Шишкин, М. А. Кострова, В. Е. Потокин, Голованов, В. Т., Ангелов, А. М., Калугин, А. И., Борис, М. Е., К. К. Тране, С. Б. Валин. Совершенствование технологии классификации в цикле измельчения апатит-нефелиновых руд. - Бюллетень “Мир серы, N, P и K”. – М., ОАО “НИУИФ”, 2, 2006. – 10-18. (Brylyakov, Yu. E., S. P. Shishkin, M. A. Kostrova, V. E. Potokin, Golovanov, V. T., Angelov, A. M., Kalugin, A. I., Boris, M. E., K. K. Trane, S. B. Valin. Sovershenstvovanie tekhnologii klassifikacii v cikle izmel'cheniya apatit nefelinovyh rud. - Byulleten' “Mir sery, N, P i K”. – M., OAO “NIUIF”, 2, 2006. – 10-18.)

Калугин, А. И., К. М. Гумениченко, А. Ю. Барабаш, С. С. Арсентьев. Опыт внедрения технологии тонкого грохочения в цикле измельчения апатит-нефелиновой руды. - Обогащение руд, 10, 2014. - 52-57. (Kalugin, A. I., K. M. Gumenichenko, A. Yu. Barabash, S. S. Arsent'ev. Opyt vnedreniya tekhnologii tonkogo grohocheniya v cikle izmel'cheniya apatit nefelinovoj rudy. - Obogashchenie rud, 10, 2014. - 52-57.)

Клемятов, А. А., В. И. Максимов, А. С. Пермяков. Анализ и прогнозирование показателей работы действующего производства на примере ОФ ОАО "Кольская ГМК". - Цветные металлы, 8/9, 2011. – 52-54. (Klemyatov, A. A., V. I. Maksimov, A. S. Permyakov. Analiz i prognozirovanie pokazatelej raboty dejstvuyushchego proizvodstva na primere OF OAO "Kol'skaya GMK". - Cvetnye metally, 8/9, 2011. – 52-54.)

Коровников, А. Н., А. А. Трофимов, А. И. Калугин. Опыт совершенствования технологии рудоподготовки в ОАО «Апатит» с применением грохотов ГСТ-72МТ - Обогащения руд, 1, 2013. – 34-38. (Korovnikov, A. N., A. A. Trofimov, A. I. Kalugin. Opyt sovershenstvovaniya tekhnologii rudopodgotovki v OAO «Apatit» s primeneniem grohotov GST-72MT - Obogashcheniya rud, 1, 2013. – 34-38.)

Сухорученков, А. И., В. В. Стаханов, Г. В. Зайцев. Тонкое грохочение – высокоэффективный метод повышения технико-экономических показателей обогащения тонковкрапленных магнетитовых руд. - Горный журнал, 4, 2001. - 48-50. (Sukhoruchenkov, A. I., V. V. Stahanov, G. V. Zajcev. Tonkoe grohochenie – vysokoeffektivnyj metod povysheniya tekhniko ehkonomicheskih pokazatelej obogashcheniya tonkovkraplennyh magnetitovyh rud. - Gornyj zhurnal, 4, 2001. – 48-50.)

THE EFFECT OF IMPURITY COMPOSITION OF PHOSPHATE ROCK ON THE TECHNOLOGY OF ITS PROCESSING AND PROPERTIES OF FINAL PRODUCTS

Norov Andrey M.[1], Pagaleshkin Denis A.[2], Fedotov Pavel S.[3]

[1] JSC "NIUIF", Russia, 162622 Cherepovets, ANorov@phosagro.ru
[2] JSC "NIUIF", Russia, 162622 Cherepovets, DPagaleshkin@phosagro.ru
[3] JSC "NIUIF", Russia, 162622 Cherepovets, PFedotov@phosagro.ru

ABSTRACT. The composition of phosphate rock and the impurities contained in it have a determining effect on the choice of processing technology, production capacity, consumption factors, properties of the final product and other important parameters. When developing methods for processing phosphate raw materials in target products, it is very important to study and take into account the impurities contained in it and their effect on technology. In this article, based on the summary of scientific and production experience and the latest researches by JSC "NIUIF", the oldest and the only scientific & research institute in Russia on phosphorus-containing fertilizers, the influence of impurities containing carbonates, calcium, iron, aluminum, magnesium, fluorine, chlorine, sodium, potassium, rare earths, silicon dioxide on process parameters of processing phosphate raw materials and properties of the final product is considered in detail. The methods of finding the optimal options for organizing of technological process of processing phosphate raw materials and stabilization of the quality of products are shown.

Keywords: phosphate rock, impurities, wet phosphoric acid, phosphorus-containing fertilizers, granule structure, caking, granule strength

ВЛИЯНИЕ НА СЪДЪРЖАНИЕТО НА ПРИМЕСИ ВЪВ ФОСФАТНИТЕ СКАЛИ ВЪРХУ ТЕХНОЛОГИЯТА ЗА ПРЕРАБОТКАТА ИМ И СВОЙСТВАТА НА КРАЙНИТЕ ПРОДУКТИ

Норов Андрей М.[1], Пагалешкин Денис А.[2], Федотов Павел С.[3]

[1] „НИУИФ" АД, Русия, 162622 Череповец, ANorov@phosagro.ru
[2] НИУИФ" АД, Русия, 162622 Череповец, DPagaleshkin@phosagro.ru
[3] НИУИФ" АД, Русия, 162622 Череповец, PFedotov@phosagro.ru

РЕЗЮМЕ. Съставът на фосфатната скала и съдържащите се в нея примеси имат определящ ефект върху избора на технология за обработка, производствен капацитет, фактори на потребление, свойства на крайния продукт и други важни параметри. При разработването на методи за преработка на фосфатни суровини в крайни продукти е много важно да се проучат и да се вземат предвид съдържащите се в тях примеси и техният ефект върху технологията. В тази статия, въз основа на научния и производствен опит и най-новите изследвания на "НИУИФ", най-старият и единствен научно-изследователски институт в Русия за торове, съдържащи фосфор, се разглежда въздействието на примеси, съдържащи карбонати, калций, желязо , алуминий, магнезий, флуор, хлор, натрий, калий, редки земни елементи, силициев диоксид върху параметрите на процеса на преработка на фосфатни суровини и свойствата на крайния продукт. Описани са методите за намиране на оптимални възможности за организиране на технологичния процес на преработка на фосфатни суровини и стабилизиране на качеството на продуктите.

Ключови думи: фосфатни скали, примеси, мокра фосфорна киселина, торове съдържащи фосфор, структура на гранулата, спичане, здравина на гранулата

Introduction

Phosphorus is quite a common element, its content in the earth's crust according to various estimates is 0.08-0.12% of its mass. In total, more than 120 phosphate minerals are known in nature, mostly chemically stable, insoluble in water and in soil solutions (Kopylev, 1981). The minerals of the apatite group are of the largest industrial value among them, as well as phosphorites that form large deposits.

Like any natural mineral substance, phosphate rock (of apatite and phosphorite nature), besides the main target component (phosphorus, usually expressed through percentage of P_2O_5 content), contains also various impurities: calcium and magnesium carbonates, compounds of iron, aluminum, silicon, fluorine, sodium, potassium, chlorine, strontium, rare earth elements, organic substances, etc. Many of these impurities, even after beneficiation of phosphate rock, have a significant influence on choosing the processing technology, the output of the target component, process mode parameters, capacity, consumption ratios of raw materials and energy resources and other indices.

Main exposition

The increased content of carbonates leads to intense foaming while processing phosphate rock via acidic methods, due to the release of carbon dioxide CO_2, especially in combination with organic impurities. This leads to reduction of operation volumes of the reactors, malfunction of the pumps, and as a result, disruption of the entire technological process. In practice, it was confirmed that phosphate rock with CO_2

content of more than 8% cannot be practically used to produce wet phosphoric acid (WPA) without special methods and means of defoaming applied (Evenchik and Brodskiy, 1987).

The specific consumption of sulfuric acid in the production of WPA (and, consequently, the production economy to some extent), and also the specific rate of production waste – phosphogypsum, depend on the calcium content in the phosphate rock.

The compounds of iron and aluminum (sesquioxides) are perhaps the most harmful impurities (especially iron), which largely determine the suitability of phosphate rock for acid processing. In sulfuric acid decomposition of phosphates with higher iron content, an excessive amount of sulfuric acid is consumed, and the recovery of P_2O_5 is greatly reduced due to precipitation of insoluble iron phosphates (P_2O_5 retrogradation). In addition, filtration of the extraction slurry gets worse. Aluminum phosphates are more soluble than iron phosphates, and therefore, are less likely to contribute to retrogradation. The content of sesquioxides in phosphate rock is limited not by their absolute content, but by their ratio to the content of P_2O_5. In practice it was confirmed that in phosphate rock suitable for sulfuric acid processing, the ratio of Fe_2O_3 content to P_2O_5 content should be not more than 8, that is:

$$\frac{C_{Fe_2O_3}}{C_{P_2O_5}} \times 100 \leq 8 \quad (1)$$

The content ratio of the sum of sesquioxides ($Fe_2O_3 + Al_2O_3$) to P_2O_5 should be not more than 12 (Kopylev, 1981; Evenchik and Brodskiy, 1987), that is:

$$\frac{C_{(Fe_2O_3+Al_2O_3)}}{C_{P_2O_5}} \times 100 \leq 12 \quad (2)$$

While processing phosphates by nitric acid and hydrochloric acid methods, the content of sesquioxides is less important due to its lower solubility in these acids (Evenchik and Brodskiy, 1987; Kononov et al., 1988), but it also leads to losses of P_2O_5. That's why, phosphate rock with ratio Fe_2O_3 to P_2O_5 of more than 12 is also unsuitable for nitric acid decomposition (Kopylev, 1981). For production of thermal phosphates by sintering, the content of sesquioxides is not significant (Evenchik and Brodskiy, 1987). And the electrothermal method allows to process practically any phosphate rocks, including low-quality ones (Pozin, 1983). The presence of sesquioxides ($Fe_2O_3 + Al_2O_3$) in the slurry (when sulfuric acid method of decomposition of phosphates is applied) affects both the size and shape of generated $CaSO_4$ crystals, which in turn affects the washing of phosphogypsum (Kopylev, 1981; Kononov et al., 1988).

The magnesium compounds in the sulfuric acid process of WPA production decrease the acid activity and increase its viscosity, so for this process it is recommended to use phosphate rock with the ratio (Kopylev, 1981; Evenchik and Brodskiy, 1987):

$$\frac{C_{MgO}}{C_{P_2O_5}} \times 100 \leq 7 \div 8 \quad (3)$$

While decomposing of phosphates with nitric and hydrochloric acid, magnesium impurities are not really significant. In the production of thermal phosphates, magnesium impurities do not cause negative effect, and they are even useful in the production of magnesium fused phosphates (Evenchik and Brodskiy, 1987).

The behavior of fluorine contained in phosphate rock is of great importance (especially in fluorapatite-based rock). When the phosphate rock is decomposed by acids, fluorine transfers into hydrogen fluoride, which then reacts with silicon-containing minerals:

$$6HF + SiO_2 \rightarrow H_2SiF_6 + 2H_2O \quad (4)$$

Part of the produced fluorosilicic acid is released in a gas phase as equimolecular mixture of $2HF + SiF_4$. The remaining amount of H_2SiF_6 transfers into the solution, where it reacts with excess SiO_2:

$$2H_2SiF_6 + SiO_2 \rightarrow 3SiF_4 + 2H_2O \quad (5)$$

The silicon tetrafluoride is volatile and also passes into gas phase. Fluorine distribution between gas, liquid and solid phases depends on the phosphate rock processed, processing mode, and other factors (Kononov et al., 1988). During concentration (evaporation) of WPA, up to 80% of fluoride contained in it, is released during the gas phase. Fluorine compounds during processing of phosphate rock primarily have a negative impact in terms of increasing corrosion. In addition, as it will be proved later, fluorine can worsen the quality characteristics of the final products.

Chlorine also significantly increases the corrosion of the equipment, therefore, for sulfuric acid processing, its content in phosphate rock should not exceed 0,03÷0,04%. Impurities of alkali metals (sodium, potassium) form poorly soluble compounds of silicon fluorides Na_2SiF_6 and K_2SiF_6. This leads to increased clogging and deposits accumulation in the piping of filtering equipment, so it is preferable that the total content of Na_2O and K_2O in the phosphate rock should not exceed 0,4÷0,6% (Kononov et al., 1988).

Compounds of rare-earth elements (REE) contained in some types of phosphate rock (for example, in the Khibiny apatite concentrate there is about 1% of REE) can adversely affect the crystallization of calcium sulfate dihydrate, worsen the filtration of phosphogypsum and increase its moist content (Kononov et al., 1988). The compounds of cerium and strontium significantly slow the hydration of calcium sulfate hemihydrate to dihydrate (Kopylev, 1981), as a result of which the two-stage hemihydrate-dihydrate process for certain kinds of phosphate rocks becomes problematic and poorly feasible.

Silicium dioxide, which is present in the form of silica and hardly soluble silicates and is part of the so-called insoluble precipitate, in most cases has no harmful effect on acid processing of natural phosphates. However, its high content in phosphate rock can lead to increased erosion of equipment and create difficulties in the filtration stage (Kononov et al., 1988). During the decomposition of phosphate rock with nitric acid, the presence of silicium dioxide, which is soluble in nitric

acid, increases the rate of nitric acid consumption and worsens the slurry filtering conditions, which in turn leads to increase of P_2O_5 and calcium nitrate losses during washing (Evenchik and Brodskiy, 1987).

Impurities can exert influence not only each one separately, but also in combination with each other. For example, the favorable effect on the shape and size of calcium sulfate crystals in the sulfuric acid production of WPA is provided by SiF_6^{2-} ions in combination with Al^{3+} ions (Kopylev, 1981). Based on the research conducted by NIUIF, our specialists proposed a method (Grinevich et al., 2016) that allowed to greatly intensify the dihydrate process of WPA production to produce the easily filtered $CaSO_4 \cdot 2H_2O$ by introducing an acid-soluble aluminum-containing additive into the decomposition zone, providing high P_2O_5 yield and shifting the crystallization zone of calcium sulfate dihydrate to higher temperatures and P_2O_5 content (high-temperature dihydrate).

In international practice there is no strict regulation for the quality of phosphate rock, however, certain requirements for exported rock have been established. Thus, phosphate rock intended for production of WPA should contain at least 31% of P_2O_5, not more than 3.5% of R_2O_3 (Fe_2O_3 + Al_2O_3), not more than 0.4% of MgO, 10,5% of insoluble precipitate and the ratio of CaO/P_2O_5 should be 1.45÷1.55 (Angelov et al., 2000).

Impurity elements can also complicate the process mode even in production of final products: mineral fertilizers and feed phosphates. When WPA is concentrated with an increased content of sesquioxides and especially magnesium, a viscous, non-transportable liquid is formed, so it is assumed that in phosphate rock used for production of concentrated acid the ratio should be (Evenchik and Brodskiy, 1987):

$$\frac{C_{MgO}}{C_{P_2O_5}} \times 100 \leq 5 \div 6 \qquad (6)$$

When the content of magnesium is high, either the technologies for production of mineral fertilizer from non-concentrated WPA are applied (Evenchik and Brodskiy, 1987; Kononov et al., 1988), or the technologies with evaporation/concentration of completely or partially neutralized slurries (Kononov et al., 1988; Grishaev et al., 2014).

The deposits on the heating surfaces of the equipment for concentration of WPA contain an increased content of impurity elements, same as various deposits and sludges in pipelines and equipment, while neutralizing WPA with ammonia during the production of mineral fertilizers (Bushuyev, 2009; Bushuyev, 2011). All of that can complicate the processing and lead to additional shutdowns for cleaning the equipment.

The increased content of impurities in the initial phosphate rock and in WPA produced from it can limit the production of some of the final products. For example, liquid complex fertilizers (LCF) of grade 11:37 cannot be produced from WPA with high content of sesquioxides and magnesium without its preliminary purification. The same impurities, as well as fluorine, can be an obstacle for the production of feed monocalcium phosphate. The impurities, passing from phosphate rock through WPA into fertilizers, can influence the quality of the latter ones. Some impurities are useful from agrochemical point of view. So, calcium, magnesium and sulfur are the macro-elements necessary for proper development of plants (Pozin, 1983). Other impurities, such as iron, copper, zinc, manganese, cobalt, molybdenum, etc., are the micro-elements, which are also very important for the realization of vital functions of plants, if not contained in excessive quantities. There is also an amount of harmful impurities - lead, mercury, arsenic, cadmium, whose content in fertilizers and feed phosphates is strictly regulated in a number of countries, including the Russian Federation. From this point of view, the Khibiny apatite concentrate used at PhosAgro plants is a unique, most environmentally friendly type of phosphate rock that does not contain harmful impurities and allows for any kinds of products to be produced from it.

Some impurities, especially such as fluorine, magnesium, iron, aluminum, can affect the physical & chemical and structural & mechanical properties of granular phosphorus-containing fertilizers. As per the research conducted by NIUIF, fluorine increases caking of granular ammonium-phosphate-based fertilizers, and also reduces their static strength (Norov et al., 2012). Figure 1 shows the dependence of caking and static strength of diammonium phosphate (DAP) granules of fertilizer grade 10:46 on the content of fluorine in it.

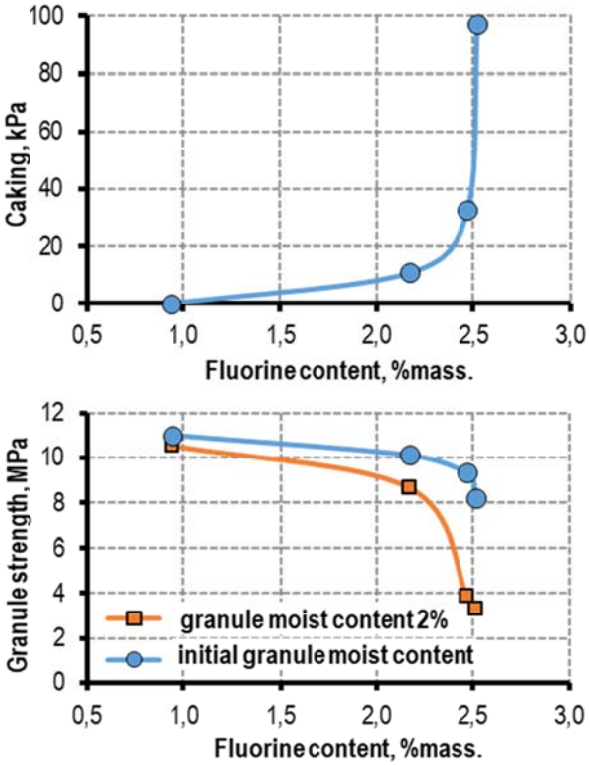

Fig. 1. Dependence of caking and static strength of industrially produced DAP granules on the content of fluorine

You can see from the graphs that with increase of fluorine content, DAP caking increases, and the strength of the granules decreases, and this becomes especially evident with a mass fraction of fluorine of more than 2%. It was also noted that the effect of fluorine increases with increase of the extent of WPA neutralization, i.e. in fertilizers based on DAP, this effect appears to a higher extent than in fertilizers based on

monoammonium phosphate (MAP). Our x-ray phase analysis proved that the fluoride compounds in MAP are represented mainly by aluminum, sodium and potassium silicofluorides, and in DAP – by fluorophosphates $NH_4AlHPO_4F_2$ and $NH_4FeHPO_4F_2$.

In the production of DAP in aqueous weak-alkaline medium, ammonium silicofluoride is hydrolyzed as per the reaction:

$$(NH_4)_2SiF_6 + 4NH_3 + (n+2)H_2O \rightarrow 6NH_4F + SiO_2 \cdot nH_2O(gel) \quad (7)$$

The obtained ammonium fluoride NH_4F is a much more hygroscopic compound than $(NH_4)_2SiF_6$. In addition, during neutralization, ammonium fluoride reacts with ammoniated iron and aluminum phosphates with formation of an amorphous, poorly filtered colloidal precipitate of fluorophosphate of ammonium, iron and aluminum (Kononov et al., 1988).

$$NH_4(Fe,Al)(HPO_4)_2 + 2NH_4F \rightarrow NH_4(Fe,Al)HPO_4F_2 + (NH_4)_2HPO_4 \quad (8)$$

Due to the formation of these compounds, the ammoniated phosphate slurries become more viscous, and to maintain their mobility, higher water content is required. This, in turn, reduces the extent of supersaturation of solutions, leads to decrease in the number of nucleating seeds, decrease of crystallization rate, and increase of crystal size during granulation.

In addition, it is known from literature that the presence of ammonium fluoride in solutions of ammonium phosphates interferes with the crystallization of diammonium phosphate and shifts it toward higher pH values (Pozin, Zinyuk et al., 1976; Dokholova et al., 1986). Increase of fluorine content in the initial WPA increases solubility of its ammonium products (Pozin, Kopylev et al., 1976; Kuvshinnikov, 1987). All of that has allowed us to conclude that the increase of the content of fluorine compounds hinders the process of mass crystallization during granulation, increases crystallization time and the size of formed crystals. As a result, the number of phase contacts between the crystals decreases, the structure of the granules becomes more porous and less stable and themobility of water-salt complexes in granules is ensured. That is why caking increases and the strength of granules decreases. This is confirmed by our microscopic studies. Figure 2a, b shows enlarged photographs of the surface and a slice of DAP granule with low and high fluorine content. You can see that DAP granules with fluorine content of less than 1% have a better, denser structure, the surface of the granules is homogeneous, even, and smoother. The slice of the granule is also homogeneous in volume, the granule is dense, monolithic, without visible agglomerates.

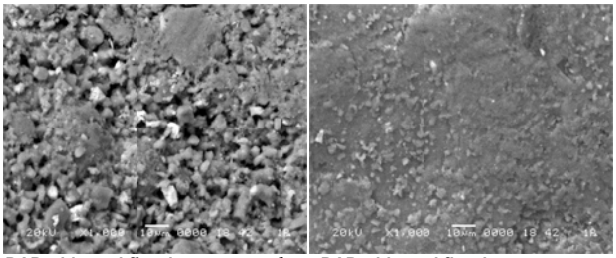

DAP with total fluorine content of more than 2 %mass. | DAP with total fluorine content less than 1 %mass.

Fig. 2a. DAP granule surfaces with different fluorine content (magnification×1000)

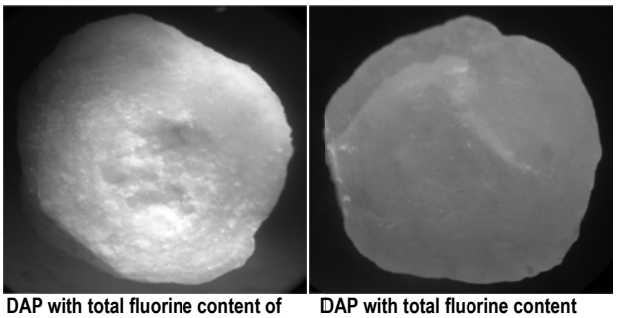

DAP with total fluorine content of more than 2 %mass | DAP with total fluorine content less than 1 %mass

Fig. 2b. DAP granule slices with different fluorine content (magnification×25)

DAP granules with fluorine content of more than 2% are heterogeneous both in surface and volume. The surface is inhomogeneous, uneven, locally formed by agglomerates of particles that creates a porous, friable structure. The slice of the granule is not homogeneous, the nucleus of the granule and the surface layer can be distinguished visibly in the photograph. The volume of the granule is represented by intergrowths of agglomerates of crystals, the packing of which is not sufficiently dense.

The silica gel $SiO_2 \cdot nH_2O$ released in the reaction (7) also negatively affects the processes of granule formation. To separately assess the extent of fluorine and silica gel effect on the properties of fertilizers, DAP granules with different fluorine content were obtained at NIUIF's Testing Center, where HF was used for changing of fluorine content in one series of testing, and H_2SiF_6 was used for this purpose in another series of testing. Then these samples were tested for strength and caking (Fig. 3).

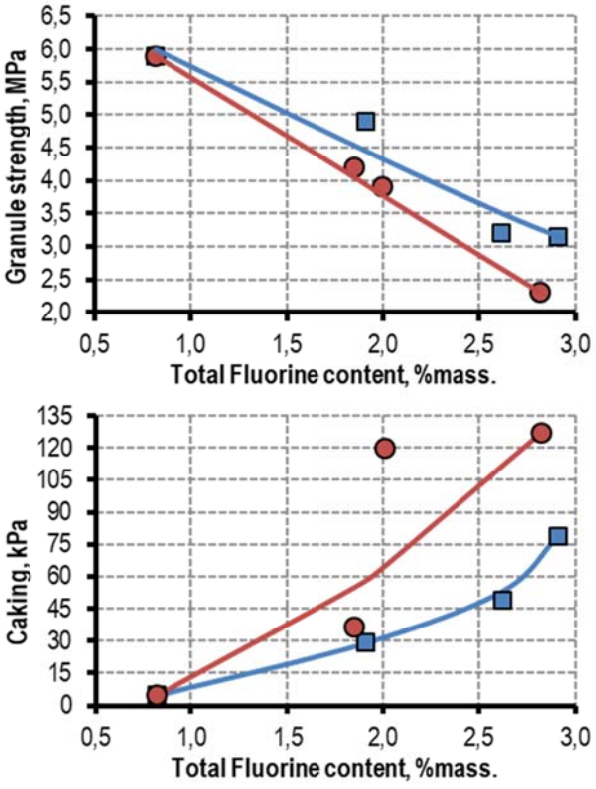

Fig. 3. Dependence of DAP granule caking and strength on the content of fluorine (red line: with addition of H_2SiF_6 (resulting in silica gel formation); blue line: with addition of HF (without formation of silica gel)

The results of these studies show that the presence of silica gel also contributes to deterioration of the structural and mechanical properties of fertilizers: the strength of the granule is reduced, and caking increases to a higher extent than with the same content of fluorine when there is no silica gel.

Some impurities, on the contrary, improve the properties of fertilizers, such as iron, aluminum and especially magnesium (Kuvshinnikov, 1987; Norov et al., 2012). The studies conducted by JSC "NIUIF" proved that even with a slight change of magnesium content (for several deciles of a percent), the properties of phosphorus-containing fertilizers significantly change (Fig. 4).

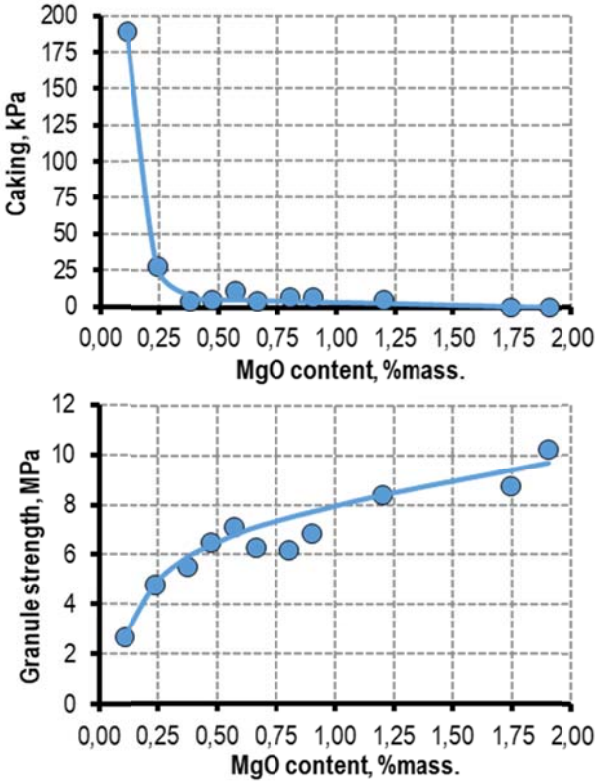

Fig. 4. Dependence of DAP caking and static strength of DAP granules on MgO content in fertilizer (fluorine content in DAP at about 2,5 %mass.)

Hereof it means that even when the magnesium content in DAP is about 0.4-0.5 percent in conversion to MgO, the caking rate decreases sharply and the static strength of the granules increases. With such insignificant change in impurity, this effect can be explained only due to change in the structure of the granules. This is also confirmed by the results of comparative studies of DAP granules under the microscope (Fig. 5a, b), which showed that granules with magnesium additives have a better, denser structure, the granules are composed of smaller crystals, have less porosity, the surface of the granules is more homogeneous, even and smooth, the slice is also homogeneous, without visible flaws.

Using the system of electronic probe energy-dispersed X-ray fluorescence analysis, the distribution of impurity elements along the surface of DAP granules was determined. The results of the analysis showed that adding of magnesium several times reduces the presence of fluorine and silicon on the surface of the granules (Table 1).

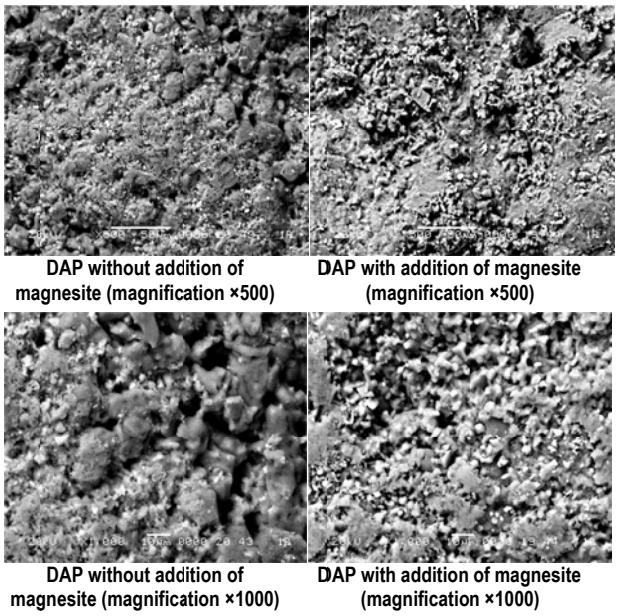

DAP without addition of magnesite (magnification ×500) | **DAP with addition of magnesite (magnification ×500)**

DAP without addition of magnesite (magnification ×1000) | **DAP with addition of magnesite (magnification ×1000)**

Fig. 5a. Electronic photographs of DAP granule surface (magnification ×500; ×1000)

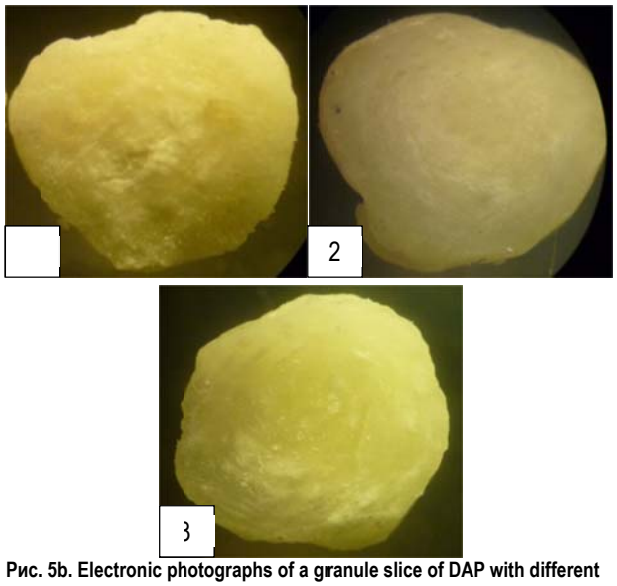

Рис. 5b. Electronic photographs of a granule slice of DAP with different MgO content (magnification ×25)
1 – without adding of MgO (0,12% MgO); 2 – 0,4% MgO; 3 – 0,5% MgO

Table 1

Fluorine and silicon content on the surface of DAP granules with and without MgO additives

Content on DAP granule surface	DAP samples			
	without MgO additive	without MgO additive	with MgO additive	with MgO additive
Fluorine, %mass.	7.07	11.63	4.90	2.15
Silicon, %mass.	0.86	1.55	0.19	0.18

This can also be explained by the fact that in the presence of magnesium, the formation rate of granule crystal structure is increased, granule crystal structure unrandomization and compaction occurs, and various impurities, amorphous and slowly crystallized, will be trapped inside the granules and their release to the surface will be complicated.

By X-ray phase and chemical analysis it was confirmed that while neutralizing of WPA with ammonia in the presence of magnesium, depending on the content of impurities in the acid and the extent of neutralization, various compounds can be formed: magnesium ammonium phosphate $MgNH_4PO_4 \cdot H_2O$, complex phosphates such as $Mg_n(Al,Fe)(NH_4)_2(HPO_4)_2F_{2n+1}$, $MgNH_4HFPO_4$, etc. The common thing for these compounds is that they are water-insoluble, finely dispersed, well-crystallized compounds (Kononov et al., 1988), which serve as seeds, accelerating crystallization processes and promoting the formation of granules with a strong structure and good physical & chemical and structural & mechanical properties. In addition, complex fluorophosphates bind water-soluble fluorine to insoluble compounds (Norov et al., 2012), therefore they partially neutralize its negative effect. In case crystalline hydrates are formed, for example, $MgNH_4PO_4 \cdot H_2O$, etc., additional water binding occurs, as well as local increase of the extent of supersaturation of solutions, which additionally accelerates crystallization. Such a mechanism, explaining the effect of magnesium on the properties of phosphorus-containing fertilizers, was proposed by NIUIF based on conducted studies and tests. Magnesium additives have a positive effect on the structure and properties of not only DAP, but also other types of granular phosphorus-containing fertilizers, for example, MAP, sulfoammophos (Norov et al., 2012). Ref. (Kuvshinnikov, 1987) tells about improving the properties of nitrate-containing NPK with magnesium. The studies carried out by JSC "NIUIF" showed that magnesium-containing additives also improve the properties of granular sulphur-containing, non-nitrate NPK-fertilizers based on phosphates and sulfates of ammonium and potassium chloride, for example, grade 15:15:15 (Fig. 6). The same is confirmed for other sulphur-free, non-nitrate NPK grades (13:19:19, 16:16:8, 8:20:30), NPS 16:20:0(14S), etc.

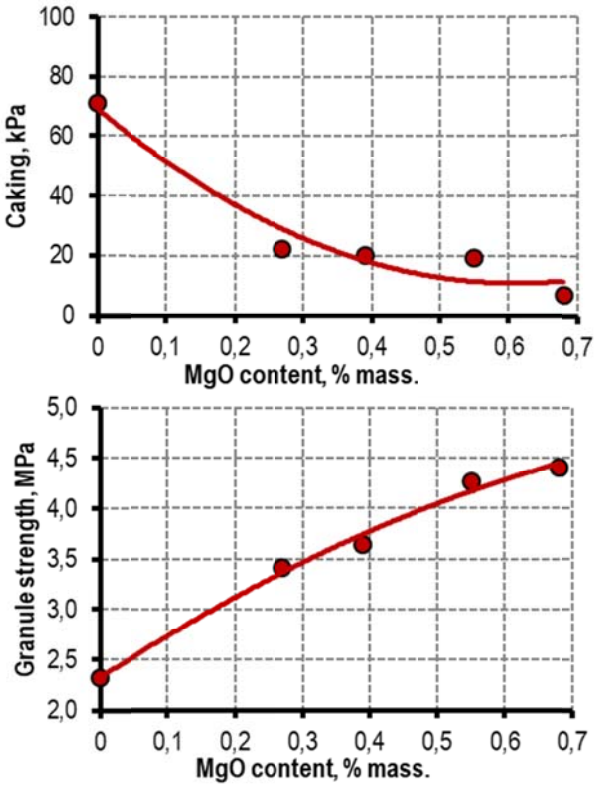

Fig. 6. Influence of magnesium content on properties of NPK fertilizer grade 15:15:15

Magnesium content in phosphorus-containing fertilizers also affects the technology of their production. Acceleration of crystal structure formation of granules with the introduction of magnesium-containing additives has a positive effect on granulation process and contributes to the formation of larger granules. As a result of compaction and hardening of granule structure, diffusion transfer of water from the granule volume to its surface becomes complicated. Generally, it can complicate a bit the drying process and increase the moist content in fertilizers, but it's not critical. According to our studies, the positive effect of using the magnesium-containing additives significantly outcompetes the negative effect of moist content increase in the product. Fig. 7 shows the results of our studies by the example of NPK-fertilizer grade 15:15:15, when the use of magnesium-containing additives makes it possible to obtain fertilizers with increased moist content without deterioration and even with improvement of fertilizer properties. This is also true for other grades of phosphorus fertilizers.

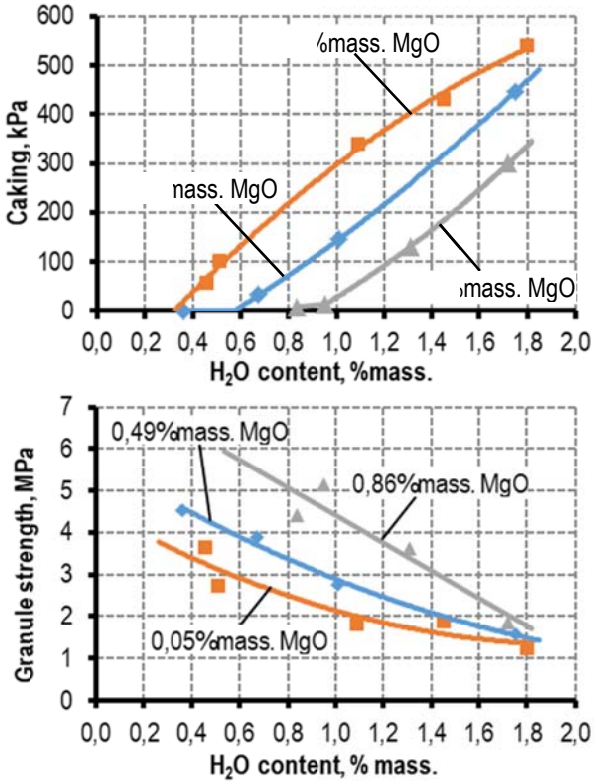

Fig. 7. Influence of content of MgO and moist on granule static strength and caking of NPK fertilizer grade 15:15:15

Since the state of granule surface also improves with the introduction of magnesium, the efficiency of its treatment with conditioning mixtures against dust and caking improves significantly as well, because air conditioners are absorbed less and longer.

Based on our research and tests, we have developed and patented a method for improving the properties of phosphorus-containing fertilizers (Chernenko et al., 2012), which has been successfully introduced at a number of Russian plants. Once the method was introduced in all these plants, the granule strength increased, while caking and dustiness of the produced fertilizers (NP, NPS, NPK and NPKS) decreased significantly.

Impurities also have a very significant effect on retrogradation of P_2O_5 and on the content of nutrients in a water-soluble, assimilable and unassimilable form, though it's a topic for another article.

Conclusion

In conclusion, it should be noted that when developing methods for processing phosphate rock into the target products, it is very important to study and take into account the impurities contained in it and their effect on the technology.

References

Angelov A.I., Levin B.V., Chernenko U.D. Phosphate rock. Reference book. M., "Nerda – Business center" LLP, 2000 - 120 p.

Bushuyev N.N., Davydenko V.V., Norov A.M., Syrchenkov A.Ya. X-ray Phase Analysis of deposits in a Pipe Reactor at phosphorus fertilizer production unit of "Balakovo Mineral Fertilizers" LLC. NIUIF works, M., 2009 - p. 115-118.

Bushuyev N.N., Davydenko V.V., Norov A.M., Syrchenkov A.Ya. Features of phase composition of diammonium phosphate produced with use of WPA obtained from Kovdor apatite. Bulletin "World of S, N, P & K", JSC "NIUIF", 2011, release No. 11 - p.18-22.

Chernenko U.D., Norov A.M., Ovchinnikova K.N., Malyavin A.S., Razmahknina G.S., Grishaev I.G., Gribkov A.B. Patent of Russian Federation No. RU 2471756. Method for reducing caking of ammonium-phosphate-based fertilizers. Published on 20.05.2012.

Dokholova A.N., Kormyshev V.F., Sidorina A.V. Production and use of ammonium phosphates. M., Chemistry, 1986 - 256 p.

Evenchik S.D., Brodskiy A.A. Phosphorus and complex fertilizers production technology. M., Chemistry, 1987 - 464p.

Grinevich A.V., Kuznetsov E.M., Kiselev A.A. Patent of Russian Federation No. RU 2583956. Way to produce wet phosphoric acid. Published on 20.03.2016.

Grishaev I.G., Norov A.M., Chernenko U.D., Malyavin A.S., Gorbovskiy K.G. Patent of Eurasian Patent Office No. 020676. Way to produce granulated ammophos. Published on 30.12.2014

Kononov A.V., Sterlin V.N., Yevdokimova L.I. Basis of the technology of complex mineral fertilzers. M., Chemistry, 1988 - 320 p.

Kopylev B.A. Wet phosphoric acid production technology. L., Chemistry, 1981 - 224 p.

Kuvshinnikov I.M. Mineral fertilizers and salts: properties and ways to improve them. M., Chemistry, 1987 - 256p.

Norov A.M., Ovchinnikova K.N., Malyavin A.S., Sokolov V.V., Pagaleshkin D.A. et al. The effect of WPA concentration and the content of fluorine and magnesium impurities in it on physical properties of ammonium phosphates. Chemical Technology, vol. 13, No.10, 2012 - p.577-586.

Pozin M.E., Zinyuk R.U., Shilling N.K., Stetsova G.S. Vapor pressure and solubility in aqueous solutions of ammonium phosphates and fluorides. Works of Saint-Petersburg State Institute of Technology in honour of LenSovet, release 5. L., 1976 - p. 59-63.

Pozin M.E., Kopylev B.A., Tsiparis A.U. The effect of anions SO_4^{2-} and F^- on the content of water-soluble components in ammoniated products of magnesium-containing phosphoric acid. Works of Saint-Petersburg State Institute of Technology in honour of LenSovet, release 5, L., 1976 - p.128-131.

Pozin M.E. Mineral fertilizers production technology. L., Chemistry, 1983 - 336p.

HIGH-STRENGTH SYNTHETIC FIBERS AND NANO-SIZED PARTICLES OF SiO_2 COMBINED INTO ONE COMPOSITE SYSTEM FOR BALLISTIC PROTECTION

Petya Gencheva[1], Lubomir Djerahov[1]

[1]University of Mining and Geology "St. Ivan Rilski", 1700 Sofia, p_gencheva@abv.bg

ABSTRACT. Aramid, polyvinyl alcohol, and nanoparticles of SiO_2, combined in a single composite system for individual ballistic protection is presented. Physico-mechanical and ballistic tests confirm that balistic resistance increases with increasing the content of polyvinyl alcohol together with nanoparticles of silicon oxide in the system thus created. Scanning electron microscopy shows a relatively uniform distribution of SiO_2 particles on the surface of the aramid before and after the ballistic studies.

Keywords: ballistic protection, aramid, SiO_2, polyvinyl alcohol

ВИСОКОЯКОСТНИ СИНТЕТИЧНИ ВЛАКНА И НАНОРАЗМЕРНИ ЧАСТИЦИ НА SiO_2 ОБЕДИНЕНИ В ЕДИННА КОМПОЗИТНА СИСТЕМА ЗА БАЛИСТИЧНА ЗАЩИТА

Петя Генчева[1], Любомир Джерахов[1]

[1]Минно-геоложки университет „Св. Иван Рилски", 1700 София, p_gencheva@abv.bg

РЕЗЮМЕ. Представена е композитна система на основата на арамид, поливинилов алкохол и наноразмерен SiO_2, предназначена за индивидуална балистична защита. Физико-механичните и балистичните тестове потвърждават, че балистичната устойчивост нараства с нарастващото съдържание на поливинилов алкохол и количества наноразмерен силициев диоксид. Сканиращата електронна микроскопия показва относително равномерно разпределение на частици SiO_2 върху повърхността на арамида, преди и след балистичните изследвания.

Ключови думи: балистична защита, арамид, SiO_2, поливинилов алкохол

Introduction

The term "nanotechnology" was first used in 1959 when the famous American physicist Richard Feynman gave a lecture on the topic "There is plenty of space on the bottom" which later became classical and has often been quoted. It proves that the principles of physics do not contradict the attempts to drive atoms by atom, as long as the necessary instruments are available.

Many experts compare the creation of nanotechnology to a second industrial revolution. From a scientific point of view, it is a way of influencing the matter below the molecular level.

Nanotechnology allows the exploration and use of very small structures and systems. The result of the use of nanotechnology is new materials, devices, and products with qualitatively different characteristics. In practice, they have the potential to be applied in every economic area and aspect of public life, including in warfare and in particular for the development of tissues for military purposes.

In recent years, the assortment of textiles has been significantly expanded by the application of chemical fibres and the blending of different fibre properties, which produce textile materials with improved hygienic properties or improved physical, mechanical, and ballistic indicators.

The complex of properties, which have the fibres together with nano powder, determine their practical significance. Through the methods and means of the special finishing, it is possible to yield new fibres that are necessary due to the different areas of their use.

The construction of the ballistic protection products requires the use of materials to create lightweight but sturdy armour. In order to be able to create such a product, it is necessary to select materials that possess strength, weather resistance, and last but not least, are of low weight. The combination of properties of metal alloys, synthetic fibres, polymeric materials, nanoparticles through their reinforcement in a single composite matrix can provide high ballistic protection.

Like other nanomaterials, the agglomeration of SiO_2 nanoparticles has seen the obstacles against their wide applications (Zhang et al., 2004, Li et al., 2004). The characteristics of nanoparticles are hardly embodied in usage because they are usually dispersed in medium in aggregation of micro-size (Ke, 2002). So, the study of improving dispersivity of nano-silica in organic solvents has raised considerable interest recently. Generally, fumed silica made by a costly method has good dispersivity while precipitated silica particles

are difficult to be dispersed into organic solvents (Wang at all, 2002). Many investigators treat precipitated nano-silica particles with coupling agents, surfactants, aliphatic acids, etc., but hardly make them well dispersive in organic solvent. This is because the unsaturated dangling bonds and hydroxyl groups are extremely active and they are saturated as soon as the SiO_2 is exposed to air. So the modifiers are difficult to react with the active groups of SiO_2. Moreover, partial agglomeration usually occurs before the modification.

Polyvinyl alcohol (PVA) is a versatile and industrially significant polymer, possesses good strength, and creates resistant roof layers. This polymer is used as a substance and creates good soldering for ceramic and metal powders. PVA, when based on nano-composites, is usually used for the production of thin films that are used in Industry. The addition of nanoparticles to polyvinyl alcohol improves its mechanical properties. The added nanoparticles, to which the surfaces have been modified, are used to provide strength by providing surface soldering between the polymer and the nanoparticles, which significantly improves the mechanical properties of the compounds. Homogeneous distribution of particles can be achieved by their organic modification which creates superficial interactions between the particles and the polymer. Broadly speaking, the reinforcement by nanoparticles in laminate compounds develops the bonding of fibers into a matrix and reinforces the properties of the matrix. With their minimum weight and small size, rigid nanofillers are used to improve the plasticity and hardness of the compounds (Obradovi et al., 2017).

The present study aims at presenting a composite system suitable for lightweight protective armour to be incorporated into a ballistic protection product. Combining the properties of heterogeneous materials in a single composite matrix can provide both reliable protection and necessary mobility during combat operations.

For the creation of sturdy armour, it is necessary to combine the properties of three types of different materials to create high strength armour: used woven synthetic fibres from the group of Aramid, nano-sized particles based on silicon oxide, and highly viscous fluid based on polyvinyl alcohol.

Experimental procedure

Preparation of the composite system

The type of aramid used was Style 363, with a mass of 180 g/m^2, thread strength of 200 cN/tex, and density between the fibres 120/120 threads/cm. Each of the layers was treated by the impregnation method by dipping, as shown in Figure 1. Each part of the samples contained ten canvases of aramid, each measuring 20 cm^2. PVA-based impregnating liquid was prepared, with a different concentration of glacial acetic acid and nano-sized particles of silicon oxide. Drying of the samples was at room temperature.

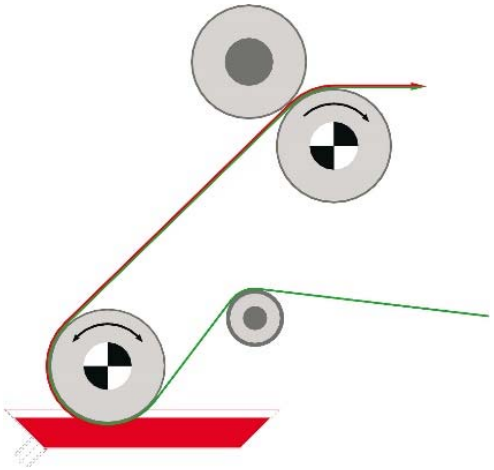

Fig. 1. Textile fabric impregnation plant, dipping method

Different concentrations and compositions of impregnating solutions are designed to track the impact of substances and nanoparticles on the strength, weight, and ballistics of composite systems. Samples of unprocessed Kevlar, aramid treated with polyvinyl alcohol (20 pph PVA), and aramid sheets treated with polyvinyl alcohol (PVA) solutions with different content of CH_3COOH and micro- and nanoparticles of SiO_2 particles were prepared where:
D_{part} = 18nm
and
S_{cn} = 210m^2/g.

Physico-mechanical test

Physical and mechanical tensile strength tests were conducted on a WPM *Shoper* dynamometer, and complied with the requirements of (BDS EN ISO 13934-1, 2013). The prepared samples were 10 mm wide and 100 mm long. The mass measurement was carried out according to standard (BDS EN 12127, 2016).

Ballistic tests

Ballistic tests were conducted in accordance with the Ballistic, (STANAG 2920 Ed.3.). The ballistic test set is shown in Figure 2.

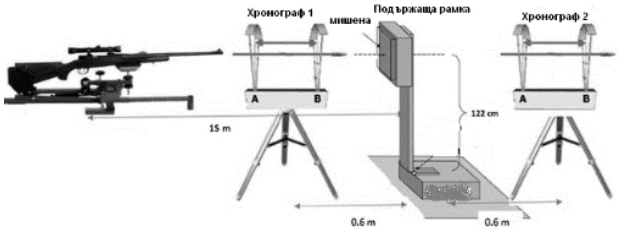

Fig. 2. Diagram of the installation for conducting ballistic tests

The boundary ballistic velocity V50 with an imitator of fragments under conditions of environmental 20 ^{0}C and a relative humidity of 82,0 ± 1,5 were defined. The shooting was conducted with a caliber of the barrel 7.62x39 mm, impersonator fragments A3/7623 mass 1.102 ± 0.02 g, direction of the barrel 00±10, and distance between the barrel end and the panel 5 m ± 50 mm. The number of projected

shots was ten punctured and ten not punched. The distance between the hits was > 30 m on the sample. Packets of 10 layers were prepared for all proportions.

Analysis of results

An analysis of the results of the tests carried out is shown in Table 1 and Fig 3, 4, and 5.

Table 1.
Data from physico-mechanical, weight, and ballistic tests and samples of different composites reinforcement materials

№	Composite system	Tensile strength [N]	Mass [g/m^2]	Average ballistic speed V_{50}, [m/s]
0	Aramid	1933	187,5	342; Δ=14
1	PVA/Aramid/	2216	250	355; Δ=23
2	PVA/aramid/10pph CH_3COOH/	2206	199	360; Δ=20
3	PVA/aramid/20pph CH_3COOH/	1617	196	344.8; Δ=29
4	PVA/aramid/30pph CH_3COOH/	1463	205	350; Δ=28
5	PVA/aramid/10pph CH_3COOH/0,5 g **SiO_2**	1961	238	393; Δ=36
6	PVA/aramid/20pph CH_3COOH/0.5 g **SiO_2**	2075	232	368.3; Δ=38
7	PVA/aramid/30pph CH_3COOH/0.5 g **SiO_2**	2143	196	369; Δ=32
8	PVA/aramid/10pph CH_3COOH/1.4g**SiO_2**	2229	242	399; Δ=34
9	PVA/aramid/20pph CH_3COOH/1.4g **SiO_2**	2143	236	389.3; Δ=35
10	PVA/aramid/30pph CH_3COOH/1.4g **SiO_2**	2387	215	409; Δ=31

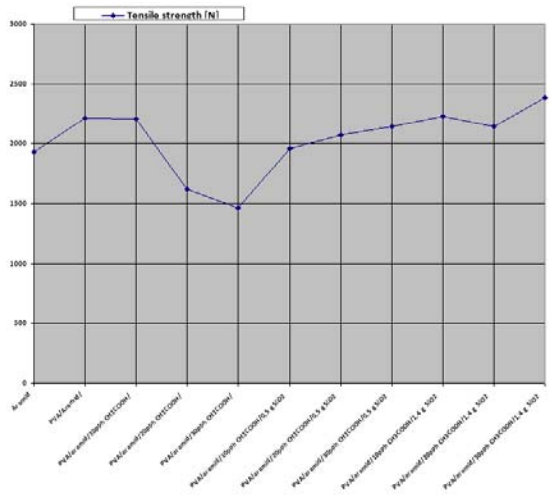

Fig 3. Results of the tensile strength tests

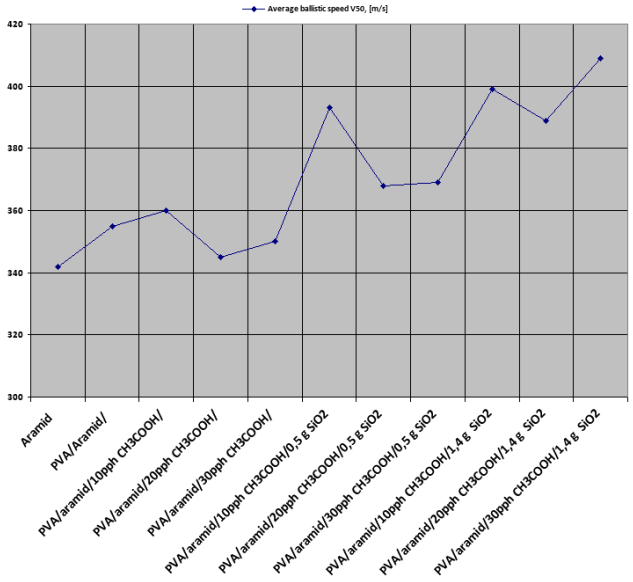

Fig 4. Results of the weight tests carried out

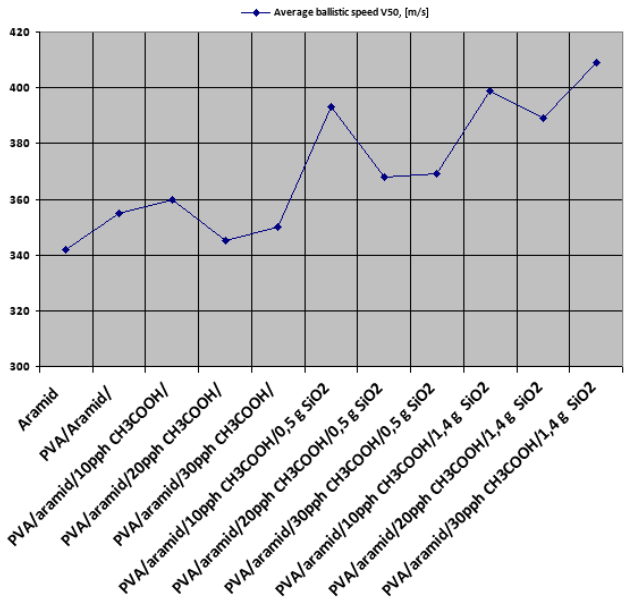

Fig 5. Ballistic test results

The results of the conducted tests show an improvement of tensile strength of the samples treated with PVA compared to the untreated samples (pure aramid). The addition of higher concentrations of 10 pph CH_3COOH to the PVA/aramid system worsened the results for two of the parameters - tensile strength and mass. The addition of nano powder SiO_2 to the PVA/Aramid system has led to an increase in the average ballistic speed of V50 in comparison to the untreated aramid, with a slight increase in weight. It should be noted that the average ballistic speed V 50 significantly increases in the PVA/aramid/10pph CH_3COOH/0.5g SiO_2 and PVA/aramid/10pph CH_3COOH/1.4g SiO_2 samples. The comparison of the results of three parameters, which were researched, shows that the PVA/aramid/30pph CH_3COOH/1.4g SiO_2 sample has the best values for tensile strength and average ballistic speed, and low for mass.

Results of scanning electron microscopy

The morphology and elemental composition of nano emulsion treated samples were screened using scanning electron microscopy and energy dispersion elemental analysis (JEOL JSM 6390 scanning electron microscope and INCA Oxford solid-state X-ray detector). Micrographs taken in secondary electrons (particle morphology and fibre thickness) were used. Figures 6 to 11 show an image in backscattered electrons. This is a semi-quantitative analysis in which the deposited particles are seen as lighter objects. A high carbon content is observed, and some oxygen, nitrogen, and significant amounts of silicon. The elements thus detected prove deposited nano particles on the surface of the aramid fibers.

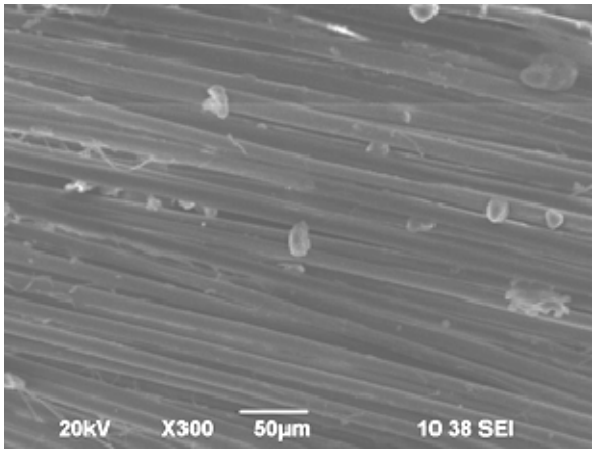

Fig 6. Scanning electron microscopy of x300, 50µm, 10 38 SEI, shows a particle with a complex embossment on the basis of Si

Table 2.
Detected elements of spectral analysis of composite: PVA/aramid/10pph CH_3COOH/0,5 g SiO_2.

Spectrum, atomic % ,till 100 %	C	O	Si
Spectrum 15	48.47	41.82	9.39
Spectrum 16	30.14	47.26	2.15

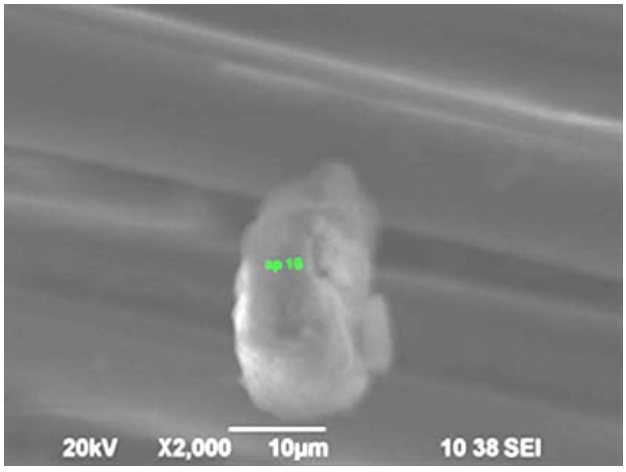

Fig 7. Scanning electron microscopy of deposited nanoparticulate SiO_2 on aramid fibers "Style 363" treated with polyvinyl alcohol at an magnification of 2000, 10µm, 10 38 SEI.i

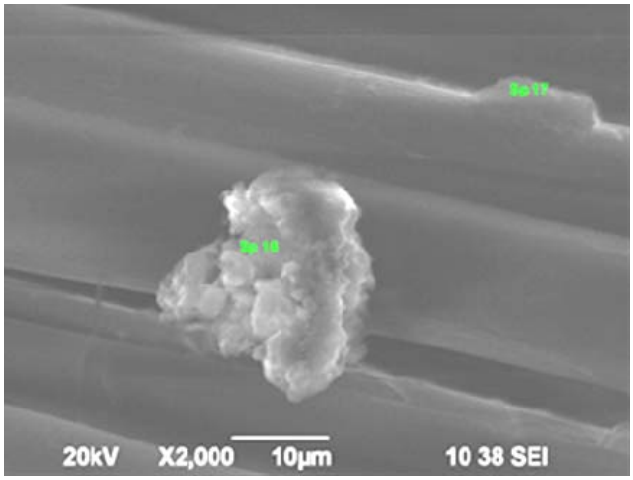

Fig 8. Scanning electron microscopy of deposited nanoparticulate SiO_2 on aramid fibers *Style 363* treated with polyvinyl alcohol at a magnification of 2000, 10µm, 10 38 SEI shows a particle with a complex embossment on the basis of Si

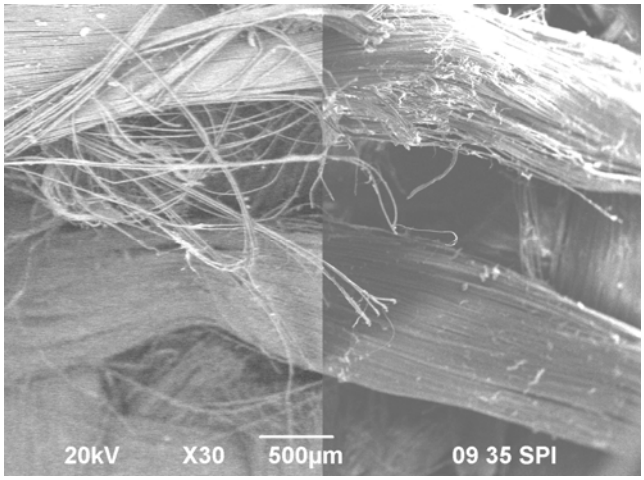

Fig 9. Scanning electron microscopy after ballistic test at a magnification of 30, 500µm, 09 35 SEI

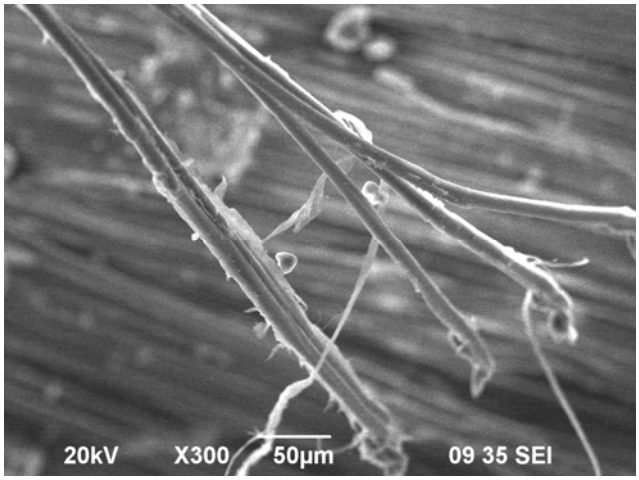

Fig 10. Scanning electron microscopy after ballistic test at a magnification of 300, 50µm, 09 35 SEI

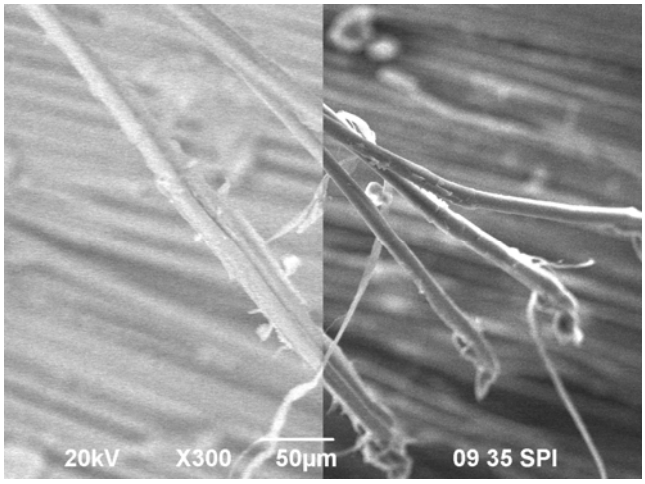

Fig 11. Scanning electron microscopy after ballistic test at a magnification of 300, 50µm, 09 35 SEI

Conclusions

As a result of the conducted experiments and the results obtained, the following conclusions can be drawn:

1. The added acetic acid to the PVA solution helps maintain the strength of the fabric and at the same time reduces the mass of the sample, which would help to completely lighten the ballistic equipment.

2. The addition of nano-sized particles of silicon oxide increases the limit ballistic velocity of the test samples.

3. The results of the scanning electron microscopy confirm the presence of deposited nano-sized silicon-based particles. Microscopic images confirm that after the ballistic tests, the reinforcement matrix of PVA, together with nanomaterial silicon oxide, remains on the surface.

The tests carried out confirm that the composite system thus created is suitable for designing ballistic protective armour not only for people but also for the paint field technique.

References

BDS EN ISO 13934-1 "Textile. Tensile properties of fabrics. Part 1: Determination of maximum force and stretch at maximum force using the STRIP method ".

BDS EN 12127 "Textiles. Fabrics. Determination of mass per unit area by using small samples".

Ke, Y. C. Polymer-Inorganic Nano-Composites, Chemical Industry Press, Beijing, 2002.

Li, X. H., Sun, R., Zhang, Z. J., Dang, H. X., Progress of polymer/inorganic nanocomposites by chemical bonds, Prog. Nat. Sci. 14 (2004) 1.

Obradovi, V., Stojanovi, D., Joki, B., Zrili, M., Radojevi, V., Uskokovi, P. S., Aleksi, R., Nanomechanical and anti-stabbing properties of Kolon fabric composites reinforced with hybrid nanoparticles, Composites Part B: Engineering, Volume 108, 1 January 2017, - 143-152.

STANAG 2920 Ed.3"Ballistic Test Method for Personal Armour Materials and Combat Clothing"

Wang, S. M., Xu, Z. X., Fu, J., Technology of Preparation on Nano-Materials, Chemical Industry Press, Beijing, 2002.

Zhang, M. L., Ding, G. L., Jing, X. Y., Hou, X. Q., Preparation, modification, and application of nanoscal SiO_2, Appl. Sci. Technol. 31 (6) (2004) 64–66.

KINETICS AND THERMODYNAMICS OF SILVER ION IMMOBILISATION BY NATURAL CLINOPTILOLITE

Marinela Panayotova[1], Neli Mintcheva[1], Lubomir Djerahov[1], Gospodinka Gicheva[1]

[1]University of Mining and Geology, Sofia 1700, Bulgaria, marichim@mgu.bg

ABSTRACT. Natural zeolites attract the attention as efficient supports of stable and monodispersed nanoparticles (NPs) for the preparation of various nanocomposites. The present work describes the results from the immobilisation of silver ions by purified natural zeolite - clinoptilolite, which is an initial step towards the production of nanocomposites "silver nanoparticles– zeolite". The effect of the concentration of silver ions in the form of $AgNO_3$ (within the range of 0.01÷0.10 M) and the ratio of the zeolite mass to the volume of $AgNO_3$ solution (ratio m:v being from 1:10 to 1:100) on the silver immobilisation has been investigated and the optimum conditions selected. The highest load of Ag^+ ions by zeolite was achieved when one gram of zeolite contacted with 40 mL of 0.05 M $AgNO_3$ solution or with 20 mL of 0.10 M $AgNO_3$ solution (equivalent to 2 mmol Ag^+ ions per 1 g zeolite). It was established that the kinetics of Ag^+ ions immobilisation by natural zeolite can best be described by the pseudo-first order kinetic equation, whereas the thermodynamics - by the Freundlich adsorption isotherm.

Keywords: natural clinoptilolite, silver nanoparticle precursor, kinetics and thermodynamics of Ag^+ immobilisation

КИНЕТИКА И ТЕРМОДИНАМИКА НА ИМОБИЛИЗАЦИЯ НА СРЕБЪРНИ ЙОНИ ОТ ЕСТЕСТВЕН КЛИНОПТИЛОЛИТ

Маринела Панайотова[1], Нели Минчева[1], Любомир Джерахов[1], Господинка Гичева[1]

[1]Минно-геоложки университет, София 1700, България, marichim@mgu.bg

РЕЗЮМЕ. Естествените зеолити представляват ефективен носител на стабилни и монодисперсни наночастици (NPs) за получаване на нанокомпозитни материали. Настоящата работа описва резултатите от имобилизирането на сребърни йони върху пречистен естествен зеолит - клиноптилолит, което е начална стъпка от процеса на получаване на нанокомпозити "сребърни наночастици-зеолит". Изследвано е влиянието на концентрацията на сребърните йони (под формата на $AgNO_3$) в интервала 0.01÷0.10 M и на съотношението маса на зеолита към обем на разтвора от 1:10 до 1:100, върху степента на задържане на Ag^+ йони. Намерено е, че оптималните условия за постигане на най-голямо натоварване на зеолита със Ag^+ йони са един грам зеолит, контактуващ с 40 mL 0.05 M разтвор на $AgNO_3$ или с 20 mL 0.10 M разтвор на $AgNO_3$ (еквивалентни на 2 mmol Ag^+ йони за 1 g зеолит). Установено е, че кинетиката на имобилизация на Ag^+ йони от естествения зеолит най-добре се описва от кинетичното уравнение за псевдо-първи порядък, а термодинамиката - от адсорбционната изотерма на Фройндлих.

Ключови думи: естествен клиноптилолит, прекурсор на сребърни наночастици, кинетика и термодинамика на имобилизация на Ag^+ йони

Introduction

The antimicrobial properties of silver ions and silver nanoparticles (AgNPs) have been well known for a long time. AgNPs and materials on their basis are an important means of disinfection of potable water (Rai et al., 2009).

Environmental applications of AgNPs require stable nanoparticles (NPs) that do not aggregate easily. The immobilisation of AgNPs on solid surfaces or their incorporation in a solid matrix provides stability and thus facilitates the reuse of NPs. The structure of natural zeolite consists of primary building units, i.e. the SiO_4 and AlO_4 tetrahedra. They are connected via oxygen ions into secondary building units which are then linked into a three-dimensional crystalline structure of zeolite. The substitution of Si by Al defines the negative charge of the zeolite framework which is compensated by alkaline and earth alkaline metal cations. Because of their negative charge on the surface, natural zeolites appear as cation exchangers (Margeta et al., 2013). Zeolites are mesoporous ion exchange materials with a stable network of hollow channels and pores within the size range of most monoatomic ions. Because of their thermal stability and unique interconnected porous microstructure, natural and synthetic zeolites have been used as templating support materials to host a variety of metallic species including silver. Studies have shown that the porous internal network structure of zeolites provides an ideal and stable template for the formation and growth of particles with nanometre dimensions. Even more, nanoparticles are physically prevented from agglomeration to form larger nanoparticles or micron-sized particles as they are individually separated within the discrete pores and channels of the zeolite interior (Yee et al., 2015).

Zeolites have a strong affinity for Ag^+ (Scacchetti et al., 2017). Silver ion-exchanged chabazite has shown the capability to precipitate silver nanoparticles at its surface after thermal reduction in air, Ar and H_2, with a size depending on the reduction environment (Liu et al., 2009).

It has been reported that the concentration and size of the formed AgNPs depend on the initial concentration of Ag-bearing solutions contacting with the zeolite and on the contact time (Guerra et al., 2012; Yee et al, 2015).

The present work aimed to explore the optimum conditions for the highest immobilisation degree of silver ions by purified natural zeolite - clinoptilolite, as an initial step to producing

nanocomposite "silver nanoparticles–zeolite". The impact of the ratio $AgNO_3$ solution volume to zeolite mass, as well as the influence of the initial concentration of the $AgNO_3$ solution that contacts with the zeolite on the silver ions uptake has been investigated. The results from this study could also be used when the aim is to adsorb Ag^+ from silver-bearing wastewater.

Methods and materials

Natural zeolitic rock containing mainly clinoptilolite was used from the East Rhodopes region of Bulgaria. It was milled and the fraction of 0.09-0.325 mm was deployed. Zeolite was purified following a procedure described by Tomašević-Čanović (2005) and modified by us. Zeolite was washed with acidified water (pH=4.6, adjusted by HCl). In a typical procedure, 350 g of zeolite were placed 3 consecutive times (each one lasting for 24 hours) in contact with 700 mL of acidified water. Then, zeolite was washed by placing it in contact with 700 mL of distilled water for 2 hours at 60°C, 6 consecutive times, while it was stirred with a magnetic stirrer. The naturally adsorbed heavy metal ions were removed with a 0.05 M solution of EDTA by the treatment of zeolite for 2 hours at 60°C at the ratio of solid:liquid = 1:10. Then, zeolite was washed with distilled water again, as it is described above. In all washing steps, the contacted water was decanted off and then a new portion of water was poured into the beaker. Finally, zeolite was separated from the liquid by filtration, dried for 24 hours at 105°C, and supplied for analysis.

The chemical composition of zeolite was determined by means of the classical silicate analysis (in mass %): SiO_2 – 70.19, Al_2O_3 – 10.90, CaO – 2.87, MgO – 0.51, K_2O – 3.41, Na_2O – 0.36, Fe_2O_3 – 0.28, MnO – 0.04, TiO – 0.06, P_2O_3 < 0.05, SO_3 < 0.05, and LOI – 10.99. The theoretical cation exchange capacity (TCEC) of the natural zeolite (the sum of exchangeable cations such as Na^+, K^+, Ca^{2+} and Mg^{2+}) was found to be 211 meq/100 g zeolite. It is of the same range as the TCEC determined by other authors for clinoptilolite from our region (Tomašević-Čanović, 2005; Margeta et al., 2013; Santiago et al, 2016). The X-ray diffraction (XRD) of purified zeolite reveals that it consists of 72.7% Clinoptilolite-Ca $[Ca_3(Si_{30}Al_6)O_{72}\cdot 20H_2O]$ and 27.3% Barrerite $[(Na,K,Ca_{0.5})_2(Al_2Si_7O_{18})\cdot 7H_2O]$.

Solutions containing different concentrations of silver ions (Ag^+) were prepared by dissolving $AgNO_3$ (p.a.) in distilled water. The accurate concentration of Ag^+ ions was determined by titration with NH_4SCN solution in acidic medium in the presence of ammonium iron(III) sulfate, $NH_4Fe(SO_4)_2\cdot 12H_2O$ (Korostelev, 1985). In the course of the analysis, the following reactions proceed:

$$AgNO_3 + NH_4SCN \rightarrow AgSCN\downarrow + NH_4NO_3$$

$$Fe^{3+} + SCN^- \rightarrow FeSCN^{2+}_{(aq)} \quad \text{(reddish brown)}$$

The conditions for all performed experiments of Ag^+ ion immobilisation by zeolite are given in Table 1.

Experiments were conducted batch-wise: a certain amount of zeolite was magnetically stirred in $AgNO_3$ solution with a predetermined concentration (0.01 M, 0.025M, 0.05 M, 0.075M, and 0.10 M). The solution pH was adjusted to 6 by 1M HNO_3 to prevent the precipitation of silver ions (Charlot, 1969). Variations in the ratio between the mass of zeolite and the volume of $AgNO_3$ solution (denoted bellow as solid to liquid ratio, or m:v) were studied, namely 1:10, 1:20, 1:40, and 1:100. Aliquot portions of 10 mL were taken at particular time (2, 5, 10, 20, 30, 45, 60, 90, 120, 180, 240 min) and the amount of Ag^+ ions remaining in the solution was determined by titration against NH_4SCN solution. Care was taken so that the total amount of the aliquots would be less than 10% of the whole volume of the solution contacting with zeolite. The process was monitored until the equilibrium was reached. Ag-loaded zeolite was collected by filtration and washed with distilled water till a negative reaction for Ag^+ in the washings was observed. It was dried at 60°C for 8 h. During all experiments, precautions were taken due to silver light sensitivity. Each experimental result was obtained by averaging the data from duplicate samples.

Table 1.
Experimental conditions of Ag^+ ion immobilisation by zeolite

Experiment №	$AgNO_3$ concentration (M)	Zeolite mass to volume of $AgNO_3$ solution ratio (m:v)
1	0.05	1:10
2	0.05	1:20
3	0.05	1:40
4	0.05	1:100
5	0.01	1:20
6	0.025	1:20
7	0.075	1:20
8	0.10	1:20

Removal of Ag^+ from the initial solution was calculated using the equation:

$$\text{Removal, \%} = [(C_o - C_\tau)/C_o] \times 100 \quad (1)$$

where C_o is the initial and C_τ is the concentration of Ag^+ at particular time τ, mg/L. Kinetic data were fitted to the following kinetic equations:

For the first order irreversible reactions:

$$\ln (C_o/C_\tau) = k \times \tau \quad (2)$$

For the second order irreversible reactions:

$$(C_o - C_\tau)/(C_o . C_\tau) = k \times \tau \quad (3)$$

For the Lagergen pseudo-first order reactions:

$$\ln (q_e - q_\tau) = \ln q_e - k_{ads} \times \tau \quad (4)$$

where k is the reaction rate constant; C_o, C_τ and τ are as described above; q_e (mg Ag^+/g zeolite) is the amount of solute adsorbed at the equilibrium; q_τ (mg/g zeolite) is the amount of solute adsorbed at time τ; k_{ads}, min^{-1} is the adsorption rate constant. The slope of the linear plot of $\ln (q_e - q_\tau)$ against τ gives k_{ads}.

Langmuir and Freundlich isotherm models were studied for their ability to describe the equilibrium sorption distribution.

The Langmuir isotherm:

$$q_e = (Q_{max} \times K_L \times C_e) / (1 + K_L \times C_e) \quad (6)$$

The Freundlich isotherm:

$$q_e = K_F \times C_e^n \quad (7)$$

where q_e is metal concentration on the zeolite at equilibrium (meq of metal ion/g of zeolite), C_e is the equilibrium metal concentration in the aqueous phase (mg/L), Q_{max} is the maximum achievable capacity (meq/g), K_L (L/mg) is the Langmuir constant, n is the Freundlich intensity parameter, and K_F is the Freundlich isotherm constant (mg/g). If the plot of C_e/q_e as a function of C_e is a straight line, the adsorption process can be described by the Langmuir isotherm. If the plot $\log q_e$ vs $\log C_e$ is a straight line, the adsorption process is best described by the Freundlich isotherm.

Results and discussion

The kinetics of Ag^+ uptake at an initial concentration of 0.05 M $AgNO_3$ and at different ratios of solid to liquid is presented in Fig. 1. The kinetics of Ag^+ uptake at the ratio of solid to liquid 1:20 and at different initial concentrations is presented in Fig. 2.

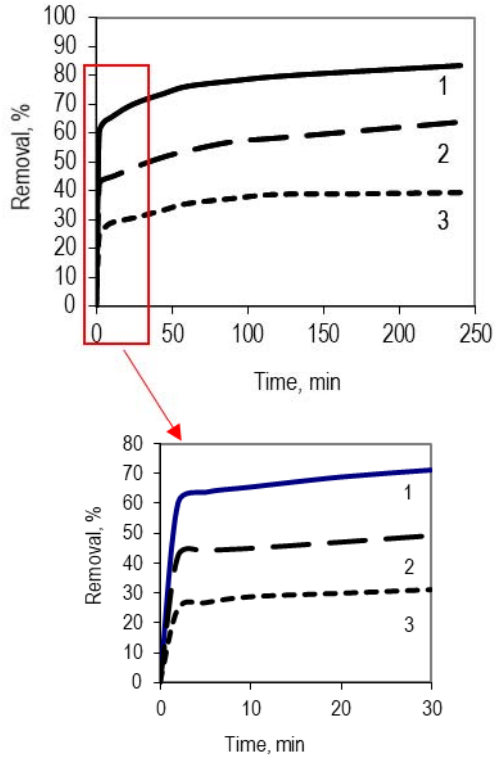

Fig. 1. Kinetics of Ag^+ uptake at an initial concentration of 0.05 M $AgNO_3$: ——— m:v = 1:10 (1), — — — m:v = 1:20 (2), - - - - - - m:v = 1:40 (3)

The kinetic curves reveal that the reaction consists of two stages, “fast” and “very slow”, at all studied m:v ratios and initial concentrations of Ag^+. Practically, the process reaches equilibrium in about 2 hours. The relatively short ion exchange time of 2 hours has been found as sufficient to produce optimum Ag^+ uptake into the zeolite pores by other authors as well (Jiraroj et al., 2014; Yee et bal., 2015).

It has been found that in all experiments, the kinetics of Ag^+ immobilisation by zeolite is best described by the pseudo-first order kinetic equation. The coefficients of determination R^2 are close to unity as presented in Table 2. Generally, this equation describes an adsorption reaction at the liquid/solid interface where a steep rise of the uptake at short times is observed (fast initial step). In such case, in calculation of the reaction rate, the data close to or at equilibrium are not included since a methodological bias is introduced (Simonin, 2016). That is why the reaction rate constants (k_{ads}) presented in Table 2 are calculated by taking into account the data for the first 90 minutes of the reaction.

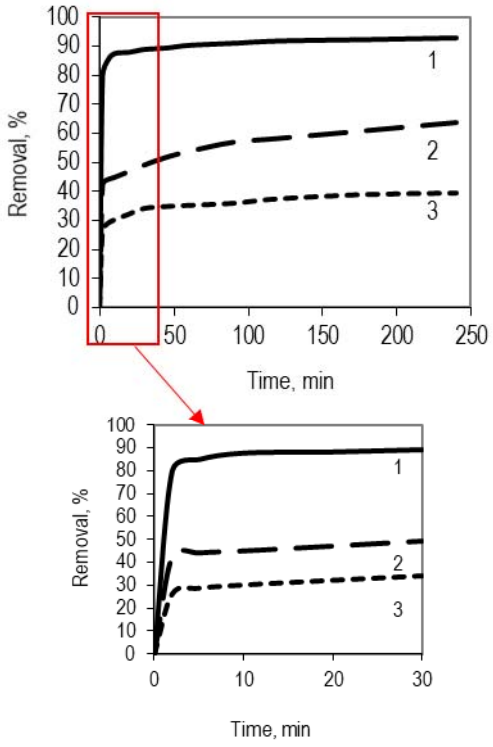

Fig. 2. Kinetics of Ag^+ uptake at the ratio of solid to liquid 1:20 and at initial concentrations of $AgNO_3$: ——— 0.01 M (1) — — 0.05 M (2)- - - - 0.10 M (3)

Table 2.
R^2values for fitting the experimental data to pseudo-first order kinetic equation and reaction rate constant

Experiment №	1	2	3	5	8
R^2	0.985	0.982	0.961	0.951	0.971
k_{ads}, min^{-1}	0.0156	0.0146	0.0224	0.0235	0.0172

The maximum uptake values of Ag^+ ions by zeolite for all samples, calculated by using the removed amount of Ag^+ from the solution at 240 min (when equilibrium was achieved), are presented in Table 3.

The amount of Ag^+ immobilised by zeolite is in the range of approximately 20-80 mg per gram zeolite (Table 3). Our findings are in line with the results of Akhigbe and coauthors (Akhigbe et al., 2016) who found the loading of 43.4 mg Ag^+/g zeolite when the process was carried out on natural British clinoptilolite at m:v =1:2.5, initial $AgNO_3$ concentration of 3% (w/v), and reaction time of 24 hours.

Table 3.
Maximum uptake of Ag^+ ions by zeolite

Experiment №	1	2	3	4	5	6	7	8
mgAg^+/g zeolite	40.4	60.3	76.8	39.7	19.0	32.2	68.0	78.2

Data presented in Tables 2 and 3 show that both factors solid to liquid ratio and the initial concentration of silver ions in the solution influence the maximum loading on zeolite.

At an initial concentration of 0.05 M $AgNO_3$ (experiments 1 - 4, Table 1), the amount of immobilised Ag^+ ions increases with the increase of the ratio m:v up to 1:40, while a further increase of the volume of Ag^+ solution gives lower loading (Table 3). The reduced immobilisation could be due to the insufficiency of adsorption sites on zeolite capable to "bind" the large number of Ag^+ present in the solution.

If the ratio solid to liquid is kept constant (m:v=1:20, experiments 5-8, Table 1), then the increase of Ag^+ concentration causes a gradual increase of Ag^+ loading and the greatest amount of Ag^+ held on zeolite is 78.2 mg/g (Table 3). It was reported by Yee and coauthors (2015) that the use of a higher concentration of the $AgNO_3$ (up to 1.0 M, m:v=1:20) led to a greater concentration of Ag^+ ions immobilised on zeolite ZSM-5 and, thus, a higher concentration of AgNPs was achieved.

The highest rate constant (0.0235 min^{-1}) was determined for experiment 5 where the ratio m:v = 1:20 and the concentration of $AgNO_3$ was the lowest (0.01 M, Table 2). At the same time, the amount of the immobilised Ag^+ per gram of zeolite was the lowest one (19.0 mg/g, Table 3). In such case, almost all available Ag^+ ions were immobilised, but because their initial concentration in the solution was low, the resulted loading was low. Although a similar value of the rate constant (0.0224 min^{-1}) was found for experiment 3 (0.05 M, m:v=1:40), the Ag^+ uptake (76.8 mg/g) was significantly higher compared to experiment 5 due to a fivefold higher concentration of initial solution in experiment 3 (Table 3).

As can be seen in Table 3, very close values were obtained for the Ag^+ loading (76.8 mg/g and 78.2 mg/g for experiment 3 and experiment 8, respectively), though a twice concentrated solution in experiment 8 was used (0.10 M and m:v=1:20). Obviously, the difference between experiments 3 and 8 is within the experimental uncertainties. Thus, one can propose that 76-78 mg/g is the optimum Ag^+ loading on zeolite ensured by the contact of 1-gram zeolite with 40 mL of 0.05 M $AgNO_3$ solution or 20 mL of 0.10 M $AgNO_3$ solution (equivalent to 2 mmol Ag^+ ions).

This amount seems to be the optimum one with respect to the capacity of zeolite to be loaded with Ag^+. Zeolite prepared under those conditions is worth undergoing further chemical reduction or calcination for obtaining AgNPs.

Experimental data fitting the isotherm equations have shown that the process is best described by the Freundlich isotherm with R^2=0.983. The values for the Freundlich intensity parameter and the Freundlich isotherm constant are graphically found and are, respectively, n=0.65 and K_F=395 mg Ag^+/g zeolite. The adsorption intensity n is less than 1and, therefore, indicates a favourable sorption of Ag^+ on the zeolite.

Conclusions

As a result of the experiments carried out on Ag^+ immobilisation by natural zeolite, the following conclusions can be drawn:

1. The kinetics of Ag^+ immobilisation by natural zeolite consisting mainly of clinoptilolite is best described by the pseudo-first order kinetic equation.

2. The uptake of Ag^+ by the natural zeolite in the studied $AgNO_3$ concentration range of 0.01-0.10 M is best described by the Freundlich adsorption isotherm with constants n=0.65 (showing the favourable sorption) and K_F=395 mg Ag^+/g zeolite, respectively.

3. Within the studied $AgNO_3$ concentration range of 0.01÷0.10 M and the ratio of solid to liquid in the range of 1:10÷1:100, the optimum conditions for achieving the highest Ag^+ loading by zeolite are one gram of the zeolite contacting with 40 mL of 0.05 M solution or with 20 mL of 0.10 M solution.

4. In our future work, the prepared silver-loaded zeolite can be used as a precursor for the synthesis of AgNPs supported on zeolite.

Acknowledgements

This work was supported by the project "Functional Composite Nanomaterials Obtained from Natural Resources for Environment Protection" funded by the Bulgarian National Science Fund – Contract № DH 17/20 - 2017.

References

Akhigbe, L., Ouki,S., Saroj, D., Disinfection and removal performance for Escherichia coli and heavy metals by silver-modified zeolite in a fixed bed column, Chem. Eng. J., 295, 2016. - 92–98.

Charlot, G. Les Reactions Chimiques en solution: L'analyse qualitative minérale, 6 ª Edición, Paris, Ed. Toray-Masson, 1969.

Guerra, R., Lima, E., Viniegra, M., Guzman, A., Lara, V., Growth of Escherichia coli and Salmonella typhi inhibited by fractal silver nanoparticles supported on zeolites, Micropor. Mesopor. Mat., 147, 2012. - 267–273.

Jiraroj, D., Tungasmita, S., Tungasmita, D. N., Silver ions and silver nanoparticles in zeolite A composites for antibacterial activity, Powder Technol, 264, 2014. - 418–422.

Korostelev, P. P., Titrimetric and gravimetric analysis in metallurgy, M., Metallurgy, 1985.

Liu, Y., Chen, F., Kuznicki, S. M., Wasylishen, R. E., Xu, Z., A Novel method to control the size of silver nanoparticles formed on chabazite, J. Nanosci. Nanotechno., 9, 2009. - 2768–2771.

Margeta, K., Logar, N. Z., Šiljeg, M., Farkaš, A., Natural Zeolites in Water Treatment – How Effective is Their Use, http://dx.doi.org/10.5772/50738, InTech, 2013.

Rai, M., Yadav, A., Gade, A., Silver nanoparticles as a new generation of antimicrobials, Biotechnol. Adv., 27, 2009. - 76–78.

Santiago, O., Walsh, K., Kele, B., Gardner, E., Chapman, J., Novel pre-treatment of zeolite materials for the removal of sodium ions: potential materials for coal seam gas co‐produced wastewater, Springer Plus, 5: 571, 2016. - 1-16.

Scacchetti, F. A. P., Pinto, E., Soares, G. M. B., Preparation and characterisation of cotton fabrics with antimicrobial properties through the application of chitosan/silver-zeolite film, Procedia Eng, 200, 2017. - 276–282.

Simonin, J. P. On the comparison of pseudo-first order and pseudo-second order rate laws in the modelling of adsorption kinetics, Chem. Eng. J., 300, 2016. - 254-263. DOI: 10.1016/j.cej.2016.04.079.

Tomašević-Čanović, M., Purification of natural zeolite-clinoptilolite for medical application - extraction of lead, J. Serb. Chem. Soc., 70, (11), 2005. - 1335–1345.

Yee, M. S. L., Khiew, P. S., Tan, Y. F., Chiu, W. S., Kok, Y. Y., Leong, C. O., Low temperature, rapid solution growth of antifouling silver-zeolite nanocomposite clusters, Micropor. Mesopor. Mat., 218, 2015. - 69-78.

STUDY ON THE AIR QUALITY DURING THE OPERATION OF THE *MIZIA* QUARRY

Marinela Panayotova[1], Gospodinka Gicheva[1], Nely Mintcheva[1], Lubomir Djerahov[1]

[1]University of Mining and Geology "St. Ivan Rilski", Sofia 1700, Bulgaria, marichim@mgu.bg

ABSTRACT. The operation of quarries is normally associated with air pollution. As a result of mining and transportation activities, particulate matter (dust), carbon monoxide (CO), carbon dioxide (CO_2), nitrogen oxides (NO_x), sulfur dioxide (SO_2), and (volatile) hydrocarbons can generally be emitted. This paper presents studies on those pollutants in the *Mizia* quarry for limestone blocks. The measured concentrations of all gaseous pollutants in the quarry air are below (or equal to) the threshold values for protecting the human health. Particulate matter concentrations determined on the territory of the quarry exceed the maximum permissible values, i.e. the hourly average norm for the protection of human health. The higher values were measured in dry weather. Since the excess of the limit values is not extremely high, wearing proper dust masks by the workers is suffices to preserve their health for the whole range of work activities except direct drilling, where additional measures are needed to decrease dust release, such as dust collection and water spraying. Concentrations of gaseous air pollutants determined at the exit of the exhaust pipe of a working Fadroma haul-dump machine, a representative of the heaviest equipment used in the quarry, are at the low edge of the ranges that are presented in the literature for the heavy duty diesel engines. Concentrations of air pollutants released by the operating quarry practically do not pose hazards to the surrounding environment.

Keywords: quarry for limestone blocks, air pollution

ИЗСЛЕДВАНЕ НА КАЧЕСТВОТО НА ВЪЗДУХА ПО ВРЕМЕ НА РАБОТАТА НА КАРИЕРА "МИЗИЯ"

Маринела Панайотова[1], Господинка Гичева[1], Нели Минчева[1], Любомир Джерахов[1]

[1]Минно-геоложки университет "Св. Иван Рилски", 1700 София, marichim@mgu.bg

РЕЗЮМЕ. Експлоатацията на кариерите обикновено се свързва със замърсяване на въздуха. В резултат на минни и транспортни дейности могат да се отделят прахови частици, въглероден оксид (CO), въглероден диоксид (CO_2), азотни оксиди (NO_x), серен диоксид (SO_2) и (летливи) въглеводороди. Докладът представя проучвания за тези замърсители в кариера „Мизия" за варовикови блокове. Измерените концентрации на всички газообразни замърсители във въздуха в кариерата са под (или равни на) праговите стойности за защита на човешкото здраве. Концентрациите на прахови частици, определени на територията на кариерата, надхвърлят максимално допустимите стойности, т.е. средната почасова норма за защита на човешкото здраве. По-високите стойности са измерени при сухо време. Тъй като превишаването на пределно допустимите стойности не е изключително високо, носенето на подходящи маски за прах от работниците е достатъчно, за да се запази здравето им за целия спектър от дейности, с изключение на пряката пробивна дейност, където са необходими допълнителни мерки за намаляване на отделянето на прах, като събиране на праха и оросяване. Концентрациите на газообразни замърсители на въздуха, определени на изхода на ауспуха на работеща фадрома - представител на най-тежкото оборудване, използвано в кариерата, са в ниския край на диапазоните, представени в литературата за тежкотоварните дизелови двигатели. Концентрациите на замърсителите на въздуха, емитирани от работещата кариера, практически не представляват опасност за околната среда.

Ключови думи: кариера за варовикови блокове, замърсяване на въздуха

Introduction

Quarrying and stone cutting industries have a significant role in our economy. However, these activities are associated with health and environmental impacts. Usually, particulate matter, or PM (dust with a diameter of 1-75 μm) is the main air pollutant released by such industries. Particles with aerodynamic diameters of less than 50 μm (termed Total Suspended Particulate matter, or TSP) can be suspended in the atmosphere, and those with aerodynamic diameters of less than 10 μm, i.e. PM_{10} (inhalable particles) can be transported over long distances and enter the human respiratory system (Sayara, 2016).

Generally, particulates from diesel engines, including those used in the quarries, contain primary carbon particles and secondary sulfate and nitrate aerosols formed from SO_2 and NO_x. The EPA found that while coarse and fine particles can increase respiratory symptoms and impair breathing, fine particles are more likely to contribute to serious health effects. Most of the particulate emissions from diesel engines are significantly smaller than 2.5 microns (Chevron Corporation, 2007).

In addition, carbon monoxide (CO), carbon dioxide (CO_2), nitrogen oxides (NO and NO_2 expressed as NO_x), sulfur dioxide (SO_2), and (volatile) hydrocarbons (VOCs) can be emitted as a result of blasting, mining and transportation activities.

Emissions of pollutants from these industries can lead to chronic health effects, such as decreased lung capacity and lung cancer resulting from long-term exposure to toxic air pollutants, as well as to a high degree of respiratory morbidity. Carbon monoxide is primarily generated by combustion processes. The toxicity of CO stems from its ability to reduce the oxygen-carrying capacity of blood by preferentially bonding to hemoglobin. While NO is non-toxic by itself, it contributes to

the ozone formation and NO_2 can irritate the lungs and lower resistance to respiratory infection. SO_2 is primarily produced by the combustion of fuels containing sulfur. It is a moderate lung irritant. Along with NO_x, it is a major precursor to acidic deposition (acid rain). VOCs are not criteria air pollutants, though some specific compounds are classified as toxic. Their importance stems from their role in forming ozone. All hydrocarbons in the atmosphere are considered VOCs, as are many other types of organic compounds. The reactivity and toxicity of hydrocarbons depends on their chemical structure. Under most conditions, alkenes and aromatics are more reactive than alkanes. The harmful effect of organic compounds depends on their structure. Most hydrocarbons are non-toxic at low concentrations; some low molecular weight aldehydes are carcinogenic, and some monocyclic and polycyclic aromatic hydrocarbons (PAH) are suspected or known carcinogens (Chevron Corporation, 2007).

Table 1 lists typical output ranges of the basic toxic material in diesel fumes, as reported by different authors (Grenier, 2005; Tschanz et al., 2010; Resitoglu et al., 2015; Nett Technologies Inc., 2018). The lower values can be found in new, tuned, and clean diesel engines using low sulfur fuels, while the higher values are characteristic for older equipment.

Table 1.
Range of emissions from diesel engines

Pollutant	Unit	Range
CO	mg/m^3	6 - 1700
CO_2	vol. %	0.5 - 12
VOCs*	mg/m^3	90 - 1860
NO_x	mg/m^3	90 - 1880
SO_2	mg/m^3	5 - 390
DPM	mg/m^3	1 - 300

DPM **-** Diesel particulate matter; * - as n-octane

Table 2 presents legal requirements for some air pollutants that can enter the air through the diesel exhaust.

Table 2.
Limit values for some air pollutants

Pollutant / Norm	1	2	3	4
SO_2 (Ordinance12, 2010)	350	125	-	20
NO_x (Ordinance12, 2010)	200	-	40	30
PM_{10} (Ordinance12, 2010)	-	50	40	-
$PM_{2,5}$ (Ordinance12, 2010)	-	-	25	-
CO (Ordinance12, 2010)	10*	-	-	-
CO_2 (NIOSH, 2007)	-	0.58**	-	-
n-octane (NIOSH, 2007)	-	350***	-	-
TSP****(Ordinance14, 1997)	0.50	0.25	0.15	-

1 - Hourly average norm for the protection of human health, $\mu g/m^3$; 2 - Daily average norm for the protection of human health, $\mu g/m^3$; 3 - Average annual norm for the protection of human health, $\mu g/m^3$; 4 - Norm for protecting natural ecosystem, $\mu g/m^3$; * - maximum average for 8 hours in one 24 hours period, mg/m^3; ** vol % - REL - TWA - recommended exposure limits - a time-weighted average concentration for up to a 10-hour workday during a 40-hour workweek; *** TWA, mg/m^3; **** - in mg/m^3 .

The degree of air pollution with the above-mentioned pollutants by the quarrying activity depends on: the type and composition of the extracted material, the mining technology, the mode of transportation, the level of mechanisation, as well as on the local microclimate conditions. That is why for obtaining a “real picture” of the situation "in situ", measurements are needed.

The work presented in this paper is aimed at determining the concentrations of the eventual pollutants emitted under real working conditions of the *Mizia* quarry, as well as to assess their possible harmful effect to the workers and to the environment. The results obtained can serve as a basis for proposing mitigation measures.

Methods and materials

The studied quarry is near the village of Varbesnitsa, the municipality of Mezdra, in Northwest Bulgaria. Climatically, the area falls within the moderate continental subregion of the European continental climatic zone. The average monthly air humidity is 72%, with a maximum in winter (December - 85%) and a minimum in summer (August - 59%). With regard to the wind, quiet weather prevails. Northwest winds with an average annual speed of 1.6 m/s are predominant.

Large premium limestone blocks are extracted in the quarry. Once the size of the block is determined, the edges of the block are determined by drilling holes. High technology diamond wire saws slice the massive beds in the quarry into blocks. Cooling water prevents the diamonds from overheating and suppresses the dust produced by the cutting equipment. The wire saws are also used to slice bigger blocks in the sealable sizes. The quarry workers pick up the stone blocks using loaders equipped with handling forks. Waste limestone, which is an unavoidable by-product of the quarrying and processing, is taken out from the production place with Fadroma haul-dump machines.

Eventual pollution can arise mainly from the drilling activities and from the work of loading and transportation machines. In addition, in windy conditions, dust from the quarry bottom can be raised. People can be exposed to limestone dust and other eventual pollutants in the workplace by inhalation and skin and eye contact.

Analyses for dust and gaseous pollutants were made at three points: first, immediately at the drilling point while the drilling was carried out; second, at the opposite end of the quarry while slicing with the wire saws and cargo operations were carried out; and third, outside the quarry in the nearby forest. In addition, exhaust gases were measured at the tailpipe end of one of the Fadroma haul-dump machines while it was working. The measurement is representative, since all haul-dump machines used in the quarry are the same age and produced by the same company.

A manual "Dräger" pump with a volume of 100 mL and two indicating tubes for each measured gas at each sampling point were used. Where necessary, tubes applicable for different concentration ranges of pollutants were used. Measurements

with tubes for CO and n-octane are generally based on oxidation-reduction processes, while measurements with tubes for CO_2, SO_2 and NO_x are generally based on changes in the pH of the substance in the tubes. Both types of reactions lead to colour change of the substances and/or added reagents-indicators in the tubes. More precisely, the following reactions were used (Dräger, 2011):

For CO:

$$5CO + I_2O_5 \xrightarrow{H_2S_2O_7} 5CO_2 + I_2$$

Color change: white → brownish green

For n-octane:

$$C_8H_{18} + I_2O_5 \rightarrow I_2$$

Color change: white → green

For CO_2:

$$CO_2 + N_2H_4 \rightarrow NH_2–NH–COOH$$

Color change: white → pale violet/blue violet

For NO_x:

a) $NO + Cr^{VI} \rightarrow NO_2$

b) NO_2 + o-diphenyl benzidine → blue grey reaction product

Color change: yellow → blue grey

For SO_2, depending on the concentration range, where the second reaction is for the lowest concentrations of SO_2:

$$SO_2 + I_2 + 2H_2O \rightarrow H_2SO_4 + 2HI$$

Color change: grey blue →white

$$SO_2 + Na_2[HgCl_4] + \text{methyl red} \rightarrow Na_2[Hg(SO_3)_2] + 4HCl$$

Color change: yellow → orange .

Personal aspirators for dust, type PAP-4S, with flow rate of 2.0 L/min and FPP-15 filters were used at sampling points 1 and 2 for 60 min and two parallel samples were taken for each point. The sampling time was 8 hours for sampling point 3. Before and after the sampling, filters were weighed on an analytical balance (±0.00001 g). Dust sampling was done in two days – on one it was sunny and slightly windy, and on the other it was cloudy, wet and quiet.

Results and discussion

Results from the in-situ measurements (averaged values from 2 parallel determinations) are presented in Table 3.

By comparing the results, presented in Table 3, with the data from Table 1 and the values from Table 2, the following can be stated:

- Concentrations of gaseous air pollutants (NO_x, CO, CO_2, SO_2, and VOCs presented as n-octane) in the working atmosphere of the quarry are below or equal to the norms for the protection of human health.

Table 3.
In-situ determined concentrations of some air pollutants

Pollutant / Point	S1	S2	S3	Pipe
SO_2, mg/m^3, dry	0.3	0.3	<0.3	6
SO_2, mg/m^3, wet	0.3	0.3	<0.3	6
NO_x, mg/m^3, dry	0.2	0.2	<0.1	0.5
NO_x, mg/m^3, wet	0.2	0.2	<0.1	0.5
CO, mg/m^3, dry	8	10	5	20
CO, mg/m^3, wet	8	10	4	20
CO_2, vol %, dry	0.4	0.4	0.2	0.8
CO_2, vol %, wet	0.4	0.4	0.2	0.75
n-octane, mg/m^3, dry	160	210	<100	525
n-octane, mg/m^3, wet	210	350	<100	630
TSP, mg/m^3, dry	31	7	0.045	-
TSP, mg/m^3, wet	25	5	-	-

S1 – site immediately at the drilling point; S2 – site at the opposite end of thequarry; S3 – site in the nearby forest; pipe - at the tailpipe end of one of the Fadroma haul-dump machines

- Concentrations of gaseous air pollutants determined at the exhaust exit of the Fadroma haul-dump machine are at the low edge of the ranges presented in the literature for the heavy duty diesel engines.

- Practically, the work in the quarry does not pollute the surroundings with NO_x, CO, CO_2, SO_2, and VOCs.

- TSP concentrations determined on the territory of the quarry exceed the maximum permissible values, i.e. the hourly average norm for the protection of human health. Significantly higher excess concentration is observed at the measuring site situated immediately at the drilling point and under dry conditions. Values are of the same order of magnitude as those measured for a similar quarry by another author at 500-700 m outside their quarry (Sayara, 2016). Higher TSP concentrations were determined in dry conditions than in wet. Summer was found as the season with the highest TSP concentration by (Sayara, 2016), too. The precipitation helps in sinking these pollutants (wet deposition) and most of the produced dust is wetted and mixed with soil and can not be easily re-suspended.

- In terms of air pollution with dust, TSP concentrations determined in the nearby forest show that the quarry activity does not pose a negative effect on the environment.

Carbon monoxide in the diesel exhaust results from the incomplete combustion of the fuel. Although CO is produced in rich mixtures during operation, a small portion of CO is also emitted under lean conditions (Resitoglu et al., 2015). Diesel engines are lean combustion engines. So, the formation of CO is minimum in the properly tuned diesel engines. Hydrocarbon emissions are composed of unburned fuels as a result of insufficient temperature which occurs near the cylinder wall. Since unburned hydrocarbons continue to react in the exhaust stream, if the temperature is above 600^{o}C and oxygen is present, diesel engines normally emit low levels of

hydrocarbons. That is why the hydrocarbon emissions from the tailpipe may be significantly lower than the hydrocarbons leaving the cylinder (Resitoglu et al., 2015). Particulate matter emissions in the exhaust gas result from the combustion process. They may originate from the agglomeration of very small particles of partly burned fuel, from partly burned lube oil, from ash content of fuel oil, and from cylinder lube oil. Diesel engines use highly compressed hot air to ignite the fuel. At high temperatures (above 1600^{o}C) in the cylinders, the nitrogen from the air reacts with oxygen and NO_x emissions are generated (Resitoglu et al., 2015).

When hydrocarbon fuel is burned with the correct amount of air in a diesel engine, the benign gases that are left are predominately water vapor, carbon dioxide, and nitrogen (Chevron Corporation, 2007).The total amount of air polluting gases and soot in the diesel exhaust is less than 1% (Resitoglu et al., 2015).

Exhaust gas recirculation (EGR) systems are usually used to reduce NO_x emissions. The exhaust gas is recirculated back into the combustion chamber and mixed with fresh air at intake stroke. A richer mix is achieved by displacing some of the intake air, but it is still lean compared to petrol engines. The lower peak temperature is achieved by a heat exchanger that removes heat before re-entering the engine, and works due to the higher specific heat capacity of exhaust gases than air. At this, the efficiency of combustion is worsened, the combustion temperature is decreased which means reducing the formation of NO_x. However, the negatively impacted efficiency leads to the production of soot particles. With the greater soot production, EGR is combined with a particulate matter filter in the exhaust gases system. EGR (with a PM filter) is widely used in high-duty diesel vehicles, including in those working in the *Mizia* quarry. The vehicles are also equipped with a diesel oxidation catalyst (DOC) which oxidizes HC and CO emissions. Most probably, the Fadroma haul-dump machines are equipped with a selective catalytic reduction (SCR) system, since the producer is amongst the world leaders implementing SCR in its high-duty vehicles. The SCR system is used to minimise NO_x emissions. Water and N_2 are released as a result of the catalytic conversion of NO_x in the exhaust gas.

The presence of the described technologies explains the low concentrations of pollutants measured in the exhaust of a working Fadroma haul-dump machine. Low concentrationsof polluting gases (below standard thresholds) have also been measured in other studies on the air quality in and around quarries and stone cutting industries (Sayara, 2016).

The presence of a visible dust cloud is a good sign that respirable dust is present, even though such clouds are mostly larger-sized particles (Organiscak et al., 2003).

Different studies obtained different values for the ratio PM_{10} / TSP but generally the reported values are in the range of 0.44-0.74 and most often - around 0.5 (Brook et al. 1997; Marcazzan et al., 2001; Kermani et al., 2003). In addition, the study of the Canadian National Air Pollution Surveillance Network showed that on average $PM_{2.5}$ accounted for 49% of the PM_{10} (Brook et al. 1997).

Considering the ratio of 0.5, it can be stated that the air outside the quarry meets the air quality standards with respect to PM_{10} and $PM_{2.5}$. However, this is not the case inside the working quarry. The limestone powder does not contain free silica and there is no danger of developing silicosis or other types of pneumoconiosis. However, powder exposure from limestone has an irritant effect on the upper respiratory tract. Some measures must be taken. Wearing proper dust masks by the workers is enough (Health and Safety Authority, 2010) for the whole range of works except for direct drilling, where additional measures are needed to decrease dust release, as described below.

Both wet and dry methods are available to reduce the drill dust (Organiscak et al., 2003). Wet drilling systems pump water into the bailing air from a water tank mounted on the drill. The water droplets in the bailing air trap dust particles as they travel up the annular space of the drilled hole, thus controlling dust as the air bails the cuttings from the hole. The drill operator controls the flow using a control valve. Dry collection systems require an enclosure around the area where the drill stem enters the ground. This enclosure is constructed by hanging a rubber or cloth shroud from the underside of the drill deck. The enclosure is then ducted to a dust collector, the clean side of which has a fan. The fan creates a negative pressure inside the enclosure, thus capturing dust as it exits the hole during drilling. The dust is removed in the collector, and clean air is exhausted through the fan. Wet systems can be more efficient, but may freeze in winter. Dry systems require careful maintenance of the drill deck shroud.

The waste limestone, an inevitable by-product of the quarrying and processing, is crushed to provide aggregate for making roads inside and around the quarry. The dust from these roads inside the quarry can be controlled by spraying plain water or water with some surfactants added by using spraying systems with suitable nozzle types (Spraying Systems Co., 2008).

Conclusions

As a result of our study the following conclusions can be drawn:

- Concentrations of gaseous air pollutants (NO_x, CO, CO_2, SO_2, and VOCs presented as n-octane) in the working atmosphere of the *Mizia* quarry for stone blocks practically do not pose hazards to the workers since they are below or equal to the norms for the protection of human health.

- TSP concentrations determined on the territory of the quarry exceed the maximum permissible values, i.e. the hourly average norm for the protection of human health. Higher amounts of dust were found in dry weather and on the measuring site situated immediately at the drilling activity.

- Wearing proper dust masks by the workers is sufficient to preserve their health. Additional measures, such as dust collection and water spraying, are needed to decrease dust release at direct drilling.

- Equipment used in the quarry is properly fitted with the air protection systems.

- Concentrations of air pollutants (NO_x, CO, CO_2, SO_2, and VOCs presented as n-octane and TSP) released by the working quarry do not pose hazards to the surrounding environment.

Acknowledgements

This work was supported by the project "COMPLEX RESEARCH OF THE DEVELOPMENT OF MINERAL WORKS IN THE QUARRY FOR THE EXTRACTION OF STONE FACING MATERIALS WITH ACCOUNTING FOR THE ECONOMIC EFFECT (on the example of "Mizia" limestone quarry) at the University of Mining and Geology – Contract № MTF -167/08.03.2018.

Rererences

Brook, J. R., Dann, T, F., Burnett, R. T., The relationship among TSP, PM_{10}, $PM_{2.5}$, and inorganic constituents of atmospheric particulate matter at multiple Canadian locations, J Air Waste Manage Association, 47, 1997. - 2-19.

Chevron Corporation, Diesel fuels technical review, Chevron Corporation ©, 2007. -116 p.

Dräger-Tubes & CMS-Handbook - Soil, water, and air investigations as well as technical gas analysis,16th Edition, Dräger Safety AG & Co. KGaA, Lűbeck, Germany, 2011. - 462 p.

Grenier, M. Measurement of carbon monoxide in diesel engine exhaust, IRSST Report (R-436), Clic Research, Canada, 2005. - 29 p.

Health and Safety Authority, A Guide to Respiratory Protective Equipment, Dublin, 2010. - 19 p.

Kermani, M., Naddafi, K., Shariat, M., Mesbah, A. S., Chemical composition of TSP and PM_{10} and their relations with meteorological parameters in the ambient air of Shariati hospital district, Iranian J Publ Health, 32, 4, 2003. - 68-72.

Marcazzan, G. M., Vaccaro, S., Valli, G., Vecchi, R. Characterization of PM_{10} and $PM_{2.5}$ particulate matter in the ambient air of Milan (Italy), Atmos Environ, 35, 27, 2001. - 4639-50.

National Institute for Occupational Safety and Health NIOSH Pocket Guide to Chemical Hazards. DHHS (NIOSH) publication no. 2005-149. NIOSH Publications, Ohio, 2007. – 454 p.

Nett Technologies Inc., 2018, www.nettinc.com/information/emissions-faq/what-are-diesel-emissions (accessed 22. 06.2018).

Ordinance No 12 of July 15, 2010 on the limit values for sulfur dioxide, nitrogen dioxide, fine particulate matter, lead, benzene, carbon monoxide and ozone in the ambient air, State Newspaper 30.07.2010.

Ordinance No 14 of 23rd September 1997 on the standards for the maximum permissible concentrations of harmful substances in the ambient air of the settlements, State Newspaper 3.10.1997.

Organiscak, J. A., Page, S. J., Cecala, A. B., Kissell F. N., Surface mine dust control, Chapter 5. In: Handbook for dust control in mining, (Ed. Kissell, F. N.). Pittsburgh Research Laboratory, National Institute for Occupational Safety and Health, Pittsburgh, PA. Information Circular 9465, DHHS (NIOSH) Publication No. 2003-147, June 2003. – 73-83.

Resitoglu, I., Altinisik, K., Keskin, A., The pollutant emissions from diesel-engine vehicles and exhaust after-treatment systems, Clean Techn Environ Policy, 17, 1, 2015. - 15–27.

Sayara, T. Environmental impact assessment of quarries and stone cutting industries in Palestine: Case study of Jammain, J Environ Prot Sustainable Development, 2, 4, 2016.- 32-38.

Spraying Systems Co., A Guide to spray technology for dust control, Bulletin No. 652, Spraying Systems Co. © U.S.A., 2008. – 20 p.

Tschanz, F., Amstutz, A., Onder, C., Guzzella, L., A Real-time soot model for emission control of a diesel engine, 6th IFAC Symposium Advances in Automotive Control, Munich, Germany, July 12-14, 2010. - 222-227.

EFFECT OF AMINES ON THE SILVER NANOPARTICLES FORMATION AT ROOM TEMPERATURE

Gospodinka Gicheva[1], Neli Mincheva[1]

[1]University of Mining and Geology "St. Ivan Rilski", 1700 Sofia, e_gospodinka@yahoo.com

ABSTRACT. Silver nanoparticles, Ag NPs, play an important role in modern technology. Their antimicrobial and catalytic properties are employed in many different fields of research – catalysis, electronics, microbiology and environmental protection. Such major involvement requires cost effective methods for synthesis of stable Ag NPs if they are applied in large scale. Here, we present an environmentally friendly method for preparation of silver nanoparticles at room temperature in the presence of amines. Two types of amines were employed in the synthesis – monoethanolamine (MEA) and triethanolamine (TEA) as a catalyst for the reduction of silver ions to Ag NPs. The resulting nanoparticles were characterized by UV-VIS spectrophotometry and scanning electron microscopy (SEM). Information about their size and morphology was obtained and was used for comparison of the effect of the amine on the process of Ag NPs formation.

Keywords: Ag NPs, nanomaterials, synthesis, amines

ВЛИЯНИЕ НА АМИНИ ВЪРХУ ПРОЦЕСА НА ФОРМИРАНЕ НА СРЕБЪРНИ НАНОЧАСТИЦИ ПРИ СТАЙНА ТЕМПЕРАТУРА

Господинка Гичева[1], Нели Минчева[1]

[1]Минно-геоложки университет "Св. Иван Рилски", 1700 София, e_gospodinka@yahoo.com

РЕЗЮМЕ. Сребърните наночастици, Ag NPs, заемат важно място в съвременните технологии. Техните антимикробни и каталитични свойства се използват в много различни научни разработки в областта на електрониката, микробиология и опазването на околната среда. Широката им област на приложение налага необходимостта от разработването на икономически изгодни методи за синтез на стабилни Ag NPs, с цел те да се прилагат в големи мащаби. В това изследване представяме екологосъобразен метод за получаване на сребърни наночастици при стайна температура в присъствието на амин. Два вида амини (моноетаноламин (MEA) и триетаноламин (TEA)) се използват при този синтез, те действат като катализатори при редукцията на сребърни йони до сребърни наночастици. Получените наночастици са охарактеризирани с UV-VIS спектрофотометрия и сканираща електронна микроскопия (СЕМ). Получена информацията за техните размер и морфология е използвана за сравнение на ефекта на двата катализатора в процеса на образуване на Ag NPs.

Ключови думи: сребърни наночастици, наноматериали, синтез, амини

Introduction

Nanosized particles and nanomaterials have attracted the interest of scientific community due to their unique properties – optical, electronic, and electrochemical (Liz-Marzán, 2006). What makes them really unique is the fact that their characteristics differ from those of the bulk materials and are size-dependant due to the quantum confinement effect. Therefore, the properties of nanomaterials can be tuned just by tuning particles' size without changing the chemical composition (Duan et al., 2000). Silver is one of the popular metals used for production of nanoparticles. Antimicrobial properties of silver ions have been well-known for long time. Silver nanoforms also show such an activity, moreover nanoparticles are much more convenient for applications such as antimicrobial textile, sterile bandages and other commercially available products based on nanosilver (Perera et al., 2013). Other applications are based on its metal conductivity and optical properties. It is applied in modern electronics and optical devices (Natsuki et al., 2011). Silver nanoparticles and materials based on them are important means for disinfection of potable water as an alternative of chlorine treatment, which leads to formation of carcinogenic by-products and derivatives (Ülküra E et al., 2005; Panacek et al. 2006; Abdel-Aziz et al., 2014).

Synthesis of uniform and stable silver nanoparticles with controllable size is also a difficult task. The optimum synthetic method should address all of the above-mention problems and additionally it should be able to yield nanoparticles with no extraneous chemicals that can potentially alter the particle's optical properties and surface chemistry. In the literature there are various methods for synthesis of silver nanoparticles (AgNPs) (Swathy B., 2014). Many of them are based on the reduction of Ag+ ions in water solution. Chemical reduction typically includes reducing agent like polyols, $NaBH_4$, N_2H_4, sodium citrate and N,N-dimethylformamide. In order to prevent the aggregation of AgNPs, the suspension is stabilized by capping agents such as sodium dodecyl sulphate (SDS), polyvinyl pyrrolidone (PVP), tri-sodium citrate (Jones et al., 2014). Some of the chemical reduction reactions can be carried out at room temperature. However, most of them need elevated temperatures for a higher reaction rate. Nanoparticles' morphology strongly depends on the reaction

temperature. For example, flower-like silver nano architecture with size of the particles 20 nm is formed in the presence of ascorbic acid at room temperature (Kimling J. et al., 2006). The other classic method involves sodium citrate as a reducing and capping agent at high temperature under reflux (Turkevich et al., 1951). Silver nanoparticles have been synthesized in the presence of supercritical carbon dioxide ($SCCO_2$), from silver nitrate used as a starting material, PVP as a stabilizer of silver clusters, and ethylene glycol as a reducing agent and solvent. Polyvinyl pyrrolidone not only protected the nanosized silver particles from aggregation, but it also promoted nucleation. The silver nanoparticles synthesized by $SCCO_2$ are smaller and possess higher monodispersity than those produced under the same conditions by the conventional heating methods. As a result, the nanosilver had lower toxicity and higher stability, and the particles were all spherical with mean diameters in the range of 2–5 nm (Jones et al., 2014).

Environmental applications of AgNPs, such as water disinfection (Pradeep A. T., 2009), dyes degradation, gas sensing etc., require stable, non-aggregable and in many cases non-hydrophobic nanoparticles. Surfactants are typically used to protect NPs from aggregation; however, the capping molecules on the surface of NPs block the mass transport and electron transfer and thus reduce their activity (Li D. et al., 2012). In addition, recovery of the AgNPs from the reaction medium is difficult and expensive. The immobilization of AgNPs on solid surfaces or incorporation in solid matrix provides stability and thus facilitates the reuse of NPs. AgNPs have been immobilized on different solid surfaces such as glass slides, silica nanofibers (Wong, C. et al., 2015), coated magnetic particles, carbon nanotubes (Yan et al., 2011) and thiol functionalized polymer–carbon nanotubes composite.

In this paper, we present the formation of silver nanoparticles obtained at room temperature using modified citrate method. It consists of addition of amines (MEA and TEA) which catalyse the reduction of silver ions by sodium citrate thus lowering the reaction temperature.

Experimental part

Chemicals

$AgNO_3$ (purum >99.8%) was purchased from Teokom Ltd (Bulgaria), tri-sodium citrate dehydrate (Na_3Cit ▪$2H_2O$; for analysis). and hexadecyltrimethylammonium bromide (CTAB; ≥99.0%) - from MERCK & CO., INC. Monoethanolamine (ethanolamine, MEA; pure p. a.) and triethanoloamine (TEA; pure p. a.) were obtained from POCH™ (Poland). All reagents were used without further purification. All the solutions were made using double distilled water.

Synthesis of AgNPs

Solution of silver nitrate in double distilled water (d.d. H_2O) was stirred on magnetic stirrer at room temperature. A solution of CTAB with different concentrations (5.10^{-4}, 1.10^{-3}, 2.10^{-3} M) was added drop wise to the $AgNO_3$ solution and the mixture was stirred for 20 minutes. Then 20 ml Na_3Cit solution (2.10^{-3} M) was added drop wise. After that 3 ml solution of 4.10^{-4} M MEA (or TEA) was injected into the reaction mixture. A pale reddish colour appeared. Aliquots of reaction mixture were taken at 15th and 30th minutes and their spectra were recorded. The amounts of reagents are given in Table 1.

Table 1.
Experimental condition for samples preparation

sample	CTAB, [M]	MEA, [M]	TEA, [M]
1	5.10^{-4}	4.10^{-4}	0
2	1.10^{-3}	4.10^{-4}	0
3	2.10^{-3}	4.10^{-4}	0
4	5.10^{-4}	0	4.10^{-4}
5	1.10^{-3}	0	4.10^{-4}
6	2.10^{-3}	0	4.10^{-4}

*The $AgNO_3$ and Na_3Cit solutions were in concentrations 2.10^{-3} M

Materials characterization

UV-Vis spectral analysis of the obtained silver nanoparticles (AgNPs) was performed. They revealed peaks characteristic for them. The nanosized structures were also observed by scanning electron microscopy (SEM).

Results and discussions

Ag NPs were formed in aqueous solution by reduction of silver ions with sodium citrate. Addition of amine as a catalyst provides an alternative pathway of the reaction and allows it to proceed at lower temperature, which is an essential advantage of this procedure. Hexadecyltrimethylammonium bromide (CTAB) was used as surfactant and stabilizing agent to prevent Ag NPs from aggregation.

In order to investigate the effect of the amine in the process on silver nanoparticles formation, we tested two types of amines – monoethanolamine (MEA) and triethanolamine (TEA). The Ag NPs formation within 30 minutes was monitored by UV-Vis spectroscopy. The UV-Vis spectra of reaction mixture of Ag NPs (samples 4-6), obtained by TEA catalyzed reduction at 15th and 30th minutes are shown on Fig. 1A and Fig. 1B, respectively.

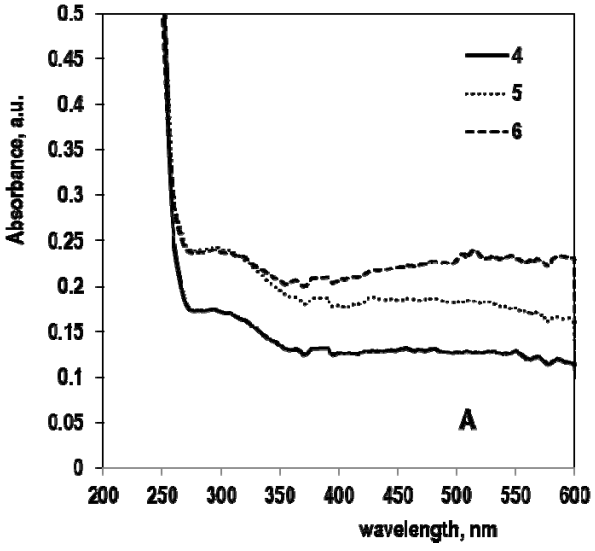

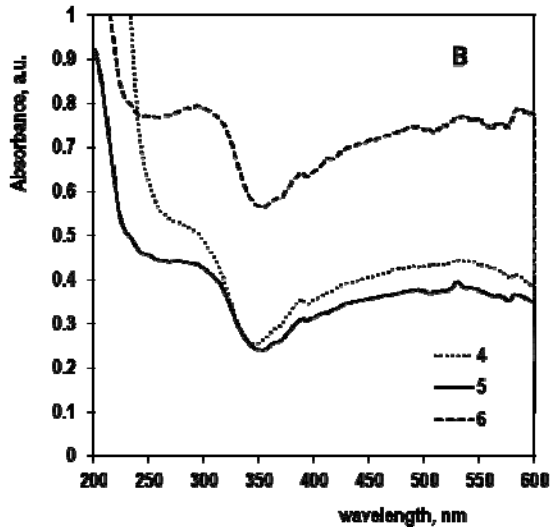

Fig. 1. UV-Vis spectra of samples 4 - 6 with TEA as catalyst and different concentration of CTAB, taken at 15th minute (A) and at 30th minute (B).

The spectra of all the samples showed two well pronounced peaks, which intensities increase with the time. The peak at 270-280 nm can be attributed to the Ag-precursor, formed between silver ions and surfactant molecule, Ag^+-CTAB complex. The longer-wavelength peaks at 480-580 nm are due to Ag NPs and give rise from nanoparticles with diameter of 100-200 nm (Fig. 1) (Agnihotri et al., 2014). This is also consistent with results shown on Fig. 2A and 2B, where the spectra of MEA-catalysed reaction mixtures are given.

Another parameter investigated in this study is the concentration of the surfactant CTAB. It was observed that the higher is its concentration, the higher is the rate of formation of the Ag NPs in both series of samples (1-3) and (4-6). Moreover, the higher concentration of CTAB leads to slight red shift of the band maximum and the increase in the intensity of both peaks (~280 nm and ~480 nm) in the spectra (Fig. 1A, 1B and Fig.2A, 2B).

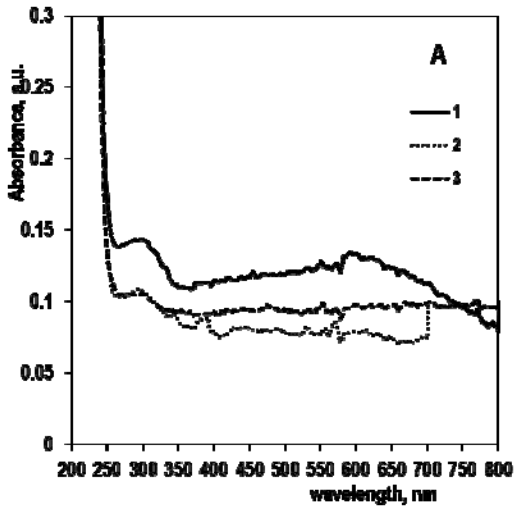

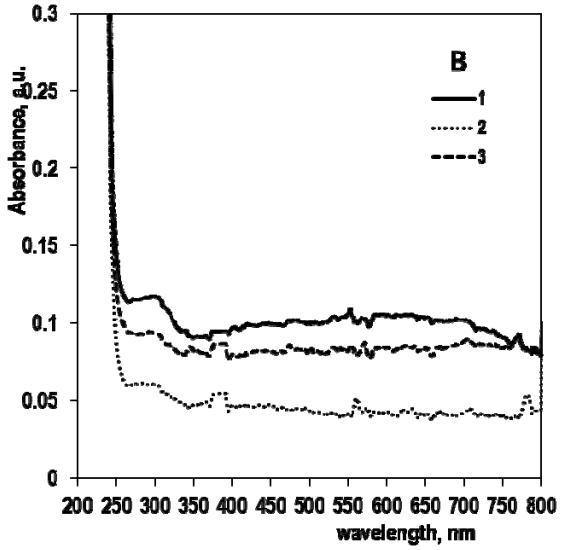

Fig. 2. UV-Vis spectra of samples 1 - 3 with MEA as catalyst and different concentration of CTAB, taken at 15 min (A) and 30 min (B)

The results from the UV-Vis spectra of the obtained Ag NPs were summarized and the data for the wavelength maxima are given in Table 2. It can be seen that the peaks for samples 1-3 are centred at 510-520 nm, while for samples 4-6 the maximum appeared at around 480 nm. It is well known that decreasing of the NPs size is associated with blue shift of the UV-Vis band. Thus, the reaction carried out in the presence of TEA leads to formation of smaller Ag NPs than that in the presence of MEA. Additionally, when the concentration of CTAB increases bigger Ag NPs are formed, as the peak shifts towards higher wavelengths.

Table 2.
The maximum wavelength determined from the UV-Vis spectra

sample	1	2	3	4	5	6
λ_{max},nm	510	515	520	480	480	490

In order to shed some light on the effect of the catalysts (MEA and TEA) we compared the spectra of Ag NPs obtained at 30th minute with the same concentration of CTAB (5.10^{-4} M). On fig.3 are shown the UV-vis spectra of the reaction mixtures containing TEA and MEA as catalysts.

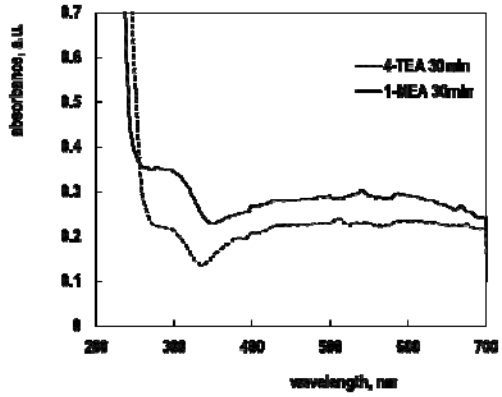

Fig. 3. UV-Vis spectra of AgNPs taken at 30 min from the reaction mixture with different catalyst – TEA and MEA and the same concentration of CTAB – 5.10-4 M

As we compare the spectra (Fig. 3) of Ag NPs, formed by MEA and TEA catalysed reaction for the same reaction time, we can observe that the MEA produced NPs are bigger in size (have maximum at higher wavelengths). The structures of both compounds are shown on Fig. 4. MEA is primary amine which generally makes it more reactive than TEA, which is a tertiary amine. Both molecules contain hydroxyl group(s) that are involved in similar chemical reactions.

(A) (B)

Fig. 4. Chemical structure of the catalysts monoethanolamine MEA (A) and triethanolamine TEA (B)

There is a proposed mechanism for the catalytic action of the amines in the literatures. It involves the addition of proton from the water molecule thus releasing hydroxyl ion. The hydroxyl ions oxidize the OH group in the citrate and free electron is generated in the process. Since the TEA is stronger base than MEA it is supposed to be more active catalyst (Natsuki et al., 2011).

The data from the SEM analysis corresponds well with the data from UV-Vis spectra. The SEM images of Ag NPs are shown on Fig. 5. The average size of the silver nanoparticles is about 200-250 nm.

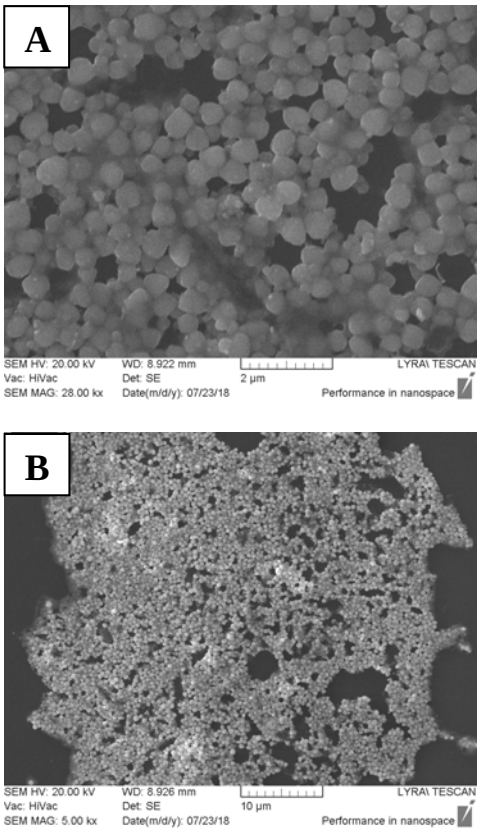

Fig. 5. SEM images at different magnification (A) and (B) of Ag NPs obtained in the presence TEA.

Conclusions

In this study a low temperature synthesis of silver nanoparticles was described and the effect of two amines was investigated. It was demonstrated that both amines (TEA and MEA) can produce Ag NPs at room temperature. This is of great impact since a large scale production of Ag NPs can be achieved only by cost effective methods which don't require heating of the mixture and energy consumption.

The reaction was conducted in water media without using expensive and toxic organic solvents. This method will be suitable for preparation of materials that will be used in water treatment and environmental protection.

The low reaction temperature is crucial for the formation of nanocomposite materials involving the reduction of silver ions adsorbed onto natural zeolite surface. It is necessary to maintain room temperature otherwise we risk desorption of silver ions at elevated temperatures. This method will allow the preparation of the desired nanocomposite material.

Acknowledgements.
The authors thank for the financial support under the project DN-17/20 – 12.12.2017 by National Research Fund and for SEM measurement of members of Faculty of Physics, University of Sofia.

References

Abdel-Aziz M.S., Shaheen M.S., El-Nekeety A.A., Abdel-Wahhab M.A., Antioxidant and antibacterial activity of silver nanoparticles biosynthesized using Chenopodium murale leaf extract. J. Saudi Chem. Soc., 18(4), 2014. - 356–363.

Agnihotri S., Mukherji S., Mukherji S., Size-controlled silver nanoparticles synthesized over the range 5–100 nm using the same protocol and their antibacterial efficacy, RSC Adv. 4, 2014. -3974-3983.

Duan X., Lieber C. M., General Synthesis of Compound Semiconductor Nanowires, Adv. Mater., 12(4), 2000. -298–302.

Jones S., Walsh-Korb Z., Barrow S. J., Henderson S. L., Barrio J., Scherman O. A., The Importance of Excess Poly(N-isopropylacrylamide) for the Aggregation of Poly(N-isopropylacrylamide)-Coated Gold Nanoparticles, ACS Nano, 110(3), 2016. -3158–3165.

Kimling J., Maier M., Okenve B., Kotaidis V., Ballot H., Plech A., Turkevich Method for Gold Nanoparticle Synthesis Revisited, J. Phys. Chem. B, 110 (32), 2006. -15700–15707.

Li D., Wang C., Tripkovic D., Sun S., Markovic N. M, Stamenkovic V. R., Surfactant Removal for Colloidal Nanoparticles from Solution Synthesis: The Effect on Catalytic Performance, ACS Catal., 2 (7), 2012. -1358–1362.

Liz-Marzán L. M, Tailoring surface plasmons through the morphology and assembly of metal nanoparticles, Langmuir. 22(1), 2006. -32–41.

Natsuki J., Abe T., Synthesis of pure colloidal silver nanoparticles with high electroconductivity for printed electronic circuits: the effect of amines on their formation in

aqueous media, J. Colloid. Interf. Sci., 359(1), 2011. -19–23.

Panacek A., Kvitek L., Prucek R., Kolar M., Vecerova R., Pizurova N., Sharma V.K., Nevecna T., Zboril R. 2006, Silver nanoparticles: Synthesis, characterization, and their antibacterial activity. J. Phys. Chem. B, 110, 2006. -16248–16253.

Pradeep A. T., Noble metal nanoparticles for water purification: A critical review, Thin Solid Films, 517, 2009, -6441–6478.

Perera S., Bhushan B., Bandara R., Rajapakse G., Rajapakse S., Bandara C. Morphological, antimicrobial, durability, and physical properties of untreated and treated textiles using silver-nanoparticles. Colloid Surface A, 436, 2013. -975–989.

Luo S., Yu S., Fang F., Lai M., Sun R., Wong C., Investigating the mechanism of catalytic reduction of silver nitrate on the surface of barium titanate at room temperature: oxygen vacancies play a key role, RSC Adv.5, 2015. -3377–3380.

Swathy B., A Review on Metallic Silver Nanoparticles, IORS Journal of Pharmacy, 4 (7), 2014. -38-56.

Turkevich J, Stevenson PC, Hillie J., A study of the nucleation and growth processes in the synthesis of colloidal gold, Discuss. Faraday Soc., 11, 1951, -55–78.

Ülküra E., Oncul O., Karagoz H., Yeniz E., Çeliköz B. Comparison of silver-coated dressing (Acticoat™), chlorhexidine acetate 0.5% (Bactigrass®), and fusidic acid 2% (Fucidin®) for topical antibacterial effect in methicillin-resistant Staphylococci-contaminated, full-skin thickness rat burn wounds. Burns, 31(7), 2005. -874–877.

Yan Y., Sun H., Yao P., Kang S., Mu J., Effect of multi-walled carbon nanotubes loaded with Ag nanoparticles on the photocatalytic degradation of rhodamine B under visible light irradiation, Appl. Surf. Sci, 257, 2011. -3620–3626.

LEADING PRINCIPLES AND PRACTICES IN THE MANAGEMENT OF CONSTRUCTION WASTES

Maria Manastirli[1], Irena Spasova[1]

[1]University of Mining and Geology "St. Ivan Rilski", 1700 Sofia, manastyrli_mariy@mail.ru

ABSTRACT. One of priorities of the ecology and protection of the natural and various technogenic media is the management of the wastes from the human activity, including their secure utilisation. In this respect, special attention is paid to the construction wastes, including activities associated with their collection, transportation, and pre-treatment with a view to their efficient recovery and recycling. This activity is connected with profound knowledge of the contemporary methods and technologies for the treatment of various types of construction waste, as well as of the specific requirements to the sites connected with the implementation of these methods and technologies. This article presents the basic principles and practices related to the management of construction waste in accordance with the national and European legislation.

Keywords: construction waste, utilisation, recycling

ВОДЕЩИ ПРИНЦИПИ И ПРАКТИКИ ПРИ УПРАВЛЕНИЕТО НА СТРОИТЕЛНИ ОТПАДЪЦИ

Мария Манастирли[1], Ирена Спасова[1]

[1]Минно-геоложки университет "Св. Иван Рилски", 1700 София, manastyrli_mariy@mail.ru

РЕЗЮМЕ. Един от основните приоритети на екологията и опазването на природната и различните техногенни среди е управлението на отпадъците от човешката дейност, в това число тяхното безопасно съхраняване и оползотворяване. Особено значение в тази насока се отделя на строителните отпадъци, включващо дейности, свързани с тяхното събиране, транспортиране и предварителна подготовка с оглед ефикасното им оползотворяване и рециклиране. Тази дейност е свързана с дълбоко познаване на съвременните методи и технологии за третиране на различните видове строителни отпадъци, както и на специфичните изисквания към площадките, свързани с реализацията на тези методи и технологии. В настоящата статия са разгледани основните принципи и практики, свързани с управлението на строителни отпадъци, съобразени с националното и европейско законодетелство.

Ключови думи: строителни отпадъци, оползотворяване, рециклиране

Introduction

The development of the economy is connected with the construction of a new infrastructure, which in turn is related to the utilisation of mineral raw materials and the generation of a large amount of construction waste that covers huge areas and pollutes the environment. According to the European statistics (EUROSTAT), 48% of the generated waste comes from the construction and demolition and 15% is generated by the mining industry, the mining of rock materials, and the excavation of earth masses. The annual quantity of such waste for the 28 EU member countries is 1750 – 1900 million tones (National strategic plan for management of the C&D waste 2011-2020).

The first step towards solving the problem with waste generation is the ecological and responsible management. According to the Directive 2008/98/EC (2008), '**waste management'** means the collection, transport, recovery, and disposal of waste, including the supervision of such operations and the after-care of disposal sites, and also including actions taken as a dealer or broker. This activity is related to a profound knowledge of the modern methods and technologies for the treatment of different types of construction waste. The present article discusses the basic principles and practices related to the waste management of construction waste in accordance with the national and European legislation.

National and European legislation in the management of the construction waste

The current EU policy in waste management is based on the concept for hierarchy in its management.

Directive 2008/98/EU implements a five-staged hierarchy in the waste prevention and management legislation and policy in all the EU member countries with the following order of priorities:

1. Prevention of waste generation;
2. Preparation for re-use;
3. Waste recycling;
4. Waste recovery , e.g. energy recovery;
5. Waste disposal;

According to the hierarchy, EU member countries must focus on the prevention of waste generation and when this is not possible, the generated waste must be reused, recycled, recovered to the fullest extent and only in the end to be eventually disposed.

In order to improve the actions of prevention of the waste generation and to facilitate the distribution of good practices, the Directive implements requirements for the EU member countries concerning the development of programs for waste generation prevention and defines the aims of their management.

The government of the Republic of Bulgaria itself has adopted a series of legislation documents ratifying the European legislation acts and ensuring sustainable economic development and environmental protection. The Ordinance for Construction Waste Management and the Use of Recycled Construction Materials (OCWM, SG No 98, 2017) is a specific subject of interest. The purpose of the Ordinance is to prevent and limit the risk of environmental pollution as a result of the collection, transportation, and treatment of the construction waste, as well as to encourage the recycling of construction waste that is not dangerous and its use for achieving the objectives of preparing it for reuse, recycling or for other use (OCWM, An. 7, art. 11, §1 - 2, SG No 98, 2017). The targeted quantity for material utilization[1] per type of waste is shown in Table 1:

Table 1
Quantitative targets for material utilisation per type of construction waste

Type of waste	Years			
	2017	2018	2019	2020 and each subseq. year
I. Waste Code				
17 01 01 concrete	85 %	85 %	85 %	85 %
17 01 02 bricks	50 %	57 %	63 %	70 %
17 01 03 roof tiles, tiles, faience and ceramics products	50 %	57 %	63 %	70 %
17 02 01 wood material	70 %	73 %	77 %	80 %
17 02 02 glass	53 %	62 %	71 %	80 %
17 02 03 plastic	63 %	69 %	74 %	80 %
17 04 05 iron and steel	90 %	90 %	90 %	90 %
17 04 01 copper, bronze, brass	90 %	90 %	90 %	90 %
17 04 02 aluminum	90 %	90 %	90 %	90 %
17 04 03 lead	90 %	90 %	90 %	90 %
17 04 04 zinc	90 %	90 %	90 %	90 %
17 04 06 tin	90 %	90 %	90 %	90 %
17 04 11 cables other than those mentioned in the code17 04 10	90 %	90 %	90 %	90 %
17 03 02 asphalt mixtures containing other substances than those mentioned in code 17 03 01	67 %	71 %	76 %	80 %
II. Sector				
Road sector	70 %	73 %	77 %	80 %
Railway sector	70 %	73 %	77 %	80 %

[1] Material utilisation – all operations of the utilsation of construction waste, such as preparation for second use, recycling, and use in reversed earth embankments, excluding the power use and secondary treatment of materials that are used for fuel.

Apart from the aim for material utilisation, there are also targets set for the limitation of the use of natural resources and materials and for their recycling to the highest extent.

Basic principles of the construction waste management

The complete management of construction waste is based on the following principles (*COM (*96*)* 399*,* 1996):

- *Hierarchy of the waste management*

Observing of the hierarchical order of the waste management is one of the most important principles. The sequence of the hierarchy defines the priority order of what represents the best opportunity for the protection of the environment.

- *Self-sufficiency and proximity when managing waste*

The principle suggests for the generated waste to be recycled and used in the community and close to the place where it was generated.

- *Best available techniques*

In the process of waste management, the best available techniques which do not require high expenses must be used.

- *Responsibility of the manufacturer and "the pollutant pays"*

The individuals, who produce or contribute to the production of waste, or pollute the environment, or the current owners of waste must cover the expenses for the waste treatment and manage the waste in a way that guarantees a high level of protection of the environment and the human health.

- *Prevention*

The potential waste problems must be foreseen and avoided at the earliest stage possible.

- *Community participation*

The concerned sides and authorities, as well as the community itself have the opportunity to participate in the development of the waste management plans and the programmes for waste prevention.

Leading practices in construction waste management

The construction waste management covers the complete cycle from waste generation to waste use or disposal. The construction waste is collected, stored, transported, and prepared for disposal separately (WML, SG No 53, 2012).

The activities of collection, storage, and material use of the construction waste may be done right on the construction site, on the site for a construction building removal, and on the site for waste treatment. The first two may be used as sites for material use only upon the wish of the contracting authority and when this has been included in the investment project and in the Plan for Construction Waste Management (PCWM, 2017). The requirements for the activities in collection and material use of the construction waste, as well as for the sites where those activities will be conducted are detailed in the Ordinance on the Management of Construction Waste and on the Use of Recycled Building Materials (OCWM, SG 98, 2017).

Technological processes and equipment in construction waste management

The process of waste management starts from the demolition of buildings and the removal of road surfaces and ends with the use of an already treated waste.

Different technologies are used for the demolition of buildings, and the choice of technology depends on a series of factors, such as type of the building, location, allowed levels of pollution, terms and desired stage of selective waste separation. The basic technologies for the demolition of the buildings include blowing up, power action, combination of a hit, cut, and pull, cutting, water jet cutting, gas-oxygen cutting, etc.

The choice of the suitable technology and equipment may be crucial for the waste separation per type and for the waste separation from the products to be reused. The selective deconstruction and the separate collection and storage of waste on the construction landing are important requirements for the receipt of high quality of the waste fractions which have the potential to be reused, to be recycled, or to be used as construction materials or products.

Depending on the technological processes, the construction waste treatment technologies may be grouped as follows:

Low technological level – technologies for crushing and sieving. The components are separated only by size without the separation of the different kinds of material.

Medium technological level - technologies for crushing, application of a sieve system, and material separation via magnet separation or sorting by hand.

High technological level - technologies for crushing, application of a sieve system, and material separation via more complex methods such as flotation, separation of ferrous and non-ferrous metals, etc.

Depending on the recycling purposes and the ensuing use of the recycled waste, the following types of recycling exist, (HCWM, https://www.moew.government.bg/static/media/ups/tiny/filebase/Waste/cdw/SO_RUKOVODSTVO_FINAL.pdf)

Primary recycling – recycling with the same purpose. For example, road – asphalt coverage which is crashed and melted on spot for a new road surface.

Secondary recycling – use of the recycled waste for a new purpose. For example, secondary use of recycled asphalt as a base for a new road surface.

Tertiary recycling – crashing of a synthetic product for the production of another one.

Quaternary recycling – transformation of raw materials into energy. For example, burning of synthetic materials and paper.

The primary and the secondary recycling methods for the recycling of construction waste are applied in Bulgaria. The level of recycling ability of the construction waste depends on a series of factors, such as level of treatment in advance, dangerous substances pollution, diversity of the waste, etc. The recycling process is done on specialised sites for recycling or directly on the construction site or on the demolition sites. The equipment may be stationary, semi-stationary or mobile.

The technological processes in the process of recycling are as follows:

Pre-fragmentation – it is performed with hydraulic scissors or a hammer and aims to reduce the size of the construction waste admitted to the crasher. It is necessary when the particle size is bigger than the entrance of the crasher or when the direct crashing would be ineffective. Concrete and reinforced concrete waste fragmentation is used as well.

Crashing – this may be done in a few steps in order to optimise the process and the workload on the equipment. Crashing is used for the major part of the construction waste, concrete, reinforced concrete, ceramics, asphalt concrete, rock materials, and polymeric construction materials.

Metal removal – this technology is applied for the reinforced concrete waste after crashing. For the purpose, magnet separators are used which remove the prestressing steel.

Sieving/fractioning – it may be performed at each level of recycling depending on the type of waste. It aims to remove the unwanted impurities or separates infractions with different size of the grain. Vibration sifters from metal nets or perforated plates are most commonly used for these purposes. The method is applicable to all kinds of construction waste.

Additional cleaning – this aims to remove unwanted impurities (for example, dust fraction on the grains of the recycled concrete since it may limit its application as an additional material). The cleaning is done via aeration or flotation.

Diagram 1 represents the technological process involved in the recycling of some types of construction waste. Every site has an incoming inspection system which ensures examination and separation of the waste, as well as waste weighing. Under Article 35 from the WML Waste Management Law, the separated waste mat that cannot be recycled on the site is recovered or submitted to the individuals who own the necessary permits for waste treatment (WML, SG No 53, art.

35, 2012). The waste suitable for recycling is crashed in jaw or rotor crushers. If necessary, the waste may be fractioned in advanced. The crasher is most commonly equipped with a magnet separator that separates metal elements such as the prestressing steel from the reinforced concrete waste. The separated metal elements are submitted to the individuals owing the respective permits for working with such waste (WML, 2012). After crushing, the waste passes through a sifter system where it is separated in different fractures. Each fracture is stored independently and after that is recovered via implementation in embankments or construction materials (for example, the recycled concrete fractions may be used for the same purpose as the natural materials: from embankment materials to supplementary materials for concrete and asphalt).

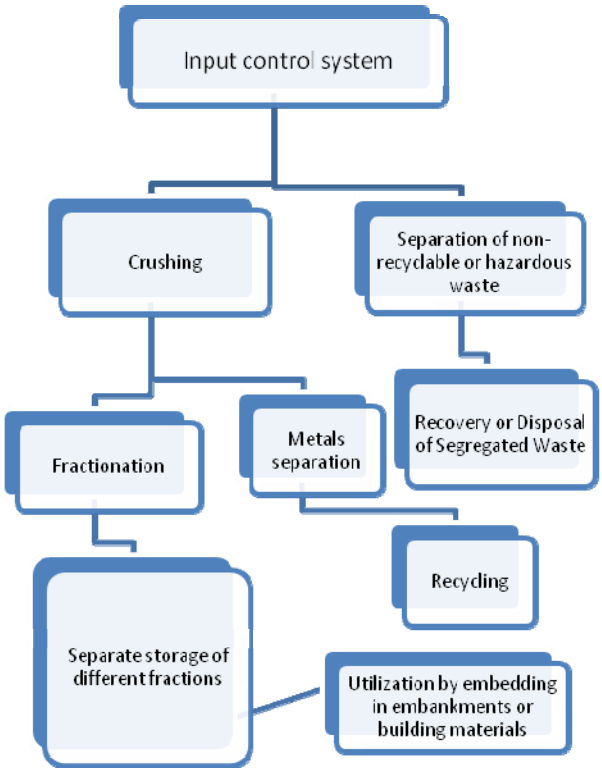

Diagram 1. Technological process involved in the recycling of some types of construction waste.

Options for the use of recycled construction waste

The recycled materials may be used in the following activities (HCWM, available at:

https://www.moew.government.bg/static/media/ups/tiny/filebase/Waste/cdw/SO_RUKOVODSTVO_FINAL.pdf).

In road construction works – as embankments, road grounds, improvement of the features of the earth bed, drainage works, supplementary materials for low-strength concrete and cement stabilisation, heat and cold recycling for road surfaces, temporary roads, etc.

In the construction of *hydro technical facilities* such as gabions and mattresses, embankments, drainage works, etc.

In the *construction of buildings and facilities* as reversed plumage, drainage works, etc.

The use of the recycled construction materials is legislated by the Regulation (EU) № 305/2011 (2011) of the European Parliament for the definition of harmonised conditions for availability on the construction products markets. In the Republic of Bulgaria, the directive is implemented via the Regulation of the Essential Requirements for the Constructions and the Evaluation of the Compliance of Construction Products (RERCECCP, 2014).

Conclusions

The legislation acts adopted by the European and the Bulgarian legislation set clear frames in the management of the construction waste. They define a hierarchical management order as a basis for the environmental protection and for the limitation of the use of natural resources.

The implementation of the legislative obligations of construction waste management and an increase in the level of their application, as well as the gradual increase in the disposal price are all good prerequisites for the increase of the quantity and the improvement of the quality of the recycled non-construction waste.

References

Communication from the Commission on the Review of the Community Strategy for Waste Management (COM (96) 399 final, 30 July 1996.

Directive 2008/98/EC of the European Parliament and of the Council on waste (Waste Framework Directive), 19 November 2008.

Handbook for construction waste management within the territory of Republic of Bulgaria, Ministry of Environment and Water, (HCWM), available at: https://www.moew.government.bg/static/media/ups/tiny/filebase/Waste/cdw/SO_RUKOVODSTVO_FINAL.pdf, (accessed 03 July 2018)

National strategic plan for the management of the construction & destruction waste of the territory of the Republic of Bulgaria for the period from 2011 to 2020.

Ordinance for Construction Waste Management and the Use of Recycled Construction Materials (OCWM), Annex №9, Article 20, Subparagraph 3, (SG No 98, promulgated 08.12.2017).

Plan for Construction Waste Management under Article 8 from the Ordinance for Waste Management and for the Input of Recycled Construction Materials (PCWM) (promulgated SG No 98, 08.12.2017).

Regulation (EU) No 305/2011 of the European Parliament and of the Council laying down harmonized conditions for the marketing of construction products, 9 March, 2011.

Regulation of the Essential Requirements for the Constructions and the Evaluation of the Compliance of Construction Products (RERCECCP), (promulgated SG No 106/2006, amended 2014).

Waste Management Law (WML), (promulgated SG No 53 of 13 July 2012.

ELECTRICITY GENERATION IN MICROBIAL FUEL CELLS BY MEANS OF DIFFERENT MICROORGANISMS

M. Nikolova[1] , I. Spasova[1], S. Groudev[1], P. Georgiev[1] ,V. Groudeva[2]

[1] University of Mining and Geology "St. Ivan Rilski", Sofia 1700, Bulgaria
[2] Sofia University "St. Kliment Ohridski", Sofia 1000, Bulgaria

ABSTRACT. Waters polluted with iron and some non-ferrous metals (Cu, Zn, Co) were subjected to treatment by means of permeable reactive multibarrier. The effluents from the multibarrier contained the metals in much lower concentrations but were enriched in dissolved organic compounds and contained anaerobic microorganisms from different physiological groups: mixed populations of mesophilic sulphate-reducing bacteria, mainly from the genera *Desulfovibrio, Desulfobacter,* and *Desulfomonas*; mixed populations of mesophilic iron-reducing bacteria of the genera *Geobacter* and *Shewanella*; mixed populations of mesophilic fermenting bacteria, mainly from the genera *Bacillus, Pseudomonas* and *Clostridium*. The electricity generated by these microorganisms in a two-section fuel cell varied from 14 to 510 mW/m^2.

Keywords: acid drainage, microorganisms, electricity generation

ГЕНЕРИРАНЕ НА ЕЛЕКТРИЧЕСТВО В МИКРОБНА ГОРИВНА КЛЕТКА ЧРЕЗ РАЗЛИЧНИ МИКРООРГАНИЗМИ

М. Николова[1], И. Спасова[1], С. Грудев[1], П. Георгиев[1], В. Грудева[2]
[1] Минно геоложки университет „Св. Иван Рилски", София 1700, България
[2] Софийски университет „Св. Климент Охридски", София 1000, България

РЕЗЮМЕ. Води, замърсени с желязо и някои цветни метали (Cu, Zn, Co) бяха подложени на обработка посредством пропусклива реактивна мултибариера. Разтворите, изтичащи от мултибариерата съдържаха метали в много по-ниски концентрации, но бяха обогатени на разтворени органични съединения и съдържаха анаеробни микроорганизми от различни физиологични групи: смесени популации на мезофилни сулфат-редуциращи бактерии, основно от родовете *Desulfovibrio, Desulfobacter* и *Desulfomonas*; смесени популации на мезофилни редуциращи желязо бактерии от родовете *Geobacter* и *Shewanella*; смесени популации на мезофилни ферментиращи бактерии, главно от родовете *Bacillus*, *Pseudomonas* и *Clostridium*. Електроенергията, генерирана от тези микроорганизми в дву-секционната горивна клетка, вариране от 14 до 510 mW/m^2.

Ключови думи: кисели дренажни води, микроорганизми, генериране на електричество

Introduction

The treatment of polluted waters, including such containing very toxic elements (heavy metals, radionuclides, arsenic), by means of different passive systems has considerably increased in the past years due to its effectiveness and the acceptable economic evaluation. In most cases, such treatment is performed by means of permeable reactive multibarriers of different types. The effluents from the multibarriers usually contain the heavy metals and other toxic elements in much lower concentrations than the waters subjected to cleaning but are usually enriched in dissolved biodegradable organic compounds. Furthermore, the microflora of the treated waters usually contains various anaerobic microorganisms most of which participate in the process of water cleaning. Such waters and their microbial inhabitants are very suitable for electricity generation by means of microbial fuel cells (Barton and Fauque, 2007; Carver et al., 2011; Dopson and Johnson, 2012; Loveley, 2008).

The present paper contains data about the treatment of waters polluted with iron and some non-ferrous metals by means of permeable reactive multibarriers inhabited by different anaerobic microorganisms from different physiological groups: mixed populations of mesophilic sulphate-reducing bacteria, mixed populations of mesophilic iron-reducing bacteria, and mixed populations of mesophilic fermenting bacteria (all of them were most active at about 37^{o}C); a mixed population of moderate thermophilic sulphate-reducing bacteria from the genus *Thermosulpobacterium* with an optimum temperature of about 55^{o}C, and mixed populations of extreme thermophilic archaea from the genus *Archaeoglobus* with an optimum temperature of about 86^{o}C. All these microorganisms were used in experiments for electricity generation by means of microbial fuel cells at the optimum temperatures relevant for each of them.

Materials and Methods

Acid drainage waters polluted with iron and some non-ferrous metals (mainly Cu, Zn, Cd) were subjected to treatment by means of permeable reactive multibarriers. The multibarriers were plastic cylindrical columns 120 cm high, with an internal diameter of 30 cm. Three columns of this type were filled with a mixture of limestone (crushed to particle size of minus 10 mm) and biodegradable organic matter consisting of

spent mushroom compost, fresh leaf compost, animal manure and saw dust. The columns were inoculated by water and soil samples inhabited by their relevant viable microflora. This microflora contained different anaerobic microorganisms: mixed populations of mesophilic sulphate-reducing bacteria, mixed populations of mesophilic iron-reducing bacteria, mixed populations of mesophilic bacteria fermenting different organic substrates, a mixed population of moderate thermophilic sulphate-reducing bacteria, and mixed populations of extreme thermophilic archaea.

Apart from the experiments on the isolation of natural representatives of microorganisms suitable for testing their ability to generate electricity, some already selected electrochemically active microorganisms were also used in this investigation. The microorganisms were added to a nutrient solution containing some biologically essential elements mentioned in the well-known 9 K nutrient medium (Silverman and Lundgren, 1959) but also containing various combinations of soluble biodegradable organic compounds, vitamins, and trace elements. Such solutions were subjected to continuous-flow circulation from the inlet to the outlet of the microbial fuel cells used for electricity generation.

The microbial fuel cells used in these investigations were of the type already efficiently used in other projects connected with the microbial generation of electricity. The cells were Plexiglas cylindrical columns 80 cm high, with an internal diameter of 12 cm. A perforated slab graphite-Mn^{4+} anode and a graphite-Fe^{3+} cathode were located in the bottom and in the top sections of the column, respectively. The two sections were separated by a permeable barrier of 5 cm thickness consisting of a 2.5 cm layer of glass wool and a 2.5 cm layer of glass beads. The feed stream containing the potential energy sources for the microorganisms was supplied to the bottom anodic section of the column and the effluents passed through the cathode section and continuously exited at the top. Biodegradable organic substrates of different types (proteins, lipids, sugars added separately or in different combinations) were used in these studies. Air was injected during the treatment to the cathode section.

Elemental analysis was done by atomic adsorption spectrometry and inductively coupled plasma spectrometry. The isolation, identification and enumeration of microorganisms were carried out by means of the classical physiological and biochemical tests (Karavaiko et al., 1988) and by the molecular PCR methods (Sanz and Köchling, 2007; Escobar et al., 2008).

Results and Discussion

The treatment of the polluted acid drainage by means of the permeable reactive multibarrier was very efficient for removing the heavy metals and, at the same time, was connected with a considerable increase in the content of biodegradable organic compounds in the waters treated in this manner (Table 1). This increase was due to the biodegradation of the initial organic matter present in the multibarriers by means of the different heterotrophic microorganisms inhabiting the multibarriers and acting at different temperatures. The microflora in the multibarrier maintained at 37°C consisted mainly of mesophilic sulphate-reducing and iron-reducing bacteria but several fermenting heterotrophic bacteria (mainly of the genera *Bacillus*, *Pseudomonas* and *Clostridium*) were also present in relatively high concentrations (within 10^3 – 10^5 cells/ml).

Table 1.
Data about the polluted waters before and after the treatment by means of different microorganisms

Parameters	Before treatment	After treatment		
		at 37°C	at 55°C	at 86 °C
pH	1.45 - 3.50	6.80 - 7.25	6.95 - 7.40	6.90 - 7.53
Eh, mV	(+370)-(+550)	(-170)-(-280)	(-175)-(-260)	(-170)-(-250)
TDS, mg/l	3520 - 5720	590 - 1380	530 - 1250	510 - 1340
Diss. O_2, mg/l	1.0 – 2.1	0.1 – 0.2	0.1	0.1 – 0.3
Diss. org. C, mg/l	1.7 – 3.5	240 - 460	230 - 450	250 - 410
Sulphate, mg/l	590 – 1850	190 - 320	250 - 440	260 - 480
Cu, mg/l	8.2 – 28	<0.1 – 0.5	<0.1 - 0.2	<0.1 - 0.3
Zn, mg/l	14 – 32	<0.1 – 0.4	<0.1 - 0.3	<0.1 - 0.3
Co, mg/l	2.8 – 12	<0.1 – 0.3	<0.1 - 0.3	<0.1 - 0.3
Cd, mg/l	0.1 – 0.5	<0.02	<0.01 - 0.03	<0.01 - 0.03
Mn, mg/l	10 – 23	0.3 – 0.5	0.2 - 0.3	0.2 - 0.3
Fe, mg/l	550 - 1670	5.1 - 8.2	<5	<5

With respect to the electricity generation among the various mesophilic bacteria tested in this study, the most active were some mesophilic sulphate-reducing bacteria (Table 2). It must be noted, however, that the different strains related to one and the same taxonomic species can differ considerably from each other with respect to their ability to generate electricity (in fuel cells of this type, at least). The efficiency of the mixed cultures of sulphate-reducing bacteria consisting from representatives of different species of such bacteria was also variable within a large range. Some strains of the *Desulfovibrio desulfuricans* and *Desulfobulbus elongatus* were the most active with respect to electricity generation not only among the sulphate-reducing bacteria but also among all microorganisms tested in this study.

Table 2.
Electricity generation by means of mesophilic sulphate-reducing bacteria

Sulphate-reducing bacteria	Power, mW/m^2
Desulfovibrio desulfuricans	203 – 510
Desulfobacter multivorans	125 – 404
Desulfobulbus elongatus	174 – 425
Desulfotomaculum nigrificans	65 – 212
Desulfococcus postgatei	25 – 170
Desulfosarcina variabilis	14 – 95
Mixed cultures	105 – 475

Note: Treatnment at 37°C.

Some of the iron-reducing bacteria were also very active with respect to their ability to generate electricity (Table 3). The different taxonomic species related to the genera *Shewanella* and *Geobacter* included strains quite different with respect to this ability. It must be noted, however, that some of the mixed cultures consisting of different species of iron-reducing bacteria were the most active among all strains and species from the two genera used in this study.

Table 3.
Electricity generation by means of mesophilic iron-reducing bacteria

Iron-reducing bacteria	Power, mW/m^2
Shewanella loihica	170 – 321
S. odeinensis	154 – 335
S. putrefaciens	20 – 215
S. alga	95 – 190
Geobacter metallireducens	161 – 212
G. ferrireducens	140 – 192
G. sulfurreducens	91 – 132
G. hydrogenofilus	48 – 97
Mixed cultures	125 – 325

Note: Treatnment at 37^{o}C.

As a whole, the electricity generation by means of different species, strains and mixed cultures of moderate thermophilic sulphate-reducing bacteria at 55^{o}C (Table 4) was lower in comparison with the electricity generation by means of mesophilic bacteria at 37^{o}C. However, it must be noted that the numbers of microbial species and strains of the mesophilic bacteria used in this study were much higher than the relevant numbers connected with the moderate thermophilic sulphate-reducing bacteria used.

Table 4.
Electricity generation by means of moderate sulphate-reducing bacteria

Sulphate-reducing bacteria	Power, mW/m^2
Thermodesulfobacterium sp.	55 – 170
T. commune	68 – 194
T. mobilis	51 – 212
Mixed cultures	86 – 280

Note: Treatnment at 55^{o}C.

The electricity generation by means of sulphate-reducing archaea at 86^{o}C was also lower (Table 5) than that achieved at 37^{o}C by means of the mesophilic sulphate-reducing bacteria. A serious reason for this is probably the same one mentioned above: about the comparative data obtained by means of the mesophilic and moderate thermophilic bacteria (i.e. the much lower number of investigations on the electricity generation by means of thermophilic microorganisms performed until now in comparison with that performed by means of mesophiles).

Table 5.
Electricity generation by means of moderate sulphate-reducing bacteria

Sulphate-reducing bacteria	Power, mW/m^2
Thermodesulfobacterium sp.	120 – 235
T. commune	73 – 203
T. mobilis	60 – 187
Mixed cultures	51 – 210

Note: Treatnment at 86^{o}C.

Acknowledgements: *The authors express their gratitude to the National Science Fund of Bulgaria for the financial support connected with this study (Project T02/2/2014).*

References

Barton, L. L., Fauque, G. D. M, 2009. Biochemistry, physiology and biotechnology of sulphate-reducing bacteria, Adv. Microbiol., 68, 41 – 48.

Carver, S. M., Vuoriranta, P., Tuovinen, O.H., 2011. A thermophilic microbial fuel cell design, J. Power Sources, 196, 3757 – 3760.

Dopson, M., Johnson, D., 2012. Biodiversity, metabolism and applications of acidophilic sulfur-metabolizing microorganisms, Environ. Microbiol., 14, 2620 – 2631.

Escobar, B., Bustos K., Morales, G., Salazar, O., 2008. Rapid and specific detection of *Acidithiobacillus ferrooxidans* and *Leptospirillum ferrooxidans* by PCR, Hydrometallurgy, 92, 102 – 106.

Karavaiko, G.I., Rossi, G., Agate, A.D., Groudev, S.N., Avakyan, Z.A. (eds.), Biogeotechnology of Metals. Mannual GKNT Center for International Projects, Moscow, 1988.

Lovely, D. R. 2008. The microbe electric conversation of organic matter to electricity, Current Opinion in Biotechnology, 19, 1 – 8.

Sanz, J. L., Köchling, T., 2007. Molecular biology techniques used in wastewater treatment: An overview. Process Biochemistry, 42, 119–133.

MICROBIAL PRE-TREATMENT OF A GOLD-BEARING FLOTATION PYRITE CONCENTRATE BY MEANS OF MESOPHILIC AND MODERATE THERMOPHILIC BACTERIA AND BY EXTREME THERMOPHILIC ARCHAEA

Irena Spasova[1], Marina Nikolova[1], Plamen Georgiev[1], Stoyan Groudev[1]

[1]University of Mining and Geology "St. Ivan Rilski", 1700 Sofia, spasova@mgu.bg

ABSTRACT. A gold-bearing flotation pyrite concentrate containing 23 g/t gold and 875 g/t silver as the most valuable components was subjected to microbial pre-treatment to liberate the precious metals from the sulphide matrix and to expose them for the subsequent extraction by means of suitable agents (thiosulphate, microbial protein hydrolysate, cyanide). The concentrate pre-treatment was performed initially in Erlenmeyer flasks and then in agitated bioreactors by means of different microorganisms: mesophilic and moderate thermophilic bacteria at 37 and 50 – 55°C, respectively, as well as by means of extreme thermophilic archaea at 75 – 90°C. The highest extractions of gold and silver (over 90%) from the pre-treated concentrate were achieved by means of moderate thermophilic bacteria at 10 – 15% pulp density, and by the extreme thermophilic archaea at pulp densities of 10%. The mesophilic bacteria were efficient for the concentrate pre-treatment at pulp density of 20%.

Key words: gold; sulphide concentrate; microbial pre-treatment; chemolithothrophs

ПРЕДВАРИТЕЛНО МИКРОБНО ТРЕТИРАНЕ НА ЗЛАТОНОСЕН, ПИРИТЕН ФЛОТАЦИОНЕН КОНЦЕНТРАТ ПОСРЕДСТВОМ РАЗЛИЧНИ МИКРООРГАНИЗМИ

Ирена Спасова[1], Марина Николова[1], Пламен Георгиев[1], Стоян Грудев[1]

[1]Минно-геоложки университет "Св. Иван Рилски", 1700 София, spasova@mgu.bg

РЕЗЮМЕ. Златоносен пиритен флотационен концентрат, съдържащ 23 g/t злато и 857 g/t сребро, бе подложен на микробиологично въздействие с цел разкриване на благородните метали от сулфидната матрица и последваща екстракция чрез различни агенти (тиосулфат, микробен белтъчен хидролизат, цианид). Предварителната обработка беше извършена в Ерленмайерови колби и след това в биореактори с разбъркване, посредством различни микроорганизми: мезофилни и умерени термофилни бактерии съответно при 37 и 50 – 55°C, както и чрез екстремни термофилни археи при 75 – 90° C. Най-висока екстракция на злато и сребро (над 90 %) от третирания концентрат бе постигната при използване на умерени термофилни бактерии при 10 – 15 % плътност на пулпа и при екстремни термофилни археи при плътност на пулпа 10%. Мезофилните бактерии бяха ефикасни при третиране на концентрата при 20% плътност на пулпа.

Ключови думи*: злато, сулфиден концентрат, микробиологично третиране, хемолитотрофи*

Introduction

The microbial pre-treatment of gold-bearing sulphide concentrates is a well-known and largely applied technological approach to liberate the gold (and silver) from the sulphide matrix and to make these precious metals accessible for the subsequent extraction by means of suitable reagents (mainly by cyanides but also by some relatively non-toxic reagents such as thiourea and thiosulphate). In most cases, these precious metals are present in pyrite and arsenopyrite but sometimes parts of them are present in other sulphides such as chalcopyrite and galena. Furthermore, it is well-known that considerable portions of other rare and expensive elements are also present in sulphides, including in the pyrite and arsenopyrite. This increases the interest in the application of the microbial pre-treatment as an efficient and economically acceptable way to facilitate the recovery of these elements from the relevant sulphides. At present, different species of chemolithotrophic bacteria and archaea are used in such investigations and even under industrial conditions characterised by microbial pre-treatment of the relevant mineral substrata at pulp densities from 10 to 30% and temperatures from 35 to 90°C (Brierley, 1995; Lawrence and Bruynesteyn, 1983; Lazer et al., 1986; Groudev et al., 1995. 1996; Wan and Brierley, 1997).

This paper contains data about investigations on the microbial pre-treatment of a gold-bearing pyrite concentrate performed under different conditions (with respect to the temperature and pulp density) by means of different microorganisms (mesophilic and moderate thermophilic bacteria at 37 and 50–55°C, respectively, and extreme thermophilic archaea at 75 and 90°C) at pulp densities from 10 to 30%.

Materials and Methods

Data about the chemical composition of the flotation concentrate used in this study are shown in Table 1. Data about the phase composition of the precious metals in the concentrate are shown in Table 2.

Table 1.
Data about the chemical composition of the flotation concentrate used in this study

Component	Content, %	Component	Content, %
S total	5.90	Zn	0.17
S sulphidic	5.14	Pb	6.10
Fe	7.10	Au	23 g/t
Cu	1.70	Ag	875 g/t

Table 2.
Phase composition of the precious metals in the concentrate

Phases	Au	Ag
	Distribution, %	
Free metal	10.7	-
Metal encapsulated in iron oxides	30.2	35.0
Metal finely dispersed in sulphide minerals	54.5	60.2
Metal finely dispersed in silicates	4.6	4.8
Total	100.0	100.0

The microbial pre-treatment of the concentrate was performed initially in Erlenmayer flasks and then in agitated bioreactors with a 1.0 l working volume by means of different chemolithotrphs able to oxidize the sulphide minerals. The pretreatment was performed in 9K nutrient medium (Silverman and Lundgren, 1959) containing the concentrate in pulp densities from 10 to 30%. The duration of the pre-treatment was up to 7 days (168 hours) at the temperature relevant for the different microorganisms: at 37 and 50–55^{o}C for the mesophilic and moderate thermophilic bacteria, respectively, and at 75 and 90^{o}C for the extreme thermophilic archaea.

The leaching of the initial concentrate and of the concentrate pre-treated by means of microorganisms was performed by means of different reagents: microbial protein hydrolisate in the presence of $KMnO_4$ or H_2O_2 in concentrations of 5 g/l each; ammonium thiosulphate in a concentration of 10 g/l in the presence of copper ions (0.5 – 1.0 g/l); and sodium cyanide.

Elemental analysis of the waters was performed by atomic absorption spectrometry and by inductively coupled plasma spectrometry.

The isolation, indentification, and enumeration of microorganisms were carried out by the classical physiological and biochemical tests (Karavaiko et al., 1988) and by the molecular PCR methods (Escobar et al., 2008; Sanz and Köchling, 2007).

Results and Discussion

The direct chemical leaching of the precious metals from the concentrate, i.e. without its pretreatment by means of the microbial oxidation, was not efficient (only 12.0% of the gold and 6.2% of the silver were extracted in this way) (Table 3). At the same time, the levels of extraction of the precious metals from the concentrate subjected to microbial pretreatment before the leaching was very efficient (the same table). It was found that the level of sulphide oxidation higher than 35% during the pretreatment was sufficient to extract more than 95% of the gold and more than 90% of the silver during the subsequent chemical leaching.

Table 3.
Leaching of precious metals from the flotation concentrate by means of different reagents before and after its pre-treatment by means of microbial oxidation

Leach solution	Initial concentrate		Pre-treated concentrate	
	Au	Ag	Au	Ag
	Extraction, %			
Protein hydrolysate	10.9	8.6	16.4	12.2
Protein hydrolysate + chemical oxidiser:				
- $KMnO_4$	40.1	32.3	90.7	85.2
- H_2O_2	30.7	24.5	86.2	84.0
Thiosulphate	46.4	34.7	90.5	88.4
NaCN	48.0	37.4	91.4	89.1

It is known that the different chemolithotrophic microorganisms attack the defect sites in the relevant mineral structures preferentially. However, the rates of oxidation by the different microbial species and even by the different strains related to one and the same taxonomic species can be quite different. In this study, the rates of microbial oxidation during the concentrate pretreatment by means of the extreme thermophilic archaea were the highest in comparison with the oxidation rates achieved by means of the moderate thermophilic and by means of the mesophilic bacteria. However, these rates were achieved during the pre-treatment performed at the relatively low pulp densities (10 – 15%) of the concentrate (Table 4).

Table 4.
Effect of the pulp density of the concentrate pre-treated by means of different microorganisms on the efficiency of the subsequent extraction of the precious metals

Pre-treatment by means of different microorganisms	Pulp density, %					
	10		15		20	
	Extraction, %					
	Au	Ag	Au	Ag	Au	Ag
Mesophilic bacteria	95.0	91.4	94.1	90.5	92.3	88.0
Moderate thermophilic bacteria	97.2	92.0	95.0	90.9	90.5	88.5
Extreme thermophilic archaea	95.2	90.5	90.1	89.4	88.5	87.5

The highest rates of pre-treatment at the highest pulp densities (20 – 30%) were achieved by means of the moderate thermophilic bacteria. It must be noted, however, that the rates of microbial pre-treatment, i.e. the rates of microbial sulphide oxidation, at these highest pulp densities were lower than those achieved at pulp densities of about 15%.

The data obtained during this study revealed that the efficient pre-treatment of the gold-bearing sulphide concentrates can be achieved by means of selected chemolithotrophic microorganisms from the three essential groups based on their optimum temperatures for growth and oxidative activity, i.e. by means of mesophilic and moderate thermophilic bacteria and by means of extreme thermophilic archaea. However, it must be noted that each of these three groups of microorganisms contains strains which can be quite different from each other with respect to many of their essential properties. Furthermore, the conditions used during the concentrate pre-treatment, especially such as the optimum temperature for the microbial growth and activity, the optimum pulp density, as well as the character of all specific properties of the relevant gold-bearing sulphide concentrate, are essential for the efficiency and the real economic effect connected with the activity of this type.

References

Brierley, C. Bacterial oxidation. Master key to unlock refractory gold ores? Engineering and Mining Journal, May, 1995. - 42–44.

Escobar, B., Bustos, K., Morales, G., Slazar, O., Rapid and specific detection pf Acidithiobacillus ferrooxidans and Leptospirillum ferrooxidans by PCR, Hydrometallurgy, 2008. 92, -102–106.

Groudev, S. N., Spasova, I. I., Ivanov, I. M., Microbial leaching of gold from refractory pyrite ore, In: VI Balkan conference on Mineral Processing, Ohrid – Macedonia, September 18 – 22, 1995.

Groudev, S. N., Spasova, I. I., Ivanov, I. M., Two-stage microbial leaching of a refractory gold-bearing pyrite ore, Mineral Engineering, 9 (7), 1996. - 707–713.

Karavaiko, G. I., Rossi, G., Agate, A. D., Groudev, S. N., Avakyan, Z. A., (eds). *Biogeotechnology of Metals. Manual,* GKNT Center for International Projects, Moscow, 1988.

Lawrence, R. W., Bruynesteyn, A., Biolocal preoxidation to enhance gold and silver recovery from refractory pyretic ores and concentrates, CIM Buletin, 76 (857), 1983. - 107.

Lazer, M. J., Southwood, M. J., Southwood, A. J., The release of refractory gold from sulphide minerals during bacterial leaching. In: Gold 100, Proceedings of the International Conference on Gold, SAIMM, Johannesburg, South Africa, vol.2, 1986. - 287-297.

Sanz, J. L., Köchling, T., Molecular biology techniques used in waste water treatment: an overview, Process Biochemistry, 42, 2007. - 119–133.

Silverman, M. P., Lundgren, D. G., Studies on the chemoautotrophic iron bacterium Ferrobacillus ferrooxidans, J. Bacteriol., 77, 1958. - 642–647.

Wan, R. Y., Brierley, J. A., Thiosulphate leaching following biooxidation pretreatment for gold recovery from refractory carbonaceous–sulfidic ore, Mining Engineering, August, 1997. - 76–80.

THE EFFECT OF THE PULP DENSITY OF A COPPER SLAG ON THE EFFICIENCY OF ITS BIOLEACHING BY MEANS OF DIFFERENT MICROORGANISMS

P. Georgiev[1] , M. Nikolova[1] , I. Spasova[1], S. Groudev[1], V. Groudeva[2]

[1] University of Mining and Geology "St. Ivan Rilski", Sofia 1700, Bulgaria
[2] Sofia University "St. Climent Ohridski", Sofia 1000, Bulgaria

ABSTRACT. Copper slag containing 0.62% Cu, 1.07% Zn, 0.08% Co, and 32.5% Fe as the most essential components was subjected to leaching by means of different chemolithotrophic microorganisms at different temperatures (from 35 to 90°C). The bioleaching was carried out by the shake-flask technique at different pulp densities (from 5 to 30%) of slag crushed to minus 100 microns. The highest rates of extraction of the non-ferrous metals and iron were achieved by means of some extreme thermophilic archaea (of the genera *Sulfolobus, Thermoplasma, Acidianus*, and *Metallosphaera*) at relatively low pulp densities (5–8% at 90°C and 10–15% at 75°C). The highest extractions by the moderate thermophilic bacteria (of the genera *Sulfobacillus, Alicyclobacillus*, and *Acidimicrobium)* were achieved at 55°C with pulp densities of 15–20%. The mesophilic bacteria (from the genera *Acidithiobacillus* and *Leptospirillum*) were efficient at 35–37°C at relatively high pulp densities (of 15–25%).

Keywords: copper slag, chemolithotrophs, leaching, valuable metals

ВЛИЯНИЕ НА ПЛЪТНОСТТА НА ПУЛПА ВЪРХУ ЕФЕКТИВНОСТТА НА БИОЛОГИЧНОТО ИЗЛУГВАНЕ НА МЕДНА ШЛАКА ПРИ ИЗПОЛЗВАНЕ НА РАЗЛИЧНИ МИКРООРГАНИЗМИ

П. Георгиев[1], М. Николова[1], И. Спасова[1], С. Грудев[1], В Грудева[2]

[1] Минно геоложки университет „Св. Иван Рилски", София 1700, България
[2] Софийски университет „Св. Климент Охридски", София 1000, България

РЕЗЮМЕ. Медна шлака, съдържаща 0.62% Cu, 1.07% Zn, 0.08% Co и 32.5% Fe, като най-важни компоненти, беше подложена на излугване с помощта на различни хемолитотрофни микроорганизми при различни температури (от 35 до 90 °C). Биологичното излугване бе проведено в колби на шейкър при различна плътност на пулпа (от 5 до 30%) с шлаки с едрина до минус 100 микрона. Най-високите скорости на извличане на цветните метали и желязото бяха постигнати чрез екстремни термофилни археи (от родовете *Sulfolobus, Thermoplasma, Acidianus* и *Metallosphaera*) при относително ниска плътност на пулпа (5-8% при 90 °C и 10-15% при 75°C). Най-високо извличане от умерените термофилни бактерии (от родовете *Sulfobacillus, Alicyclobacillus* и *Acidimicrobium*) бе постигнато при 55°C и плътност на пулпа от 15-20%. Мезофилни бактерии (от родовете *Acidithiobacillus* и *Leptospirillum*) бяха ефикасни при 35-37°C и при относително високи плътности на пулпа (от 15-25%).

Ключови думи: медна шлака, хемолитотрофи, излугване, ценни метали

Introduction

The pyrometallurgical slags, mainly these from the copper recovery, are wastes containing considerable quantities of valuable components, mainly non-ferrous metals (especially copper, zinc, and cobalt) but also iron and manganese, aluminum and silicon. At present, the slags are used mainly in the construction of roads and for the preparation of cements of different types. However, the investigations on the possibilities to extract the different more valuable components of the slags, especially the non-ferrous metals, as real commercial-scale products, are steadily increasing in numbers. In this respect, special interest is paid to the possibility to use various chemolithotrophic microorganisms, both bacteria and archaea, to efficiently extract the various metal components of the slags by means of leaching in agitated bioreactors (Panda et al., 2015; Kaksonen et al., 2016; Potysz et al., 2016; Georgiev et al., 2017; Spasova et al., 2017). Such treatment is performed on finely ground slags present in the relevant optimum concentrations and treated at conditions optimum for the microorganisms (bacteria and archaea) used as the relevant leaching agents. The present paper contains data in this aspect.

Materials and Methods

The slag used in this study contained 0.62% Cu, 1.07% Zn, 0.08% Co, 0.09% Mn, 2.91% Al, 32,5% Fe, 1.90% S, and 16.3% Si as the most essential components of the chemical composition. The fayalite (Fe_2SiO_4) and diopside ($CaMgSi_2O_6$) were the main mineral phases in the slag but some oxides, mainly of iron, such as hematite (Fe_2O_3) and magnetite (Fe_3O_4), were also present, as well as some plagioclases, quartz and calcite. The content of pyrite (FeS_2) was relatively low but considerable portions of the non-ferrous metals were present as the relevant sulphides. Copper was present mainly in sulphides (bornite, covellite, and chalcopyrite) but also in oxides and as its elemental form (Cu^0). Zinc was present as the relevant oxide (ZnO) but also in its own elemental form (Zn^0).

The bioleaching of the slags was performed by means of microorganisms related to three different groups on the basis of the optimum temperature for their growth and activity: mesophilic bacteria of the genera *Acidithiobacillus* and *Leptospirillum*, as well as an archaeon related to the genus *Ferroplasma*, all tested at their optimum temperatures of 30–37°C; moderate thermophilic bacteria, with temperature optimum within 50–60°C; and extreme thermophilic archaea, with temperature optimum of 65–80°C but able to grow and active even at higher temperatures.

The comparative experiments for the leaching of the slag were performed in 9K nutrient medium using some components of the slag (ferrous iron and sulphidic sulphur) as energy sources. However, in some experiments, Fe^{2+} (in the form of ferrous sulphate) and sulphur (in its elemental form) were also added as energy sources.

The bioleaching was performed in agitated Erlenmeyer flasks of 300 ml volume each containing 100 ml leach solution inoculated by microorganisms and slag with a particle size of minus 100 microns added in quantities to form pulp densities from 5 to 30%. Aeration by air enriched with CO_2 to 0.10–0.20% was used in some of the tests.

The activity of some microbial strains from the different taxonomic species was increased to some extent by means of consecutive cultivations in the nutrient medium 9K supplied by slag with a step-by-step increasing of the relevant pulp densities.

In some experiments, the leaching of the slag was performed in agitated bioreactors with a volume of 1 L each. Apart from the batch leaching, such bioreactors were also used for performing the continuous-flow leaching.

Elemental analysis of the liquid samples was performed by atomic absorption spectrometry (AAS) and inductively coupled plasma spectrometry (ICP). The isolation, identification, and enumeration of microorganisms were carried by the classical physiological and biochemical tests and by the molecular PCR methods (Karavaiko et al., 1988; Sanz and Köchling, 2007; Escobar et al., 2008).

Results and Discussion

The level of extraction (in % for 48 hours, i.e. until about the end of the logarithmic growth phase) of the non-ferrous metals from the slag by means of mesophilic bacteria at 37°C decreased with the increase of the pulp density from 10 to 25% (Table 1). At the same time, the rates of extraction of these most valuable components of the slag (present in mg.l/h) were increased to some extent. However, the residual contents of the non-ferrous metals in the slag after the leaching were still quite high, especially in the tests with the higher pulp densities.

The levels of extraction of the non-ferrous metals by means of moderate thermophilic bacteria at 55°C also decreased with the increase of the pulp density from 10 to 20% (Table 2). The best results were achieved by means of *Sulfobacillus thermosulphidooxidans* which possessed both ferrous- and sulphur-oxidizing abilities. However, some of the mixed cultures of moderate thermophilic bacteria, especially such consisting of *S. thermosulphidooxidans* and a strain of *Acidithiobacillus caldus* (not able to oxidize Fe^{2+} but possessing sulphur-oxidizing ability), were very efficient, especially at pulp densities of 10 and 15%.

Table 1.
Bioleaching of slag by means of mesophilic bacteria at 37°C

Pulp density	Components	Extraction, % for 24 h	Rate of extraction, mg/l.h
10%	Cu	82	10.59
	Zn	70	15.60
	Co	87	1.14
15%	Cu	73	14.14
	Zn	62	20.73
	Co	80	1.19
20%	Cu	68	17.56
	Zn	55	24.52
	Co	77	1.71
25%	Cu	60	19.36
	Zn	48	26.74
	Co	71	1.97

Note: The results in the table are obtained by means of a mixed culture consisting of *At. ferrooxidans, L. ferrooxidans*, and *At. thiooxidans.*

Table 2.
Bioleaching of slag by means of moderate thermophilic bacteria at 55°C

Microorganisms	Components	Pulp density, %		
		10	15	20
		Extraction, % for 48 h		
Sulfobacillus thermosulphidooxidans	Cu	88	77	71
	Zn	75	68	60
	Co	91	84	78
Alicyclobacillus tolerans	Cu	84	73	70
	Zn	71	64	59
	Co	88	80	75
Sulfobacillus acidiphilus	Cu	82	70	65
	Zn	73	62	56
	Co	85	80	77
Mixed cultures	Cu	80-88	71-79	71-75
	Zn	71-77	62-68	59-62
	Co	82-90	79-84	73-80

The bioleaching of the slag by means of extreme thermophilic archaea at 75 and even at 86°C (Tables 3 and 4), specifically by means of pure cultures of *Sulfolobus metallicus* and of *Metallosphaera sedula*, as well as by means of some mixed cultures of these two species, was the most efficient during this study. It must be noted, however, that similar results were also achieved by means of mixed cultures of these two species but containing representatives of two additional species (*Thermoplasma acidophilum* and *Acidianus infernus*), especially at pulp densities of 10–12%. However, mixed cultures consisting only of *T. acidophilum* and *Ac. infernus* were not so active.

The economic evaluation of the whole treatment process, starting from the grinding of the slag intended for bioleaching to the optimum particle size (usually minus 100 microns), and the selection and adaptation of the most suitable microbial cultures

intended for leaching of the real slag under the real optimum conditions, are all essential steps in the development of an efficient industrial-scale process of this type.

Table 3.
Bioleaching of slag by means of moderate thermophilic bacteria at 75°C

Microorganisms	Components	Pulp density, %		
		10	15	20
		Extraction, % for 48 h		
Sulfolobus metalicus	Cu	91	90	82
	Zn	80	79	68
	Co	93	91	87
Metallosphaera sedula	Cu	90	89	80
	Zn	80	77	65
	Co	91	89	86
Acidianus infernus	Cu	86	84	77
	Zn	77	73	64
	Co	88	86	82
Mixed cultures	Cu	87-91	86-92	79-84
	Zn	77-82	78-82	68-71
	Co	87-93	88-91	84-88

Table 4.
Bioleaching of slag by means of extreme thermophilic archaea at 86°C

Microorganisms	Components	Pulp density, %	
		5	10
		Extraction, % for 48 h	
Sulfolobus metalicus	Cu	93	91
	Zn	82	80
	Co	95	91
Metallosphaera sedula	Cu	91	89
	Zn	82	80
	Co	93	90
Thermoplasma acidophilium	Cu	93	90
	Zn	84	81
	Co	93	90
Mixed cultures	Cu	88-95	86-91
	Zn	80-86	78-84
	Co	88-93	90-93

References

Escobar, B., Bustos K., Morales, G., Salazar, O., Rapid and specific detection of *Acidithiobacillus ferrooxidans* and *Leptospirrilim ferrooxidans* by PCR, Hydrometallurgy, 92, 2008. - 102–106.

Georgiev, P. S., Spasova, I. I., Groudeva, V. I., Nikolova, M. V., Lazarova, A. I., Iliev, M., Ilieva, R., Groudev, S. N., Bioleaching of valuable components from a pyrometallurgical final slag, In: Solid State Phenomena, Trans Tech Publications, Swithzerland, vol., 262, 2017. - 696–699.

Kaksonen, A. H., Särkijärvi, S., Puhakka, J. A., Peuraniemi, J., Junnikkala, S., Tuovinen, O. H., Chemical and bacterial leaching of metals from a smelter slag in acid solutions, Hydrometallurgy, 159, 2016. - 46–53.

Karavaiko, G. I., Rossi, G., Agate, A. D., Groudev, S. N., Avakyan, Z. A. (eds.), Biogeotechnology of Metals. Mannual, GKNT Center for International Projects, Moscow, 1988.

Panda, S., Mishra, S., Rao, D. S. Pradhan, N., Mohapatsa, U. B., Angadi, S. K., Mishra B. K., Extraction of copper from copper slag: Mineralogical; insights, physical beneficiation and bioleaching studies, Korean J. Chem. Eng., 32 (4), 2015. - 667–676.

Potysz, A., Kiezczak, J., Fuchs, Y., Grybos, M., Guiband G., Lens, P. N. L., van Hullebush, E. D., Bacterially-mediated weathering of crystalline and amorphous Cu-slags, Applied Geochemistry, 64, 2016**. -** 92–106.

Sanz, J. L., Köchling, T., Molecular biology techniques used in wastewater treatment: An overview. Process Biochem.42, 2007. - 119–133.

Spasova, I. I., Groudev, S. N., Georgiev, P. S., Nikolova, M. V., Lazarova, A. I., Bioleaching of copper slags by means of different microbial cultures, In: XIV Int. Congress "Machines, Technologies, Materials", Borovetz, Bulgaria, March 15 – 18, 2017. - 57–58.

ANALYTICAL EXPRESSIONS FOR STRESSES IN STEEPLY STRATIFIED ROCK MASS AROUND AN OPENING IN THE SHAPE OF AN ELLIPSE

Violeta Trifonova-Genova

University of Mining and Geology "St. Ivan Rilski", 1700 Sofia, violeta.trifonova@yahoo.com

ABSTRACT. The article discusses the question of analytically determining stresses around an opening. Its cross-section is an ellipse. The rock mass consists of homogenous, parallel and steep layers. They are isotropic or have the plane of isotropy that is parallel to the stratification. The thickness of layers is greater than the dimensions of the opening. The influence of stresses which is due to the passage of the work extends into the rectangular area around the opening. The specified class of tasks is solved by the methods of two theories: the theory of elasticity and the mechanics of the stratified random.
The approach applied here is to determine the analytical expressions of stresses at random points of two layers. In these expressions, the stresses in a generalised field in polar coordinates are involved.
The obtained analytical results are applied to a real rock mass with layers considered as homogeneous and isotropic environments. A diagram of the normal tangential stresses along the contour of the opening is given.

Keywords: stratified random, theory of elasticity, analytical solution, stress state, opening in the shape of an ellipse.

АНАЛИТИЧНИ ИЗРАЗИ ЗА НАПРЕЖЕНИЯТА В СТРЪМНОНАПЛАСТЕН МАСИВ ОКОЛО ИЗРАБОТКА С ФОРМА НА ЕЛИПСА

Виолета Трифонова-Генова

Минно-геоложки университет "Св. Иван Рилски ", 1700 София, violeta.trifonova@yahoo.com

РЕЗЮМЕ. В статията се разглежда въпросът за аналитично определяне на напреженията около изработка. Нейното напречно сечение е елипса. Масивът се състои от хомогенни, успоредни и стръмни пластове. Те са изотропни или притежават равнина на изотропия, която е успоредна на напластяването. Дебелини на пластовете са по-големи от размерите на изработката. Влиянието на напреженията, дължащо се на прокарване на изработката, се простират в правоъгълна област около отвора. Този вид задачи се решават с методите на теорията на еластичността и механика на напластените среди.
Тук е приложен е подход за определяне на аналитичните изрази за напреженията в произволни точки от два пласта. В тези изрази участват напреженията в обобщена среда в полярни координати. Физико-механичните характеристики на тази среда са функции на същите на всеки пласт.
Получените аналитични резултати са приложени за реален масив с пластове, разгледани като еднородни и изотропни среди. Дадена е диаграмата на нормалните тангенциални напрежения по контура на изработката.

Ключови думи: напластените среди, теория на еластичността, аналитично решение, напрегнато състояние, изработка с форма на елипса.

Introduction

The analytical and numerical methods are applied in calculating the stresses around a circular opening drawn in a stratified rock mass (Trifonova-Genova, 2012; Trifonova-Genova, June 2012; Minchev, 1960). The rock mass consists by homogeneous layers which are parallel to one another and to the axis of the opening. The layer thickness is commensurate with the dimensions of the opening. These thicknesses participate in the analytical expressions for stresses. These expressions are suitable for low sloping layers.

In the case when the layers are steep and their thickness is greater than the dimension of the circular opening, other expressions are offered (Trifonova-Genova, 2017; Trifonova-Genova, 2018).

The present work focuses on obtaining the analytical expressions for stresses around an opening in the shape of an ellipse.

Methods

Formulation of the problem

A horizontal opening with elliptic cross section is drawn at a sufficiently large depth H. The influence on the distribution of stresses does not reach the boundary of the half-plane. The latter is accepted as an infinite linear deformable environment. The width of the opening is $2b$ and the height is $2a$. The influence of the opening on the distribution of stresses encompasses the rectangular area with a width of $12b$ and a height of $12a$. The beginning of the Oxz coordinate system is chosen in the center of the opening. The layers are isotropic or transversally isotropic with the plane of isotropy parallel to the stratification. The plane forms an angle α with the horizontal axis.

Stresses in a generalized field

By the theory described in (Minchev, 1968), the stratified field is replaced by a generalized field with a volume of weight

designed as $\gamma^{(o)}$. When the layers are isotropic, $E^{(o)}$ is Young's modulus and $\mu^{(o)}$ is Poisson's ration (Trifonova-Genova, 2017). If the layers are transversally isotropic, the field is transversally isotropic with two types of physical and mechanical characteristics. The former are in the direction parallel to the plane of isotropy ($E_1^{(o)}$, $\mu_1^{(o)}$), but the latter are in the direction perpendicular to the plane of isotropy ($E_2^{(o)}$, $\mu_2^{(o)}$). These characteristics are expressed for each layer respectively (Trifonova-Genova, 2012; Minchev, 1968).

The task assigned is reduced to the task of the plane theory of elasticity with an opening that is loaded to infinity with the stresses of the undisturbed rock. The complex variable theory is used to obtain the stresses in the generalised field in a polar coordinate system. This theory describes the stresses and the displacements by the complex potentials. The view of them for an isotropic rock mass can be found in (Minchev, 1960; Bulychev, 1982).

The stresses on the contour of the opening are:

$$\sigma_r^{(o)} = 0;$$
$$\tau_{r\theta}^{(o)} = 0; \qquad (1)$$
$$\sigma_\theta^{(o)} = -\gamma^{(o)} H\left[\lambda_1 + \frac{\lambda m + (m_1 + \lambda m_2)\cos 2\theta_*}{1 + m^2 + 2m\cos 2\theta_*}\right],$$

where

$$m_1 = \frac{1+m^2}{2}; \quad m_2 = \frac{1-m^2}{2}; \quad \lambda = \frac{\mu^{(o)}}{1-\mu^{(o)}};$$
$$\lambda_1 = 1+\lambda; \quad m = \frac{a-b}{a+b}; \quad \theta_* = \theta - 90^\circ.$$

Here, r_o and θ are polar coordinates of points on the plane.

Stresses in layers

The layers around the opening in the shape of an ellipse are two (Fig.1). Their thickness is greater than the dimensions of the opening. The rectangular area of influence is loaded by vertical and horizontal stresses (Trifonova-Genova, 2018). There are stresses in the corresponding layers in undamaged rock.

The transformation formulae from an article by Trifonova-Genova (2018) and the opposite of them are used there. The stresses in each layer are expressed by adduced stresses of a generalised field. In the polar coordinate system, these expressions are:

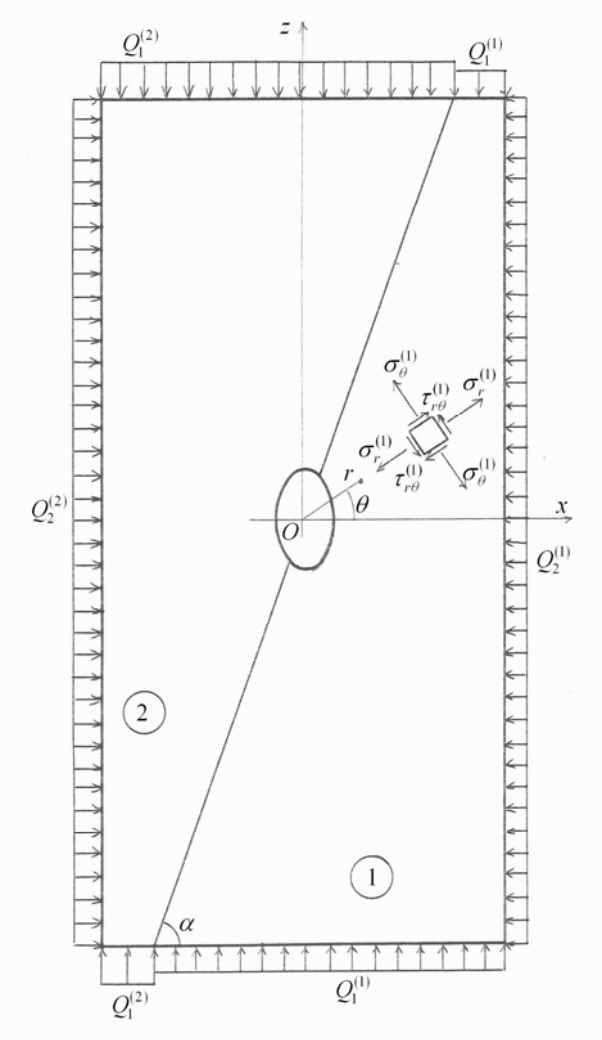

Fig.1. Calculation scheme for determining stresses

$$\sigma_r^{(i)} = T_{11}^{(i)}\sigma_r^{(o)} + T_{12}^{(i)}\sigma_\theta^{(o)} + T_{13}^{(i)}\tau_{r\theta}^{(o)};$$
$$\sigma_\theta^{(i)} = T_{21}^{(i)}\sigma_r^{(o)} + T_{22}^{(i)}\sigma_\theta^{(o)} + T_{23}^{(i)}\tau_{r\theta}^{(o)}; \qquad (2)$$
$$\tau_{r\theta}^{(i)} = T_{31}^{(i)}\sigma_r^{(o)} + T_{32}^{(i)}\sigma_\theta^{(o)} + T_{33}^{(i)}\tau_{r\theta}^{(o)}; \; i = 1.2,$$

where

$$T_{11}^{(i)} = 0.25 s_2^2 B_1^{(i)} + c^4 B_2^{(i)} + s^4 + 0.5 s_2^2;$$
$$T_{12}^{(i)} = c^4 B_1^{(i)} + 0.25 s_2^2 B_2^{(i)} - 0.25 s_2^2;$$
$$T_{13}^{(i)} = s_2 c^2 \left[B_1^{(i)} - B_2^{(i)} + 1\right];$$
$$T_{21}^{(i)} = 0.25 s_2^2 B_{21}^{(i)} + s^4 B_1^{(i)} - 0.25 s_2^2;$$
$$T_{22}^{(i)} = 0.25 s_2^2 B_1^{(i)} + s^4 B_2^{(i)} + c^4 + 0.5 s_2^2;$$
$$T_{23}^{(1)} = s_2 s^2 \left[B_1^{(i)} - B_2^{(i)} + 1\right];$$
$$T_{31}^{(i)} = -s_2 c^2 B_1^{(i)} + c^4 B_2^{(i)} + s^4 + 0.5 s_2 (c_2 - s_2);$$
$$T_{32}^{(i)} = c^4 B_1^{(1)} + 0.25 s_2^2 B_2^{(i)} + 0.5 s_2 s^2;$$
$$T_{33}^{(i)} = s_2 c^2 \left[B_1^{(i)} - B_2^{(i)} + 0.5(1 + c_2^2)\right].$$

In these expressions, the following trigonometric functions are designed with a lower case letter:

$$c^2=\cos^2\beta;\quad s^2=\sin^2\beta;$$
$$s_2=\sin(2\beta);\ c_2=\cos(2\beta);\qquad (3)$$
$$c^4=\cos^4\beta;\quad s_2^2=\sin^2(2\beta);\quad \beta=\theta-\alpha.$$

The coefficients $B_1^{(i)}$ and $B_2^{(i)}$ in expressions (2) are constants, linked to Young's modulus and Poisson's rations. For the isotropic layers, these coefficients are:

$$B_1^{(1)}=A_2.A_{**}.A_*;\quad B_1^{(2)}=-A_1.A_{**}.A_*;$$
$$B_2^{(i)}=A.A_*.E^{(i)};\quad A_*=\left[A_1E^{(1)}+A_2E^{(2)}\right]^{-1};\qquad (4)$$
$$A_{**}=\mu^{(1)}E^{(2)}-\mu^{(2)}E^{(1)},$$

where $E^{(i)}$ is Young's modulus and $\mu^{(i)}$ is Poisson's ration.

When the layers are transversal and isotropic, these coefficients are determined by:

$$B_1^{(1)}=\frac{A_2A_{**}^tE_1^{(1)}E_1^{(2)}}{E_2^{(1)}E_2^{(2)}A_*^t};\ B_1^{(2)}=\frac{-A_1A_{**}^tE_1^{(1)}E_1^{(2)}}{E_2^{(1)}E_2^{(2)}A_*^t};$$
$$B_2^{(1)}=\frac{AE_1^{(1)}}{A_*^t};\quad B_2^{(2)}=\frac{AE_1^{(2)}}{A_*^t};\qquad (5)$$
$$A_{**}^t=-\mu_2^{(2)}E_2^{(1)}+\mu_2^{(1)}E_2^{(2)};\ A_*^t=A_2E_1^{(2)}+A_1E_1^{(1)}.$$

The physical and mechanical characteristics of the layers in expressions (5) are two types. There are the ones that are in the direction parallel to the plane of isotropy and are denoted by an index lower than 1 ($E_1^{(i)}$, $\mu_1^{(i)}$). The others are in the direction perpendicular to the plane of isotropy and are denoted by an index lower than 2 ($E_2^{(i)}$, $\mu_2^{(i)}$).

The total area under consideration around the opening in expressions (4) and (5) is designated as A. The areas of the layers are designated as A_1 and A_2 (Fig.1).

The stresses in polar coordinates to the contour of the opening are obtained by the stresses in a generalised field:

$$\sigma_r^{(i)}=0;$$
$$\tau_{r\theta}^{(i)}=0;\qquad (6)$$
$$\sigma_\theta^{(i)}=\left\{\left[B_1^{(i)}c^2+B_2^{(i)}s^2\right]s^2+c^4+0.5s_2^2\right\}\sigma_\theta^{(o)}.$$

Numerical example

An opening in the shape of an ellipse has a width of $2b=3m$ and a height of $2a=4.8m$. It draws at a depth of $H=320m$. The inclination of the plane between two steep layers is $\alpha=70°$. The equation of the straight line corresponding to the plane is $z=2.747x-3$. The total rectangular area of influence is $A=518.4\ m^2$ (Fig.1). The areas of the first and the second layers correspond to $A_1=217.3\ m^2$ and $A_2=301.1\ m^2$.

The values of Young's modulus ($E^{(1)}$, $E^{(2)}$), Poisson's rations ($\mu^{(1)}$, $\mu_2^{(2)}$), and the volume of weight ($\gamma^{(1)}$, $\gamma^{(2)}$) for two isotropic layers are determined and can be viewed in Table 1, rows four and five (Trifonova-Genova, 2012). The parameters of the generalised field are given in row six in the same table.

Table 1
Physical and mechanical characteristics of layers

i	$E^{(i)}$	$\mu^{(i)}$	$\gamma^{(i)}$
dimension	MPa		MN/m^3
multiplier	10^3		10^{-2}
1	0.148	0.154	0.28
2	0.595	0.237	0.25
o	0.4075	0.2	0.263

The intersection points of the straight line between the two layers and the ellipse are added to the fixed numbers of points on the contour. For them, the polar angular coordinates and the trigonometric functions take part in the expressions of normal tangential stresses in the first and the second layers and the generalised field. The coefficient of lateral pressure $\lambda^{(o)}$ of the generalised field is equal to 0.25. The vertical stress in the same field is $Q_1^{(o)}=\gamma^{(o)}H=8.32MPa$.

The results of the calculations for the stresses without dimension are given in Table 2. It must be noted that the values of stresses in each layer depend considerably on the values of Young's modulus. Then, in layer 2, the stresses are greater than the same in the generalised field. But in layer 1, these values are smaller than the same in the generalised field. Comparing the values of these stresses, we have established a peak in the diagrams of the boundary between the two layers.

The diagrams of the normal tangential stresses are shown in Figure 2. Here, the stresses in the generalised field are marked with a dotted line and the stresses in the layers with a thick line. The peak in the diagrams of the boundary between the two layers can be seen in points two and eleven.

Key findings

Given analytical expressions of stresses in each layer are applied in a rock mass in which the layers are steep and isotropic or transversally isotropic.

The diagram of normal tangential stresses in a rock consisting of two layers is obtained for an opening in the shape of an ellipse.

Table 2.
Normal tangential stresses in a generalized field in two layers

№	θ [°]	$\frac{\sigma_\theta^{(o)}}{Q_1^{(o)}}$	$\frac{\sigma_\theta^{(1)}}{Q_1^{(o)}}$	$\frac{\sigma_\theta^{(2)}}{Q_1^{(o)}}$
1	0	1.713	0.876	
2	31.148°	1.532	1.409	-1.621
3	60	0.928		-0.927
4	90	0.258		-0.258
5	120	0.928		-1.062
6	150	1.546		-2.212
7	180	1.714		2.319
8	210	1.546		-1.646
9	240	0.928		-0.927
10	270	0.258		-0.258
11	275.538°	0.292	-0.374	-0.294
12	300	0.928	-0.742	
13	330	1.546	0.623	
14	360	1.714	0.876	

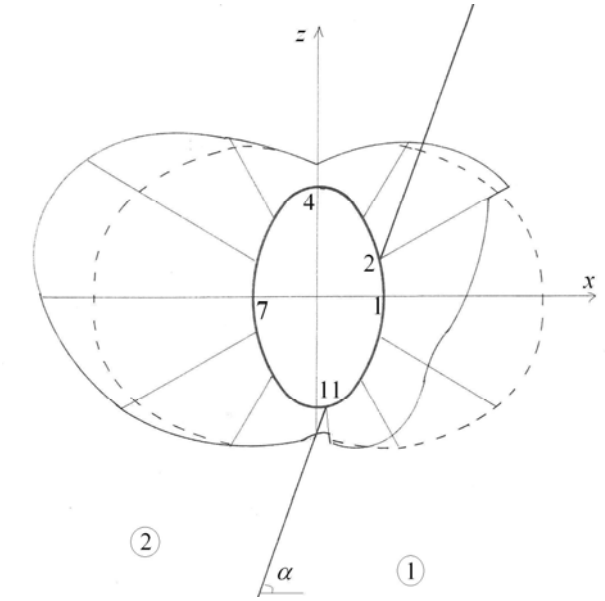

Fig.2. Diagram of normal tangential stresses along the contour of the opening

Conclusion

The method described in this article has the following advantages:

-It is very easy to apply;

-It uses affordable means of calculating (a computer, a calculator, the Exell software product, and others);

-It can be adapted to openings drawn in the rock with other shapes of the cross-section.

References

Булычев, Н. С. Механика подземных сооружений, М., Недра, 1982. - 282 с. (Bulichev, N. S., Mehanika podzemnih soorujenii, M., Nedra, 1982. - 282 p.)

Минчев, И. Тр. Механика на анизотропното тяло в минното дело, Д.И. „Техника“, С., 1960. - 126 с. (Minchev, I. Tr., mehanika na anizotropnoto tialo v minnoto delo, Sofia, D. I. “Tehnika”, 1960. - 126 p.)

Минчев, И. Тр. Механика на напластените среди, Д.И. „Техника“, С., 1968. (Minchev, I. Tr., Mechanika na naplastenite sredi, Sofia, D. I. “Tehnika”, 1968.)

Трифонова-Генова, В. М. Върху определяне на напреженията в стръмно напластен масив около хоризонтална изработка с кръгово напречно сечение, *VIII-та Международна научна конференция по геомеханика, Сборник от доклади, Варна*, 02-06.07.2018. (Trifonova-Genova, V. M. Varhu opredelyane na naprejeniata v strumno naplasten masiv okolo horizontalna izrabotka s kragovo naprechno sechenie, - Sbornik ot dokladi, Varna, 02-06.07.2018.)

Трифонова-Генова, В. М. Деформирано състояние на разномодулен масив в околността на вертикална изработка, *V-та Международна научна конференция по геомеханика, Сборник от доклади, Варна*, 18 - 20.06.2012. - 294-299. (Trifonova-Genova, V. M. Deformirano sastoyanie na raznomodulen masiv v okolnostta na verikalna izrabotka, - *V-ta Mejdunarodna nauchna konferencia po geomehanika, Sbornik ot dokladi, Varna,* 18-20.06.2012. - 294-299.)

Трифонова-Генова, В. М. Напрегнато състояние в напластен масив около кръгла изработка, София: ИК “Св. Иван Рилски”, 2012. 132 с. (Trifonova-Genova, V. M. Napregnato sastoyanie v naplasten masiv okolo kragla izrabotka, Sofia: I. K. “Sv. Ivan Rilski”, 2012. - 132 p.)

Trifonova-Genova, V. Analytical expression for stresses in a steeply layered rock mass around a circular opening, In: Journal of Mining and Geological Sciences, Vol. 60, Part II, 2017. - 59-62.

SELF-CLEARING OF VIBRATING SCREENING SYSTEMS

Stefan Pulev

University of Mining and Geology "St. Ivan Rilski", 1700 Sofia, st_pulev@yahoo.com

ABSTRACT. During the screening process, particles can block the system by becoming trapped in the screening surface which causes a decrease in performance called blinding. This paper studies the forces acting on a blocked particle from the sample and the conditions under which it becomes free again. Self-clearing is the ability of sieves to dislodge blocked particles by no means other than the forces created by the sieving itself. The determinant factors for self-clearing are correctly selected vibration frequency, amplitude and direction, as well as screen slope. The purpose of this work is to investigate the effects of these on the ability to self-clear with forces of friction taken into account. The relationships between particle dimensions and the size of surface openings that permit self-clearing are determined.

Key words: vibrating screening system, self-clearing

САМООЧИСТВАНЕ НА ВИБРАЦИОННИТЕ ПРЕСЕВНИ УРЕДБИ

Стефан Пулев

Минно-геоложки университет "Св. Иван Рилски", 1700 София, E-mail st_pulev@yahoo.com

РЕЗЮМЕ. В процеса на пресяване така наречените трудни зърна засядат в отворите на ситото и причиняват задръстване, с което понижават производителността. Изследват се силите, действащи върху една заседнала частица от пресявания материал и условията за нейното излизане от това състояние. Самоочистването е свойство на ситото да се освобождава от заседналите трудни зърна без различни помощни средства, а само с помощта на действащите сили. Решаващи фактори за самоочистването на пресевните повърхности са правилно подбраните честота, амплитуда и направление на трептенията и наклон на пресевната повърхност. Целта на тази работа е изследване на влиянието на споменатите фактори върху способността на ситото да се самоочиства при отчитане и на силите на триене. Изведени са зависимости между размерите на частиците и големината на отворите на ситото, осигуряващи самоочистването.

Ключови думи: вибрационни пресевни уредби, самоочистване

Introduction

Screen blinding degrades screening performance and efficiency. It is of particular importance to formulate the exact reasons and identify means to prevent it from occurring.

It is clear from the practice of mining enterprises that the main factors for blinding are the physical properties of material screened (Denev, 1964; Tsvetkov, 1988). The particle-size distribution is particularly important. The larger the "under-size" particle groups and smaller the "limit-size" (or "near-size") particle groups, the lower the risk of blinding. The general rule is that small particles easily pass through the openings and the screen proves to be large enough for near-limit particles.

High material humidity also contributes to intensified blinding. Finer particles stick together and form larger pieces which cause congestion. Sieving is made difficult not by the humidity itself, but by the water on the surfaces of particles. Water connects particles pulling them together. Increased humidity prevents screening only up to certain limits. Screening beyond these is called wet screening.

Contamination in the feed also creates conditions for blinding of the screen surface. Even in low humidity, loamy impurities form lumps which remain in the material bed and block the openings. Fine dust can also adhere to surface openings and reduce their size.

The shape of the particles and their relative weight are also important. Objects with flat and elongated shapes can cover openings more easily. It is of paramount importance that the shape of the openings be suitable for the shape of the particles. Round holes are recommended for spheres and cubes. Rectangular ones are suitable for flat and elongated particles.

Self-clearing is the ability of sieves to dislodge blocked particles by no means other than forces created by the sieving itself. The determinant factors for self-clearing are correctly selected vibration frequency, amplitude, and direction, as well as screen slope. The purpose of this work is to investigate the effects of these on the ability to self-clear with forces of friction taken into account. This work is a continuation of the quoted study by Pulev (2015).

Analysis

The most common cause of screen blinding is openings blocked by near-sized particles. These are particles with a size d greater than or equal to the size of the holes l (Fig. 1).

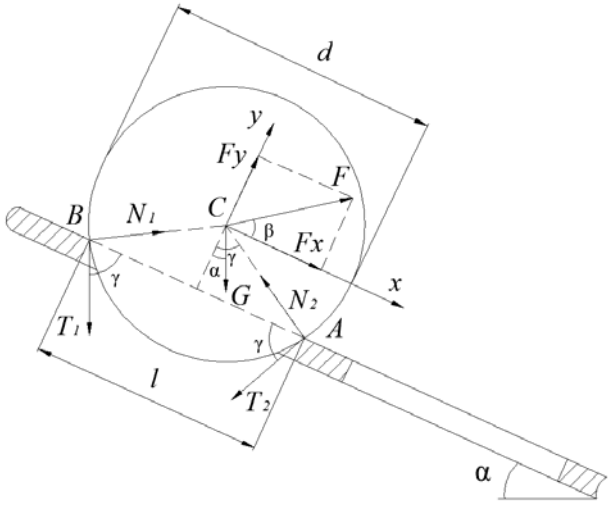

Fig. 1. Diagram of forces acting on a near-sized particle

We investigate a screening surface sloped at an angle α relative to the horizon that performs rectilinear vibrations governed by the law

$$\eta = h\sin\omega t .$$

The amplitude and frequency are denoted by h and ω, respectivley, and the angle β determines the direction of vibrations . Fig. 1 presents a blocked particle that has covered the screen opening, modelled as a completely rigid body with a spherical shape and mass m. A coordinate system Cxy is introduced with the x axis parallel to the screening surface. The active forces acting on the particle are the force of gravity

$$G = mg$$

and the periodically changing inertia force

$$F = mh\omega^2 \sin\omega t$$

with components

$$G_x = mg\sin\alpha$$
$$G_y = mg\cos\alpha$$
$$F_y = mh\omega^2 \sin\omega t.\sin\beta$$
$$F_x = mh\omega^2 \sin\omega t.\cos\beta .$$

The normal forces with which the screen acts on the particle at the ponints of contact with the screen surface A and B are denoted by N_1 and N_2. Sliding friction forces of type

$$T_1 = \mu N_1 \text{ and } T_2 = \mu N_2$$

are applied at the same points. The coefficient of friction between the particle and the screen is μ. The border state in which the particle separates from the screen in the positive direction of the y axis is examined. It is assumed that separation is possible at the maximum value of the inertia ($\sin\omega t = 1$); then

$$F_y = mh\omega^2\sin\beta \qquad (2.1)$$
$$F_x = mh\omega^2\cos\beta .$$

As there are no external causes, it is considered there is no possibility for the particle to rotate around its center O. The conditions for equilibrium of this setup are:

$$F_x + G_x + (N_1 - N_2)\sin\gamma + (T_1 - T_2)\cos\gamma = 0$$
$$F_y - G_y + (N_1 + N_2)\cos\gamma - (T_1 + T_2)\sin\gamma = 0$$

Following transformations, the expression below is derived:

$$2N_1 = \frac{F_x + G_x}{\sin\gamma + \mu\cos\gamma} + \frac{G_y - F_y}{\cos\gamma - \mu\sin\gamma} . \qquad (2.2)$$

From Fig. 1, the following holds for the geometric dimensions:

$$\cos\gamma = \frac{\sqrt{d^2 - l^2}}{d}, \ \sin\gamma = \frac{l}{d} .$$

The concept of relative particle size is introduced. It is denoted by

$$a = \frac{d}{l}$$

and represents the ratio between particle size and sceen opening size. The size of the particle is relative. The following equations then hold:

$$\cos\gamma = \frac{\sqrt{a^2 - 1}}{a}, \ \sin\gamma = \frac{1}{a} . \qquad (2.3)$$

It is considered that the release of the particle will occur when the particle does not exert pressure on the screening surface, i.e.

$$N_1 = 0 \qquad (2.4)$$

After taking into account conditions (2.1) to (2.4), we can derive the expression for the relative particle size

$$a = \sqrt{1 + \frac{g(\cos\alpha + \mu\sin\alpha) - h\omega^2(\sin\beta - \mu\cos\beta)}{g(\sin\alpha - \mu\cos\alpha) + h\omega^2(\cos\beta + \mu\sin\beta)}}^{\,2} \qquad (2.5)$$

The relative particle size determined by (2.5) gives an idea of the ability of the screen to self-clear. At values close to 1,

particles fall deep into the openings, block them, and release becomes harder. As values become greater than 1, the particle center of gravity is more distant from the surface and the probability of self-clearing increases.

Numerical experiment and discussion

The analysis of (2.5) shows that the the following four factors influence self-clearing:

– vibration frequency ω ;

– vibration amplitude h ;

– vibration direction determined by angle β ;

– screen slope α .

To investigate their impact, charts (see Fig. 2, 3, 4, and 5) have been plotted using (2.6) with the following parameters set at:

$$h = 2\ mm\ ,\ \omega = 400\ s^{-1},\ \alpha = 9°,$$
$$\beta = 15°,\ \mu = 0{,}2\ .$$

Fig. 2 shows changes of relative particle size against an amplitude variation from 1 to 10 mm. It can be seen that self-clearing improves as amplitude increases. The reason is that a larger inertial force pulls near-sized particles out from the openings more easily.

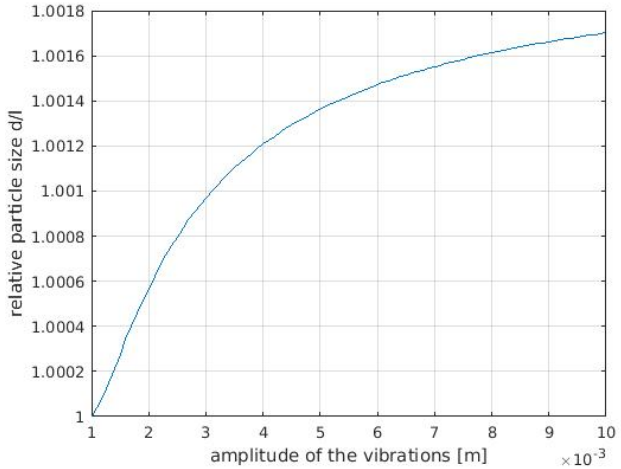

Fig. 2. Influence of vibration amplitude on self-clearing ability

Figure 3 illustrates relative particle size against a vibration frequency varying from 50 to 250 s^{-1}. As can be seen, high vibratoin frequency adversely affects self-clearing.

Fig. 4 shows how screen surface slope affects self-clearing. The angle α varies from 0 to 40º. Increases in slope only sightly imporove self-clearing because they reduce the gravity component $G_y = mg\cos\alpha$. At the same time, steep slope increases material movement speed and can negatively affect screening efficiency.

Fig. 5 illustrates the influence of vibration direction determined by the angle β . The anble varies from 0 to 40º. At smaller angles, self-clearing is weak, but the magnitude of the horizontal component F_x of the inertial force is large. This leads to improved transport of material over the screen surface. Increasing β causes an increase in the vertical component of the inertial force and improvements in self-clearing, but it can adversely affect the vibration stability of individual particles.

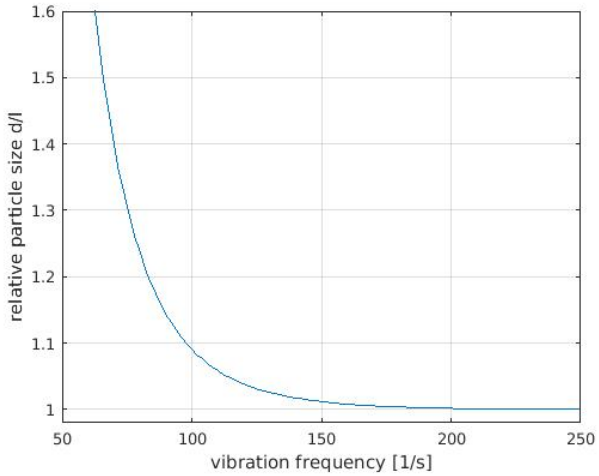

Fig. 3. Influence of vibration frequency on self-clearing ability

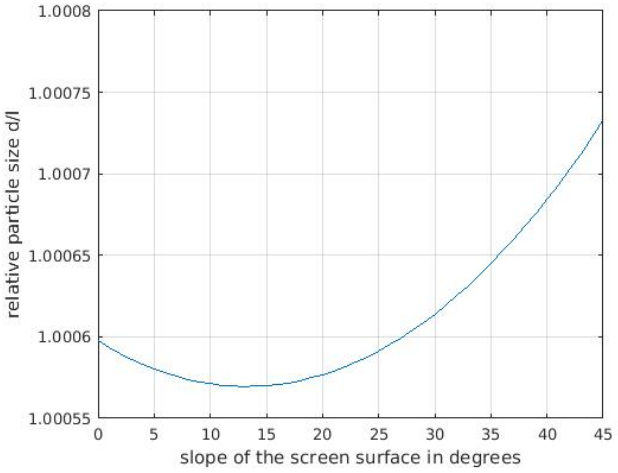

Fig. 4. Influence of screen slope on self-clearing ability

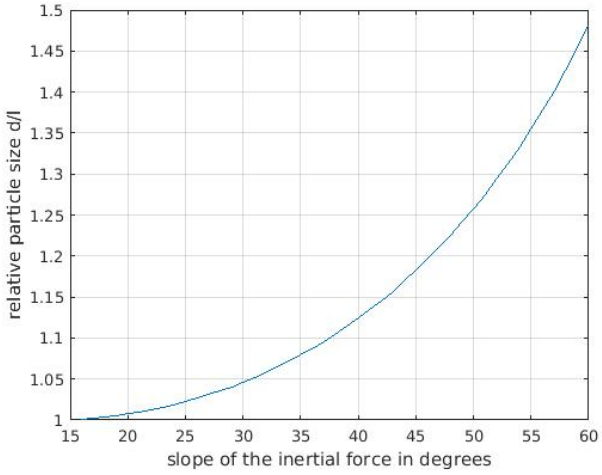

Fig. 5. Influence of vibration direction on self-clearing ability

Conclusion

The ability of the screen to self-clear is an extremely important for increasing the performance and efficiency of vibrating screening systems. It is a complex dependency on the parameters of the vibration and on the slope of the screening surface. The deduced formula (2.5) and its analysis can be used to correctly select the amplitude, frequency and direction of oscillation, as well as screen slope. The results of this study can aid technologists in mining enterprises.

References

Денев, С. И. Трошене, смилане и пресяване на полезни изкопаеми. С., Техника, 1964. (Denev, S. I. Troshene, smilane i presiavane na polezni izkopaemi. Sofia, Tehnika, 1964.)

Пулев, Ст. Условия на самоотчистване на вибрационните пресевни уредби, XV международна научна конференция ВСУ'2015, 4-5 юни 2015, София, Доклади том II, - 65-70.(Pulev, S. Uslovia za samoochistvane na vibracionnite presevni uredbi, XV mejdunarodna nauchna konferencia VSU'2015, 4-5 yuni 2015, Sofia, Dokladi tom II, - 65-70.

Цветков, Х. Ц. Обогатителни машини. С.,Техника, 1988. (Tsvetkov H. Ts. Obogatitelni mashini. Sofia, Tehnika, 1988.)

IRON DOPED CARBON NANODOTS AS EFFICIENT ELECTROCATALYSTS

Ivan Nikolov[1], Alexandre Loukanov[1,2], Elena Ustinovich[3], Anatoliy Angelov[1], Seiichiro Nakabayashi[2]

[1] Laboratory of Engineering NanoBiotechnology, Department of Eng. Geoecology, University of Mining and Geology "St. Ivan Rilski" – Sofia, Bulgaria, ivan_nikolov.1985@abv.bg; tonyagev@mgu.bg
[2] Division of Strategic Research and Development, Graduate School of Science and Engineering, Shimo − Ohkubo 255, Sakura − Ku, Saitama 338-8570, Japan, loukanov@mail.saitama-u.ac.jp, sei@chem.saitama-u.ac.jp
[3] Plekhanov Russian University of Economics, Stremyanny per. 36, 117997, Moscow, Russian Federation, lenausti@mail.ru

ABSTRACT. Carbon nanodots (C-dots) doped with iron cations were synthesized as efficient electrocatalysts for oxygen reduction reaction. For that purpose the nanoparticles were immobilized on a graphite rods used as a working electrode. The ultra small iron-doted carbon nanodots produced a substantial reduction peak at –0.18 V in acidic media indicating that the oxygen was reduced at the modified electrode. In conclusion, we consider that iron-doted C-dots are a promising candidate as an alternative to theplatinum based catalysts for fuel cells applications.

Keywords: carbon nanodots, environmentally friendly electrocatalysts, oxygen reduction reaction

ВЪГЛЕРОДНИ НАНОТОЧКИ ДОТИРАНИ С ЖЕЛЕЗНИ КАТИОНИ КАТО ЕФИКАСНИ ЕЛЕКТРОКАТАЛИЗАТОРИ

Иван Николов[1], Александър Луканов[1,2], Елена Устинович[3], Анатолий Ангелов[1], Сейчиро Накабаяши[2]

[1]Лаборатория Инж. Нанобиотехнология, Катедра „Инженерна геоекология", Минно-геоложки Университет „Св.Иван Рилски" – София, България, ivan_nikolov.1985@abv.bg ; tonyagev@mgu.bg
[2]Отдел за стратегически изследания и развитие, Факултет по наука и инженерство, Университет Сайтама, Шимо-Окубо 255, Сакура-ку, Сайтама 338-8570, Япония, loukanov@mail.saitama-u.ac.jp , sei@chem.saitama-u.ac.jp
[3]Плеханов Руски икономически университет, ул. "Стремяни" 36, 117997, Москва, Руска федерация, lenausti@mail.ru

РЕЗЮМЕ. Въглеродните наноточки (C-dots) дотирани с железни катиони бяха синтезирани, като ефикасни електрокатализатори за редукция на кислород. За тази цел наночастиците бяха имобилизирани върху графитни пръчки, използвани, като работен електрод. Ултрамалките въглеродни наноточки, дотирани с железни йони произвеждат значителен редукционен пик при at –0.18 V в киселинна среда, което показва, че кислорода се редуцира на модифицирания електрод. В заключение, считаме че тези наночастици са обещаващ кандидат, като алтернатива на катодните катализатори, базирани на платината за приложения в горивни клетки.

Ключови думи: въглеродни наноточки, *екологосъобразни електрокатализатори, редукция на кислород*

Introduction

The electrochemical oxygen reduction reaction is regarded as a key step for the development of green ecotechnologies, including solar fuel production, fuel cells, rechargeable batteries, etc. (Trotochaud et al., 2012; Suntivich et al., 2011). Nowadays, the fuel cells are in the focus of the research efforts, because they produce water as the main product of the reaction with a few byproducts (Lastovina et al., 2017). Their efficiency is limited by the rate of oxygen reduction reaction (ORR) (Becknell et al., 2015). In the widely used fuel cells the commercially available cathodic catalysts usually contain platinum and its alloys (Pt/C, Pt3Co/C). These catalysts are too expensive for common use and they can degrade over time. The high cost of the other noble metal catalysts (as iridium and ruthenium oxides) is a motive to concentrate the efforts on developing high-efficient and cost-effective alternatives, known as efficient platinum-free electrocatalysts. Different compounds have been employed as alternative catalysts for the ORR. Recently, metal-organic frameworks, some nanoparticles and oxide compounds of cheap and environmental friendly 3d-metals as iron, cobalt, nickel and etc. were investigated as promising electrocatalysts under mild reaction conditions (Liang et al., 2011; Yeo & Bell, 2011; Subbaraman et al., 2012; Gao et al., 2013). Among them, the metal nanocrystals as iron/cobalt nitride, Co_xO_y, Fe_xO_y and Mn_xO_y coordinated to nitrogen-doped carbon materials are of considerable interest. These nano-electrocatalysts produce high oxygen reduction reaction activity due to synergetic chemical coupling effects between the nitrogen-doped carbon and the metal nanocrystals (Liang et al., 2011). The electrocatalytic activity can be increased by change of nanoparticle design as decreasing of its diameter, co-doping with other metals, modification with organic ligands, etc. (Lv et al., 2016). As another kind of electrocatalysts based on metals, the combination of nitrogen doped carbon nanomaterials and nanoparticles synthesized from some transition d-elements is a desired way to promote efficiently ORR catalytic activity (Bo et al., 2015). Previous reports found that the introduction of a trace transition metal as iron effectively increases the activity of nitrogen-doped carbon materials (Liu et al., 2013). Recently it

has been found that catalysts based on iron, nitrogen and carbon can be synthesized by pyrolyzing a wide variety of nitrogen and carbon precursors in the presence of iron sources at high temperature (Byon et al., 2011). Nanocatalysts prepared in such a way exhibited good activity for ORR.

The aim of this report was to develop electrochemically active nitrogen-doped carbon dots with incorporated iron ions as effective ORR catalyst. For that purpose highly-fluorescence nitrogen-doped carbon dots (C-dots) nanoparticles were synthesized by microwave-assisted pyrolysis and iron ion was incorporated into the aromatic core and carboxyl groups by complex-formation chemical reaction. Such prepared nanoparticles were immobilized on the graphite electrode and tested for ORR activity.

Experimental Procedures

Materials. All chemicals were purchased from Wako Company, they are of analytical grade and were used without future purification. The chemicals used in our experiments are as follow, citric acid, 1,2-ethylenediamine, sodium nitrite, sodium bicarbonate, potassium hydroxide, sulfur acid and concentrated hydrochloric acid. The solutions were prepared with ultrapure water (18.0 M 18.2MΩ·cm, 25°C, Water Purifying System). Commercial graphite rods with 1.2 nm diameter were purchased from Uni 0.5 Mm Hb Nano Dia Blended Hi-quality Mechanical (made in Japan) and used as a working electrode.

Fabrication of C-dots-Fe^{3+} modified graphite electrodes. The nanoparticles were prepared by the so called microwave assisted pyrolysis, which is a "bottom up" method. For this synthesis 1 g of citric acid was mixed with 10 ml deionized water and 0.2 ml of 1,2- ethylenediamine was subsequently injected into the reaction mixture. Then the precursors were energetically mixed by magnetic stirrer to obtain a final clean and transparent solution. Then the solution was subject to microwave pyrolysis in 150 ml Beher glass for 180 sec in a conventional microwave oven (600 W). After the pyrolytic reaction a yellow-brown pellet was formed at the bottom of the glass vessel. Its aqueous solution was with acidic pH = 3.5. The pellet was dissolved again in 10 ml deionized water and the dispersion was centrifuged at 13500 RPM for 30 min to remove coarse graphite particles and second byproducts. The bare C-dots reacted with solution of $FeCl_3$ at pH = 4.2 and the reaction solution was neutralized. The reacted nanoparticles were separated from the unreacted iron salt by size-selective desalting column (PD-10 desalting column, GE Healthcare Life Sciences). The supernatant was oven dried at 80°C. The size and morphology of the nanoparticles were characterized by transmission electron microscope. UV-VIS absorption spectra of C-dots were measured using Jasco V-630 UV/VIS spectrophotometer. The commercial graphite electrodes were modified with C-dots-Fe^{3+} using simple drop-coating method. Simply, 15 μL of C-dots-Fe^{3+} dispersion was dropped onto the graphite electrode surface followed by coating with 4 μL of Nafion solution (0.5 wt%). Then, the prepared electrode was dried in an oven at 80°C for 60 min.

Electrochemical characterization. The modified graphite electrodes were characterized by Cyclic voltammetry (CV) using a Potentiostat (PARSTAT 2263, Princeton Applied Res) in aqueous solution of hydrochloric acid (0.01 M HCl). The applied scan rate was 100mVs^{-1} within a potential scan range of – 0.5 to + 0.5 V. The electrochemical measurements were performed at ambient temperature in nitrogen and oxygen-saturated solutions, respectively. A conventional three-electrode electrochemical cell was used, including modified with C-dots-Fe^{3+} graphite rod as a working electrode, an Ag/AgCl (saturated KCl) electrode as the reference electrode and polished platinum wire as the counter electrode.

Result and discussion

Physicochemical characterization of the nanoparticles. The preparation of nitrogen-doped carbon nanodots with iron complex is presented on Fig. 1.

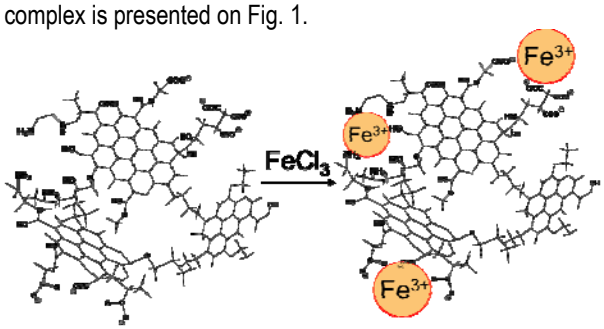

Fig.1. Schematic representation of the formation of chelate complex between iron ions and the surface functional groups of the carbon nanoparticle

It is known that the C-dots contain abundant number of surface functional groups as carboxylates, amines, hydroxyl and etc. The iron ions possess certain affinity to the oxygen atoms from the organic shell and the result is association between the metal ions and the carboxylate groups (Dhenadhayalan & Lin, 2015).

The microscopic data show uniformly dispersed ultra-small nanoparticles with a diameter less than 3 nm (d < 3 nm). Their hydrophilic surface as explained above was abundant with organic groups as carboxyl, amino, hydroxyl and etc., which favors their good solubility in aqueous solutions. The UV-visible spectrum displays the typical for C-dots absorption peaks at 245 nm and 344 nm, which indicate π–π^* transition of the aromatic sp^2 domains and n–π^* transition attributed to C=O and C=N groups, respectively (Roy et al., 2015) as shown on Figure 2. The dynamic light scattering analysis confirmed the nanoparticles size distribution in the range 1.0–3.0 nm with 2 nm average diameter. The reaction with iron ions causes quenching of the C-dots emission intensity but does not change the absorption maximum peak. However, the solution color of treated nanoparticles changes to dark, which causes enhancing of the absorbance in the visual wavelength range. This effect remains even after purification of C-dots-Fe^{3+} with size-selective desalting column. The darkest color of nanoparticle solution after purification can be seen even with naked eyes. This was an indication that the iron ions are chemically attached to the functional groups of the nanoparticle and they are not in equilibrium with the surrounded aqueous media.

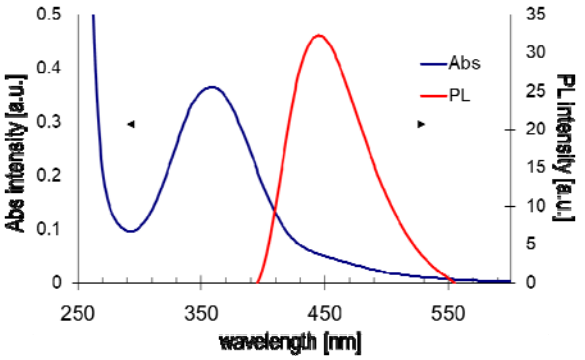

Fig.2. Optical properties of the highly fluorescent C-dots

Electrochemical oxygen reduction reaction activity of the modified with C-dots-Fe^{3+} graphite working electrode. The electrochemical ORR activity of the unmodified and modified graphite electrode was investigated by cyclic voltammetry. For that purpose the electrode rod was used as a working electrode or cathode in the electrochemical experimental cell. Several parameters were modulated in order to optimize the production of achievable current density of the modified working electrodes. Dilute solution of hydrochloric acid was chosen as it is commonly used as the electrolyte in many electrochemical reactions in fuel cells. Thus, the highest current intensity was achieved by using of 0.01 M HCl as electrolyte. On Fig. 3 are shown the cyclic voltammograms of bare (unmodified) and modified with nanoparticles graphite electrode. The electrode modified with nanoparticles exhibited a remarkably higher anodic peak current intensity as compared with the intensity of the unmodified bare electrode.

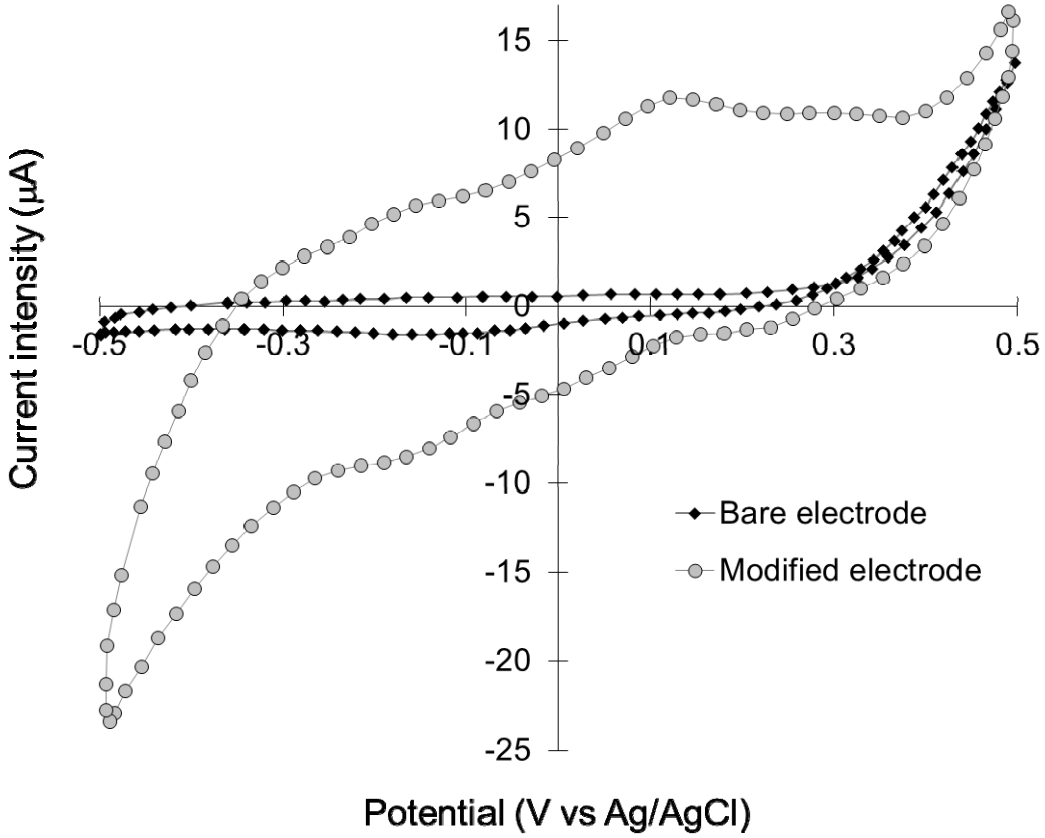

Fig.3. Cyclic voltammogram of bare electrode and modified electrode with C-dots-Fe^{3+} nanoparticles in 0.01 M HCl solution, saturated with oxygen at a scan rate of 100 mVs^{-1}

This is an indication that the deposition of C-dots-Fe^{3+} nanoparticles had substantially enhanced the overall electrical conductivity of the graphite rod. Additional experiments by cyclic voltammetry proved that the current intensity of the modified electrode increased linearly with the increasing of the amount of nanoparticles and iron ions, respectively incorporated in them. This increasing effect could be attributed to the amount of iron ions which are bound to the carboxylate groups on the nanoparticle surface. It is known that $–COO^-$ groups have strong coordination affinity towards Fe^{3+} ions in aqueous media as shown on Fig. 1. Thus, they led to higher electrical conductivity of the C-dots-Fe^{3+} modified graphite electrode. The cyclic voltammograms of the immobilized nanoparticles show also that in nitrogen-saturated electrolyte C-dots-Fe^{3+} produced pseudocapacitive behavior, whereas in oxygen-saturated electrolyte a substantial reduction peak occurred at – 0.18 V as shown on the figure above, indicating that O_2 was reduced on the working electrode. Just for comparison, the commercial Pt/C catalysts exhibit a reduction peak at + 0.53 V for ORR (Bo et al., 2015). If methanol is

introduced into the testing electrochemical cell, then an identical response was observed for C-dots-Fe^{3+} modified electrode. This indicates a good selectivity for ORR against methanol. Again, in comparison with the case of commercial Pt/C, the disappearance of oxygen reduction reaction current and methanol oxidation indicated that the ORR process was strongly retarded by the alcohol. These results indicate that the presented graphite electrode with electrocatalytic nano-layer was a potential alternative to platinum as a cathode catalyst.

C-dots modified electrode as electrochemical sensor for selective detection of metal ions. The specific electrochemical properties of the carbon nanodots modified electrode can be applied also as a sensor for detection of metal ions in aqueous media. The analytical performance of this electrochemical sensor can be achieved by cyclic voltammetry as well as electrochemical impedance spectroscopy, because of the specific opto-electronic properties as explained above. In our experiment we found that under optimized condition, the electrochemical sensor electrode exhibited a linear detection range of iron ions detection in the interval between 0.5 to 30 ppm with a limit of detection of around 0.4 ppm. The selectivity of the electrode was investigated with a wide range of metal ions (Hg^{2+}, Cd^{2+}, Co^{2+}, etc.), which are commonly associated with heavy metal pollution in natural water. The solubility of these metal ions is dependent on pH of solution. Due to this reason, in the performed sensor analysis we used HCl and H_2SO_4 for sample preparation. In our experiment the current intensity of the modified electrode was highest in the case of iron ions among the other evaluated metal ions. The selectivity is attributed to the specific chemical affinity of C-dots to Fe^{3+} as we have explained in the text. The investigation of the sensor research project is still under progress.

Conclusion

An electrode modified with iron-doped carbon nanodots has been fabricated. The electrode has ORR activity in acidic solution and produces higher current density. Therefore, we concluded that C-dots-Fe^{3+} nanoparticles are a promising potential candidate as electrocatalytic cathode for oxygen reduction. The obtained data provide also potential alternative approach for preparation of efficient and low-cost metal-doped C-dots electrocatalysts with practical application in fuel cells. In addition, the fabricated graphite electrodes modified with C-dots can be used also as a sensor for electrochemical detection of iron in polluted natural water.

Competing Interests

The authors declare that there no competing interests regarding the publication of this research article.

Acknowledgment

Funding from the Bulgarian National Science Fund, Grant № DN07/7, 15.12.2016. This study was accomplished within the bilateral agreement between Saitama University-Japan and the University of Mining and Geology "St. Ivan Rilski"-Bulgaria.

References

Becknell, N., Kang, Y., Chen, C., Resasco, J., Kornienko, N., Guo, J., et al., (2015) Atomic structure of Pt_3Ni nanoframe electrocatalysts by in situ X-ray absorption spectroscopy. J Am Chem Soc 137, 15817–15824.

Bo, X., Li, M., Han, C., Zhang, Y., Nsabimana, A., Guo, L., (2015) Noble metal-free electrocatalysts for the oxygen reduction reaction based on iron and nitrogen-doped porous graphene. J Mater Chem A 3, 1058–1067.

Byon, H. R., Suntivich, J., Shao-Horn, Y., (2011) Graphene-based non-noble-metal catalysts for oxygen reduction reaction in acid. Chem Mater 23, 3421–3428.

Dhenadhayalan, N., Lin, K. C., (2015) Chemically induced fluorescence switching of carbon-dots and its multiple logic gate implementation. Sci Rep 5, 10012.

Gao, M. R., Xu, Y. F., Jiang, J., Yu, S. H., (2013) Nanostructured metal chalcogenides: synthesis, modification, and applications in energy conversion and storage devices. Chem Soc Rev 42, 2986–3017.

Lastovina, T., Pimovona, J., Budnyk, A., (2017) Platinum-free catalysts for low temperature fuel cells. IOP Conf. Series: Journal of Physics: Conf Series 829, 012007.

Liang, Y. Y., Li, Y. G., Wang, H. L., Zhou, J. G., Wang, J., Regier, T., Dai, H., (2011) Co_3O_4 nanocrystals on graphene as a synergistic catalyst for oxygen reduction reaction. Nat Mater 10, 780–786.

Liu J., Sun, X., Song, P., Zhang, Y., Xing, W., Xu, W., (2013) High-performance oxygen reduction electrocatalysts based on cheap carbon black, nitrogen, and trace iron. Adv Mater 25, 6879–6883.

Lv, H., Li, D., Strmcnik, D., Paulikas, A. P., Markovic, N. M., Stamenkovic, V. R., (2016) Recent advances in the design of tailored nanomaterials for efficient oxygen reduction reaction. Nano Energy 29, 149–165.

Roy, P., Chen, P. C., Periasamy, A. P., Chen, Y. N., Chang, H. T., (2015) Photoluminescent carbon nanodots: synthesis, physicochemical properties and analytical applications. Materials Today 18, 447–458.

Subbaraman, R., Tripkovic, D. Chang, K. C., Strmcnik, D., Paulikas, A. P., Hirunsit, P., Chan, M., Greeley, J., Stamenkovic, V., Markovic, N. M., (2012) Trends in activity for the water electrolyser reactions on 3d M (Ni, Co, Fe, Mn) hydr(oxy)oxide catalysts. Nat Mater 10, 780–786.

Suntivich, J., May, K. J., Gasteiger, H. A., Goodenough, J. B., Horn, Y. S., (2011) A perovskiteoxide optimized for oxygen evolution catalysis from molecular orbital principles. Science 334, 1383–1385.

Trotochaud, L., Ranney, J. K., Williams, K. N., Boettcher, S. W., (2012) Solution-cast metal oxide thin film electrocatalysts for oxygen evolution. J Am Chem Soc 134, 17253–17261.

Yeo, B. S., Bell, A. T., (2011) Enhanced activity of gold-supported cobalt oxide for the electrochemical evolution of oxygen. J Am Chem Soc 133, 5587–5593.